TECHNISCHE
UNIVERSITÄT
DRESDEN

Architectural Principles for Database Systems on Storage-Class Memory

Dissertation

zur Erlangung des akademischen Grades
Doktoringenieur (Dr.-Ing.)

vorgelegt an der
Technischen Universität Dresden
Fakultät Informatik

eingereicht von
Ismail Oukid, M.Sc.
geboren am 19. Mai 1989 in Blida, Algerien

Gutachter:	**Prof. Dr.-Ing. Wolfgang Lehner** Technische Universität Dresden
	Prof. Dr. Stefan Manegold Universiteit Leiden & Centrum voor Wiskunde en Informatica
Tag der Verteidigung:	5. Dezember 2017

Walldorf, den 15. Dezember 2017

Ismail Oukid: *Architectural Principles for Database Systems on Storage-Class Memory* ©December 15, 2017.

To my parents.

ABSTRACT

Database systems have long been optimized to hide the higher latency of storage media, yielding complex persistence mechanisms. With the advent of large DRAM capacities, it became possible to keep a full copy of the data in DRAM. Systems that leverage this possibility, such as main-memory databases, keep two copies of the data in two different formats: one in main memory and the other one in storage. The two copies are kept synchronized using snapshotting and logging. This main-memory-centric architecture yields nearly two orders of magnitude faster analytical processing than traditional, disk-centric ones. The rise of Big Data emphasized the importance of such systems with an ever-increasing need for more main memory. However, DRAM is hitting its scalability limits: It is intrinsically hard to further increase its density.

Storage-Class Memory (SCM) is a group of novel memory technologies that promise to alleviate DRAM's scalability limits. They combine the non-volatility, density, and economic characteristics of storage media with the byte-addressability and a latency close to that of DRAM. Therefore, SCM can serve as *persistent main memory*, thereby bridging the gap between main memory and storage. In this dissertation, we explore the impact of SCM as persistent main memory on database systems. Assuming a hybrid SCM-DRAM hardware architecture, we propose a novel software architecture for database systems that places primary data in SCM and directly operates on it, eliminating the need for explicit I/O. This architecture yields many benefits: First, it obviates the need to reload data from storage to main memory during recovery, as data is discovered and accessed directly in SCM. Second, it allows replacing the traditional logging infrastructure by fine-grained, cheap micro-logging at data-structure level. Third, secondary data can be stored in DRAM and reconstructed during recovery. Fourth, system runtime information can be stored in SCM to improve recovery time. Finally, the system may retain and continue in-flight transactions in case of system failures.

However, SCM is no panacea as it raises unprecedented programming challenges. Given its byte-addressability and low latency, processors can access, read, modify, and persist data in SCM using load/store instructions at a CPU cache line granularity. The path from CPU registers to SCM is long and mostly volatile, including store buffers and CPU caches, leaving the programmer with little control over when data is persisted. Therefore, there is a need to enforce the order and durability of SCM writes using persistence primitives, such as cache line flushing instructions. This in turn creates new failure scenarios, such as missing or misplaced persistence primitives.

We devise several building blocks to overcome these challenges. First, we identify the programming challenges of SCM and present a sound programming model that solves them. Then, we tackle memory management, as the first required building block to build a database system, by designing a highly scalable SCM allocator, named PAllocator, that fulfills the versatile needs of database systems. Thereafter, we propose the FPTree, a highly scalable hybrid SCM-DRAM persistent B^+-Tree that bridges the gap between the performance of transient and persistent B^+-Trees. Using these building blocks, we realize our envisioned database architecture in SOFORT, a hybrid SCM-DRAM columnar transactional engine. We propose an SCM-optimized MVCC scheme that eliminates write-ahead logging from the critical path of transactions. Since SCM-resident data is near-instantly available upon recovery, the new recovery bottleneck is rebuilding DRAM-based data. To alleviate this bottleneck, we propose a novel recovery technique that achieves nearly instant responsiveness of the database by accepting queries right after recovering SCM-based data, while rebuilding DRAM-based data in the background. Additionally, SCM brings new failure scenarios that existing testing tools cannot detect. Hence, we propose an online testing framework that is able to automatically simulate power failures and detect missing or misplaced persistence primitives. Finally, our proposed building blocks can serve to build more complex systems, paving the way for future database systems on SCM.

ACKNOWLEDGEMENTS

This thesis would not have been possible without the contributions, support, and companionship of many whom I would like to acknowledge.

First and foremost, I would like to express my deepest gratitude to my supervisor and mentor Prof. Wolfgang Lehner for his unconditional support throughout my thesis, both *personally* and *professionally*. Wolfgang has always been a positive presence. He had my back from day one until today and continuing, ensuring I was always in the best possible conditions to succeed, even beyond my thesis. By always offering constructive criticism and enthusiastically encouraging me to aim high, he gave me confidence and guided me to strive for excellence.

Furthermore, I would like to thank Prof. Stefan Manegold for taking on the role of co-examiner of my thesis, for his invaluable feedback, and for his hospitality during my visit at CWI.

Moreover, I would like to express my gratitude to the SAP HANA Campus team, where I had the privilege to conduct my thesis. I enjoyed my time as a PhD student in great part thanks to their companionship. First, there is Arne Schwarz, the heart and soul of the campus, who works hard so that we only need to worry about our research. Then there is my fellow PhD students and friends: Ingo Müller, Michael Rudolf, Marcus Paradies, Iraklis Psaroudakis, David Kernert, Elena Vasilyeva, Hannes Rauhe, Robert Brunel, Thomas Bach, Florian Wolf, Matthias Hauck, Lucas Lersch, Frank Tetzel, Robin Rehrmann, Stefan Noll, Georgios Psaropoulos, Jonathan Dees, Philipp Große, Martin Kaufmann, and Francesc Trull. Ingo influenced me the most as a researcher and as a person. I looked up to him as a mentor from day one; from him I learned scientific rigor, critical thinking, and that *quality needs time*. I have been looking up to him as a big brother since and still strive to follow his footsteps. Michael's willingness to help is unmatched; he came to the rescue countless times for technical and non-technical issues. My time in Germany surely would not have been as enjoyable without his help. I was lucky to travel with Marcus several times to conferences; he surely knows how to organize a trip – the Yosemite excursion is unforgettable. I had such an exciting time with Iraklis, Ingo, Frank, Matthias, and Thomas during the SIGMOD programming contests – I learned a lot from each one of them. Frank was the perfect night owl partner for the late evenings in the office, and Georgios made my social life a thing again during the last year of my PhD. Additionally, I would like to thank Robin, Frank, Lucas, Stefan, Michael, Marcus, Thomas, Matthias, and Ingo for reviewing parts of this dissertation. I am grateful to all of you guys!

Special thanks go to my SAP supervisors Daniel Booss, Anisoara Nica, and Peter Bumbulis, as well as my Intel supervisor Thomas Willhalm for their help and guidance throughout my thesis. Daniel's technical expertise was key in jump starting the PAllocator. Peter was influential in laying out the vision for SOFORT during my visit to SAP Waterloo in April 2014. Ani supported me in several of my papers and was instrumental in devising the adaptive recovery mechanism of SOFORT. Thomas was always prompt to give me feedback and get me access to the latest and fanciest Intel hardware. Moreover, I would like to thank Norman May, Alexander Boehm, Roman Dementiev, Otto Bruggeman, and Abelkader Sellami for their support and insightful input. A special appreciation goes to Oliver Rebholz, my manager in my new role at SAP, for allowing me to finish my dissertation by easing my load in the first few months of my employment.

During my thesis, I was blessed with talented students that were of great help in building my prototype SOFORT: Adrien Lespinasse worked on early versions of PAllocator and the testing framework, Johan Lasperas worked on the FPTree, Daniel Bossle worked on SCM-optimized concurrency control, and Grégoire Gomes worked on the defragmentation scheme of PAllocator.

I would also like to thank my colleagues at the TU Dresden Database Systems Group for their warm welcome whenever I visited: Lars Dannecker, Ulrike Fischer, Katrin Braunschweig, Julian Eberius, Tim Kiefer, Robert Ulbricht, Ines Funke, Ulrike Schöbel, Dirk Habich, Maik Thiele, Martin Hahmann, Hannes Voigt, Thomas Kissinger, Tobias Jäkel, Tomas Karnagel, Till Kolditz, Claudio Hartmann, Kai Herrmann, Kasun Perera, Rihan Hai, Ahmad Ahmadov, Johannes Luong, Annett Ungethüm, Patrick Damme, Lars Kegel, Juliana Hildebrandt, Alexander Krause, Mikhail Zarubin, Elvis Koci, Nusrat Lisa Jahan, Muhammad Idris, and Rana Faisal Munir. A special appreciation goes to Hannes, Kai, Till, and Maik for their help regarding the PhD administrative procedure, and to Thomas for his contribution to the *instant recovery* paper.

I warmly thank my long-time friends Hamza Rihani and Amine Bentaiba who have always been there for me and provided me with an outlet to escape my thesis whenever I needed to. Last but not least, I would like to thank my family, especially my parents, for believing in me more than anyone, for their unconditional support, constant encouragement, and for indulging my character in stressful periods.

Ismail Oukid
December 15, 2017

CONTENTS

Abstract v

Acknowledgements vii

1 Introduction 5

2 Leveraging SCM in Database Systems 11

2.1 Storage-Class Memory 11
2.1.1 Architecting SCM 12
2.1.2 SCM Performance Implications 14

2.2 SCM Emulation Techniques 15
2.2.1 NUMA-Based SCM Emulation 16
2.2.2 Quartz 17
2.2.3 Intel SCM Emulation Platform 17

2.3 SCM and Databases: State-of-the-Art 18
2.3.1 Storage and Recovery 19
2.3.2 Query Optimization and Execution 24

2.4 Overview of SOFORT 27
2.4.1 Design Principles 27
2.4.2 Architecture Overview 27
2.4.3 Persistent Memory Management 28
2.4.4 Data Layout 28
2.4.5 Concurrency Control 29
2.4.6 Recovery Mechanisms 30

2.5 Conclusion 31

3 Persistent Memory Management 33

3.1 Persistent Memory Challenges 34
3.1.1 Data consistency 34
3.1.2 Data recovery 35
3.1.3 Persistent memory leaks 36
3.1.4 Partial writes 36
3.1.5 Persistent memory fragmentation 37
3.1.6 Address space fragmentation 37

3.2 SCM Programming Models 38

3.2.1 Recoverable Addressing Scheme 38
3.2.2 Consistency Handling 38
3.2.3 Persistent Memory Leak Prevention 39
3.2.4 Related Work 40

3.3 Persistent Memory Allocation 42
3.3.1 Pool Structure 42
3.3.2 Allocation Strategies 42
3.3.3 Concurrency Handling 43
3.3.4 Garbage Collection 44
3.3.5 Related Work 45

3.4 PAllocator Design and Implementation 46
3.4.1 Design goals and decisions 46
3.4.2 Programming Model 49
3.4.3 PAllocator Architecture 50
3.4.4 SmallPAllocator 51
3.4.5 BigPAllocator 52
3.4.6 Defragmentation 54
3.4.7 Recovery 55

3.5 Evaluation 56
3.5.1 Standalone allocation and deallocation 58
3.5.2 Random allocation and deallocation 60
3.5.3 Larson benchmark 61
3.5.4 Recovery time 63
3.5.5 Defragmentation 64
3.5.6 Allocator impact on a persistent B-Tree performance 64

3.6 Summary 65

4 PERSISTENT DATA STRUCTURES 67

4.1 Related Work 68
4.1.1 CDDS B-Tree 69
4.1.2 wBTree 69
4.1.3 NV-Tree 70
4.1.4 Discussion 71

4.2 FPTree Design Principles 73
4.2.1 Selective Persistence 73
4.2.2 Fingerprints 74
4.2.3 Amortized Persistent Memory Allocations 76
4.2.4 Selective Concurrency 76

4.3 FPTree Base Operations 78
4.3.1 Fixed-Size Key Operations 78
4.3.2 Variable-Size Key Operations 84
4.3.3 Leaf group management 87

4.4 Evaluation . . . 89
4.4.1 Experimental Setup . . . 90
4.4.2 Single-Threaded Microbenchmarks . . . 90
4.4.3 Concurrent Microbenchmarks . . . 93
4.4.4 End-to-End Evaluation . . . 97
4.5 Summary . . . 100
5 SOFORT: A HYBRID SCM-DRAM TRANSACTIONAL STORAGE ENGINE 101
5.1 Design Space Exploration . . . 102
5.1.1 Concurrency Control . . . 102
5.1.2 Version Storage . . . 105
5.1.3 Index Management . . . 106
5.1.4 Garbage Collection . . . 107
5.2 SOFORT Architecture . . . 108
5.2.1 Concurrency Control . . . 109
5.2.2 Version Storage . . . 109
5.2.3 Index Management . . . 111
5.2.4 Garbage Collection . . . 112
5.3 SOFORT Implementation . . . 113
5.3.1 MVCC Structures . . . 113
5.3.2 Start Transaction . . . 115
5.3.3 Select . . . 116
5.3.4 Insert . . . 117
5.3.5 Delete . . . 118
5.3.6 Update . . . 118
5.3.7 Commit Transaction . . . 119
5.3.8 Abort Transaction . . . 120
5.3.9 Recovery . . . 122
5.3.10 Garbage Collection . . . 124
5.4 Continuing Unfinished Transactions . . . 125
5.5 Evaluation . . . 126
5.5.1 Experimental Setup . . . 127
5.5.2 OLTP Performance . . . 127
5.5.3 Data Placement Impact on OLTP Performance . . . 128
5.5.4 Durability Cost . . . 130
5.5.5 Recovery Time . . . 131
5.6 Summary . . . 132
6 SOFORT RECOVERY TECHNIQUES 133
6.1 Recovery of Secondary Data Structures . . . 134
6.1.1 System Responsiveness . . . 135
6.1.2 Balancing Query Performance with Recovery Performance . . . 135

6.1.3 Discussion . . . 136

6.2 Adaptive Recovery . . . 136
6.2.1 Characterization of Secondary Data Structures . . . 136
6.2.2 Benefit Functions for Secondary Data . . . 137
6.2.3 Benefit Functions Benefit$_{\text{dep}}$ and Benefit$_{\text{indep}}$ . . . 139
6.2.4 Recovery Manager . . . 141

6.3 Evaluation . . . 142
6.3.1 Experimental Details . . . 142
6.3.2 Secondary Data Placement Impact on Recovery Performance . . . 143
6.3.3 Recovery Strategies . . . 144
6.3.4 Adaptive Resource Allocation Algorithm . . . 146
6.3.5 Resilience to Workload Change . . . 148
6.3.6 Impact of SCM Latency . . . 148
6.3.7 Limits of Adaptive Recovery . . . 149

6.4 Related Work . . . 150

6.5 Summary . . . 151

7 TESTING OF SCM-BASED SOFTWARE 153

7.1 Background . . . 154
7.1.1 Related Work . . . 155
7.1.2 Memory Model . . . 156

7.2 Testing of SCM-Based Software . . . 156
7.2.1 Crash Simulation . . . 156
7.2.2 Faster Testing with Copy-on-Write . . . 159
7.2.3 Faster Code Coverage with Call Stack Tracing . . . 159
7.2.4 Memory Reordering . . . 160
7.2.5 Crash Simulation During Recovery . . . 161
7.2.6 Crash Simulation in Multi-Threaded Programs . . . 163
7.2.7 Limitations and Complementarity with Yat . . . 163

7.3 Evaluation . . . 164

7.4 Summary and Future Work . . . 166

8 CONCLUSION 167

8.1 Summary of Contributions . . . 167

8.2 Future Work . . . 169

BIBLIOGRAPHY 173

LIST OF FIGURES 185

LIST OF TABLES 187

LIST OF ALGORITHMS 188

1

INTRODUCTION

> *"The arrival of high-speed, non-volatile storage devices, typically referred to as storage class memories (SCM), is likely the most significant architectural change that datacenter and software designers will face in the foreseeable future."* **Nanavati et al. "Non-Volatile Storage: Implications of the datacenter's shifting center". In Communications of the ACM. Jan, 2016.**

Companies rely heavily on extracting insights from a continuous flow of new data for their business operations and strategic planning. Traditionally, they have used dedicated systems for ingesting and analyzing their data. Incoming data is first ingested by several transactional systems. Then, the accumulated data is sent periodically, e.g., once a week, to a data warehouse that prepares it for analytical processing. Thereafter, the data warehouse is queried to extract relevant business insights. A major disadvantage of this approach is that business insights reflect the past rather than the present. With the rise of Big Data, businesses became eager to process their ever-growing data and extract business insights in real-time, a capability that traditional systems cannot provide.

Hybrid Transactional and Analytical Processing (HTAP) database systems, such as SAP HANA [44] and IBM DB2 Blu [140], are a new type of database systems that provide the ability to ingest updates while providing real-time analytics at the same time [142]. As a result, they provide business insights that reflect the most recent data, which allows companies to discover and react to trends while they are happening, thereby giving them a competitive edge. These systems are made possible thanks to advancements in hardware. Indeed, the advent of large main-memory capacities and high core counts has spurred a shift in software design towards main-memory-centric architectures, which yield orders of magnitude faster access characteristics than traditional, disk-centric approaches. HTAP database systems are a salient example of this new class of main-memory-centric systems.

Scale-up (shared memory) is the preferred architecture of HTAP database systems because of the need to tightly integrate their transactional and analytical capabilities. In fact, some business applications cannot be efficiently scaled out. For instance, certain Enterprise Resource Planning (ERP) transactional workloads touch nearly the whole database, which renders efficient partitioning of the data for scale-out impractical. Furthermore, the rise of Big Data emphasized the importance of these systems with an ever-increasing need for larger main memory capacities. However, they have become constrained by the scalability limits of DRAM: The largest available shared memory server for database systems can embed up to 48 terabytes of DRAM [61].

While the cost per bit of DRAM has steadily decreased over the years, the capacity and bandwidth per core have worsened [112]. As a matter of fact, it is intrinsically hard to further increase the density of

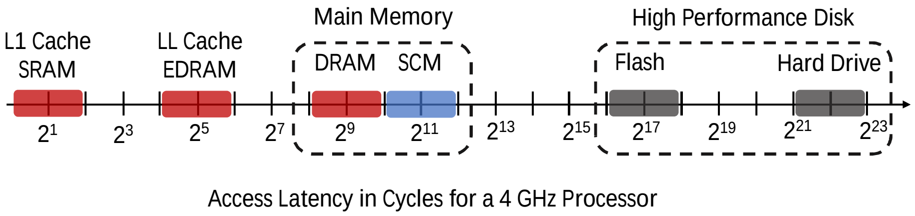

Figure 1.1: Comparison of access latency of different memory technologies. Adapted from [137].

DRAM [67]: The smaller the DRAM cell, the more it leaks energy which interferes with the state of neighboring cells, thereby exponentially increasing error rates. Another concern is that a significant share of the energy consumption in data centers can be attributed to DRAM [30], either directly or indirectly (e.g., through the cooling system). Consequently, DRAM can no longer satisfy the demand for ever growing main memory capacities.

Storage-Class Memory[1] (SCM) is a class of novel memory technologies that exhibit characteristics of both storage and main memory: They combine the non-volatility, density, and economic characteristics of storage (e.g., flash) with the byte-addressability and a latency close to that of DRAM (albeit higher), as illustrated in Figure 1.1. Examples of such memory technologies include Resistive RAM [50] (researched by Hynix, SanDisk, Crossbar, Nantero), Magnetic RAM [37] (researched by IBM, Samsung, Everspin), and Phase Change Memory [87] (researched by IBM, HGST, Micron/Intel). In particular, Intel and Micron announced an SCM technology, called 3D XPoint [1], in the Dual Inline Memory Module (DIMM) form factor. SCM technologies are expected to exhibit asymmetric latencies, with writes being noticeably slower than reads, and limited write endurance (although SCM may be significantly more durable than flash memory, e.g., 3D XPoint [1] by three orders of magnitude). Moreover, SCM will be denser than DRAM, yielding larger memory capacities. Finally, in contrast to DRAM that constantly consumes energy to refresh its state, idle SCM does not consume energy – only active cells do. Hence, SCM has the potential to lift the scalability issues of DRAM, both in terms of capacity and energy consumption.

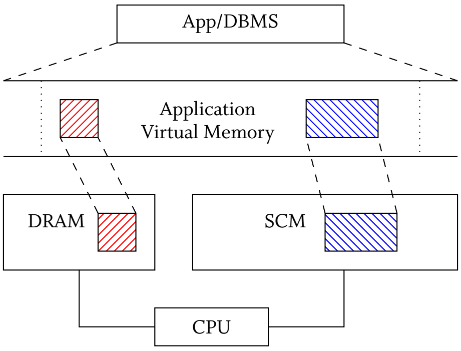

Figure 1.2: SCM is mapped directly into the address space of the application, allowing direct access with load/store semantics.

Given its unique characteristics, SCM can serve as fast storage or as DRAM replacement. However, while SCM is projected to be cheaper than DRAM, it will be too expensive to replace flash. Additionally, it is too slow to replace DRAM. Nevertheless, we foresee that SCM will be invaluable in extending main memory capacity in large scale-up systems. Additionally, it can serve as a cheaper DRAM alternative when performance is not paramount. We argue, however, that these use cases do not harness the full potential of SCM: They do not exploit its non-volatility. In this dissertation we make the case for a third option: using SCM as *persistent main memory*, i.e., as memory and storage at

---

[1] SCM is also referred to as Non-Volatile RAM (NVRAM) or simply Non-Volatile Memory (NVM).

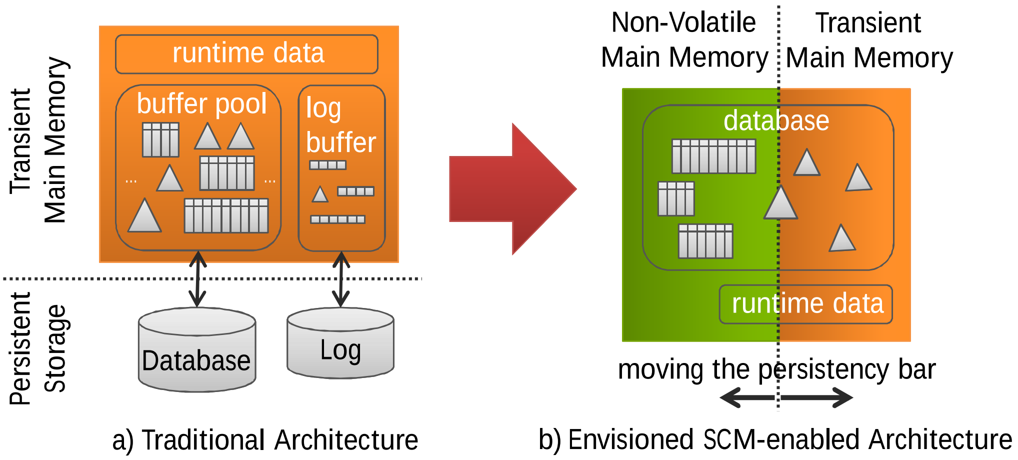

Figure 1.3: Towards a hybrid SCM-DRAM single-level database storage architecture.

the same time. Given its byte-addressability and low latency, processors will be able to access SCM directly with load/store semantics. Current file systems, such as ext4 Direct Access (DAX) [35], already support this access method by offering zero-copy memory mapping that bypasses DRAM and offers the application layer direct access to SCM, as illustrated in Figure 1.2.

Two factors have traditionally spurred shifts in database architectures: new business needs, such as the need for high transaction rates following the advent of the Internet, and – maybe more importantly – advancements in hardware technology [151]. In fact, we often find in the literature decades-old research works that investigated database architectures that were reinvented decades later, mainly because hardware advancements empowered them. For instance, main-memory databases have been researched and recognized, as early as the 1980s, as superior in performance to disk-based counterparts [34, 91, 47]. Nevertheless, it took until the late 2000s, and the advent of large main memory capacities, before main-memory databases took off. SCM databases are no exception: They have been investigated since the late 1980s [27, 2]. However, these works, as well as recent ones, leverage SCM to improve only the logging component as the main bottleneck for transaction processing. Nevertheless, other components of the database do not benefit from SCM. In contrast, we argue that the two ingredients to trigger a rewrite of database systems are present: scaling up HTAP database systems represents the business need, and SCM represents the advancement in hardware. Therefore, we endeavor in this dissertation to explore a novel database architecture that leverages SCM as persistent main memory.

Figure 1.3 outlines the move from a traditional database architecture towards our envisioned system design. Due to the block-oriented nature of today's non-volatile devices (e.g., hard disk or flash), both traditional disk-based and modern main-memory database systems rely on additional logging and snapshotting components to efficiently guarantee consistency and durability. The demarcation line between transient memory and persistent storage is explicit, as illustrated on the left-hand side of Figure 1.3. SCM, however, is byte-addressable and offers a latency close to that of DRAM. Thus, we envision a novel main-memory database architecture that directly operates on SCM, eliminating the need for explicit I/O. We anticipate that the performance gained by removing I/O will compensate for the performance lost because of the higher latency of SCM. Still, we see the need to keep DRAM next to SCM for performance-critical data structures, as illustrated on the right-hand side of Figure 1.3.

Our envisioned hybrid SCM-DRAM architecture allows for a radical change in the database architecture: First, it eliminates the traditional recovery bottleneck of main-memory database systems, namely reloading data from storage to main memory, as data is discovered and accessed directly in

SCM. Second, the use of SCM-based persistent data structures in combination with an adequate concurrency scheme (e.g., Multi-Version Concurrency Control) allows for completely replacing the traditional logging infrastructure by fine-grained, cheap micro-logging at data-structure level. Third, it can be dynamically decided where to store certain database objects as long as their loss can be tolerated, e.g., index structures may be stored in DRAM and reconstructed during recovery, potentially based on recent workload patterns. Fourth, system runtime information can easily be stored in SCM to improve recovery time. Finally, the system may retain and continue running transactions in case of system failures. For large main-memory database systems running in business-critical environments (e.g., e-commerce), this is a major advancement compared to traditional log-based systems.

While SCM brings unprecedented opportunities as a potential universal memory, it fulfills the *no free lunch* folklore conjecture and raises unprecedented challenges as well. To store data, software has traditionally assumed block-addressable devices, managed by a file system and accessed through main memory. The programmer holds full control over when data is persisted and the file system takes care of handling partial writes, leakage problems, and storage fragmentation. As a consequence, database developers are used to ordering operations at the logical level, e.g., writing an undo log before updating the database. SCM invalidates these assumptions: It becomes possible to access, read, modify, and persist data in SCM using load and store instructions at a CPU cache line granularity. The journey from CPU registers to SCM is long and mostly volatile, including store buffers and CPU caches, leaving the programmer with little control over when data is persisted. Even worse, compilers and CPUs might speculatively reorder writes. Therefore, there is a need to enforce the order and durability of SCM writes at the system level (in contrast to the logical level) using persistence primitives, such as memory barriers and cache line flushing instructions, often in a synchronous way. This in turn creates new failure scenarios, such as missing or misplaced persistence primitives, which can lead to data corruption in case of software or power failure. As a consequence, leveraging SCM as persistent main memory requires devising a novel programming model.

Given the absence of a standard SCM programming model, SCM memory management, and SCM-based data structures, it is unclear how to achieve our envisioned architecture. Therefore, we set forth two main goals for this dissertation: (1) devising fundamental building blocks that can be used to build SCM-based database systems, and (2) using these building blocks to demonstrate how to achieve our envisioned database architecture. For the latter part, we target HTAP capabilities. Hence, we opt for a columnar data representation, as it is easier to tame a column-store for OLTP than to tame a row-store for OLAP (see Section 2.4.5 for a more detailed discussion). In fine, the work presented in this dissertation can be regarded as a pathfinding effort, or as technology scouting, for future SCM-based database systems.

Dissertation Outline and Contributions

Our extensive pathfinding work on SCM led us to devise several building blocks that are necessary for enabling our envisioned single-level architecture [127]. In the following we give an overview of our contributions:

- **SCM Programming Model [124].** Exploring the implications of leveraging SCM as persistent main memory led us to identify several programming challenges. Examples of these challenges are data consistency, data recovery, persistent memory leaks, and partial writes. To address them, we survey state-of-the-art SCM programming models and make the case for the most suitable techniques for database systems. We assemble these techniques into a sound SCM programming model that forms the foundation of the work presented in this dissertation.

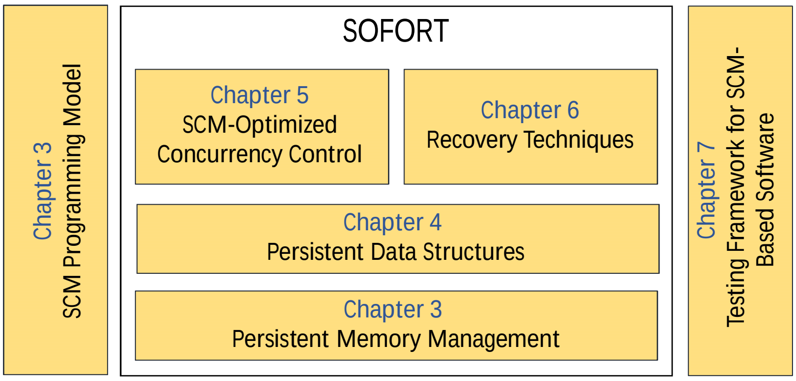
Chapter 3
SCM Programming Model
SOFORT
Chapter 5
SCM-Optimized Concurrency Control
Chapter 6
Recovery Techniques
Chapter 4
Persistent Data Structures
Chapter 3
Persistent Memory Management
Chapter 7
Testing Framework for SCM-Based Software

Figure 1.4: Organization of our contributions across the dissertation.

- **Persistent Memory Management [124].** Memory management is the first building block needed to build a database system. We survey state-of-the-art transient memory and SCM allocators and make the observation that they are designed for general-purpose applications. However, database systems have all but general-purpose needs. We identify the unique needs of database systems and use them as guidelines to design a highly scalable SCM allocator, named PAllocator.
- **Persistent Data Structures [126].** With SCM memory management, it becomes possible to build SCM-based data structures. While surveying state-of-the-art SCM-based data structures, we noticed that they are significantly slower than their DRAM-based counterparts because of the higher latency of SCM. To close this performance gap, we propose the FPTree, a highly scalable hybrid SCM-DRAM B^+-Tree that places its inner nodes in DRAM and its leaf nodes in SCM. Upon recovery, inner nodes are rebuilt from leaf nodes. Furthermore, the FPTree implements a novel concurrency scheme that uses Hardware Transactional Memory (HTM) for the concurrency of inner nodes and fine-grained locking for that of leaf nodes.
- **SOFORT [122, 128].** Equipped with efficient SCM memory management and SCM-based data structures, we realize our envisioned database architecture in SOFORT[2], a hybrid SCM-DRAM columnar transactional engine. SOFORT is a single-level store, i.e., the working copy is the same as the durable copy of the data. We propose an adaptation of MVCC to SCM in a way that eliminates traditional write-ahead logging from the critical path of transactions. SOFORT allows placing secondary data either in SCM or in DRAM. Since SCM-based data is near-instantly available upon recovery, the new recovery bottleneck is rebuilding DRAM-based data.
- **Recovery Techniques [129].** To tackle the new recovery bottleneck, namely rebuilding DRAM-based data, we propose two recovery techniques: instant recovery and adaptive recovery. Instant recovery allows SOFORT to provide instant-responsiveness by accepting queries right after recovering SCM-based data, while DRAM-based data is rebuilt in the background. Adaptive recovery improves upon instant recovery by ordering the rebuild of DRAM-based data structures according to their importance to the currently running workload.
- **Testing Framework for SCM-Based Software [123].** SCM brings new failure scenarios that existing testing tools cannot detect. To tackle this issue, we propose an online testing framework that is able to automatically simulate power failures and detect missing or misplaced persistence primitives. Furthermore, our testing framework uses a set of optimizations, such as limiting duplicate testing by leveraging call stack information, to achieve fast crash simulation.

Figure 1.4 illustrates the organization of these contributions across the chapters of this dissertation. We motivate each contribution in detail at the beginning of its corresponding chapter. Furthermore, each chapter is concluded with a summary of its main insights. Moreover, we show the advantages of each of our devised building block through a thorough qualitative as well as experimental comparison

---

[2] "*sofort*" is a German word that means "instantly".

with state-of-the-art competitors. In brief, our proposed building blocks can be used to build more complex systems, such as SOFORT, thereby paving the way for future database systems on SCM.

This dissertation is organized as follows: In Chapter 2 we elaborate on the characteristics of SCM, how to emulate it, and the performance implications of its higher latency. Then, we survey state-of-the-art database research on SCM [125]. We conclude Chapter 2 by giving an overview of SOFORT and its different components, while contrasting its design decisions with those of state of the art. Thereafter, Chapter 3 details the programming challenges of SCM and explores how to solve them. Then, we detail our SCM programming model and devise PAllocator, our highly scalable persistent memory allocator. Next, in Chapter 4 we survey existing SCM-based data structures. Then, we present the FPTree, our hybrid SCM-DRAM B^+-Tree. Afterwards, Chapter 5 demonstrates how we assemble our devised building blocks to build SOFORT. In particular, we elaborate on how we adapt MVCC to SCM. Furthermore, Chapter 6 presents SOFORT's recovery techniques, namely instant recovery and adaptive recovery. Later, we showcase in Chapter 7 our online testing framework for SCM-based software. Finally, Chapter 8 summarizes the contributions of this dissertation and presents an extended view on promising future work directions. In particular, we present our vision on how to extend our work to account for hardware and media failures to achieve high availability by leveraging SCM and Remote Direct Memory Access (RDMA).

2

LEVERAGING SCM IN DATABASE SYSTEMS

SCM is emerging as a viable alternative to lift DRAM's capacity limits. Since it exhibits characteristics of both storage and main memory, SCM can be architected in different ways: as main memory extension, as disk-replacement, or as persistent main memory, i.e., as main memory and storage at the same time. These unique properties enable several optimizations and architectural enhancements for database systems. In this chapter we position our work with regards to state-of-the-art research on leveraging SCM in database systems. To do so, we first survey database optimization opportunities enabled by SCM that were explored in the literature, starting from the most straightforward ones to completely revising database architectures. Then, we highlight the gaps in state-of-the-art that our work ambitions to fill. We show that placing all data in SCM compromises performance, and argue instead for a hybrid SCM-DRAM architecture. While related works have mostly focused on transactional row-store systems, we target hybrid analytical and transactional (HTAP) systems. In this context, we propose *SOFORT*, a hybrid SCM-DRAM single-level columnar storage engine, designed from the ground up to explore the full potential of SCM.

This chapter is organized as follows: In Section 2.1 we present SCM, discussing how it can be integrated in the memory hierarchy, and exploring its performance implications with microbenchmarks. Since SCM is not available yet, we elaborate in Section 2.2 on practical ways to emulate its performance characteristics. Thereafter, Section 2.3 surveys state-of-the-art research on the use of SCM in database systems, with an emphasis on works that enhance database logging and storage architectures. Then, Section 2.4 positions our work with regards to related work and gives an overview of SOFORT. Finally, Section 2.5 summarizes this chapter.

2.1 STORAGE-CLASS MEMORY

Leon Chua predicted in the early 1970s the existence of the *memristor* [23], a fundamental circuit element that is capable of storing and retaining a state variable. It the late 2000s, a team at HP Labs discovered the memristor in the form of Resistive RAM (RRAM) [50] [153]. It turned out that several works had already stumbled upon the memristor property, but they could not identify it as such and deemed it an anomaly. Since then, several other memory technology candidates that exhibit the memristor property have been identified, e.g., Phase Change Memory (PCM) [87] and Spin Transfer Torque Magnetic RAM (STT-MRAM) [59]. In the industry, these novel memory technologies are

Parameter	NAND	DRAM	PCM	STT-RAM
Read Latency	25 µs	50 ns	50 ns	10 ns
Write Latency	500 µs	50 ns	500 ns	50 ns
Byte-addressable	No	Yes	Yes	Yes
Endurance	10^4–10^5	$>10^{15}$	10^8–10^9	$>10^{15}$

Table 2.1: Comparison of current memory technologies with SCM candidates [107].

grouped under the umbrella term *Storage-Class Memory* (SCM). SCM promises to combine the low latency and byte-addressability of DRAM, with the density, non-volatility, and economic characteristics of traditional storage media. Most SCM technologies exhibit asymmetric latencies, with writes being noticeably slower than reads. Table 2.1 summarizes current characteristics of two SCM candidates, PCM and STT-MRAM, and compares them with current memory technologies. Like flash memory, SCM supports a limited number of writes; yet, from a material perspective, some SCM candidates promise to be as enduring as DRAM. These candidates also promise to feature even lower latencies than DRAM. However, while its manufacturing technology matures, we expect the first few generations of SCM to exhibit higher latencies than DRAM, especially for writes. Given its non-volatility, idle SCM memory cells do not consume energy, contrary to DRAM cells that constantly consume energy to refresh their state. Consequently, SCM has the potential to drastically reduce energy consumption, although except for embedded systems, this potential has yet to be shown. Given SCM's byte-addressability and low latency, data in SCM can be accessed via load and store semantics through the CPU caches without buffering it in DRAM.

In this work, we assume that the issue of SCM's limited write endurance will be addressed at the hardware level. In fact, works like [138, 98] already proposed wear-leveling techniques at the hardware level to increase the lifetime of SCM.

The advent of SCM seems to be imminent. Intel and Micron demonstrated large capacity DIMMS of a new byte-addressable non-volatile memory technology called 3DXPoint [1]. Furthermore, there has been recently a breakthrough in the industry efforts to standardize different Non-Volatile DIMMs (NVDIMMs) form factors [71]. Microsoft Server [162] and Linux [97] have both announced support for NVDIMMs. In the following section, we discuss different alternatives on how SCM can be integrated in the memory hierarchy.

2.1.1 Architecting SCM

SCM can be architected as main memory extension to alleviate DRAM's scalability limits. In this scenario, the non-volatility of SCM is not leveraged. Several works have investigated this approach. For instance, Lee et al. [86] discussed how to use Phase Change Memory as a scalable DRAM alternative. We expect this architecture option to be rapidly adopted, especially in large main-memory systems where the cost of DRAM is a major factor in the total cost of ownership (TCO). Indeed, SCM is projected to be cheaper than DRAM. We foresee that the first adopters will be cloud providers such as Google, Amazon, and Microsoft, as well as large-scale main-memory database systems such as SAP HANA.

Figure 2.1 depicts two options for architecting SCM as *transient* main memory. The first one, illustrated in Figure 2.1a, is to introduce SCM as a new memory tier on top of which DRAM serves as a hardware-managed cache (e.g., as a fully associative cache). Qureshi et al. [139] investigated this option and showed that a buffer of 1GB of DRAM can efficiently hide the higher latency of up to 32GB

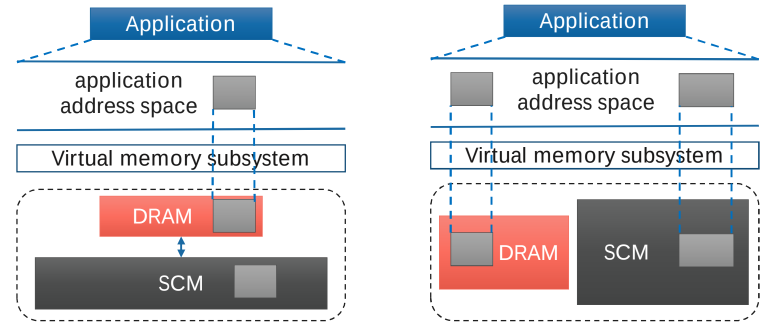

(a) DRAM as hardware-managed cache for SCM

(b) SCM next to DRAM

Figure 2.1: SCM as transient main memory extension.

of SCM. The second option, shown in Figure 2.1b is to have SCM next to DRAM, at the same hierarchical level, thereby introducing the notion of fast and slow memory and the corresponding data placement problem.

SCM can be alternatively used as persistent storage, hence leveraging its non-volatility. There are again two options, as depicted in Figure 2.2: The first one is to use SCM as a fast block device, managed by a traditional file system, and accessed through DRAM. Note that this use case does not leverage the byte-addressability of SCM. We do not foresee this architecture option to be widely adopted, as SCM is projected to be much more expensive than flash memory. The second option is to use SCM as persistent main memory, i.e., as main memory and storage at the same time, hence leveraging the full potential of SCM– we assume this architecture in this work. We elaborate in the next paragraph on how SCM is managed as persistent main memory.

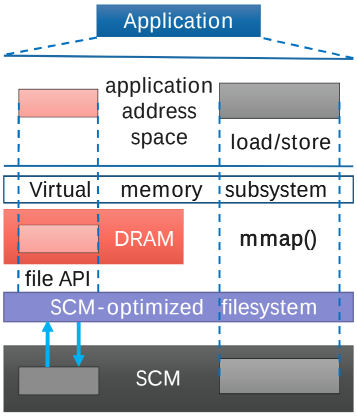

Figure 2.2: SCM as disk replacement or as persistent main memory.

There seems to be a consensus that SCM will be managed by a special file system that provides zero-copy memory mapping – as recommended by the Storage Networking Industry Association (SNIA) [150] – bypassing the operating system page cache and providing the application layer with direct access to SCM, as illustrated in Figure 2.2. Several such file systems have already been proposed, such as BPFS [26], SCMFS [175], PMFS [39], NOVA [179], and HiNFS [121]. Additionally, Linux kernels 4.7 and higher already embed such a functionality through the new Direct Access (DAX) feature [35], currently supported by the ext4 file system [42]. However, the Linux page table presents a major roadblock for the integration of SCM in large-scale systems: The Linux page table currently implements concurrency using a global lock, which makes memory reclamation upon shutdown of a multi-terabyte main memory process very slow, although SCM pages do not need to be reclaimed as they do not correspond to any DRAM memory. Worse, both DRAM and SCM page entries are scanned to reclaim the memory of the DRAM ones. For example, our measurements, depicted in Figure 2.3[1], show that it takes up to 15 minutes to reclaim 10 terabytes of main memory upon process termination. Moreover, memory mapping millions of files will stress the (lack) of scalability of the Linux page table and the file system indexing [29], significantly slowing down startup time of large-scale main memory systems. Most of these issues can addressed by using SCM-aware file systems – instead of building sub-optimal SCM support on top of existing ones – and by making the virtual memory component of operating systems SCM-aware.

---

[1] Figure 2.3 is courtesy of Robert Kettler and Daniel Booss.

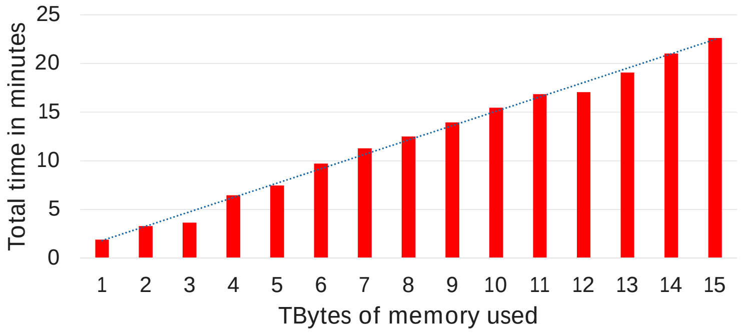

Figure 2.3: Measuring process termination duration. Experiment: memory map memory, touch it, then kill the process and measure termination duration. The experimental system has 32 E7-8890 v3 processors (1152 cores total) and 16 terabytes of DRAM.

2.1.2 SCM Performance Implications

To understand the performance implications of a hybrid SCM-DRAM hardware architecture, we designed three microbenchmarks:

Synthetic read. We evaluate the performance of pure sequential and random reads in DRAM and in SCM. The size of the dataset is 1 GB. Pure sequential read is implemented as a cache ping, i.e., one byte is read from every cache-line-sized piece of the dataset, making the whole dataset go through L1 cache. As for pure random read, one byte from the dataset is randomly read – which counts as a full cache line read – until the amount of read data is equal to the size of the dataset.

SIMD-Scan. As a real-world example of sequential reads, we evaluate the *SIMD Range Scan* [173], an OLAP scan operator over bit-packed integers usually representing dictionary-coded values in a columnar representation, in SCM and in DRAM. In this experiment, each integer value is represented with 11 bits, and the size of the dataset is set to 200 million values, i.e., 262 MB.

B^+-Tree and Skip List. As a real-world example of random reads, we evaluate the read and write performance of a B^+-Tree and a Skip List in DRAM and in SCM. In each experiment, we first populate the tested structure with 10 million tuples, then, we execute 5 million either read or write operations. Each tuple is a pair of 8-Byte integers.

In all experiments, we use the Intel SCM Emulation Platform, described in Section 2.2.3, to vary the latency of SCM from 90 ns (i.e., the latency of DRAM) up to 700 ns. Figure 2.4 depicts the experimental results. The y-axis represents the slowdown incurred by using SCM over DRAM. For an SCM latency of 200 ns, we notice that the slowdown for pure sequential read and SIMD-Scan is only 1.05× and 1.04× respectively, while for an SCM latency of 700 ns the slowdown increases but is limited to 1.81× and 1.65×, respectively. This is explained by hardware and OS-level prefetching that hide the higher latency of SCM when detecting a sequential memory access pattern. Additionally, we partially attribute the slowdown surge to the hardware prefetcher that fails to prefetch data at the right time. Indeed, the prefetcher has to prefetch data *timely*; if the data is prefetched too early, then it might be evicted from the cache before it is used by the CPU; if the data is prefetched too late, then prefetching will not hide the whole memory latency. Since the hardware prefetcher is calibrated for DRAM's latency, it prefetches data too late when SCM's latency is too high. Hence, the prefetcher becomes unable to hide the whole memory latency. This is a limitation of the emulator and can be fixed in real hardware by calibrating the hardware prefetcher for SCM's latency. We conclude that workloads with sequential memory access patterns hardly suffer from the higher latency of SCM.

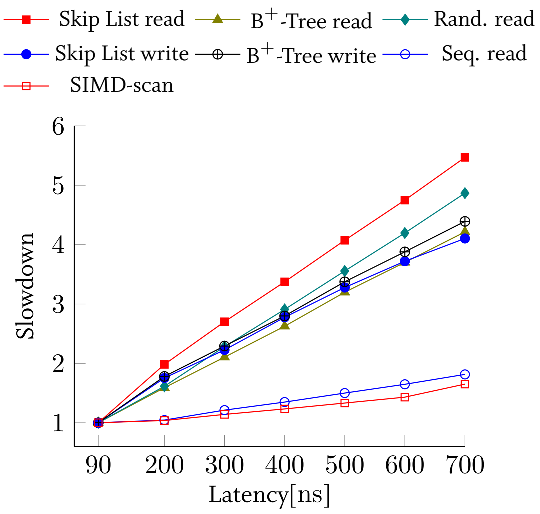

Figure 2.4: Slowdown incurred by using SCM over DRAM in different microbenchmarks.

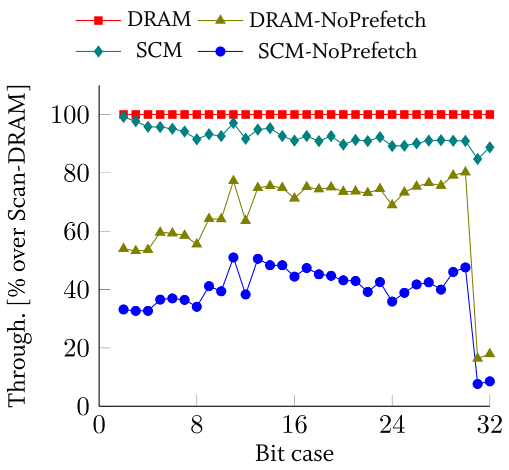

Figure 2.5: SIMD Scan performance on SCM relative to DRAM with and without hardware and software prefetching.

To validate our analysis, we fix the latency of SCM to 200 ns and ran again the SIMD-Scan experiment for different bit-cases, with and without hardware and software prefetching. Figure 2.5 shows that the average performance penalty for the different bit cases is 8% compared with using DRAM. With hardware and software prefetching disabled for both SCM and DRAM [36], we observe that the average performance penalty of using SCM rises to 41% compared with using DRAM. If we compare similar memory technologies, disabling prefetching incurs a slowdown of 34% for DRAM and 56% for SCM.

On the side of random memory accesses, Figure 2.4 shows that the performance of pure random read, Skip List read/write, and B$^+$-Tree read/write quickly and linearly deteriorates as we increase the latency of SCM: For an SCM latency of 200 ns, the slowdown is already $1.61\times$, $1.98\times/1.75\times$, and $1.59\times/1.78\times$, respectively, and increases for an SCM latency of 700 ns up to $4.86\times$, $5.47\times/4.10\times$, and $4.21\times/4.40\times$, respectively. This is explained by the fact that Skip Lists and B$^+$-Trees have a random access pattern that triggers several cache misses per read/write, amplifying the overhead of the higher access latency of SCM. We conclude that workloads with random access patterns significantly suffer from the higher latency of SCM.

This result motivates the need to keep DRAM to enable faster query execution, as keeping latency-sensitive data structures in SCM leads to a significant performance penalty.

2.2 SCM EMULATION TECHNIQUES

Researchers are often reluctant to dive into systems research on SCM due to the lack of real hardware. To a certain extent, their concerns are justified as several SCM performance characteristics and their interplay with modern CPU architectures are yet to be seen. One solution would be to use cycle-accurate simulators, such as PTLSim [183], a cycle-accurate out-of-order x86-64 simulator. However, these solutions are not attractive to systems developers because: (1) they are slow; (2) their simulated architecture does not reflect the latest CPUs, thereby limiting their accuracy; and (3) they often require extensions to account for non-supported instructions. Nevertheless, if we assume the DIMM form factor and an access interface similar to that of DRAM, we can reliably emulate SCM latency and bandwidth in different ways, which we detail in the following.

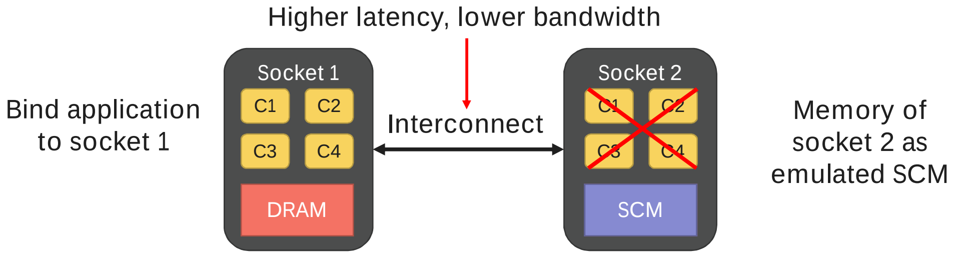
Higher latency, lower bandwidth
Bind application to socket 1
Socket 1
C1
C2
C3
C4
DRAM
Interconnect
Socket 2
C1
C2
C3
C4
SCM
Memory of socket 2 as emulated SCM

Figure 2.6: NUMA-based SCM emulation on a two-socket system.

2.2.1 NUMA-Based SCM Emulation

Non-Uniform Memory Access (NUMA) can be used to emulate a higher latency and a lower bandwidth. This can be achieved, as illustrated in Figure 2.6, by binding a program to the memory and computing resources of a socket (processor), and using the memory of another socket as emulated SCM, which will have the latency and throughput characteristics of remote memory accesses through socket interconnect links. While Figure 2.6 depicts a two-socket system, where only a single emulated latency and bandwidth configuration is possible, larger systems such as 4 or 8-socket systems can offer additional emulation configurations. In fact, the number of interconnect hops determines the latency and bandwidth metrics. Furthermore, some interconnect links can be switched off in the BIOS to force additional interconnect hops between two sockets. This is useful, for instance, when the sockets of a system are fully connected with each other.

The main advantage of NUMA-based SCM emulation is that it does not affect the micro-architectural behavior of the CPU such as speculative execution, memory parallelism, and prefetching, thereby ensuring a reliable and accurate performance evaluation of programs that use SCM. Additionally, as we explain below, it requires little effort. However, it offers limited latency and bandwidth settings and delivers a symmetric (instead of the expected asymmetric) SCM latency.

Binding a program to a socket can be done on Linux using *libnuma* or simply using the *numactl* command [115], among other widely available and simple-to-use possibilities. Using the memory of a socket as emulated SCM can be done in two ways. The first one is to mount a temporary file system, i.e., *tmpfs* [158], on the memory of a specific socket, and use the resulting device as emulated SCM. This can be done in two steps:

1. create a *tmpfs* device with, e.g., 1 GB size in */mnt/pmem*:
   ```
   mount -t tmpfs -o size=1G tmpfs /mnt/pmem
   ```
2. remount the device to bind its memory to a specific socket (e.g., socket 1):
   ```
   mount -o remount,mpol=bind:1 /mnt/pmem
   ```

A drawback of this approach is that the operating system still manages the memory and allocates it to the device when needed at a page granularity.

The second way to use the memory of a socket as emulated SCM is to reserve a DRAM region upon boot time and mount an SCM-aware file system on it (e.g., ext4 DAX) [60]. This memory region will be invisible to the operating system and will be treated as an SCM device, which contrasts with the *tmpfs* approach where the operating system still manages the memory. This approach be carried in three steps:

- reserve a DRAM region using the *memmap* kernel boot parameter. For example, to reserve 32 GB starting from physical address 64 GB, the parameter is:

  ```
  memmap=32G!64G
  ```

- format the resulting SCM device to a file system format that supports DAX, e.g., ext4:

  ```
  mkfs.ext4 /dev/pmem0
  ```

- mount the device with the DAX option:

  ```
  mount -o dax /dev/pmem0 /mnt/pmem
  ```

In summary, NUMA-based SCM emulation is easy to use and requires little effort.

2.2.2 Quartz

Quartz [167] is a DRAM-based, software-based SCM performance emulator that leverages existing hardware features to emulate different latency and bandwidth characteristics. Instead of injecting delays to every single SCM access, which the authors argue is infeasible in software without a significant overhead, Quartz models the average application perceived latency by injecting delays at boundaries of *epochs*. An *epoch* has a fixed time duration upon which hardware performance counters are read. A delay is then introduced based on the number of stalled cycles induced by references to SCM. The delay is computed as follows:

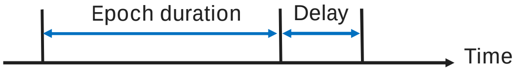

Delay = (Stalled cycles / Average latency) X latency differential

Hence, Quartz can vary the emulated latency of SCM by changing the latency differential between DRAM and SCM in the formula above. The authors evaluated the emulation accuracy of Quartz by comparing it with NUMA-based emulation and reported an error rate no higher than 9%. Quartz can emulate either a system with only SCM, or a system with fast memory (DRAM) and slow memory (SCM). The latter is achieved by combining Quartz with NUMA-based emulation; Quartz would add delays that correspond to only remote memory accesses, which can be quantified by means of hardware performance counters.

Quartz consists of two parts: a user-mode dynamic library that manages *epochs*, and a kernel module that manages performance counters. Using Quartz is as easy as pre-loading the user-mode, which will register the threads of the program and manage delay injection. To sum up, Quartz has the advantage of relying counters available in commodity hardware and offering a wide range of latency and bandwidth setting. However, it might interfere with the micro-architectural behavior of the processor, emulates a symmetric SCM latency, and is less accurate than NUMA-based emulation. HP has recently open-sourced Quartz [136], enabling its adoption by some works [90].

2.2.3 Intel SCM Emulation Platform

Intel has made available an SCM emulation platform [38] to several academic and industry partners, and many publications have already used it [39, 122, 6]. It is equipped with four Intel Xeon E5

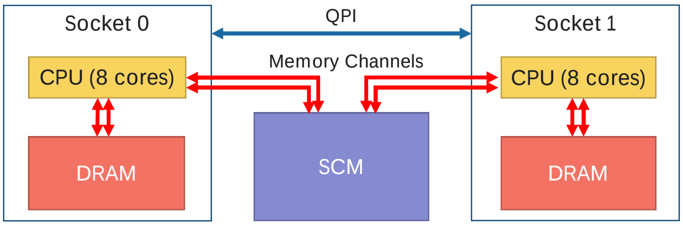

Figure 2.7: Architecture overview of Intel's SCM emulation platform.

processors, two of which are deactivated and their memory is interleaved at a cache line granularity to form an emulated SCM region. Each processor has 8 cores, running at 2.6GHz and featuring each 32 KB L1 data and 32 KB L1 instruction cache as well as 256 KB L2 cache. The 8 cores of one processor share a 20 MB last level cache. The two active processors have four DDR3 memory channels each, two of which are attached to local memory, and the other two are attached to the emulated SCM region, as illustrated in Figure 2.7. This contrasts with NUMA-based emulation and Quartz which rely on remote memory accesses via socket interconnect links. The emulated SCM region is managed by an SCM-aware file system, such as PMFS [39] or ext4 with DAX support [42, 35], that provides direct access to the memory region with *mmap*.

Similarly to Quartz, the memory bandwidth of emulated SCM can be changed utilizing the DRAM thermal control [58]. To emulate different latencies, the system relies on a special BIOS and microcode which introduces delays upon accesses to the emulated SCM region. More precisely, the emulator relies on the fact that the number of cycles stalled for Last Level Cache (LLC) misses is proportional to memory latency. The emulator injects additional stall cycles using debug hooks and special microcode every 32 LLC miss – smaller windows lead to better emulation but incur tangible emulation overhead. The number of additional injected stall cycles is computed as follows:

$$Count_{added\ stalls} = Count_{stalled} \times \frac{Latency_{scm}}{Latency_{dram}}$$

where $Count_{stalled}$ is provided by hardware counters and represents the number of stalled cycles due to LLC misses during a window. This is more accurate, yet more complex to implement, than the software-based average latency approach of Quartz.

In brief, the advantage of Intel's SCM emulation platform is that it is a hardware-based emulation, yet it enables a wide range of bandwidth and latency settings. Moreover, tampering with the CPU's micro-architectural behavior is limited since delays are introduced at a much narrower window granularity and independent of software logic. However, in addition to emulating symmetric SCM latencies, it has the drawback of not being widely available: (1) it is a special piece of hardware; (2) there exist only a few such systems; and (3) access to such a system can be granted only through Intel. In our work, Intel provided us with access to such a system which we used in our experiments.

2.3 SCM AND DATABASES: STATE-OF-THE-ART

SCM impacts all layers of database systems. First and foremost, the storage and recovery layer, which is the focus of this dissertation, can be completely re-architected. We present in Section 2.3.1 several works that leveraged this opportunity. The most advanced SCM-based architectures require novel data structures, which in turn require SCM allocation schemes. We elaborate on both topics in Chapters 3 and 4, respectively. Moreover, the asymmetry in SCM read/write latency and bandwidth calls for revising the cost models of query optimizers and the trade-offs of query execution operators. We present in Section 2.3.2 relevant works that investigated this challenge.

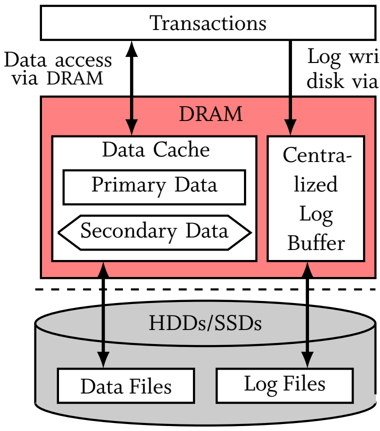

Figure 2.8: Traditional database architecture.

2.3.1 Storage and Recovery

In this section we discuss optimization opportunities brought by SCM to database storage and recovery architecture. We classify related work into two categories: (1) works that focus solely on improving the logging infrastructure using SCM; and (2) works that go further and propose to re-architect database storage and logging using SCM.

Traditional database architecture

In the traditional disk-based database architecture, shown in Figure 2.8, the data cache and log buffer are associated with storage devices for durability. All database objects in the data cache reflect a (potentially modified) copy of the database state. Runtime information is stored in main memory and re-built during system startup. The border line between transient memory and persistent storage is explicit and the database system manages cross-border traffic using an eviction policy, a log buffer, etc. The last decade has seen the emergence of main-memory database systems which assume that the whole database fits in main memory, enabling them to simplify away the data cache. Nevertheless, they still require a log buffer.

To ensure transaction durability, both disk-based and main-memory database systems rely on Write-Ahead Logging (WAL) [56] on traditional storage media (HDDs, SSDs), which constitutes a bottleneck for transactional workloads. To mitigate this bottleneck, database systems usually implement group commit [34]: log durability is enforced per batch of transactions to amortize disk access cost. Furthermore, WAL entries are usually coalesced in the log buffer to transform multiple random writes into amortized sequential disk writes [109]. This is achieved by keeping a centralized log buffer and employing page latches, which constitute a contention point for high-performance transactional systems. Recovery is performed by replaying the log starting from the latest consistent durable database state (redo phase), then undoing the effects of in-flight transactions at failure time (undo phase). To shorten the redo phase, database systems employ checkpointing, which consists in periodically taking snapshots database state.

Improving the logging infrastructure using SCM

SCM-based database systems have been investigated as early as in the 1980s. For instance, Copeland et al. [27] made the observation that a system with battery-backed DRAM – an economically viable technology at the time – would allow to remove disk I/O from the critical path of transactions, thereby alleviating the need for group commit [34] and reducing transaction latencies. Agrawal et al. [2] investigated database recovery algorithms assuming a back-then hypothetical non-volatile main-memory system. While using two-phase locking for concurrency control, they devised optimized recovery algorithms for both page locking and record locking schemes. While these works only look at how to optimize existing logging and recovery algorithms in presence of non-volatile main memory in a non-disruptive way, Copeland et al. [27] recognize the possibility of devising novel counterparts.

The advent of SCM has spurred a renewed interest in non-volatile main memory database systems. Fang et al. [43] were the first to introduce SCM in the database architecture. They propose to place the database log, access it, and update it directly in SCM, which simplifies the log architecture since the log buffer is not required anymore. The log can be asynchronously written to disk for archival purposes. This architecture has two advantages: (1) As Copeland et al. [27] previously observed, group commit is not needed anymore, because SCM is several orders of magnitude faster than disks; and (2) transaction logs are traditionally grouped in contiguous pages to amortize disk access, which necessitates the use of page latches; being a random-access, byte-addressable memory, SCM alleviates this constraint, making log page latches unnecessary. These two advantages result in lower transaction latencies and higher transaction throughput.

Gao et al. [46] propose to use SCM as a new, persistent buffering layer between main memory and disks. They introduce PCMLogging, a new logging scheme that integrates implicit logs into modified pages. PCMLogging flushes the modified pages of a transaction from main memory to SCM upon commit, which ensures that the database state is always up-to-date. Therefore, checkpointing is not required anymore. However, undoing the effects of unfinished transactions during recovery is still needed. Indeed, a full main memory cache might need to flush modified pages to SCM. To handle this case, PCMLogging keeps in SCM a list of all running transactions and their respective modified pages that were flushed to SCM. To provide undo capabilities, PCMLogging writes flushed pages out-of-place in SCM. Recovery is performed by scanning the pages in SCM, retrieving their transaction ID, and rolling back the ones modified by in-flight transaction at failure time. We argue that, contrary to Fang et al. [43], PCMLogging introduces additional complexity in durability management and does not leverage the byte-addressability of SCM. Additionally, the authors compare PCMLogging only to a traditional database architecture with emulated PCM as main memory, which does not allow to draw compelling conclusions.

Wang et al. [170] make the observation that while distributed logging has been historically a no-go for single node systems because of I/O overheads, the characteristics of SCM make it relevant for multi-socket systems. Hence, they propose a distributed logging scheme that maintains one SCM log buffer per socket, thereby relieving log contention. A log object is considered durable as soon as it is written to the SCM log buffer. When the latter becomes full, it is flushed to disk. The authors investigate two flavors of distributed logging: page-level and transaction-level log space partitioning. In page-level log space partitioning, a transaction can write log records to any log partition, which might incur expensive remote memory accesses. Additionally, transactions lose access to the previous Log Sequence Number (LSN) of each log record, because LSNs are bound to a single log partition. This compromises the ability of a transaction to undo its changes when it aborts. To remedy this problem, the authors propose to keep a private DRAM undo buffer per transaction. In transaction-level log space partitioning, transactions write log records only to their local log partition. This poses an issue during recovery as the order of log records per page is lost, thereby compromising the redo and undo phases. To solve this issue, the authors propose to uniquely identify log records using *global* *sequence numbers* (GSNs) based on a logical clock [82] for each page, transaction, and log record. The order of log records can therefore be established during the log analysis phase of recovery.

SCM log buffers are marked as write-combining, meaning that read and write operations to SCM bypass the CPU cache. Writes are lazily drained from the write-combining buffers to SCM. Therefore, it is necessary to employ memory fences which (among other things) drain the contents of the write-combining buffers. Nevertheless, a memory fence drains the buffers of only its local core, which poses a challenge for transaction commit. Indeed, before committing, a transaction must ensure the persistence of all its log records, in addition to all log records that logically precede them. To solve this problem, the authors introduce *passive group commit*. The general idea is as follows: (1) every committing transaction issues a memory fence and updates a variable (*dgsn*) in its working thread to its GSN; (2) committing transactions are registered into a group commit queue; and (3) a daemon fetches the smallest *dgsn* across working threads (i.e., the upper bound GSN of persisted log records) and dequeues any transaction that has a GSN smaller than this minimum. Following an empirical evaluation, the authors conclude that transaction-level log space partitioning is more promising that the page-level counterpart.

Huang et al. [62] focus on the most cost-effective use of SCM. Since SCM will be more expensive than disks, they propose to restrict the use of SCM to the database log, which is the main bottleneck for OLTP systems. Doing so shifts the logging bottleneck from I/O to software overheads, mainly incurred by contention on the centralized log buffer. Therefore, the authors propose *NV-logging*, a per-transaction decentralized logging scheme. Basically, transactions keep private logs in the form of a linked-list of transaction objects. Log objects are first constructed in DRAM, then flushed to a global circular log index, which is truncated upon checkpointing. A global counter is used to generate LSNs. The internal structure of log objects is similar to that of ARIES [109], except that NV-logging keeps a backward pointer instead of keeping the LSN of the previous log object. The recovery procedure follows the ARIES protocol. While the authors claim that NV-logging is the most *cost-effective* use of SCM in OLTP systems, it misses out on the opportunity of introducing SCM in the main-memory layer, SCM being projected to be cheaper than DRAM.

Re-architecting database storage and logging using SCM

While the logging component might be a target of choice for SCM in the short term, SCM can spur a more radical change in database architecture. For instance, Pelley et al. [133] investigated three architecture alternatives for SCM in database systems. The first one is to use SCM as a drop-in disk replacement, which enables near-instantaneous recovery since dirty pages can be flushed at a high rate, significantly reducing the redo phase during recovery. However, this architecture retains all the software complexity introduced to amortize costly disk I/O. The second architecture option, denoted In-Place Updates and illustrated in Figure 2.9a, assumes that SCM reads are optionally performed through a software-managed DRAM cache, while writes are performed directly to SCM. The centralized log that keeps a total order of updates is not needed anymore: Undo logs are distributed per transaction (i.e., each transaction keeps a private log), which is possible since in-flight transactions modify mutually exclusive sets of pages. In-Place Updates completely removes redo logging and page flushing, but it is highly sensitive to the latency of SCM writes.

To lift this shortcoming, the authors introduced a third architecture option, named NVRAM group commit. It executes transactions in batches, which are then either all committed or aborted. The changes of a transaction batch are buffered in a DRAM staging buffer and flushed to SCM upon commit, as depicted in Figure 2.9b. Aborting batches can undo their changes in the staging buffer by leveraging the transactions' private undo logs. Note that, in contrast to in-place updates, these logs are

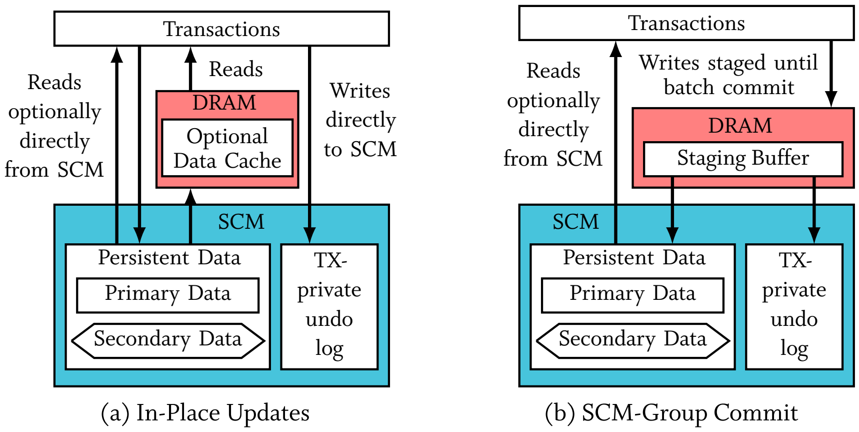

(a) In-Place Updates (b) SCM-Group Commit

Figure 2.9: Database architecture with SCM as a primary data store.

not persisted. For failure recovery, NVRAM Group Commit relies on a database-wide undo log. When the staging buffer is not large enough, or in presence of long-running transaction, NVRAM Group Commit falls back to traditional, ARIES-style logging. The authors assume a *persist* barrier primitive that ensures the durability of all pending SCM writes. They show that In-Place Updates, respectively NVRAM Group Commit, exhibits the highest transaction throughput when the latency of the persist barrier is lower, respectively greater, than 1 µs. Nevertheless, we argue that both suffer from the fact that updates are still done at a page granularity, which does not leverage SCM's byte-addressability.

Debradant et al. [31] showed that, when SCM is used as disk-replacement, the OLTP performances of disk-based and main-memory databases converge (in the absence of skew) and become bound by the logging overhead, suggesting that neither architecture is suitable for SCM. This result motivated Arulraj et al. [5] to conduct an empirical study of three storage architectures, namely namely In-Place Update (InP), Copy-on-Write (CoW), and Log-Structured Updates (Log), and their enhanced SCM counterparts. The authors assume an SCM-only system. The InP architecture is based on the VoltDB [169] main-memory database system. It keeps checkpoints on disk and uses the STX B^+-Tree library for all its in-memory indexes. To ensure durability, InP employs WAL to record transaction changes between two checkpoints. Recovery consists in loading the latest checkpoint, replaying the log, then undoing the changes of in-flight transactions. The SCM-enhanced version of InP, denoted NVM-InP, uses persistent versions of the STX B^+-Trees. It alleviates the need for checkpointing and the redo phase during recovery, since all committed transactions are guaranteed to have persisted their changes. WAL is still needed to undo the effects of in-flight transactions. However, instead of copying the previous state of a record, NVM-InP simply stores a non-volatile pointer in the log, thereby reducing data duplication.

The CoW architecture is based on LMDB's CoW B^+-Tree [22]. The SCM-optimized counterpart, namely NVM-CoW, modifies LMDB's CoW B^+-Tree to leverage the byte-addressability of SCM. For instance, only the nodes involved in an update are copied instead of the whole B^+-Tree, thereby reducing the storage footprint. Recovery in both variants does not involve any operation since the system is always guaranteed to be in a consistent state.

The Log architecture employs LevelDB's Log-Structured Merge Tree (LSM) [48]. The LSM tree keeps a *memtable* (B^+-Tree) in DRAM and ensures its durability using WAL. When a *memtable* reaches a certain size, it is compacted into a Sorted String Table (SST) and spilled to persistent storage. The WAL log is then truncated and a new *memtable* is created. The LSM tree can have multiple layers of SSTs. A background process merges SSTs together to reclaim space and limit read amplification. The

SCM version of Log, namely NVM-Log, implements the *memtable* as a non-volatile B$^+$-Tree. NVM-Log keeps the same structure of the LSM Tree, except that instead of compacting *memtables* into SSTs, it keeps their structure intact and simply marks them as immutable. For recovery, WAL is not needed anymore for the redo phase, but similarly to NVM-InP, it is still needed for the undo phase.

Following an extensive empirical evaluation, the authors observe that in OLTP scenarios, the NVM-InP architecture performs the best out of the three evaluated architectures. However, this architecture is still tied to WAL, which we argue can be completely removed. Moreover, they conclude that SCM latency is the most significant factor in the performance of these SCM-enabled systems, which motivates the need to keep DRAM for latency-sensitive data structures, as already stated in Section 2.1.2.

To *hide* WAL from the critical path of transactions, Arulraj et al. [6] propose Write-Behind Logging (WBL). The authors assumes a two-tier memory architecture encompassing DRAM and SCM, and multi-version concurrency control [84]. WBL flushes transaction updates to SCM before writing the corresponding log entry. This enables it to store only the location of modified tuples instead of their before-images. While the redo phase during recovery is not needed anymore, the undo phase is still required. To support the latter, WBL logs two timestamps that delimit a batch of transaction: the first one corresponds to the last committed transaction in the previous batch, and the second one corresponds to the upper bound timestamp of any transaction executing in this batch. This interval is denoted a *commit timestamp gap*. Moreover, WBL logs timestamps of long running transactions that span multiple batch windows. During recovery, the log is scanned to retrieve the latest active commit timestamp gap and the timestamps of in-flight long-running transactions. Then, the database considers the tuples that fall within this gap or these timestamps as invisible. A background garbage collector cleans the tuples that correspond to the aforementioned gap and timestamps, then removes them from tuple visibility checks. While WBL dramatically reduces the size of the log and improves transaction throughput, it is still centralized and relies on group commit which compromises transaction latency.

Hideaki Kimura presented FOEDUS, a database engine designed for future many-core servers with SCM [79]. FOEDUS assumes a two-tier memory hierarchy consisting of DRAM and SCM. It is targeted for scenarios where data does not fit in main memory. This case has been traditionally addressed in main-memory database systems by keeping hot data in DRAM and cold data in storage. However, existing systems have either physical dependency (e.g., H-Store [76] with Anti-Caching [32]) or logical inequivalence (e.g., Siberia [41]) between hot and cold data. The key idea of FOEDUS is to keep logically equivalent, but physically independent volatile pages in DRAM, and snapshot pages in SCM. Logical equivalence means that if a volatile page exists, then it is guaranteed to have the latest version of the data; if it does not exist, then the snapshot page is guaranteed to have the latest version of the data. The physical independence between volatile and snapshot pages is achieved by building the snapshot pages from transaction logs instead of the volatile pages. Therefore, no synchronization between the two forms of pages is needed. A *log gleaner* process constructs snapshot pages in DRAM, then writes them sequentially to SCM, similarly to LSM Trees [119]. However, contrary to LSM Trees, FOEDUS avoids read amplification thanks to its dual page scheme. Indeed, a read operation involves only a single page. Furthermore, FOEDUS employs an enhanced optimistic concurrency control scheme based on the Masstree [101] and the Foster B-Tree [55]. Recovery consists in invoking the *log gleaner* to create updated snapshot pages based on the WAL log starting from the latest checkpoint. While FOEDUS exhibits impressive scaling, it relies on traditional logging. Additionally, it does not leverage the byte-addressability of SCM as it accesses it through file I/O.

A straightforward use case for leveraging the non-volatility of SCM is to place read-only data in it. This use case is particularly suitable for HANA, SAP's hybrid transactional and analytical main-memory database. HANA splits data in a large read-only part, compressed and read-optimized for analytical processing, and a smaller dynamic part for transaction processing that is merged periodically into the read-only part. Andrei et al. [3] showed that the read-only part can be placed in SCM at a low performance cost since it is read-optimized and cache-efficient, while the dynamic part kept in DRAM for better transactional performance. This has the additional advantage of significantly speeding up restart time since the read-only, larger part stored in SCM is immediately accessible after a restart and does not need to be loaded from storage to main memory.

Finally, Schwalb et al. [148] proposed Hyrise-NV, an SCM-enabled version of the Hyrise main-memory storage engine [57], tailored for hybrid transactional and analytical workloads. Hyrise employs the same *main/delta* approach of SAP HANA. Hyrise-NV persists all its data structures in SCM, including secondary indexes. It relies on an append-only strategy and multi-versioning to achieve consistency. Moreover, it persists metadata of currently running transactions, which enables it, in case of failure, to undo in-flight transactions without using traditional WAL. Nevertheless, similar to the NVM-InP architecture, its performance highly depends on the characteristics of SCM. Worse, assuming an SCM latency equal to that of DRAM (i.e., best-case scenario), Hyrise-NV incurs a 20% performance penalty in transactional workloads compared to the WAL-based Hyrise.

Table 2.2 summarizes the discussed approaches for re-architecting database storage and logging, including our own database prototype, named SOFORT, which we introduce in the Section 2.4. The in-place updates architecture on SCM seems to be the one that leverages SCM the best so far.

2.3.2 Query Optimization and Execution

Despite being out of the scope of this dissertation, we briefly cover, for the sake of completeness, related work on adapting query optimization and execution for SCM. On the one hand, disk-based database operators are optimized for block-based devices with a stark difference between sequential and random accesses, while SCM is byte-addressable and has a low latency. On the other hand, main-memory database operators are optimized for cache efficiency, but they assume symmetric read/write latencies, while SCM writes are slower than reads. Therefore, SCM invalidate the assumptions of both disk-based and main-memory databases, mandating to revisit their operators and cost-models in light of SCM.

A much anticipated use of SCM is as a main memory extension next to DRAM, alleviating the latter's capacity limits, but without leveraging the non-volatility of SCM. The database has to implement some logic on whether to place data in DRAM or in SCM; it is a similar problem to that of NUMA data placement, but complicated with an additional dimension. Since SCM is slower than DRAM, a straightforward idea is to place cold data (i.e., data that is seldom accessed) in SCM, and hot data (i.e., data that is frequently accessed) in DRAM for better performance. To the best of our knowledge, the problem of data placement in presence of SCM has not been investigated yet.

Chen et al. [20] revisited the design trade-offs of two core main-memory database algorithms, namely B^+-Tree indexes and hash joins, assuming a PCM-based main memory[2]. In addition to being significantly slower than reads, PCM writes consume more energy. Therefore, the authors focus on decreasing the number of PCM writes. They propose to replace the traditionally sorted B^+-Tree nodes with unsorted ones. Indeed, an insertion in a sorted node moves half of the records in average, while an insertion in an unsorted node is a simple append operation. Additionally, a bitmap can be used to track valid entries and indicate free ones that an insertion can use. On the downside, search operations have to scan the whole unsorted node, instead of a binary search in an unsorted node. Furthermore, the authors investigate hash joins for PCM. In particular, they consider the simple hash join and the

---

[2] The analysis of the authors is valid for any kind of SCM technology that exhibits asymmetric read write latencies.

Approach	Target Systems	Contributions	Advantages	Limitations
Fang et al. [43]	OLTP systems (IBM SolidDB[a])	Write the log and persist it directly in SCM	Remove log buffer, group commit, and log page latches	Assume special hardware support (persist barrier); Only the log benefits from SCM
Gao et al. [46]	OLTP systems	Use SCM as disk buffer; Write log implicitly in data pages; Flush modified pages out-of-place upon commit	Remove checkpointing and centralized log buffer; Near-instant recovery.	SCM accessed via DRAM; Rely on paging; Byte-addressability of SCM not leveraged; More complexity in durability management
Wang et al. [170]	OLTP systems (Shore-MT [73])	Distribute transactional log across the sockets of a single node; SCM directly accessed with the write-combining CPU caching policy.	Remove log buffer; Improve concurrency	Only the log benefits from SCM;
Huang et al. [62]	OLTP systems (Shore-MT)	Keep transaction-private log buffers in DRAM, coupled with a global log index in SCM	Decentralize log buffer; Improve concurrency	Only the log benefits from SCM;
Pelley et al. [133]	OLTP systems (Shore-MT)	Place data in SCM, read it optionally via DRAM, modify it directly in SCM; Three architectures considered: SCM as disk-replacement, in-place updates, and NVRAM group commit. Each transaction keeps a private log.	Remove checkpointing and redo phase; Near-instant recovery.	Assume special hardware support (persist barrier); In-place updates highly-sensitive to the latency of SCM; Use WAL.
Arulraj et al. [5]	OLTP systems (VoltDB, LMDB, LevelDB)	Place data, read it, and modify it directly in SCM; Three storage architectures investigated: in-place, copy-on-write, and log-structured updates; Keep references (instead of copies) of the data in the log.	Remove checkpointing and redo phase; Near-instant recovery; Reduced log size.	Architecture highly-sensitive to the latency of SCM; Use WAL.
Arulraj et al. [6]	HTAP systems (Peloton [134])	Use DRAM as cache for SCM; Transaction persists changes out-of-place (using multi-versioning) before writing the log; Keep references (instead of copies) of the data in the log.	Remove checkpointing and redo phase; Reduced log size; Log partially hidden from the critical path of transactions.	SCM accessed via DRAM; Rely on group commit.
Hideaki Kimura [79]	OLTP systems (FOEDUS)	Use DRAM as cache for SCM; Make SCM and DRAM pages logically equivalent and physically independent.	Scalability on hundreds of cores.	Use traditional WAL; SCM accessed via DRAM with file I/O.
Schwalb et al. [148]	HTAP Systems (Hyrise-NV)	Place data, read it, and modify it directly in SCM; Append-only architecture; Persist transaction information.	Remove checkpointing, group commit, and redo phase; No transactional log in the critical path of transactions; Near-instant recovery;	highly-sensitive to the latency of SCM; Require heavy software rewrite; More complex durability management; slower than WAL-based counterpart.
Andrei et al. [3]	OLAP systems (SAP HANA [44])	Place the large read-only part of HANA in SCM.	No need to load data from disk to main memory, leading to significantly reduced restart time.	The read-write, transactional part does not benefit from SCM.
Oukid et al. [122]	HTAP systems (SOFORT)	SCM next to DRAM; Primary data placed, read, and modified directly in SCM; Secondary, latency-sensitive data in DRAM; columnar data organization.	Decreased SCM latency-sensitivity; Remove checkpointing, group commit, and redo phase; No transactional log in the critical path of transactions; Near-instant recovery; Good OLTP performance in a column store.	Require heavy software rewrite; More complex durability management.

Table 2.2: Summary of state-of-the-art research on re-architecting database storage and recovery in presence of SCM.

---

[a] SolidDB has been acquired in 2014 by UNICOM Systems, Inc.

cache partitioning algorithms. They note that the simple hash join is better in presence of variable-size, large keys, while the cache partitioning algorithm is better in presence of small, fixed-size keys. The latter first hash-partitions the two joined relations into parts that fit in the CPU cache, then joins each partition pair. To decrease the number of writes incurred by the partitioning phase, the authors propose *virtual cache partitioning*, which consists in keeping compacted references to the records instead of physically copying them; this reduces the number of writes during partitioning, but increases the number of reads during the join phase because records are scattered. In brief, both unsorted nodes and virtual cache partitioning trade writes for reads.

Stratis D. Viglas [166] proposes a framework for trading writes for reads, assuming SCM is used as DRAM replacement. The framework distinguishes between two classes of algorithms. In the first one, the input is split between a write-incurring part and a write-limited part of the algorithm. The second class is based on lazy processing; the algorithm trades reads for writes, keeping track of the cost of reads versus savings ratio. When the costs exceed the savings, the algorithm writes an intermediate result, then starts a new lazy processing phase. The author devised several sorting and join algorithms that correspond each to one of the classes. As an example of the first class, *Segment sort* partitions the data into two parts: The first part is sorted using the write-intensive external merge sort, and the second part is sorted using the slower, read-intensive selection sort. The latter has quadratic read complexity but writes a value only once in its final position. The ratio between the two parts can be tuned depending on different constraints, such as an upper bound operator latency or a limited number of writes. The *hybrid Grace-nested-loops join* algorithm follows a similar approach by partitioning the input between a write-inducing Grace join [80] and a read-only nested-loops join. Another example is the *segmented Grace join* which, assuming a partitioned input, materializes only some partitions and processes the remaining ones by scanning the remainder of the input.

As an example of the second class, the *lazy sort* algorithm compares for each iteration of a selection sort, the cost of materializing the input of the next iteration to the cost of scanning the current input. If the latter is higher, then the next input is materialized; otherwise, the current input is scanned. The *lazy join* algorithm, which is based on the cache partitioning algorithm, follows a similar approach. The vanilla algorithm partitions the input in several passes; during each pass, a hash table partition is populated, and the remainder input is materialized for the next pass. However, the *lazy join* algorithm decides for each pass whether to materialize the next input, or whether to scan the current input in the next pass, based on the cost of each. In brief, similar to the approach of Chen et al. [20], the above algorithms induce read-amplification for the sake of decreasing the number of expensive writes.

Modern query optimizers are no strangers to asymmetries in storage devices. Indeed, while traditional disks have a symmetric read/write cost with sequential writes faster than random writes, SSDs exhibit have asymmetric read/write costs, with converging sequential and random read costs. We find, nevertheless, two conflicting conclusions in the literature. On the one side, Pelley et al. [132] compare the performance of several database operators using an SSD-aware and an SSD-oblivious query optimizer. They conclude that making optimizers SSD-aware brings only marginal benefits which are not worth the effort, although they interestingly note that this conclusion may change with SCM. On the other side, Bausch et al. [9] devised SSD-aware cost models for several database operators, which led to significant performance improvements for certain TPC-H queries, justifying the need to make query optimizers SSD-aware. We argue that similar efforts need to be conducted to investigate SCM-aware query optimization. For instance, Arulraj et al. [4] propose to adapt the cost model of query optimizers to take into account, e.g., that table or index scans are reads, while materializations are writes.

In conclusion, the characteristics of SCM invalidate the design assumptions of database operators and cost models. We argue that cache-efficiency is paramount for SCM since its latency is higher than that of DRAM. Therefore, cache-efficient main-memory algorithms and data structures are a good starting point for designing SCM-optimized counterparts. The challenge will be to account for the latency differential between reads and writes, and to adapt cost models accordingly. Finally, the algorithm theory community has picked up interest in SCM and works that formalize algorithms and cost models for SCM are starting to emerge [14, 10]

2.4 OVERVIEW OF SOFORT

To explore the full potential of SCM, we decided to opt for a greenfield approach. Our exploration work was conducted concurrently to most of the works we surveyed in the previous section. This endeavor led us to design and implement a novel hybrid SCM-DRAM columnar transactional engine, named SOFORT, tailored for hybrid OLTP and OLAP workloads and fast data recovery. In this section, we first state our design principles, then we give an overview of the different components of our system SOFORT[3].

2.4.1 Design Principles

A hybrid SCM-DRAM hardware architecture allows for a radical change and a novel database system architecture in different perspectives:

- There is no need to copy data out of the storage system since directly modifying the data stored in SCM becomes possible;
- The use of persistent data structures in combination with an adequate concurrency scheme allows for completely dropping the logging infrastructure;
- It can be dynamically decided where to store certain database objects as long as their loss can be tolerated;
- It is possible to achieve near-instant recovery.

We realize the above design principles in SOFORT, our prototype storage engine which we implemented from scratch for this purpose. In the following, we give an overview of SOFORT and contrast our design decisions with state-of-the-art.

2.4.2 Architecture Overview

Among all researched architecture alternatives, in-place updates on SCM stands out as the most promising one. However, as observed by Arulraj et al. [5], and as shown in Section 2.1.2, this architecture is highly sensitive to the latency of SCM. Therefore, instead of the all-in-SCM state-of-the-art approach, we adopt a hybrid SCM-DRAM architecture that offers better performance trade-offs.

Most previous works have focused solely on improving OLTP performance in row-stores. In comparison, SOFORT is a hybrid SCM-DRAM main-memory transactional storage engine intended for hybrid analytical and transactional workloads. It is a single-level store, i.e., it keeps a single copy of the primary data in SCM, directly operates on it, and persists changes in-place in small increments. As illustrated in Figure 2.10, SOFORT offers the flexibility to keep secondary data either in SCM or in DRAM. To achieve good OLAP performance, tables are stored column-wise. Similar to SAP HANA, data is split into a larger read-optimized, read-only *main* storage for OLAP, and a smaller write-optimized, read-write *delta* storage for OLTP, with periodic merges from the *delta* to the *main* to do garbage collection and keep the size of the *delta* bounded. We envision that the *main* will be entirely kept in SCM and is instantly recovered after failure at a negligible cost [3]. If the *main* contains performance-critical latency-sensitive indexes, these can be shadowed partially or fully in DRAM to avoid the cost of higher SCM latencies. Given our architectural choices, we expect SOFORT to have high OLAP performance. In our work, we focus on the most challenging part: durable transaction processing in the *delta*. In the following, we give a brief overview of the different components of SOFORT.

---

[3] The material in this section is partially based on [122, 128, 129]

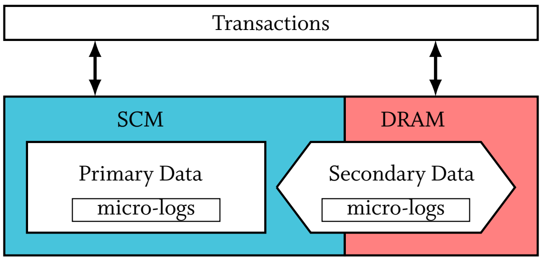

Figure 2.10: Hybrid SCM-DRAM architecture of SOFORT.

2.4.3 Persistent Memory Management

While popular in the operating systems community, SCM memory management remains an almost unexplored topic in database systems. With few exceptions [5], works that leverage SCM as persistent main memory do not elaborate on how they allocate memory, or on how they recover data. This section gives an overview on how we fill this gap.

SCM is managed using a file system. User space access to SCM is granted via memory mapping using *mmap*. The mapping behaves like *mmap* for traditional files, except that the persistent data is directly mapped to the virtual address space, instead of to a DRAM-cached copy.

When a program crashes, its pointers become invalid since the program gets a new address space when it restarts. This implies that these pointers cannot be used to recover persistent data structures. To solve this problem, we propose a new pointer type, denoted Persistent Pointer (PPtr), that remains valid across restarts. It consists of a base, which is a file ID, and an offset within that file that indicates the start of the block pointed to. To manage SCM, we propose a persistent memory allocator (PAllocator) that provides a mapping of SCM to virtual memory, enabling the conversion of PPtrs to regular pointers. We denote *work pointers* regular pointers that are conversions of PPtrs. This is a similar approach to *pointer swizzling* [174], where disk pointers are converted to virtual memory pointers at page fault time. While our pointer conversion principle is the same as in [174], we convert pointers only at restart time and not for every page fault.

PAllocator uses big SCM files that are cut into smaller blocks for allocation. It maps these files to virtual memory to enable the conversion of PPtrs to work pointers. At restart time, a new mapping to virtual memory is created, allowing to re-convert PPtrs to new valid work pointers. PAllocator is also persistent. It maintains a persistent file counter to know how many files it has created. It also stores meta-data for every allocated block.

To perform recovery, we need to keep track of an entry point. One entry point is sufficient for the whole storage engine since every structure is encapsulated into a larger structure up to the full engine. An entry point can simply be two PPtrs: the first points to the root object of SOFORT and the second to the root object of PAllocator. The entry point is kept in SCM in a special file at a known offset. We give a full description of SOFORT's persistent memory management in Chapter 3.

2.4.4 Data Layout

The closest works to ours are the Peloton [6, 134] and Hyrise-NV [148] hybrid OLTP and OLAP database systems. To achieve good OLTP and OLAP performance, Peloton organizes data in *tiles* [157].

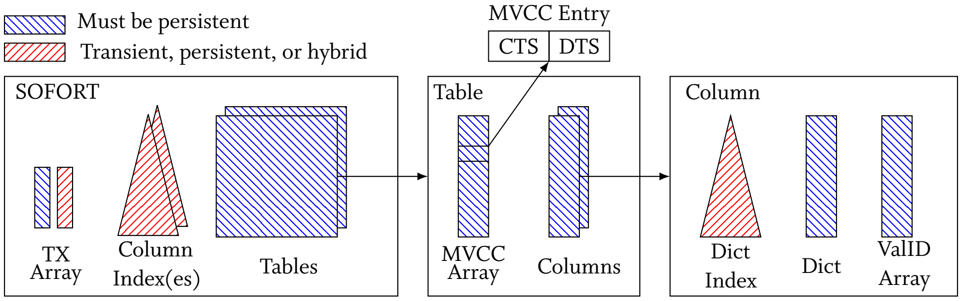

Figure 2.11: Data layout overview in SOFORT.

A *tile* stores subsets of attributes of a table row-wise, resulting in a middle ground between the row-oriented and the column-oriented representations. In contrast, SOFORT is a column-oriented main-memory storage engine that uses dictionary compression. Hyrise-NV is similar to SOFORT in that regard. The remainder of this section gives an overview of data organization in SOFORT.

Figure 2.11 gives an overview of data organization in SOFORT. Tables are stored as a collection of append-only columns. Each column consists of an unsorted dictionary stored as an array of the column's unique data values, and an array of value IDs, where a value ID is simply a dictionary index (position). These two arrays are sufficient to provide data durability and constitute the *primary* data. SOFORT stores primary data, accesses it, and updates it directly in SCM. Other data structures are required to achieve reasonable performance including, for each column, a dictionary index that maps values to value IDs, and for each table, a set of multi-column inverted indexes that map sets of value IDs to the set of corresponding row IDs. We refer to these structures as *secondary* data since they can be reconstructed from the primary data. SOFORT can keep secondary data in DRAM or in SCM. Putting all indexes in DRAM gives the best performance but might stress DRAM resources, while placing indexes in SCM exposes them to its higher latency which compromises performance. To solve this issue, we devise novel hybrid SCM-DRAM data structures that exhibit nearly the same performance as DRAM-based counterparts, while using only a small portion of DRAM. We elaborate on SOFORT's hybrid data structures in Chapter 4.

2.4.5 Concurrency Control

A columnar data layout preserves analytical performance, but poses great challenges for transactional performance. Indeed, materializing rows in a column-store necessitates several random memory accesses, which exacerbates the cost of higher SCM latencies. Moreover, most previous works still rely on some sort of write-ahead logging. In this section, we highlight how SOFORT gets completely rid of traditional logging in the critical path of transactions and manages to achieve competitive OLTP performance despite its columnar data layout.

Multi-Version Concurrency Control (MVCC) [84, 81] is a natural design decision for SOFORT, as versioning simplifies durability management with regards to partial writes. SOFORT adapts to SCM a similar MVCC scheme to that of the Hekaton main-memory database system [84]. As shown in Figure 2.11, SOFORT keeps a transaction object array that stores the metadata of currently running transactions. Contrary to Hyrise-NV which persists the whole transaction object, SOFORT splits it into a transient and a persistent part. The transient part consists of a transaction ID, the start timestamp of the transaction, a read set containing the row IDs of all visited rows, and a status variable. The persistent part encompasses the commit timestamp of the transaction, and a write set containing the row IDs of all modified rows. To undo the effects of aborted transactions or in-flight transactions during recovery, it is sufficient to update the MVCC timestamps of inserted or deleted rows, which are tracked in the persistent write set of each transaction. Therefore, SOFORT does not require a traditional transaction log to achieve durability, as changes are applied directly to the primary, persistent data, and undo capability is provided by persisting the transactions' write sets. Additionally, SOFORT implement a background garbage collection mechanism that cleans indexes and enables the reuse of deleted rows. A detailed description of the concurrency control mechanism and garbage collection of SOFORT is available in Chapter 5.

2.4.6 Recovery Mechanisms

Previous works either assume that secondary indexes are persistent, or they do not account for their rebuild when measuring recovery time. Yet, rebuilding transient data will become the new bottleneck in database systems that access data directly in SCM. This section briefly elaborates on how we tackle this issue in SOFORT.

SOFORT recovers by first recovering primary data that is persisted in SCM at a negligible cost, then undoing the effects of unfinished transactions. The last phase of the recovery procedure, that is, rebuilding secondary data, can be handled in three different ways: in the first approach, denoted *Synchronous Recovery*, SOFORT does not accept requests until the end of the recovery process, i.e., until all secondary data structures have been rebuilt. The main advantage of this approach is that it rebuilds secondary data structures as fast as possible since all system resources are allocated to recovery. However, this approach suffers from the fact that the database is not responsive during the whole recovery period, which might be long as its duration depends directly on the size of secondary data structures to be rebuilt.

The second approach, named *Instant Recovery*, starts accepting requests right after recovering primary data. Instant recovery follows a *crawl before run* approach: it uses primary data, which is recovered at a negligible cost, to answer queries, while secondary data structures, whose purpose is to speed up query processing, are rebuilt in the background. For example, lookups to a dictionary index and an inverted index are replaced by scans of the corresponding dictionary array and the value IDs arrays, respectively. Partially rebuilt DRAM-based indexes can be progressively leveraged as they are being rebuilt. For instance, a regular dictionary index lookup is replaced by the following sequence: look up the partially rebuilt dictionary index; if the value is not found, then scan only the portion of the dictionary array that has not been indexed yet. Hybrid SCM-DRAM indexes, however, need to be fully recovered in order to be leveraged. The main advantage of this approach is that it enables instant recovery, i.e., instant responsiveness of the database after failure. However, it takes the database longer than for synchronous recovery to approach peak performance observed before failure. This is because system resources are split between recovery and query processing, while in synchronous recovery, all system resources are allocated to recovery.

To cure the shortcomings of both approaches, SOFORT has a third recovery technique, named *Adaptive Recovery*. It dynamically ranks transient secondary data structures based on their importance to the current workload. During recovery, it prioritizes the rebuild of the most highly ranked data structures. Furthermore, adaptive recovery employs a dynamic resource allocation algorithm that releases resources from the recovery process to query execution when it detects that system has approached peak performance. Therefore, adaptive recovery achieves instant responsiveness while reaching peak performance quickly, well before the end of the recovery process. We present the details of SOFORT's recovery techniques in Chapter 6.

2.5 CONCLUSION

SCM is driving a necessary rethink of database architectures. In this chapter we presented several works that propose to re-architect parts or all of the traditional database storage architecture. Contrary to the state-of-the-art that focuses mostly on OLTP row-store systems, we focus on HTAP systems which usually adopt a columnar data representation. We showed that a hybrid SCM-DRAM storage architecture enables better performance than an SCM-only one. Furthermore, we anticipate that it is possible to completely remove traditional WAL from the critical path of transactions. We materialize our design principle in SOFORT, a hybrid single-level transactional storage engine that makes the most out of both DRAM and SCM. SOFORT persists its primary data directly in SCM at cache-line granularity.

While a single-level architecture brings many benefits, such as instant recovery, it does not come as a *free lunch*: it requires heavy software rewrite and introduces unprecedented programming challenges, on which we elaborate in the next chapter.

3

PERSISTENT MEMORY MANAGEMENT

Memory allocation has always been a topic in database systems. In the disk-based database systems era, memory management was mostly synonymous of buffer pool management. For instance, Traiger [160] investigated how to optimize the operating system virtual memory component such that it is efficiently used as replacement for the buffer pool. In the era of main-memory database systems, we switched to using transient allocators, such as jemalloc [72], tcmalloc [49], and Hoard [11]. However, these allocators are general-purpose and database systems have all but general-purpose needs. Hence, to no surprise, several database system vendors, such as SAP, IBM, and Oracle implement their own memory management [145, 156, 120]. The rise of SCM might spur a major change in the architecture of database systems, and in this incoming era of SCM-based database systems, everything is yet to be done, starting from persistent memory management as a fundamental building block. However, SCM as persistent main memory is still at its pathfinding stages. Therefore, we explore in the first part of this chapter the programming challenges of SCM, then survey state-of-the-art techniques on how to solve them. Thereafter, we devise a sound SCM programming model that takes into account database system requirements.

In the second part of this chapter, we present SOFORT's memory management component, called PAllocator, a highly scalable, fail-safe, and persistent allocator for SCM, specifically designed for databases that require very large main memory capacities[1]. PAllocator uses internally two different allocators: SmallPAllocator, a small block persistent allocator that implements a segregated-fit strategy; and BigPAllocator, a big block persistent allocator that implements a best-fit strategy and uses hybrid SCM-DRAM trees to persist and index its metadata. The use of hybrid trees enables PAllocator to also offer a fast recovery mechanism. Moreover, PAllocator addresses fragmentation in persistent memory, which we argue is an important challenge, and implements an efficient defragmentation algorithm that is able to reclaim the memory of fragmented blocks by leveraging the hole punching feature of sparse files. To the best of our knowledge, PAllocator is the first SCM allocator that proposes a transparent defragmentation algorithm as a core component for SCM-based database systems. Our evaluation shows that PAllocator improves on state-of-the-art persistent allocators by up to two orders of magnitude in operation throughput, and by up to three orders of magnitude in recovery time. Furthermore, we integrate PAllocator and a state-of-the-art persistent allocator in a persistent B^+-Tree, and show that PAllocator enables up to 2.39x better operation throughput than its counterpart.

This chapter is organized as follows: We contribute in Section 3.1 an analysis of the challenges posed by SCM that we drew from our experience in designing and implementing SOFORT. Then, Section 3.2

---

[1] Parts of the material in this chapter are based on [124].

discusses existing programming models for SCM and contrasts their advantages and disadvantages. Thereafter, Section 3.3 explores the design space of persistent memory allocators following different dimensions, e.g., allocation strategies, concurrency handling, and garbage collection. Afterwards, Section 3.4 presents the design and implementation of our PAllocator, including its defragmentation algorithm and its recovery mechanism. Section 3.5 presents a detailed performance evaluation of PAllocator against state-of-the-art SCM allocators. Finally, Section 3.6 summarizes the contributions of this chapter.

3.1 PERSISTENT MEMORY CHALLENGES

With the unique opportunities brought by SCM comes a set of novel programming challenges, from which we identify: (1) data consistency; (2) data recovery; (3) persistent memory leaks; (4) partial writes; (5) persistent memory fragmentation; and (6) virtual address space fragmentation. We detail these challenges in the following.

3.1.1 Data consistency

SCM is managed using an SCM-aware file system that grants the application layer direct access to SCM through memory mapping. This enables CPUs to access SCM directly with load and store semantics. The path from SCM to CPU registers is long and mostly volatile, as illustrated in Figure 3.1. It includes store buffers and CPU caches, over all of which software has little control. Additionally, modern CPUs implement complex out-of-order execution and either partial store ordering (Intel x86) or relaxed-memory ordering (ARM, IBM Power). Consequently, memory stores need to be explicitly ordered and persisted to ensure consistency. Current x86 CPUs provide the CLFLUSH, MFENCE, SFENCE, and non-temporal store instructions (MOVNT) to handle memory ordering and data durability. Additional instructions, namely CLFLUSHOPT and CLWB, have been announced for future platforms [64]. CLFLUSH evicts a cache line and writes it back to memory. It is a synchronous instruction and does not require a memory fence to be serialized. SFENCE is a memory barrier that serializes all pending stores, while MFENCE serializes both pending loads and stores. Non-temporal stores bypass the cache by writing to a special buffer, which is evicted either when it is full, or when an SFENCE is issued, as shown in Figure 3.1. CLFLUSHOPT is the asynchronous version of CLFLUSH. It is not ordered with writes, which improves its throughput. Finally, CLWB writes back a cache line to memory but without evicting it from the CPU cache, which benefits performance when data is accessed shortly after it is persisted. It executes asynchronously and is not ordered with writes. Both CLFLUSHOPT and CLWB require two SFENCEs to be serialized, as illustrated in Figure 3.1; the first SFENCE ensures that the latest version of the data is being flushed, while the second SFENCE ensures that the flushing instruction finishes executing.

To highlight the data consistency challenge, we consider the example of the following simplified persistent array append operation:

```
void append(int val) {
    array[size] = val;
    clwb(&array[size]);
    size++;
    clwb(&size);
}
```

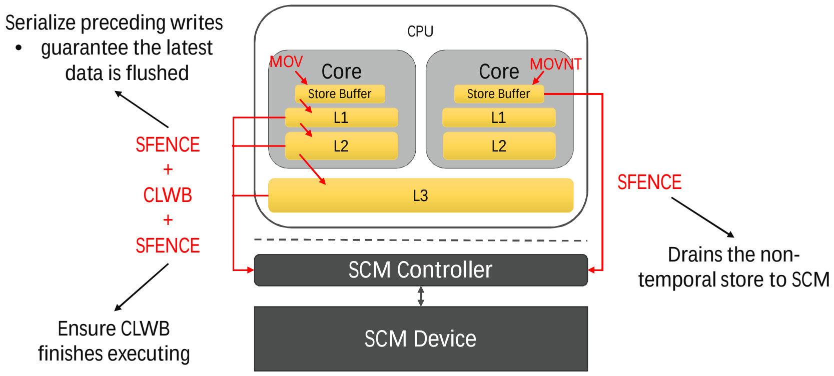
Serialize preceding writes
• guarantee the latest data is flushed
SFENCE
+
CLWB
+
SFENCE
Ensure CLWB finishes executing
CPU
MOV
Core
Store Buffer
L1
L2
Core
MOVNT
Store Buffer
L1
L2
L3
SCM Controller
SCM Device
SFENCE
Drains the non-temporal store to SCM

Figure 3.1: Illustration of the volatility chain in a 2-core x86-like processors.

Assume we want to append value 2017. Lines 2 and 3, and/or lines 4 and 5 could be reordered since CLWB is not ordered with writes, which might leave the array in one of the following (potentially inconsistent) states:

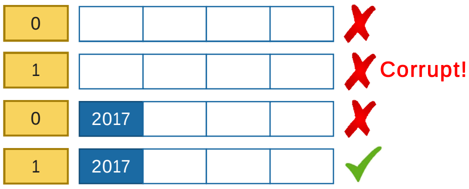

Therefore, we must wrap CLWB with two SFENCEs as follows:

```
1 void append(int val) {
2     array[size] = val;
3     sfence(); clwb(&array[size]); sfence();
4     size++;
5     sfence(); clwb(&size); sfence();
6 }
```

Until recently the memory controller buffers were considered to be part of the volatility chain. Since then Intel has announced support for Asynchronous DRAM Self-Refresh (ADR) in all platforms that will support persistent memory [33]. ADR protects data still pending in the memory controller buffers from power failures using capacitors. Hence, it is safe to assume that a cache line flush guarantees persistence.

3.1.2 Data recovery

When a program restarts, it loses its previous virtual address space, including its memory mappings, invalidating any stored virtual pointers, as illustrated in Figure 3.2. Hence, there is a need to devise ways of discovering and recovering data stored in SCM. Using a file system on top of SCM provides a way of discovering data after a restart. Reads and writes to a file created and memory mapped by an SCM-aware file system are made with direct load and store instructions. Hence, SCM-aware file systems should not have a negative performance impact on the application. Therefore, a potential solution would be to create one file per data object. However, database systems can have millions of objects of different sizes, ranging from a few bytes to several gigabytes, rendering this solution unrealistic because:

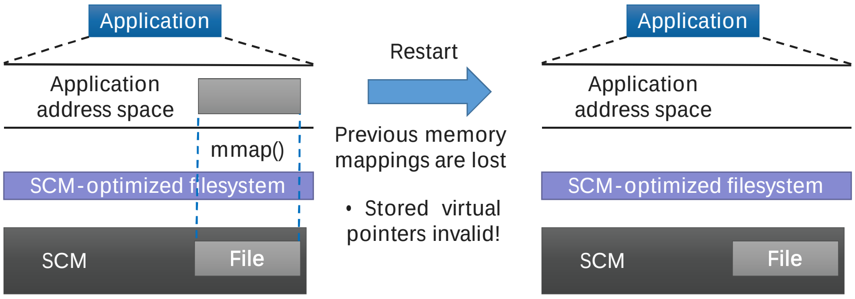
Application
Application address space
mmap()
SCM-optimized filesystem
SCM
File
Restart
Previous memory mappings are lost
• Stored virtual pointers invalid!
Application
Application address space
SCM-optimized filesystem
SCM
File

Figure 3.2: Illustration of process address space loss upon restart.

- it incurs a large space overhead for small objects (e.g., file metadata);
- today's file systems are not tailored to handle millions of files;
- recovery would consist of memory mapping millions of files, which does not scale on Linux systems because the page table is protected by a global lock.

We cover state-of-the-art data recovery techniques in Section 3.2.

3.1.3 Persistent memory leaks

Memory leaks pose a greater problem with persistent memory than with volatile memory: they are *persistent*. Additionally, persistent memory faces a new class of memory leaks resulting from software or power failures. To illustrate this problem, consider the example of the following linked list:

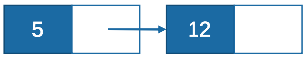

If a crash occurs during an append operation after a new node was allocated but before it was linked to the tail node, the persistent allocator will remember the allocation while the data structure will not, leading to a persistent memory leak, as depicted blow:

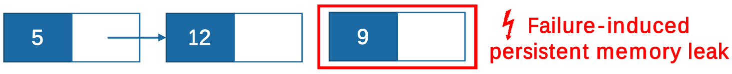

Hence, there is a need to devise techniques to avoid failure-induced memory leaks. We elaborate on existing approaches in Section 3.2 .

3.1.4 Partial writes

We define a *p-atomic* store as one that is retired in a single CPU cycle; that is, a store that is immune to partial writes. Current x86 CPUs support only 8-byte p-atomic stores; larger write operations are prone to partial writes since the CPU can speculatively evict a cache line at any moment. For example, suppose we want to write the string below that spans two cache lines:

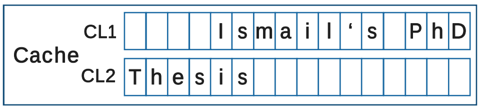

If a failure occurs during the write operation, assuming we write 8-bytes at a time, the corresponding SCM string location might be in one of the following states:

1. “”: no write has propagated to SCM;
2. “Ismail’ ”: a failure occurred after the first 8 bytes were written and flushed to SCM;
3. “Ismail’s PhD”: a failure occurred after the string was written, but only the first cache line was flushed to SCM;
4. “\0\0\0\0\0\0\0\0\0\0\0Thesis”: a failure occurred after the string was written, but only the second cache line was flushed to SCM.
5. “Ismail’s PhD Thesis”: the whole string was correctly flushes to SCM.

Cases 2, 3, and 4 can result, for instance, from the writing thread being descheduled. Meanwhile, the CPU might speculatively flush the first or the second cache line due to a set conflict. A failure at this time would corrupt the string in SCM. A common way of addressing this problem is using flags that can be written p-atomically to indicate whether a larger write operation has completed.

3.1.5 Persistent memory fragmentation

Persistent memory allocations have a longer lifespan than transient ones, and therefore have more impact on the overall application. While a restart remains a valid, but last-resort way of defragmenting volatile memory, it is not effective in the case of persistent memory. This is a similar problem to that of file systems. However, file system defragmentation solutions cannot be applied to SCM, because file systems have an additional indirection step: they use virtual memory mappings and buffer pages in DRAM, which enables them to transparently move physical pages around to defragment memory. In contrast, persistent memory mappings give direct physical memory access to the application layer without buffering in DRAM. Hence, persistent memory cannot be transparently moved as it is bound to its memory mapping. As a consequence, we argue that fragmentation avoidance is a core requirement for any persistent memory allocator. Within our PAllocator solution we propose a defragmentation algorithm, detailed in Section 3.4.6.

3.1.6 Address space fragmentation

Given the existence of systems with tens of TBs of main memory, and given the currently limited amount of address space supported by both software and hardware, we anticipate that the larger main memory capacities SCM enables will pose the unprecedented challenge of address space fragmentation. Indeed, SCM enables main memory capacities of hundreds of TBs. Current Intel x86 processors use 48 bits for address space, which amounts to a maximum capacity of 256 TB. However, Linux uses only 47 bits as one bit is reserved for the kernel. Hence, Linux currently supports up to 128 TB of address space. Two challenges arise: this capacity will not be sufficient for next-generation servers that use SCM, and the amount of physical memory approaches the limits of available virtual address space making the latter prone to fragmentation. Hence, memory mapping a file that resides in SCM might fail because of the lack of a large-enough contiguous *virtual* memory region. To remedy this issue, starting from Linux kernel v4.12, the page table will be extended to 5 levels instead of 4, enabling support for 128 PB of virtual address space [28].

From all these challenges, we conclude that there is a need for novel programming models for SCM, which must provide the following: (1) data discovery and recovery mechanisms; (2) data consistency model; (3) failure-induced memory leak prevention. A persistent memory allocator must build on top of a sound programming model that provides the above features. Furthermore, it should minimize fragmentation, or even better, offer a defragmentation mechanism. Our PAllocator fulfills all of the above requirements.

3.2 SCM PROGRAMMING MODELS

In the previous section, we identified three main requirements, namely providing a recoverable addressing scheme, handling data consistency, and preventing failure-induced persistent memory leaks, that a programming model for SCM must fulfill. In this section we elaborate in detail on existing techniques to fulfill each one of of them. These techniques are usually provided in libraries that serve as an interaction interface between SCM and the programmer.

3.2.1 Recoverable Addressing Scheme

A recoverable addressing scheme must provide two features: persistent pointers, that is, a way to reference objects that remains valid across restarts, and a recovery scheme that maps back the objects of the program into its virtual address space. We find two approaches in the literature: The first one consists in using fixed-address memory mappings. Upon restart, the program would always memory map its SCM files to the same virtual address ranges, which preserves the validity of virtual pointers. Hence, the program can use virtual pointers as persistent pointers. The advantage of this approach is that it retains the familiar virtual pointer interface and incurs no runtime overhead. Its disadvantage, however, is that fixed-address memory mappings are usually prohibited in the industry because they constitute a security issue. Furthermore, the operating system offers no guarantees that the desired virtual address ranges are available. Hence, fixed-address memory mappings might unmap existing objects.

The second approach uses regular, unrestricted memory mappings. Upon restart, the program would memory maps its SCM files into arbitrary virtual address ranges, rendering any stored virtual pointers invalid. To reference objects in a recoverable way, this approach relies on persistent pointers that consist of a file ID and an offset within that file, as depicted in Figure 3.3. A persistent pointer can be swizzled (converted) into a virtual pointer by adding the start address of the file (returned by *mmap*) to the offset [174]. The program can then buffer the virtual pointer to avoid the cost of conversion during normal execution. A persistent pointer to the root object of the program is kept at a known offset, which enables the program to recover its data. The advantage of this approach is that it is a safe, easy-to-implement, and portable approach. The disadvantage, however, is that it incurs a memory overhead since persistent pointers are larger than virtual pointers, in addition to the space overhead of the buffered converted virtual pointers. Note that when the SCM pool consists of a single file, we can abstract away the file ID and use only file offsets as persistent pointers. We argue that unrestricted memory mappings, which we adopt PAllocator, is the safest approach.

3.2.2 Consistency Handling

To address the challenges of data consistency, state-of-the-art works have followed mainly two approaches. The first one strives to provide global solutions in the form of software libraries, mostly following a transactional-memory-like approach, with the goal of making programming against SCM easy and accessible for programmers. However, this approach introduces the overhead of systematic write-ahead logging, which is exacerbated in presence of higher SCM latencies. For example, the code of our previous persistent array append operation example would look like this under this approach:

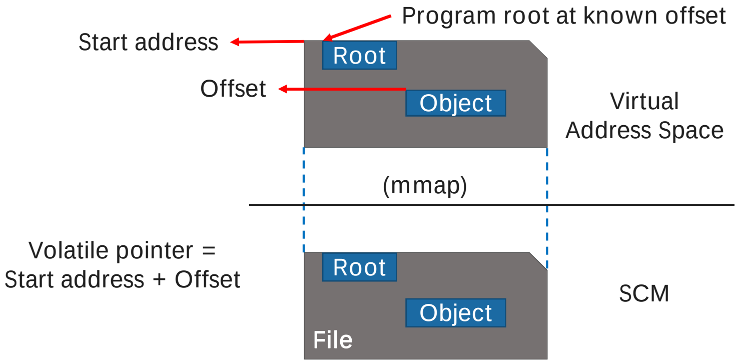

Figure 3.3: Example of data recovery using persistent pointers consisting of a file ID and an offset within that file.

```
void append(int val) {
    TX_BEGIN {
        array[size] = val;
        size++;
    } TX_END
}
```

Each modification triggers at least two writes: the first one logs the current value of the changed variable (assuming an undo log), and the second one updates the variable. Hence, the array append operation would necessitate at least 4 writes to SCM.

The second approach, that we denote *lightweight primitives*, relies on existing CPU persistence primitives, namely cache line flushing instructions (CLFLUSH, CLFLUSHOPT, and CLWB), memory barriers (MFENCE and SFENCE), and non-temporal stores (MOVNT), to enforce consistency and durability. The advantage of this approach is that it allows low-level optimizations. For instance, the code of the previous example would be as follows:

```
void append(int val) {
    array[size] = val;
    persist(&array[size]);
    size++;
    persist(&size);
}
```

Where *persist* is a wrapper function for a serialized flush. Indeed, this approach can provide utility functions that abstract away the explicit usage of persistence primitives. Note that the array append operation requires only 2 writes to SCM, in contrast to the 4 writes required by the transactional approach. We conclude that devising high-performance SCM-based data structures calls for using the lightweight primitives approach, which we do in this work. However, the ability to do low-level optimizations comes at a price: the programmer must reason about the application state, which makes the lightweight primitives approach more error-prone and harder to use than the transactional approach.

3.2.3 Persistent Memory Leak Prevention

The traditional allocation interface suffers from a blind spot. Consider the following example:

```
1 pptr = allocate(size);
2 persist(&pptr);
```

Where *pptr* is a persistent pointer belonging to the calling data structure. If a failure occurs between lines 1 and 2, the allocator will have completed the allocation request and will remember that it allocated this block, while the data structure might loose its reference to that block because it was not persistent before the failure occurred. We find three approaches that remedy this issue in the literature. The first one uses reference passing; the allocator interface is modified to take a reference to a persistent pointer that belongs to the calling data structure and that must reside in SCM:

```
allocate(PPtr& p, size_t size);
```

The allocator will set the persistent pointer to the address of the allocated memory and persist it before returning, hence removing the aforementioned blind spot. Note that reference passing, which we adopt in this work, is ideal for the lightweight primitives approach.

The second approach consists in to wrap code that is prone to persistent memory leaks inside a fail-atomic transaction, e.g., as follows:

```
TX_BEGIN {
    pptr = allocate(size);
    persist(&pptr);
} TX_END
```

Finally, the third approach consists in using offiline garbage collection [13]. It consists in scanning allocated blocks during recovery to detect persistent memory leaks. We elaborate on the latter approach in more details in Section 3.3.4.

3.2.4 Related Work

Table 3.1 summarizes existing libraries that aim to address the programming challenges of SCM. Among early works, Volos et al. [168] proposed Mnemosyne, a library collection to program SCM that require kernel modifications and compiler support. Following a similar approach, Coburn et al. [24] proposed NV-Heap, a persistent heap that implements garbage collection through reference counting. Later, Chakrabarti et al. [18] and Chatzistergiou et al. [19] proposed respectively Atlas and REWIND, two log-based user-mode libraries that manage persistent data structures in SCM in a recoverable state using undo/redo logging. An original characteristic of Atlas is that it assumes that the consistency-critical code sections are protected with locks. Atlas then transforms these locked scopes into fail-atomic transactions at compile time. This means, however, that single-threaded programs need to be modified by inserting locks where changes to SCM-based structures occur. Most recently, Avni et al. [8] proposed PHyTM, a persistent hybrid transactional memory system that leverages hardware transactional memory, while assuming hardware support for single-bit atomic commit to SCM. Intel's NVML [117] offers an elaborate collection of libraries that spans both the raw and the transactional approaches. Additionally, it offers a middle-ground approach based on the raw one augmented with useful transaction support, such as atomic execution of object constructors upon persistent memory allocation, which greatly simplifies fail-safe atomicity management. In our work we follow the lightweight primitives approach.

Library	Consistency Handling	Recoverable Addressing Scheme	Memory Leak Prevention	Compiler Support	Reference
Mnemosyne	Transactional + Lightweight primitives	**PPtr:** file offset; **Recovery:** new mmap in reserved address space	Transactional logging + reference passing	Yes	Volos et al. [168]
NV-Heaps	Transactional	**PPtr:** file ID + offset; **Recovery:** new mmap	Transactional logging	No	Coburn et al. [24]
NVML	Transactional + Lightweight primitives	**PPtr:** file ID + offset; **Recovery:** new mmap	Transactional logging + reference passing	No	`http://pmem.io`
Atlas	Transactional (sections identified by locks)	**PPtr:** virtual pointer; **Recovery:** fixed-address mmap	Transactional logging	Yes	Chakrabarti et al. [18]
REWIND	Transactional	**PPtr:** Undefined. Hints suggest **PPtr:** virtual pointer; **Recovery:** fixed-address mmap	Transactional logging	Yes	Chatzistergiou et al. [19]
PAllocator	Lightweight primitives	**PPtr:** file ID + offset; **Recovery:** new mmap	Reference passing	No	Oukid et al. [124]

Table 3.1: Summary of existing libraries that address some or all of the programming challenges of SCM. PPtr stands for persistent pointer.

3.3 PERSISTENT MEMORY ALLOCATION

In this section we explore the design space of persistent memory allocators. Then, we summarize related work, highlighting the design decisions of each approach and contrasting them with those of our PAllocator.

3.3.1 Pool Structure

A persistent memory pool can comprise either one large SCM file (pool) or multiple ones. The advantage of using a single file is that it is easier to implement and it enables abstracting away the unique file ID in persistent pointers. Therefore, persistent pointers can consist of only the offset within the single file. The disadvantages, however, are threefold: (1) while growing the pool can be done by increasing the size of the file, shrinking it is much harder; (2) huge block allocations (e.g., several megabytes and higher) are an issue since, because they most likely require the global pool to be expanded, but it cannot shrink back in most cases after a deallocation, hence exacerbating fragmentation; and (3) the segregated-fit allocator must use the best-fit allocator to create its chunks, resulting in a contention point – we explain segregated-fit and best-fit allocators in the next section.

Using multiple files, which we adopt in PAllocator, remedies most of these issues. First, it is easier to grow and shrink the pool since huge block allocations can be serviced by creating a new file, avoiding any fragmentation at the allocator level. Second, it becomes possible to defragment persistent memory by leveraging the *hole punch* feature of sparse files (see Section 3.4.6 for more details). Finally, the segregated-fit and best-fit allocators can operate independently by creating and maintaining their own files. The disadvantage, however, is that persistent pointers must include both the file ID (8 bytes) and the offset (8 bytes), resulting in a 16-byte structure.

3.3.2 Allocation Strategies

We distinguish three main allocation strategies. The first one, and the simplest, is creating one file per allocation. The advantage of this approach is that it is suitable for huge block allocations (several megabytes and above). Moreover, it avoids creating any fragmentation at the allocator level – fragmentation handling is pushed to the file systems. Nevertheless, this approach is not suitable for smaller block allocations as a program such as a database system might allocate millions of objects.

The second allocation strategy is denoted *segregated-fit* allocation and is illustrated in Figure 3.4. It is particularly suitable for small block allocations (from a few bytes to a few kilobytes). It consists in creating chunks of memory of a few kilobytes that specialize in allocating one specific block size, denoted the *size class*. Basically, the chunk is split into an array of its size class. It also contains a header that tracks which blocks from this array are allocated. The header can be implemented in several ways; Figure 3.4 illustrates an implementation based on a bitmap. Given the existence of a non-full chunk of the appropriate size class, an allocation can be performed by simply flipping one bit in the chunk header. Assuming a moderate number of class sizes, an advantage segregated-fit allocation is that it limits fragmentation for small blocks. Having too many class sizes might have the opposite effect. State-of-the-art allocators usually have between 30 and 40 class sizes.

Segregated-fit allocation is not suitable for large block allocation (from a few kilobytes to a few megabytes). Indeed, a chunk should contain an array of several times the size of its class size in order to amortize

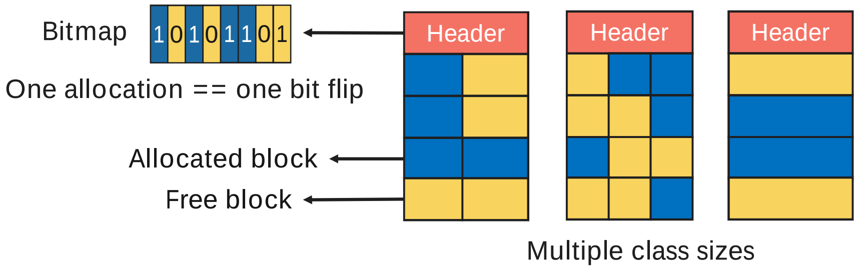

Figure 3.4: Illustration of the segregated-fit allocation strategy for small block allocations.

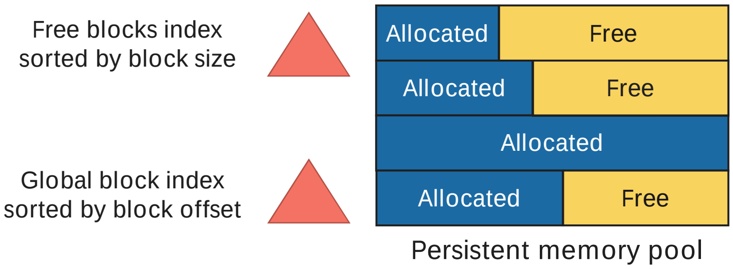

Figure 3.5: Illustration of the best-fit allocation strategy for large block allocations.

the cost of chunk creation. In the case of large blocks, the size of the chunks and the number of class sizes would be simply too big, which brings us to the third allocation strategy, denoted *best-fit* allocation; Figure 3.5 how the data layout might look like. This approach keeps a large pool (file) that is divided into blocks equal in size to the allocation request sizes, rounded up to the closest multiple of a predefined granularity (e.g., a system-page-size, typically 4 KB). Metadata consists of two indexes: The first one indexes all free blocks and is sorted by the block size. It is used during allocations to determine the smallest block that is greater or equal to the requested size. In case it is greater than the requested size, the found block is split into two blocks, one of which is used to service the allocation request, and the second remains a free block. The second index keeps metadata on all existing blocks (e.g., whether they are free or allocated) and is sorted by the block offset. It is used to identify the left and right neighboring blocks of a deallocated block to be coalesced together in case they are free. A drawback of this approach is that it is prone to fragmentation, an issue which we address in Section 3.4.6. In PAllocator, we use all three allocation strategies.

3.3.3 Concurrency Handling

The state-of-the-art technique for concurrency handling in transient allocators is thread-local caching. It consists in keeping one sub-allocator with its own cached memory per thread. Sub-allocators request chunks of memory from the global allocator and use them as a local cache to service allocation requests triggered by the host thread. This technique is mostly used for segregated-fit small block allocators, because they requests only small amounts of memory at a time, in the form of chunks, from the global allocator. A best-fit large block allocator would need to request and maintain large local pools which renders its space overhead too great to be considered in the general-purpose case. When a thread terminates, the memory of its local sub-allocator must be merged back into the global pool, which might be difficult to be executed fail-atomically in the case of a persistent allocator. Another drawback of thread-local allocation is that it does not scale under high concurrency, because the number of sub-allocators depends on the number of threads, and not on the number of available CPU cores.

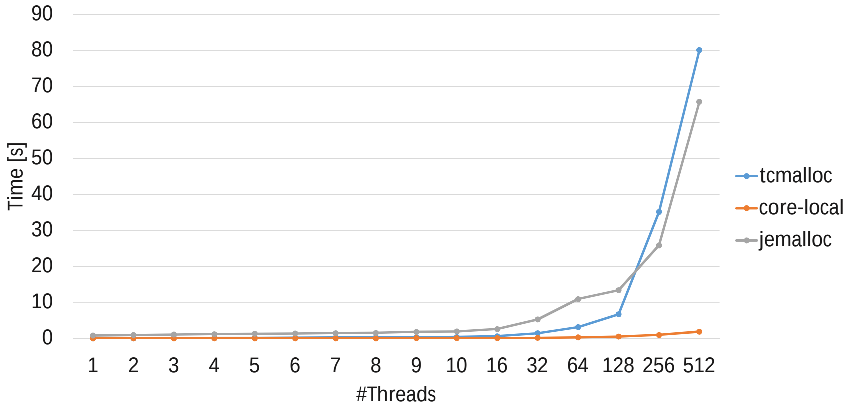

Figure 3.6: 16 KB allocation performance on an Intel Xeon CPU X5550 2.67GHz (16 cores). The core-local allocator scales better under high concurrency than thread-local counterparts.

To circumvent this shortcoming, a second technique that we denote *core-local allocation*, keeps one sub-allocator per physical CPU, completely independent of the number of running threads. Allocations are serviced by the sub-allocator of the core on which the requesting thread is executing. Furthermore, the sub-allocators are created only once when the program is started, and and their number is optimal and independent of the number of threads. This enables the allocator to retain its performance under very high concurrency.

To validate the above qualitative analysis, we measure the performance of 16 KB allocations of an SAP in-house core-local transient allocator with that of two state-of-the-art thread-local transient allocators, namely jemalloc [72] and tcmalloc [49]. The results are depicted in Figure 3.6[2]. We observe that the performance of the jemalloc and tcmalloc deteriorates greatly when the number of threads exceeds the number of available CPU cores. The core-allocator, however, exhibits robust performance and retains good performance even under very high concurrency, which verifies our qualitative analysis. Hence, we use core-local allocation in PAllocator.

3.3.4 Garbage Collection

We find two uses of garbage collection in the literature of persistent memory allocators. The first one is traditional reference counting, which is used for instance in NVHeap [24]. The main challenge in adapting this technique to persistent allocators are deallocations. Indeed, a deallocation might call the destructor of the deallocated object, which might trigger recursive deallocations. Hence, there is a need to ensure the fail-atomicity of recursive deallocations.

The second approach, introduced in the Makalu allocator [13], is offline garbage collection. The novelty of this approach is not in the garbage collection algorithm itself, but in its original use. Indeed, garbage collection is usually run online, while the program is executing. When a program terminates, its transient memory is reclaimed by the operating system. Hence, there is by definition no garbage at start time. However, in the case of persistent memory, the persistent memory allocation topology survives restarts, which means that garbage might exist at start time. Makalu employs garbage collection in this context. It runs a mark-and-sweep garbage collection algorithm during recovery, and considers any blocks that could not be reached as memory leaks. This enables Makalu to relax its metadata persistence constraints, which results in faster small block allocations. Nevertheless, offline garbage

---

[2] Figure 3.6 is courtesy of Daniel Egenolf and Daniel Booss.

collection has two main drawbacks. First, it imposes some constraints on the programming language, such as forbidding generic pointers. Second, recovery is significantly slowed down since persistent memory needs to be scanned by the garbage collection process. Note that we do not employ garbage collection in PAllocator

3.3.5 Related Work

Among transactional approaches, Mnemosyne [168] uses an SCM-aware version of Hoard [11] for small block allocations, and a transactional version of *dlmalloc* [85] for large allocations. NVHeap [24] uses a persistent heap that implements garbage collection through reference counting. While these approaches are laudable, we argue that transactional-memory-like approaches suffer from additional overhead due to systematic logging of modified data, which is amplified by the higher latency of SCM.

Moraru et al. [110] proposed NVMalloc, a general purpose SCM allocator whose design emphasizes wear-leveling and memory protection against erroneous writes. The authors propose to extend CPU caches with line counters to track which lines have been flushed. Yu et al. [184] proposed WAlloc, a persistent memory allocator optimized for wear leveling. In contrast to NVMalloc and WAlloc, we focus on performance and defragmentation, and ignore wear-leveling which we envision will be addressed at the hardware level. Indeed, several works, such as [138], have already addressed proposed wear-leveling techniques at the hardware level to increase the lifetime of SCM.

Schwalb et al. [147] propose nvm_malloc, a general purpose SCM allocator based on jemalloc [72]. It uses a three-step allocation strategy, first proposed by *libpmem* from NVML, namely reserving memory, initializing it, and then activating it. nvm_malloc creates a single, dynamically resizable pool and uses link pointers, which represent offsets within the pool, to track objects. nvm_malloc uses a segregated-fit algorithm for blocks smaller than 2 KB, and a best-fit algorithm for larger blocks.

NVML [117] is an open-source, actively developed collection of persistent memory libraries from Intel. The most relevant library to our work is *libpmemobj*, which provides, among other features, an advanced fail-safe memory allocator, which is the only one, in addition to our PAllocator, to account for fragmentation, a very important challenge as explained in Section 3.1. It uses a best-fit algorithm for memory allocations larger than 256 KB, and a segregated-fit algorithm with 35 size classes for smaller allocations. In the latter case, to minimize fragmentation, a chunk of 256 KB is divided into blocks of 8× the class size, which are then inserted into a tree. Hence, each chunk can service allocations of up to 8× their class size. Nevertheless, in contrast to our PAllocator, NVML does not have a defragmentation mechanism. NVML handles concurrency by maintaining thread local caches.

More recently, Bhandari et al. [13] presented Makalu, a fail-safe persistent memory allocator that relies on offline garbage collection to relax metadata persistence constraints, resulting in faster small-block allocations, and enabling Makalu to catch persistent memory leaks that stem from programming errors. Makalu's allocation scheme is similar to that of nvm_malloc, but differs in that it enforces the persistence of only a minimal set of metadata, and reconstructs the rest during recovery. Potential inconsistencies that might arise during a failure are cured using garbage collection during recovery. Makalu relies on normal volatile pointers, and keeps them valid across restarts by memory mapping its pool at a fixed address (using the MAP_FIXED flag of *mmap*). However, in addition to being a security issue, fixed-address mappings will unmap any objects that are mapped in the requested range. Finally, garbage collection can limit certain functionalities of unmanaged-memory languages, such as C++, that are usually used for building database systems.

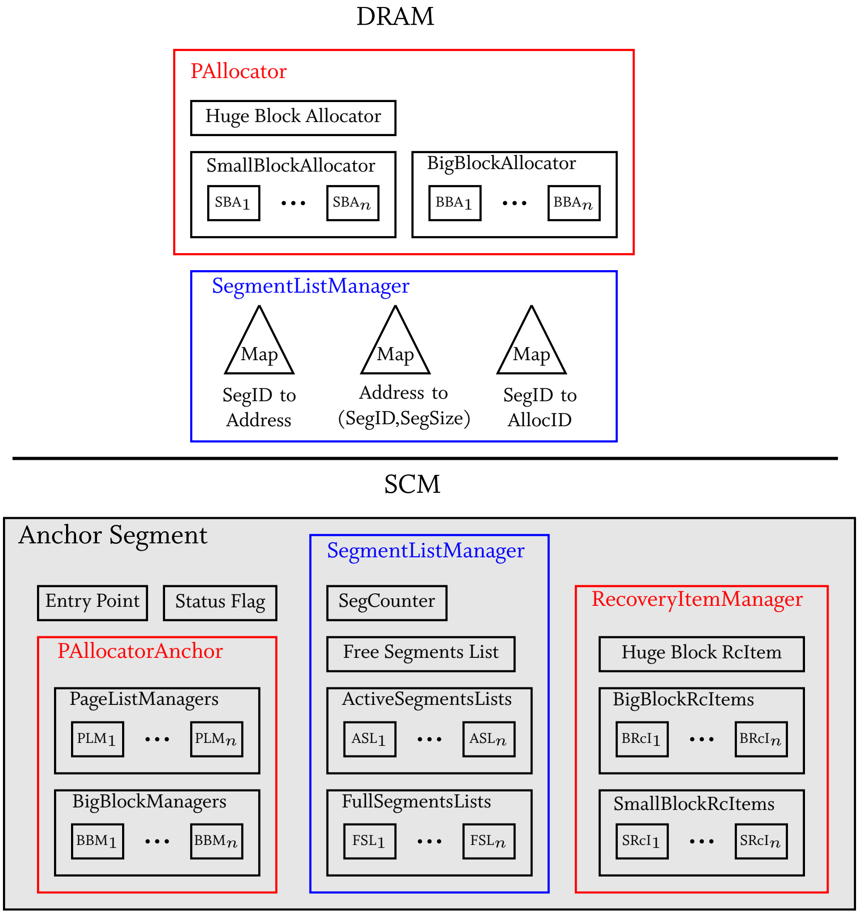

Figure 3.7: Architecture overview of PAllocator.

To the best of our knowledge, Mnemosyne, NVML, nvm_malloc, Makalu, and NVMalloc are the only persistent allocators publicly available. We compare the performance of PAllocator against NVML, Makalu, and nvm_malloc; we exclude NVMalloc since it does not provide a recovery mechanism (see Section 3.5 for further details), and Mnemosyne since its default allocator is outperformed by Makalu [13].

Table 3.2 summarizes the design characteristics of existing persistent memory allocators. PAllocator exhibits radically different design characteristics than state-of-the-art persistent allocators. This difference stems from our design goals on which we elaborate in the next section.

3.4 PALLOCATOR DESIGN AND IMPLEMENTATION

In this section we present our proposed PAllocator and its different components.

3.4.1 Design goals and decisions

We identify the following design goals for persistent memory allocators tailored for large-scale SCM-based systems:

Allocator	Purpose	Pool Structure	Allocation Strategies	Concurrency Handling	Garbage Collection	Defragmentation	Reference
Mnemosyne	General	Multiple files	Segregated-fit + best-fit	Thread-local for small blocks; global lock for large blocks	Yes	No	Volos et al. [168]
NV-Heaps	General	Single file	Undefined	Thread-local	Yes	No	Coburn et al. [24]
nvm_malloc	General	Single file	Segregated-fit + best-fit	Thread-local for small blocks; global lock for large blocks	No	No	Schwalb et al. [147]
NVML	General	Single file	Segregated-fit + best-fit	Thread-local for small blocks; global lock for large blocks	No	No	`http://pmem.io`
Makalu	General	Single file	Segregated-fit + best-fit	Thread-local for small blocks; global lock for large blocks	Yes (offline)	No	Bhandari et al. [13]
PAllocator	Special (large-scale systems)	Multiple files	Segregated-fit + best-fit + file	Core-local for small and large blocks; global lock for huge blocks	No	Yes	Oukid et al. [124]

Table 3.2: Summary of the design characteristics of existing persistent memory allocators. There are salient differences in the design decisions of PAllocator and state-of-the-art persistent allocators.

- The ability to adapt to changes in available memory resources. This is particularly important in a cloud environment.
- High concurrency scalability. Large main-memory systems run on multi-socket systems with up to 1000 cores. Thus, it is important for the persistent allocator to provide robust and scalable performance.
- Provide robust performance for all sizes of allocations, as database-system allocation sizes cover a wide range, from a few bytes to hundreds of gigabytes.
- Fast recovery. Currently there are instances of single-node main-memory database systems such as SAP HANA [44] with up to 48 TB of main memory. With SCM this capacity will quickly exceed 100 TB. Thus, the persistent allocator must exhibit fast recovery and should not rely on scanning memory to recover its metadata.
- Defragmentation ability; Database systems run for a very long time, much longer than general-purpose applications, making fragmentation much more likely to happen.

So far, state-of-the-art persistent allocators, such as NVML, nvm_malloc, and Makalu have been engineered as general-purpose allocators, taking inspiration from state-of-the-art general-purpose transient allocators. We argue that they are unfit for large-scale SCM-based database systems because:

- They all use a single pool (file), which is difficult to both grow and shrink (to the best of our knowledge, none of them can grow or shrink their pool beyond its initial size).
- They put an emphasis on the scalability of small-block allocations (from a few bytes up to a few kilobytes), and neglect that of middle-sized and large-block allocations.
- They do not provide defragmentation capabilities.
- They often rely on scanning memory to recover their metadata during recovery.

PAllocator is not a general-purpose allocator. It fulfills the above design goals following radically different design decisions than state-of-the-art persistent allocators:

- We use multiple files instead of a single pool, which allows us to easily grow and shrink our pool of persistent memory.
- We use large files to avoid having a large number of them which would hit the limitations of current file systems.
- We use three different allocation strategies for small, big, and huge allocation sizes, mostly independent from each other, to ensure robust performance for all allocation sizes.
- We aggressively cache free memory by not removing free files. Instead, we keep them to speed up future allocations. This is acceptable since main-memory database systems usually have dedicated resources.
- Instead of thread-local pools, we use one allocator object per physical core. Database systems can create and terminate threads at a high rate during query processing. Using thread-local pools in this case might hurt performance and complicates fail-safety management as the local pool has to be given back and integrated in the global pool upon thread termination. Using striping per physical core combined with aggressive caching provides a stable, robust, and scalable allocation and deallocation performance.
- To defragment memory, we leverage the hole punching feature of sparse files. This is an additional advantage of using multiple files.
- To provide fast recovery, we persist most of PAllocator's metadata and rely on hybrid SCM-DRAM trees to trade off between performance and recovery time when necessary.

3.4.2 Programming Model

We assume that SCM is managed by a file system that provides direct access to the application layer through memory mapping. To retrieve data, we use *persistent pointers*, which consist of an 8-byte file ID and an 8-byte offset within that file. We devise two classes: PPtrBase and PPtr. PPtrBase is an untyped persistent pointer, equivalent to `void*`. PPtr inherits from PPtrBase and is a template, that is, it is aware of its type, and it also provides a cast function:

```
class alignas(16) PPtrBase {
    uint64_t fileID;
    ptrdiff_t offset;
    void* toPtrBase(); // Swizzling function
};
template<typename T>
class PPtr : PPtrBase {
    T* toPtr(); // Swizzling function
    template<typename U>
    PPtr<U>& as(); // Cast function
};
```

Persistent pointers are aligned to 16-bytes to make sure that the file ID and the offset reside in the same cache line. Since persistent pointers are 16-byte large, they cannot be assigned p-atomically. To remedy this issue, we adopt the convention that a null pointer is a pointer with fileID equal to -1. Thus, by setting the offset first, then the file ID, we ensure that the persistent pointer is moved p-atomically from a null value to a valid value. As will be explained in Section 3.4.3, persistent pointers can be swizzled (converted) to ordinary, virtual memory pointers and vice versa.

To prevent memory leaks, we changed the allocation interface to take as argument a reference to a PPtrBase:

```
allocate(PPtrBase &p, size_t allocationSize)
deallocate(PPtrBase &p)
```

The data structure must provide a persistent pointer that resides in SCM, where the allocate function can write the address of the allocated memory before returning. This ensures that the data structure has always a handle on its requested allocation, even in case of a crash. Hence, the responsibility of avoiding memory leaks is split between the allocator and the requesting data structure: If a crash occurs before the allocate function has persistently written the address of the allocated memory into the provided PPtrBase, it is the allocator's responsiblity to catch the memory leak during recovery; otherwise, the allocator considers that the allocation has successfully completed, and the data structure has a handle on the allocated memory. Additionally, the deallocate function resets the provided persistent pointer to null in order to prevent dangling persistent pointers.

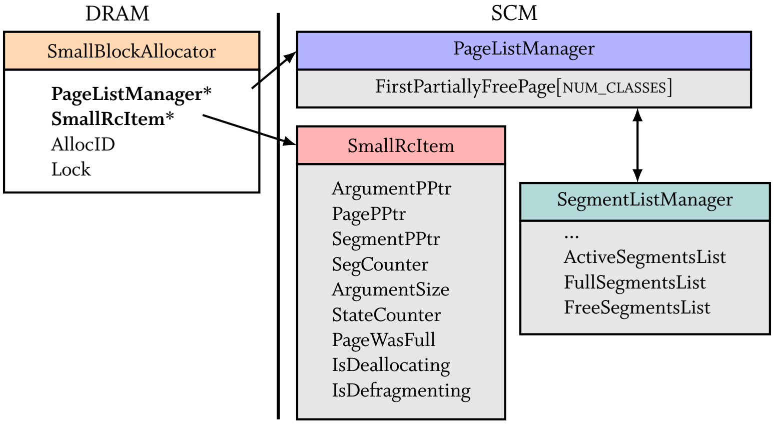

Figure 3.8: Architecture overview of SmallPAllocator.

3.4.3 PAllocator Architecture

PAllocator is a highly scalable persistent allocator specifically designed for SCM-based systems that use large amounts of memory. PAllocator does not keep a single memory pool like previous works. Instead, it creates multiple files, referred to as *segments*, on a need basis.

Figure 3.7 illustrates the architecture of PAllocator. It uses three different allocators: SmallPAllocator, BigPAllocator, and HugePAllocator. SmallPAllocator handles allocations in the range [64 B, 16 KB), while BigPAllocator handles allocations in the range [16 KB, 16 MB). Larger allocations are handled by HugePAllocator. For concurrency, PAllocator maintains one SmallPAllocator and one BigPAllocator object per core, while maintaining only a single HugePAllocator, as huge allocations are bound by the operating system and file system performance. Indeed, HugePAllocator creates one segment per allocation, and deletes that segment on deallocation. Although simple, this approach has the advantage of avoiding any memory fragmentation. SmallPAllocator and BigPAllocator objects are instantiated in transient memory and initialized with references to their persistent metadata. The internals of SmallPAllocator and BigPAllocator are detailed in Sections 3.4.4 and 3.4.5, respectively.

PAllocator maintains a special segment, called *Anchor Segment*, where it keeps critical metadata for recovery purposes (See Figure 3.7). Furthermore, PAllocatorAnchor keeps one PageListManager (PLM_i) and one BigBlockManager (BBM_i) for each SmallPAllocator and BigPAllocator, respectively. The use of these structures is detailed in Sections 3.4.4 and 3.4.5, respectively. Additionally, the different allocators rely on micro-logs to ensure the atomicity of allocations and deallocations across failures. These micro-logs are referred to as *Recovery Items*. The RecoveryItemManager maintains one such recovery item for each allocator object.

SegmentListManager is a central component of our design and is responsible for creating segments. It has a transient part and a persistent part. The persistent part maintains a global segment counter, a shared list of free segments, and for each SmallPAllocator, a list of active segments (ASL_i) as well as a list of full segments (FSL_i). The use of these lists is explained in Section 3.4.4.

The transient part of SegmentListManager maintains the following segment mappings (See DRAM side of Figure 3.7):

- SegIDToAddress: It maps segment IDs to their corresponding virtual addresses. This map is used to swizzle persistent pointers to ordinary pointers by fetching the address of a segment and adding the offset.

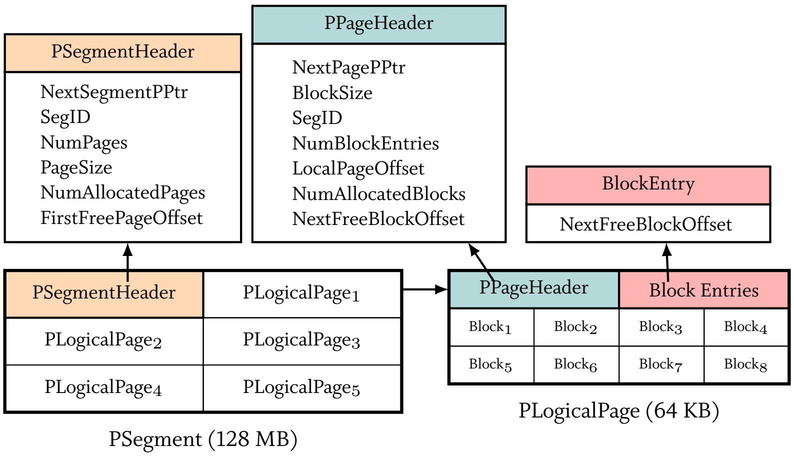

Figure 3.9: Data organization in SmallPAllocator.

- AddressToSegInfo: It maps the virtual address of a segment to its ID and size. This map is used to swizzle ordinary pointers to persistent pointers by getting an upper bound of the address, checking whether it is in the address range of the returned segment using its size, computing the offset and returning the corresponding persistent pointer.
- SegIDToAllocID: It maps a segment ID to its owner allocator ID. Segments are not shared between allocator objects, which implies that the allocator object that allocated a block is also responsible for deallocating it. Indeed, allocator objects operate independently from each other. This map is used in deallocations to identify the allocator object that should perform the deallocation.

These mappings are stored in transient memory for better performance, and are easily retrieved from persistent metadata during recovery, as detailed in Section 3.4.7.

3.4.4 SmallPAllocator

SmallPAllocator relies on a segregated-fit allocation algorithm. It has 40 size classes, ranging from 64 B to 15 KB. We align all allocations to a cache-line-size (typically 64 B) in order to avoid false sharing of cache lines which could unintentionally evict adjacent data when flushed. Figure 3.8 gives an overview of the architecture of SmallPAllocator. Its two main auxiliary data structures are PageListManager and SmallRcItem. PageListManager consists of an array that contains a persistent pointer to the first partially free page of a class size. It interacts with SegmentListManager to get new free pages when needed upon allocations, and to return completely free pages upon deallocation. Each SmallPAllocator owns a set of segments which are represented by the ActiveSegmentsList and FullSegmentsList in SegmentListManager. SmallRcItem is a 64-byte long recovery item. It is used to log ongoing allocation or deallocation information to ensure their atomicity in case of a crash. For instance, ArgumentPPtr stores the persistent address of the persistent pointer provided by the requester, which enables SmallPAllocator to inspect it upon recovery to see if it completed the allocation process.

Figure 3.9 illustrates data organization in SmallPAllocator. Each segment is 128 MB large, and is divided into logical pages of 64 KB, the first of which serves as the segment header. Segments are chained together using NextSegmentPPtr to form either the active or the full segments list whose heads are stored in SegmentListManager. Similarly, pages of the same size class are linked using NextPagePPtr to a list whose head is stored in PageListManager. Pages are in turn divided into blocks of the same size. To track its blocks, a page stores one 2-byte BlockEntry per block, which represents

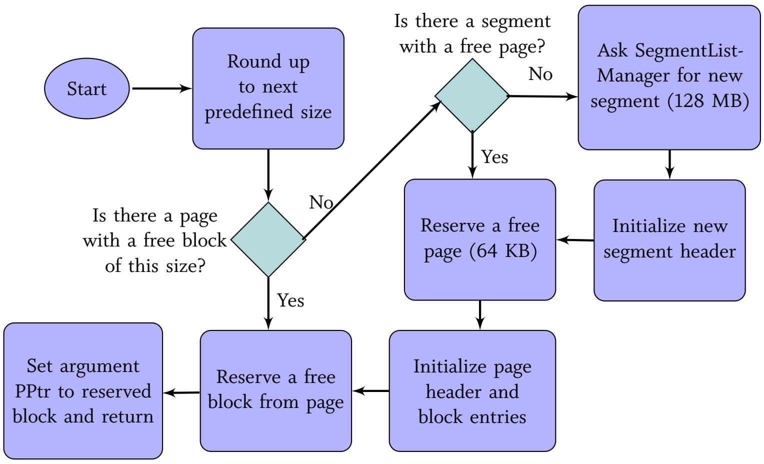
Start
Round up to next predefined size
Is there a page with a free block of this size?
No
Yes
Is there a segment with a free page?
No
Yes
Ask SegmentList-Manager for new segment (128 MB)
Initialize new segment header
Reserve a free page (64 KB)
Initialize page header and block entries
Reserve a free block from page
Set argument PPtr to reserved block and return

Figure 3.10: Allocation process of SmallPAllocator.

the offset of the next free block, hence forming a list whose head is referenced by NextFreeBlockOffset in the page header.

To illustrate how all the components of SmallPAllocator interact together, we depict in Figure 3.10 its allocation process. For the sake of clarity, we do not include operations on recovery items. First, the requested size is rounded up to the nearest predefined size class. Then, PageListManager checks whether there is a partially free page of this size, in which case it reserves the block pointed to by NextFreeBlockOffset in the page header by popping the head of the list of blocks; or if no free page is available, then PageListManager requests a free page from SegmentListManager, which returns a page from the head of the active segments list, creating a segment in the process if the latter is empty. Thereafter, the page header and block entries are initialized and a block is reserved.

Note that if a segment becomes empty after a deallocation, it is not returned to the system. Rather, free segments are chained in the FreeSegmentsList of SegmentListManager to avoid the cost of segment creation and page faults. This is a commonly used technique for transient memory in main-memory databases which implement their own internal memory management [44, 106].

3.4.5 BigPAllocator

BigPAllocator is a tree-based allocator that uses a best-fit algorithm. It is responsible for allocating blocks ranging from 16 KB to 16 MB. To enable defragmentation (see Section 3.4.6), all blocks are aligned to a system page size (usually 4 KB). Figure 3.11 gives an overview of BigPAllocator. It comprises two main auxiliary data structures: BigBlockManager and BigRcItem, which is a 128-byte recovery item used to ensure fail-safe atomicity of BigPAllocator's operations. BigBlockManager is responsible for keeping the topology of allocated and free blocks. To this aim, it comprises two trees:

- *Free blocks tree*: a set of pairs of a block size and its persistent pointer. It keeps track of free blocks.
- *BlockInfo tree*: a maps of the persistent pointers of all existing blocks to their corresponding BlockInfo.

A BlockInfo is 8-bytes long and consists of the block size and three flags: IsUsed indicates whether a block is allocated; IsLastBlock indicates whether a block is at the end of a segment; and IsHole indicates whether a block is a hole.

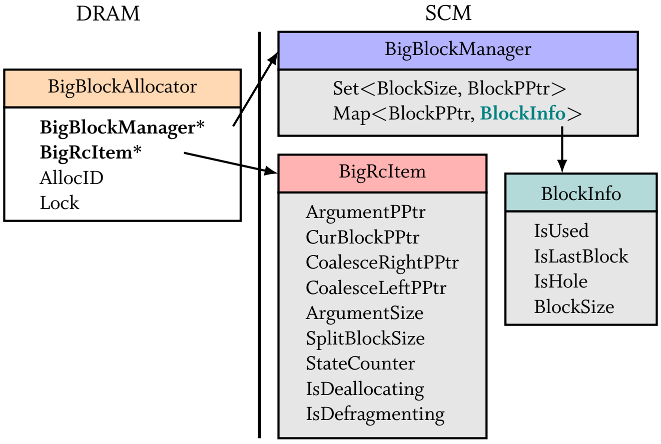

Figure 3.11: Architecture overview of BigPAllocator.

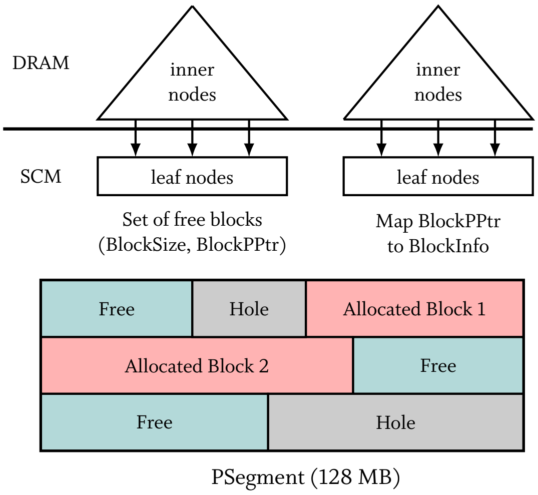

Figure 3.12: Data organization in BigPAllocator.

Figure 3.12 illustrates data organization in BigPAllocator. Similarly to SmallPAllocator, it uses segments of 128 MB that are then divided with a best-fit strategy into blocks of different sizes. We purposefully make SmallPAllocator and BigPAllocator segments of the same size to enable both to fetch segments from FreeSegmentsList. The trees of BigBlockManager are implemented using the FPTree [126], a hybrid SCM-DRAM persistent tree, which store a linked list of leaf nodes in SCM and keep inner nodes in DRAM for better performance. Upon recovery, the leaf nodes are scanned to rebuild the inner nodes. These hybrid trees use the small block allocators to allocate their leaf nodes. We chose to use the FPTree because it provides near-DRAM performance while recovering up to two orders of magnitude faster than a full rebuild of a transient counterpart.

To illustrate how the different components of BigPAllocator interact together, we depict its allocation process in Figure 3.13. For the sake of clarity, we do not include operations on recovery items. First, with a lower bound operation on the free blocks tree, using as search key the requested size and a null pointer, the smallest free block that is larger than the requested block is retrieved. If no block was found, then a request for a new segment is made to SegmentListManager, and the returned segment is inserted in the free blocks tree. Thereafter, if the block is larger than the requested size, it is split into two blocks: the left one is kept free and its size updated both in the free blocks tree and its BlockInfo, while the right one, whose size is equal to the requested size, is inserted as a new allocated block in the BlockInfo tree.

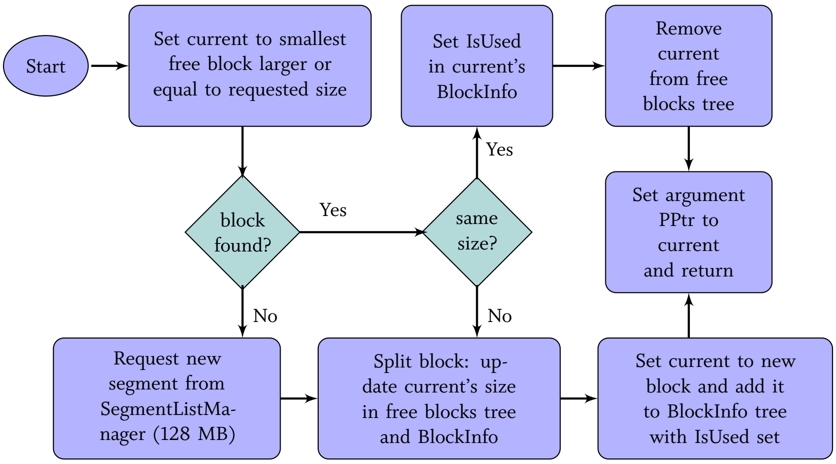
Start
Set current to smallest free block larger or equal to requested size
block found?
Yes
No
same size?
Yes
No
Set IsUsed in current's BlockInfo
Remove current from free blocks tree
Set argument PPtr to current and return
Request new segment from SegmentListManager (128 MB)
Split block: update current's size in free blocks tree and BlockInfo
Set current to new block and add it to BlockInfo tree with IsUsed set

Figure 3.13: Allocation process of BigPAllocator.

3.4.6 Defragmentation

NVML and nvm_malloc do not have any mechanism to defragment persistent memory. Both create a single memory pool which exacerbates fragmentation in the presence of frequent large allocations and deallocations. The segregated-fit approach of PAllocator, NVML, and nvm_malloc already limits fragmentation for small blocks. In contrast, the tree-based big block allocators of the aforementioned allocators are more prone to fragmentation. To make matters worse, NVML and NVMalloc service huge allocation requests through their respective pool, which makes them fail when no matching free contiguous block exists in the pool. PAllocator, however, creates one segment per huge allocation, enabling it to avoid any fragmentation that might arise from huge allocations. This highlights the benefits of having multiple segments instead of a single large pool. Additionally, PAllocator implements an efficient defragmentation mechanism that we detail in this section.

To defragment memory, PAllocator relies on the hole punching feature of sparse files. When an allocation fails because PAllocator was unable to create a segment, the allocation request is first redirected to the other allocator objects in a round-robin fashion, until one of them succeeds, because one of them might have a partially free segment with a matching free block. If all of them fail, then a defragmentation request of the requested segment size is made. The defragmentation process first checks the free segments list in SegmentListManager and removes as many of them as needed. If that is not enough, then the segments of BigPAllocator are defragmented. The latter process is illustrated in Figure 3.14.

The defragmentation process starts by getting the largest free block available in the free blocks tree. Then, it updates its BlockInfo by setting IsHole to true, and punches a hole of the size of the block in the corresponding segment. We use *fallocate*[3] with the flags FALLOC_FL_PUNCH_HOLE and FALLOC_FL_KEEP_SIZE to perform the hole punch. Note that the latter flag enables the segment to keep its apparent size, which is required since collapsing the punched hole could invalidate the offsets of existing persistent pointers. Punching holes in free blocks is safe because they are aligned to a system page size. Thereafter, the defragmentation process erases the current block from the free blocks trees, and gets handles on its left and right neighbors from the BlockInfo tree. If the left neighbor is a hole, then it is coalesced with the current block by updating its size and erasing the current block from the BlockInfo tree. The current block is then set to the left neighbor. If the right neighbor is a hole, then it is coalesced with the current block by updating the size of the current block

---

[3] `http://man7.org/linux/man-pages/man2/fallocate.2.html`

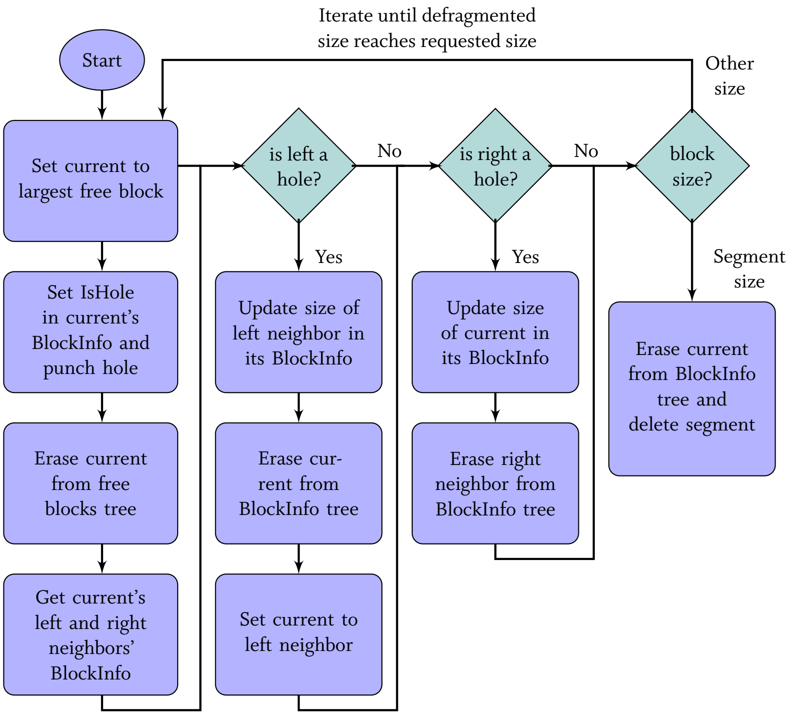
Iterate until defragmented size reaches requested size
Start
Set current to largest free block
Set IsHole in current's BlockInfo and punch hole
Erase current from free blocks tree
Get current's left and right neighbors' BlockInfo
is left a hole?
No
Yes
Update size of left neighbor in its BlockInfo
Erase current from BlockInfo tree
Set current to left neighbor
is right a hole?
No
Yes
Update size of current in its BlockInfo
Erase right neighbor from BlockInfo tree
block size?
Other size
Segment size
Erase current from BlockInfo tree and delete segment

Figure 3.14: Defragmentation process of BigPAllocator.

and erasing the right neighbor from the BlockInfo tree. Finally, if the size of the current block is equal to that of a segment, then the whole segment is a hole, in which case it is deleted both from the BlockInfo tree and from the file system. This process is repeated until either we reach the requested size, or no more free blocks exist.

Figure 3.14 does not show the use of the recovery items. Nevertheless, the defragmentation process uses them to achieve fail-safe atomicity. In case of a failure during defragmentation, PAllocator rolls forward during recovery only the defragmentation iteration that was ongoing at failure time. The recovery is greatly simplified since removing from a tree and punching a hole in a file are both idempotent operations.

One limitation of our defragmentation algorithm is that holes are still memory mapped, hence blocking address space. To mitigate this issue, we propose to collapse holes that are located at the end of a segment and remap the latter by shrinking the existing memory mapping.

Additionally, SmallPAllocator can also be defragmented by punching holes in free logical pages, and subtracting them from the number of pages in the segment header, which allows us to account for logical page holes when deciding if a segment if empty.

3.4.7 Recovery

PAllocator uses the status flag in the anchor segment to check whether a failure occurred before the end of the initialization process, in which case the initialization is restarted from scratch. If a failure occurs after the initialization completed, then PAllocator starts recovery by memory mapping all existing segments and reconstructing SegIDToAddress and AddressToSegInfo of SegmentListManager. Thereafter, PAllocator instantiates the allocator objects and calls their respective recovery functions,

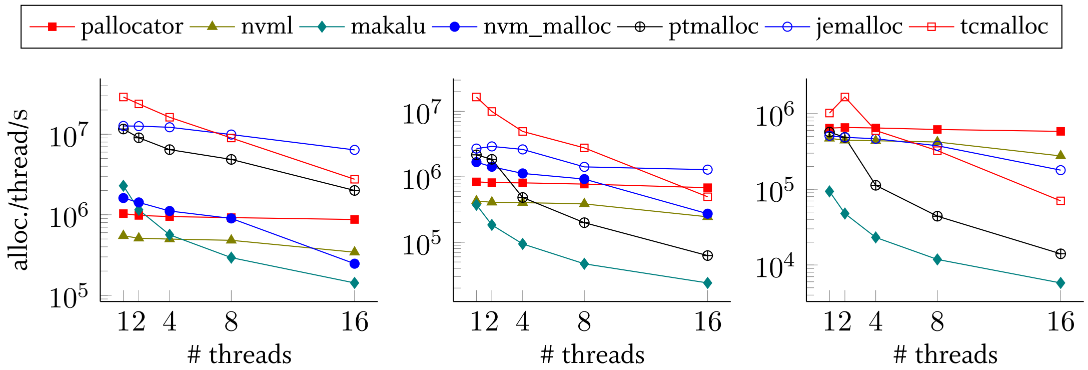

(a) 128 B (b) 1 KB (c) 8 KB

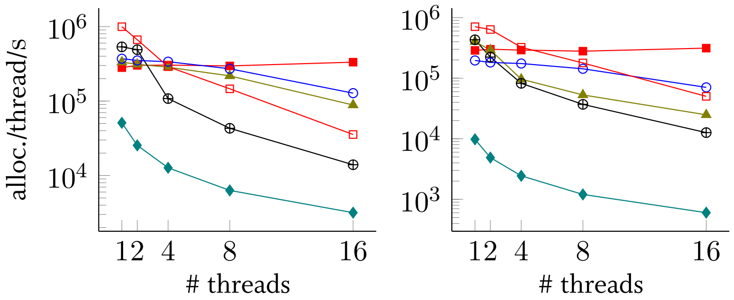

(d) 64 KB (e) 512 KB

Figure 3.15: Allocations concurrency scalability for different object sizes.

which check the recovery items and restore the allocator to a consistent state in case the failure happened during an allocation or a deallocation. Note that the recovery of BigPAllocator involves reconstructing the inner nodes of its hybrid trees from the persistent leaf nodes. Finally, PAllocator recovers the SegIDToAllocID map as follows:

1. All segments are initially assigned to HugePAllocator.
2. The active segments list and full segments list, located in SegmentListManager, of each SmallPAllocator are scanned. This enables to restore segment ownership information of all SmallPAllocators.
3. The recovery of a hybrid tree involves scanning the persistent leaf nodes to retrieve the max key in each one of them, which are in turn used to reconstruct the inner nodes. We extend the recovery of the BlockInfo tree to extract a list of encountered segments while scanning the leaf nodes, which is sufficient to restore segment ownership information of all BigPAllocators.
4. The segments present in the FreeSegmentsList are not assigned to any allocator.
5. The segments whose ownership has not been updated remain assigned to HugePAllocator.

Recovery time is dominated by the recovery of the trees of BigPAllocator when these are large. Nevertheless, hybrid trees recovery is one to two orders of magnitude faster than that of transient counterparts. Note that the recovery of segments that contain holes does not pose any challenge and are recovered in the same way as segments without holes.

3.5 EVALUATION

Experimental setup. We run our experiments on an SCM emulation system provided by Intel. It is equipped with 4 8-core Intel Xeon E5-4620 v2 processors clocked at 2.60 GHz. Each core has 32 KB

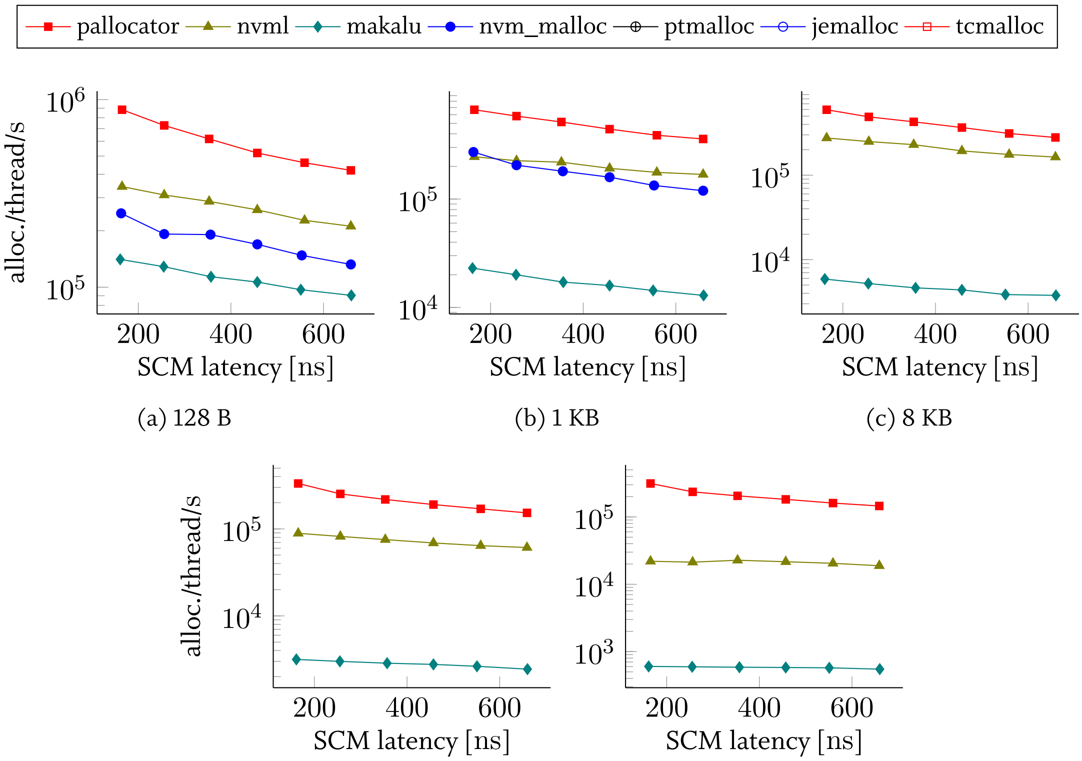

(a) 128 B (b) 1 KB (c) 8 KB

(d) 64 KB (e) 512 KB

Figure 3.16: Allocations performance for different object sizes and SCM latencies.

L1 data and 32 KB L1 instruction cache and 256 KB L2 cache. The cores of one processor share a 20 MB last level cache. To emulate SCM, two sockets are disabled and their memory is interleaved at a cache-line granularity and reserved as a separate persistent memory region. Thanks to a special BIOS, the latency of this memory region can be configured to a specified value. A detailed description of this system is publicly available [38]. The system has 64 GB of DRAM and 359 GB of emulated SCM on which we mount *ext4* with DAX. The system runs Linux kernel *4.8.0-rc4*.

In addition to PAllocator, we evaluate the following state-of-the-art persistent allocators:

- NVML v1.1[4]: We use `libpmemobj`'s POBJ_ALLOC to allocate and POBJ_FREE to deallocate.
- nvm_malloc[5]: We use nvm_reserve + nvm_activate to allocate, and nvm_free to deallocate. To keep track of allocated objects, we provide the allocation and deallocation functions with a single link pointer.
- Makalu[6]: We use MAK_malloc/MAK_free to allocate/deallocate. We track allocated objects using a linked list.

We intentionally exclude NVMalloc[7] from our experiments because it uses anonymous memory mapping as a means to emulate SCM, and does not provide any recovery mechanism. As a baseline, we also include in our experiments the following state-of-the-art transient memory allocators:

- *ptmalloc*: The GNU C library allocator. We use *glibc* v2.19.

---

[4] `https://github.com/pmem/nvml/releases`

[5] `https://github.com/IMCG/nvm-malloc`

[6] `https://github.com/HewlettPackard/Atlas/tree/makalu`

[7] `https://github.com/efficient/nvram/`

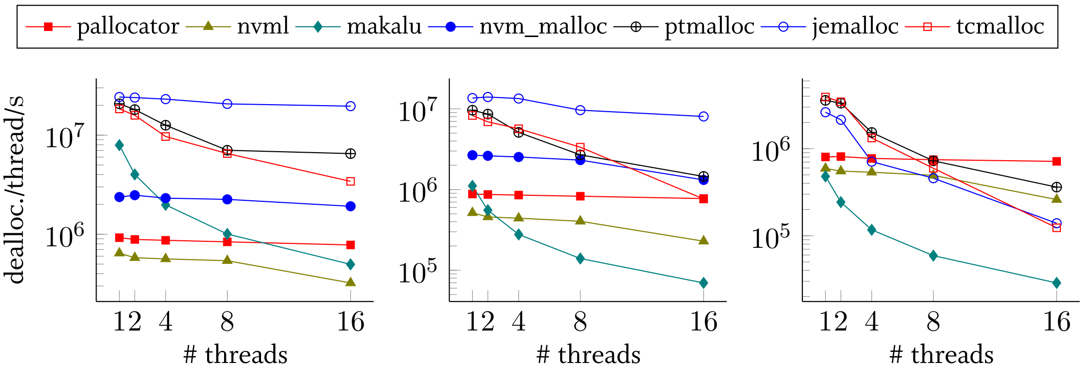

(a) 128 B (b) 1 KB (c) 8 KB

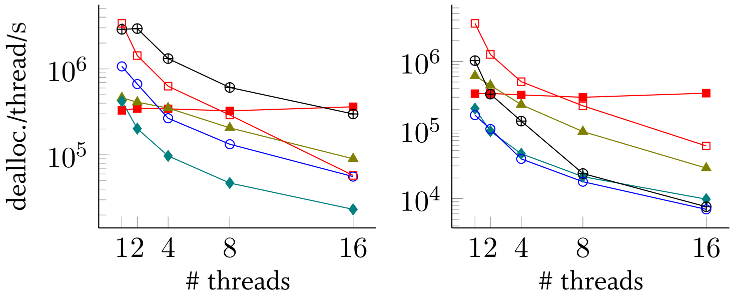

(d) 64 KB (e) 512 KB

Figure 3.17: Deallocation concurrency scalability for different object sizes.

- *jemalloc* v4.2.1: An allocator designed for fragmentation avoidance and high concurrency scalability.
- *tcmalloc (gperftools v2.5)*: An allocator designed for high concurrency scalability through thread-caching.

We compile all tests with *gcc-4.8.5* with full optimizations. We let the operating system schedule the threads but we forbid thread migration between sockets in order to get more stable results. In all experiments where we vary the number of threads, we set the latency of SCM to the minimum latency, namely 160 ns, which corresponds to the normal remote-socket latency. This gives us the best performance evaluation since higher latencies are emulated using microcode and do not account for out-of-order execution and instruction prefetchers. All reported results are the average of 5 runs.

3.5.1 Standalone allocation and deallocation

To evaluate standalone allocation and deallocation performance, we designed a benchmark that takes as parameters a fixed object size, a number of threads, and the number of allocations per thread N. The program first executes the requested allocations as a warm-up, then it deallocates all objects and allocates them again. We measure the time of the latter deallocation and allocation phases separately. We set $N = 500k$ for object sizes 128 B, 1 KB, and 8 KB, $N = 80k$ for 64 KB, and $N = 10k$ for 512 KB. The goal of the warm-up phase is to trigger all page faults to decouple the performance of the allocators from kernel operations. This is especially important in concurrent environments where kernel locking can be an important performance factor. We report the results in Figure 3.15 and Figure 3.17. Note that we depict results of nvm_malloc only for object sizes 128 B and 1 KB, because nvm_malloc uses a non-balanced binary tree to index allocated and free blocks greater than

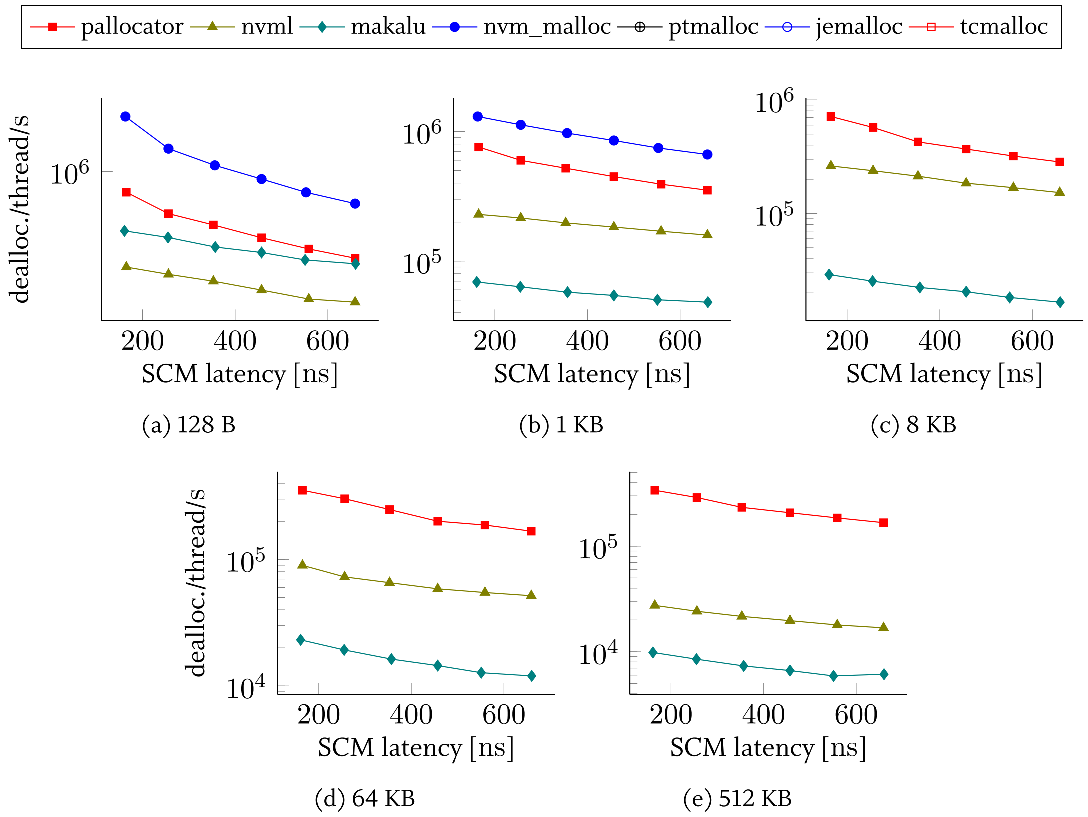

(a) 128 B (b) 1 KB (c) 8 KB

(d) 64 KB (e) 512 KB

Figure 3.18: Deallocation performance for different object sizes and SCM latencies.

2 KB. Since the object size is fixed in this experiment, the binary trees degenerate into linked-lists, thus incurring severe performance issues.

Figures 3.15a-3.15e show allocation throughput per thread for different allocation sizes. For small sizes (128 B and 1 KB), we observe that PAllocator scales linearly; it retains nearly the same throughput per thread with 16 threads as with one thread. NVML scales nearly linearly as well, but with a drop from 8 to 16 threads. In contrast, Makalu and nvm_malloc scale less than the aforementioned counterparts. Indeed, Makalu and nvm_malloc are the fastest single-threaded but the slowest with 16 threads. Worse, Makalu's performance degrades linearly for sizes 1 KB and higher, because it uses thread-local allocation only for small blocks, and relies on a global structure for larger blocks, which results in poor scalability. Overall, PAllocator scales better and significantly outperforms NVML and Makalu, and nvm_malloc with 16 threads. For 128 B allocations, transient allocators are one to two orders of magnitude faster than the persistent ones. This is expected since persistent allocators use expensive flushing instructions. Yet, the performance gap narrows significantly at 16 threads, except for jemalloc which remains one order of magnitude faster. For 1 KB allocations however, only tcmalloc is one to two orders of magnitude faster than persistent counterparts with one thread. With 16 threads, PAllocator outperforms ptmalloc and tcmalloc, and performs in the same order of magnitude as jemalloc.

For medium sizes (8 KB and 64 KB), we observe that PAllocator still scales linearly, while NVML scales less compared with the small objects case. This is because the design of NVML emphasizes fragmentation avoidance and thus grants chunks of only 256 KB at once to local thread caches. This leads to lock contention as thread local caches request more often chunks with 1 KB allocations than with 128 B ones. PAllocator is able to significantly outperform all transient allocators with 16 threads. In fact, the larger the allocation size, the less the transient allocators scale, especially ptmalloc which is outperformed by both PAllocator and NVML with only two threads.

For large sizes (512 KB), we observe that PAllocator is the only allocator that scales linearly, and it outperforms NVML and all transient allocators with only 2 threads. We note that NVML is faster than PAllocator with one thread: NVML uses transient trees to index its large blocks, while we use hybrid SCM-DRAM trees which incur a small additional overhead but enable much faster recovery (see recovery experiments below).

Figures 3.16a-3.16e show allocation throughput per thread for different allocation sizes, varying SCM latencies, and 16 threads. We observe that performance degrades with higher latencies, but the overhead does not exceed 54%, 43%, 44%, and 57% for PAllocator, NVML, Makalu, and nvm_malloc, respectively, with an SCM latency of $650\,\text{ns}$ compared with $160\,\text{ns}$. We also observe that for allocation sizes 64 KB and 512 KB, PAllocator seems to suffer more from higher SCM latencies than NVML. This is explained by two factors: (1) the bottleneck for NVML with 16 threads is synchronization rather than persistence; and (2) accessing the leaf nodes of PAllocator's hybrid trees becomes more expensive with higher SCM latencies.

Figures 3.17a-3.17e show deallocation throughput per thread for different allocation sizes. Similar to allocations, PAllocator scales linearly for all allocation sizes. NVML exhibits similar behaviour to its allocations as well and has lower throughput than PAllocator except for sizes 64 KB and 512 KB with up to 4 threads. This is again explained by the fact that PAllocator uses its big block allocator for these allocation sizes, which involves operations on its hybrid trees that incur an extra overhead compared with NVML's transient counterparts. We note that nvm_malloc has $2\times$ higher throughput for deallocations than for allocations for sizes 128 B and 1 KB, and outperforms PAllocator even with 16 threads. Indeed, in contrast to its allocations, nvm_malloc deallocations scale linearly. As for Makalu, it is the fastest for 128 B, but its performance drops linearly in all cases. Interestingly, with 16 threads and for 8 KB and larger, PAllocator outperforms again all allocators including transient ones.

Figures 3.18a-3.18e show deallocation throughput per thread for different allocation sizes, varying SCM latencies, and 16 threads. We observe the same patterns as with allocations. We note that the performance of all persistent allocators degrades gradually with increasing SCM latencies up to 60%, 46%, 48%, and 64% for PAllocator, NVML, Makalu, and nvm_malloc, respectively, with an SCM latency of $650\,\text{ns}$ compared with $160\,\text{ns}$. We argue that this drop is still acceptable given the $4\times$ higher latency.

3.5.2 Random allocation and deallocation

In this experiment we evaluate the performance of mixed random allocations and deallocations. The experiment consists in executing 10 iterations of N allocations followed by N deallocations of random size per thread. We fix the range of object sizes between 64 B and 128 KB, and we consider three different object size distributions: (1) Uniform distribution; (2) Binomial distribution with skew factor 0.01 to emphasize smaller sizes; (3) Binomial distribution with skew factor 0.7 to emphasize larger sizes. We set $N = 500k$ for Binomial small, and $N = 50k$ for Uniform and Binomial large. Figure 3.19 depicts the results.

Figures 3.19a-3.19c show operation throughput per thread. We observe that PAllocator scales linearly for all distributions. Additionally, it manages to outperform all transient allocators in the Uniform and Binomial large cases, while outperforming only ptmalloc in the Binomial small case. In the Uniform case, PAllocator outperforms NVML, Makalu, and nvm_malloc by up to $7.5\times$, $49.7\times$, and $6.7\times$, respectively. nvm_malloc's performance degrades significantly in the case of Binomial large because

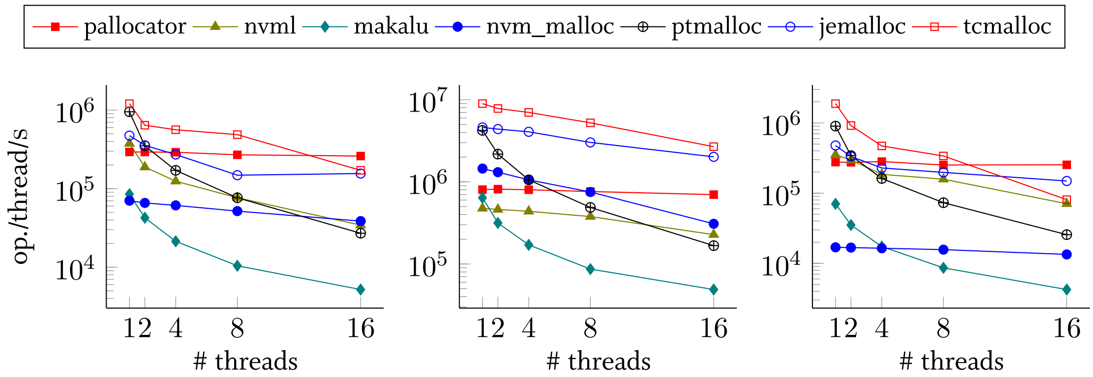

(a) Uniform (b) Binomial small (c) Binomial large

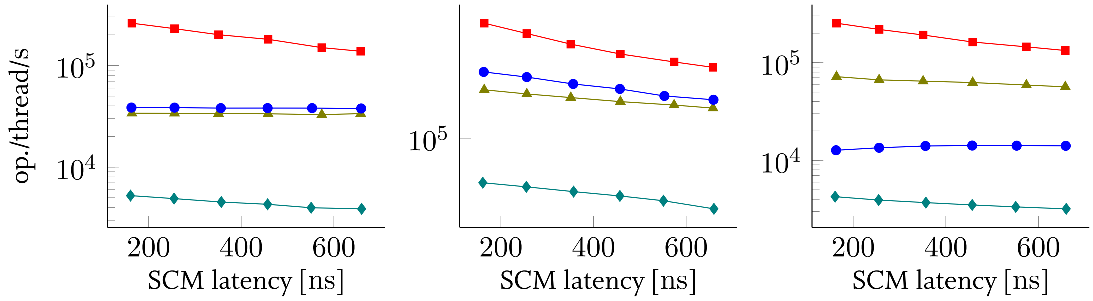

(d) Uniform (e) Binomial small (f) Binomial large

Figure 3.19: Random allocation/deallocation benchmark with different distributions.

of its binary trees and is 19× slower than PAllocator. Makalu's behavior is similar to the previous experiment as its performance degrades linearly with increasing threads.

Figures 3.19d-3.19f show operation throughput per thread for varying SCM latencies with 16 threads. The drop in the performance of PAllocator is limited to 47% with an SCM latency of $650\,\text{ns}$ compared with $160\,\text{ns}$. Nevertheless, PAllocator still outperforms Makalu, NVML, and nvm_malloc. The latter two show little performance degradation with higher SCM latencies since with 16 threads, their bottleneck is synchronization in addition to the binary trees for nvm_malloc.

3.5.3 Larson benchmark

We adapt the Larson benchmark from the Hoard[8] allocator benchmark suite [11] to the evaluated persistent allocators. The Larson benchmark simulates a server. In its warm-up phase, it creates N objects of random size per thread and shuffles the ownership of these objects between the threads. Thereafter, in a loop, it randomly selects a victim object to deallocate and replaces it with a newly allocated one of random size. After the warm-up phase, each thread executes in a loop $N \times L$ times the last sequence of the warm-up phase, where $N = 1k$ and $L = 10k$ in our experiments. We experiment with three object size ranges: 64 B–256 B (small), 1 KB–4 KB (medium), and 64 KB–256 KB (large). Results are depicted in Figure 3.20.

Figures 3.20a-3.20c show operation throughput per thread for different object size ranges. We observe that PAllocator is the only allocator to scale linearly in all three object size ranges. It outperforms NVML, Makalu, and nvm_malloc by up to $4.5\times$, $1.6\times$, and $3.9\times$, respectively, and is able to

---

[8] https://github.com/emeryberger/Hoard/

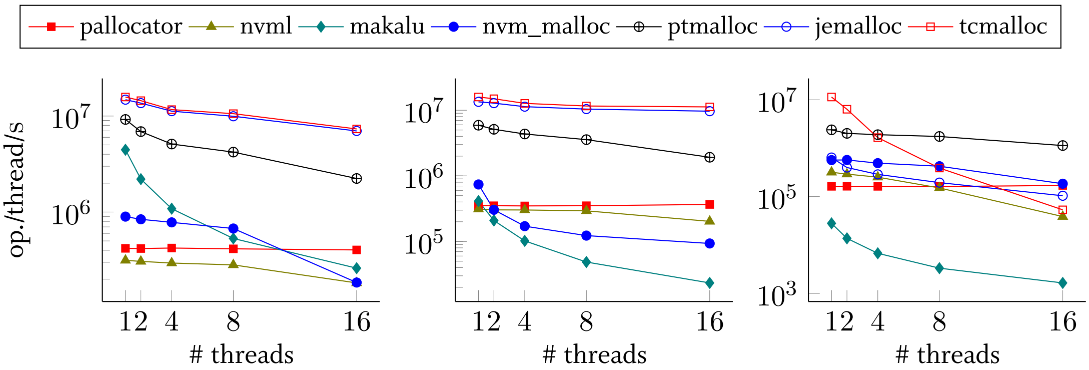

(a) 64 B - 256 B (b) 1 KB - 4 KB (c) 64 KB - 256 KB

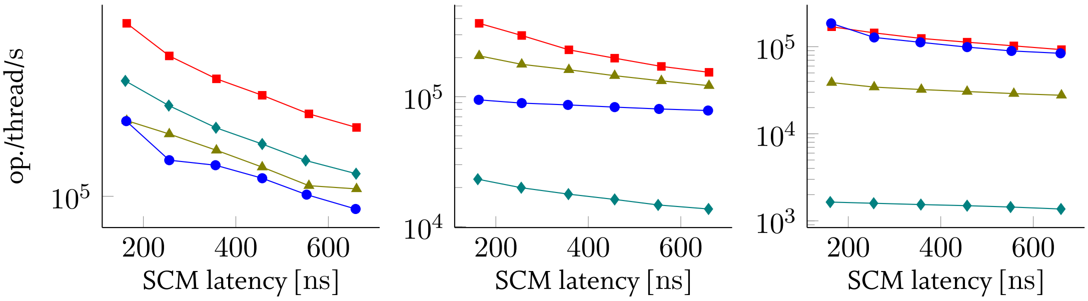

(d) 64 B - 256 B (e) 1 KB - 4 KB (f) 64 KB - 256 KB

Figure 3.20: Larson benchmark with different random allocation ranges.

outperform jemalloc and tcmalloc in size range 64 KB–256 KB with 16 threads. We note, however, that Makalu outperforms PAllocator in size range 64 B– 256B until 4 threads, partially thanks to the fact that the total size of allocated objects does not grow. Also, we note that nvm_malloc outperforms PAllocator in size range 64 B– 256B until 8 threads, and in size range 1 KB– 4 KB with one thread. Surprisingly, nvm_malloc scales well in size range 64 KB–256 KB, in contrast to size range 1 KB–4 KB, and outperforms PAllocator until 16 threads where the performances of the two allocators meet. This is explained by two factors: (1) the small number of allocated objects in this experiment maintains the binary trees of nvm_malloc very small; and (2) nvm_malloc rounds up allocation sizes to multiples of 4 KB starting from 2 KB requests. Consequently, in the range 1 KB–4 KB, half of the allocations are rounded up to 4 KB allocations, making the binary trees degenerate into linked-lists, while these are relatively balanced for size range 64 KB–256 KB.

Figures 3.20d-3.20f show operation throughput per thread for different object size ranges, different SCM latencies, and 16 threads. We observe that for size ranges 64 B–256 B and 64 KB–256 KB, the performance of the persistent allocators degrades in a similar way: up to 57%, 45%, 54%, and 56% for PAllocator, NVML, Makalu, and nvm_malloc, respectively, for an SCM latency of 160 ns compared with 160 ns. For size range 1 KB–4 KB however, we note that PAllocator is more sensitive to higher SCM latencies than NVML, Makalu, and nvm_malloc. This is partly explained by the fact that NVML, Makalu, and nvm_malloc suffer from other bottlenecks (synchronization) than persistence with 16 threads. Nevertheless, we found that NVML was consistently the least sensitive allocator to higher SCM latencies throughout all previous experiments.

We expect significant performance improvements with the new CLWB instruction, because PAllocator reads and flushes recovery items multiple times per operation. CLFLUSH evicts the recovery items from the CPU cache, leading to repeated cache misses as recovery items are accessed again shortly after. CLWB would remedy this issue.

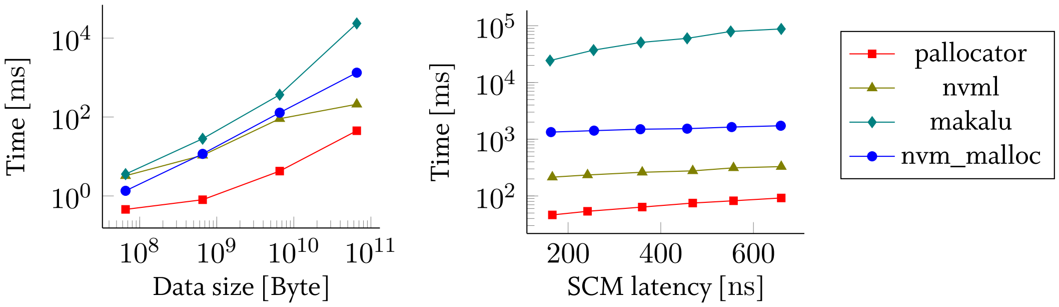

(a) Varying allocations size (b) Varying SCM latency

Figure 3.21: Recovery time for varying total allocation sizes and SCM latencies.

3.5.4 Recovery time

In this experiment we measure recovery time of PAllocator, NVML, and nvm_malloc– we exclude transient allocators. To do so, we first execute a fixed amount of allocation requests of sizes uniformly distributed between 64 B and 128 KB using 16 threads. Then, in a second run we measure the recovery time of the persistent allocator.

nvm_malloc re-creates upon recovery its arenas as if they were full, that is, all their chunks have no free blocks. Chunks can be recovered in two ways: (1) either nvm_malloc receives a deallocation request of a block that resides in a not-yet-recovered chunk, in which case the chunk is discovered and recovered; (2) or by a background thread created by the recovery process. If nvm_malloc receives an allocation request before its chunks have been recovered, it will create new ones, even if the non-recovered ones contain enough free space to service the allocation request. This has the effect of exacerbating (permanent) fragmentation, which is not acceptable, especially since nvm_malloc cannot defragment its memory. Hence, to avoid this, and to measure the total recovery time of nvm_malloc, we changed its recovery function to recover fully existing chunks before returning.

Makalu has two recovery modes: Upon normal process shutdown, Makalu flushes its metada to SCM and considers that garbage collection is not needed upon restart. If, however, the process was terminated due to a failure, Makalu will run an offline garbage collection process during recovery. In this experiment, we consider the second case.

Figure 3.21 depicts the results. In Figure 3.21a we fix the latency of SCM to 160 ns and vary the total size of allocations. We observe that PAllocator recovers significantly faster than NVML and nvm_malloc, and significantly faster than Makalu: with a total size of allocations of 61 GB, PAllocator recovers in 45 ms, while NVML, Makalu, and nvm_malloc recover in 210 ms, 23.5 s and 1.3 s, respectively. Makalu is the slowest to recover because it needs to execute an offline garbage collection, in addition to scanning its persistent metadata to rebuild its transient metadata. nvm_malloc is the second slowest to recover because it needs to scan persistent memory for existing blocks, while PAllocator and NVML keep enough metadata persisted to swiftly recover their allocation topology. The difference between PAllocator and NVML comes from the fact that NVML indexes metadata in transient trees, while PAllocator employs hybrid SCM-DRAM trees that are more than one order of magnitude faster to recover than the transient counterparts. Note that all three allocators implement only single-threaded recovery and could benefit from parallelizing their recovery process.

In Figure 3.21b we fix the total size of allocations to 61 GB, and vary the latency of SCM between 160 ns and 650 ns. We note that recovery time increases slowly with higher SCM latencies. Indeed, at

Allocator	#allocs	Defrag.	Runtime	Max block
Pallocator	2.1m	512 GB	358 s	2 GB
NVML	55.6k	na	8 s	128 KB
Makalu	303k	na	172 s	128 KB
nvm_malloc	0	na	na	64 KB

Table 3.3: Fragmentation stress test results.

an SCM latency of 650 ns, recovery times increased compared to those at an SCM latency of 160 ns by 100%, 54%, 260%, and 1.29% for PAllocator, NVML, and nvm_malloc, respectively. These increases are reasonable for an SCM latency increase of 4×. This is explained by the fact that the recovery processes of all three allocators involve mainly sequential reads which are more resilient to higher memory latencies thanks to hardware prefetching. The higher increase for PAllocator is explained by the recovery of the hybrid trees which dominates total recovery time. Since their leaf nodes are persisted in SCM as a list, scanning them during recovery involves sequential reads within a leaf node, but breaks the prefetching pipeline when accessing the next leaf node, hence resulting in a higher sensitivity to SCM latencies.

Extrapolated to a total allocations size of 1 TB, recovery times would be 0.75 s, 3.5 s, 394.5 s, and 22.5 s for PAllocator, NVML, Makalu, and nvm_malloc, respectively.

3.5.5 Defragmentation

In this experiment we focus on testing resilience to memory fragmentation of PAllocator, NVML, and nvm_malloc – we exclude transient allocators. NVML's pool size is set to the maximum available emulated SCM (359 GB). The warm-up phase consists of allocating 256 GB of 64 KB objects. Thereafter, we perform in a loop: (1) deallocate every other object until half of the allocated memory (i.e. 128 GB) is freed; and (2) allocate 128 GB of objects of double the previous allocation size. We deallocate objects in a sparse way to exacerbate fragmentation. We repeat this process until either the first allocation fails or we reach object size of 2 GB. The experiment is run single-threaded. We report the total number of allocated objects, the amount of defragmented memory for PAllocator, and the total runtime (excluding the warm-up phase) in Table 3.3. We notice that NVML and Makalu fail early and manage to execute only a small number of allocations, while nvm_malloc does not even complete the warm-up phase. Note that for Makalu, we had to increase the maximum number of sections in its configuration file from 1 K to 1 M for the warm-up phase to run through. PAllocator manages to reach the 2 GB object size threshold by defragmenting 512 GB of memory through several iterations, managing to execute 2.1 M allocations. This demonstrates the ability of PAllocator to efficiently defragment memory. Note that for sizes larger than 16 MB, in contrast to NVML and nvm_malloc, PAllocator does not create any fragmentation as it creates one segment per allocation.

3.5.6 Allocator impact on a persistent B-Tree performance

In this experiment we study the impact of allocator performance on a persistent B$^+$-Tree, a popular data structure in database systems. To do so, we use the concurrent, variable-size key version of the FPTree [126] (in contrast to the single-threaded, fixed-size key version used in BigPAllocator), which stores keys in the form of a persistent pointer. Thus, every insertion and deletion operation involves a key allocation or deallocation, respectively. The tested FPTree version employs Hardware

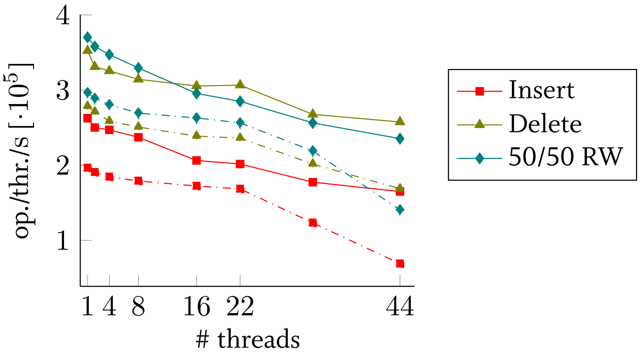

Figure 3.22: Allocator impact on FPTree performance. Solid lines represent PAllocator and dash-dotted lines NVML.

Transactional Memory (HTM) in its concurrency scheme. Unfortunately, the emulation system does not support HTM. Hence, we use for this experiment a system equipped with two Intel Xeon E5-2699 v4 processors that support HTM. Each one has 22 cores (44 with HyperThreading) running at 2.1GHz. The local-socket and remote-socket DRAM latencies are respectively 85 ns and 145 ns. We mount *ext4* with DAX on a reserved DRAM region belonging to the second socket, and bind our experiments to the first socket to emulate a higher SCM latency. We measure the performance of FPTree insertions, deletions, and a mix of 50% insertions and 50% find operations, using PAllocator and NVML. In all experiments, we first warm up the tree with 50M key-values, then execute 50M operation for a varying number of threads. Keys are 128-byte strings while values are 8-byte integers. We report the normalized throughput per thread in Figure 3.22. The solid lines represent PAllocator results while the dash-dotted lines represent NVML results. We observe that with one thread, using PAllocator yields 1.34x, 1.26x, and 1.25x better throughput than using NVML for insertions, deletions, and mixed operations, respectively. These speedups surge up to 2.39x, 1.52x, and 1.67, respectively, with 44 threads. This shows that the FPTree scales better with PAllocator than with NVML, especially when using hyperthreads. We conclude that the performance of a persistent allocator does impact the performance of database data structures.

3.6 SUMMARY

In this chapter we tackled the problem of SCM allocation as a fundamental building block for SCM-based database systems. We first laid down the foundations of a sound SCM programming model, taking into account the requirements of database systems. Then, we presented PAllocator, a highly scalable fail-safe persistent allocator for SCM that comprises three allocators, one for huge blocks, one for small blocks, and one for big blocks, where metadata is persisted in hybrid SCM-DRAM trees. Additionally, we highlighted the importance of persistent memory fragmentation, proposing an efficient defragmentation algorithm. Through an experimental analysis, we showed that PAllocator scales linearly for allocations, deallocations, mixed operations with different size distributions, and server-like workloads. Overall, it significantly outperforms NVML, Makalu, and nvm_malloc, both in operation performance and recovery time. Throughout all experiments, PAllocator showed robust and predictable performance, which we argue is an important feature for an allocator. Finally, we showed that a persistent B^+-Tree performs up to 2.39x better with PAllocator than with NVML, demonstrating the importance of efficient memory allocation for SCM-based data structures.

4

PERSISTENT DATA STRUCTURES

Given the characteristics of SCM, it is theoretically possible to persist data structures in SCM and at the same time obtain near-DRAM performance. This potential has been acknowledged by recent works and new systems that adopt this novel paradigm are emerging [5, 128, 79]. We devised in the previous chapter the foundations for a sound programming model and efficient, fail-safe persistent memory allocation techniques, both of which are necessary building blocks for SCM-based persistent data structures. In this chapter we investigate the design of persistent index structures as one of the core database structures, motivated by the observation that traditional main memory B^+-Tree implementations do not fulfill the consistency requirements needed for such a use case[1]. Furthermore, while expected in the range of DRAM, SCM latencies are higher and asymmetric with writes noticeably slower than reads. We argue that these performance differences between SCM and DRAM imply that the design assumptions made for previous well-established main memory B^+-Tree implementations might not hold anymore. Therefore, we see the need to design a novel, persistent B^+-Tree that leverages the capabilities of SCM while exhibiting performance similar to that of a traditional transient B^+-Tree.

Designing persistent data structures comes with unprecedented challenges for data consistency since SCM is accessed via the volatile CPU cache over which software has only little control. Several works proposed SCM-optimized B^+-Trees such as the CDDS B^+-Tree [164], the wBTree [20], and the NV-Tree [180], but they fail to match the speed of an optimized DRAM-based B^+-Tree. Additionally, they do not address all SCM programming challenges we identify in Chapter 3, especially those of persistent memory leaks and data recovery.

To lift this shortcoming, we propose the *Fingerprinting Persistent Tree* (**FPTree**) that is based on four design principles to achieve near-DRAM-based data structure performance:

1. **Fingerprinting**. Fingerprints are one-byte hashes of in-leaf keys, placed contiguously in the first cache-line-sized piece of the leaf. The FPTree uses unsorted leaves with in-leaf bitmaps – originally proposed in [20] – such that a search iterates linearly over all valid keys in a leaf. By scanning the fingerprints first, we are able to limit the number of in-leaf probed keys to **one** in the average case, which leads to a significant performance improvement.
2. **Selective Persistence**. The idea is based on the well-known distinction between primary data, whose loss infers an irreversible loss of information, and non-primary data that can be rebuilt from the former. Selective persistence consists in storing primary data in SCM and non-primary data in DRAM. Applied to the FPTree, this corresponds to storing the leaf nodes in SCM and the inner nodes in DRAM. Hence, only leaf accesses are more expensive during a tree traversal compared to a fully transient counterpart.

---

[1] Parts of the material in this chapter are based on [126].

3. **Selective Concurrency**. This concept consists in using different concurrency schemes for the transient and persistent parts: The FPTree uses Hardware Transactional Memory (HTM) to handle the concurrency of inner nodes, and fine-grained locks to handle that of leaf nodes. Selective Concurrency elegantly solves the apparent incompatibility of HTM and persistence primitives required by SCM such as cache line flushing instructions. Concurrency control techniques such as key-range locking [51] and orthogonal key-value locking [54] are orthogonal to our work as we focus on concurrency of physical operations.
4. **Sound Programming Model**. We identified several SCM programming challenges in the previous chapter: *data consistency*, *partial writes*, *data recovery*, and *memory leaks*, the last two of which are not fully addressed in related work. We solve all these challenges by relying on the sound programming model we devised in the previous chapter that encompasses the use of *Persistent Pointers*, an optimized, crash-safe, persistent allocator, and a memory leak prevention scheme. Contrary to existing work, this allows us to take into account the higher cost of persistent memory allocations in the performance evaluation.

Additionally, to amortize the higher cost of persistent memory allocations, we propose an optimization that consists of allocating several leaves at once, and explain how these leaf groups are managed.

We implemented the FPTree and two state-of-the-art persistent trees, namely the NV-Tree and the wBTree. Using microbenchmarks, we show that the FPTree outperforms the implemented competitors, with respectively fixed-size and variable-size keys, by up to 2.6× and 4.8× for an SCM latency of 90 ns, and by up to 5.5× and 8.2× for an SCM latency of 650 ns. The FPTree achieves these results while keeping less than 3% of its data in DRAM. Additionally, we demonstrate how the FPTree scales on a machine with 88 logical cores, both with fixed-size and variable-size keys. Moreover, we show that the FPTree recovery time is 76.96× and 29.62× faster than a full rebuild for SCM latencies of 90 ns and 650 ns, respectively. Finally, we integrate the FPTree and the implemented competitors in *memcached* and our prototype database SOFORT. Compared with fully transient trees, results show that the FPTree incurs only 2% overhead in *memcached* using the *mc-benchmark* and that performance is network-bound. When using the TATP benchmark on the prototype database, the FPTree incurs a performance overhead of only 8.7% and 12.8% with an SCM latency of respectively 160 ns and 650 ns, while the overheads incurred by state-of-the-art trees are up to 39.6% and 51.7%, respectively.

The rest of the chapter is organized as follows: Section 4.1 surveys related work, while Section 4.2 presents our design goals and a description of our contributed design principles. Then, Section 4.3 explains the base operations of the FPTree. Thereafter, we discuss the results of our experimental evaluation in Section 4.4. Finally, Section 4.5 summarizes the contributions of this chapter.

4.1 RELATED WORK

Data structures are traditionally persisted using undo-redo logging and shadowing techniques. Some works investigated how to make persistent data structures asymmetry aware. For instance, Viglas [165] studies the case of replicated storage, where reads are faster than writes. He proposes to decrease the number of writes in B^+-Trees by allowing it to be unbalanced. This is achieved by delaying node splits until the cost of re-balancing can be amortized with sequential I/O. However, we argue that this optimization is not fit for SCM which has orders of magnitude lower latency than SSDs and HDDs. The rise of flash memory lead to the emergence of new optimized data structures such as the Bw-Tree [95]. However, these remain intrinsically tied to the logging and paging mechanisms, which SCM can completely do without. Indeed, the advent of SCM enables novel and more fine-grained techniques in designing persistent data structures, but it presents unprecedented challenges as discussed in Chapter 3.

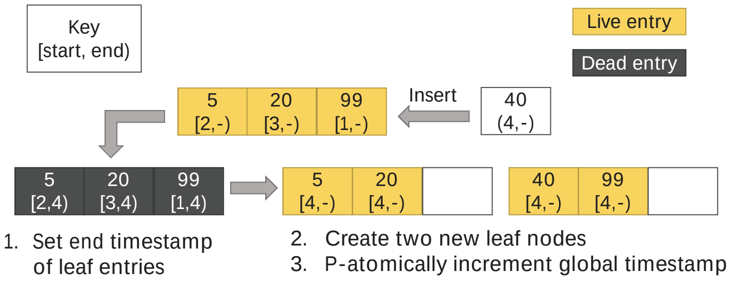

Figure 4.1: Node split after an insertion in the CDDS B$^+$-Tree.

Several works proposed global solutions to these challenges, such as NVHeap [24], Mnemosyne [168], and REWIND [19], which are based on garbage collection and software transactional memory. However, these solutions incur additional overhead due to systematic logging of changed data, which adds up to the overhead caused by the higher latency of SCM. Another line of work relies on the persistence primitives provided by the CPU, namely memory barriers, cache line flushing instructions, and non-temporal stores to design persistent data structures that are stored in and accessed directly from SCM.

SCM-based data structures focus mainly on achieving fail-atomicity and reducing the number of expensive SCM writes. In the following, we cover the main SCM-based data structures that have been proposed in the literature.

4.1.1 CDDS B-Tree

Venkataraman et al. [164] proposed the CDDS B$^+$-Tree, a persistent and concurrent B$^+$-Tree that relies on versioning to achieve fail-atomicity. Figure 4.1 shows the different steps of an insertion in the CDDS B$^+$-Tree that involves a node split. Records have a start time-stamp and an end time-stamp. If a node split is required, the records in the full node are all deleted by setting their end time-stamp; then, two new nodes are created, in which the values of the full node are inserted with a new start time-stamp. The values become visible only when the global time-stamp counter is p-atomically incremented. The CDDS B$^+$-Tree recovers from failures by retrieving the version number of the latest consistent version and removing changes that were made past that version. Nevertheless, its scalability suffers from using a global version number, and it requires garbage collection to remove old versions.

4.1.2 wBTree

Chen et al. [20] proposed to use unsorted nodes with bitmaps as flags to achieve p-atomicity. As a result, updates are performed out-of-place and made visible by p-atomically updating the bitmap. Figure 4.2 compares insertions in a sorted and an unsorted node. Sorted insertions involve a shift of data to make place for the new key, which might leave the node in an inconsistent state in case of a failure. Unsorted insertions remedy this issue by inserting the record into a free slot, then p-atomically updating the bitmap to set the new record as valid. Therefore, unsorted nodes decrease the number of expensive writes to SCM and greatly simplify fail-atomicity management. Nevertheless, a key lookup would necessitate a linear scan, which might be, proportionally to the size of the node, more expensive than a binary search.

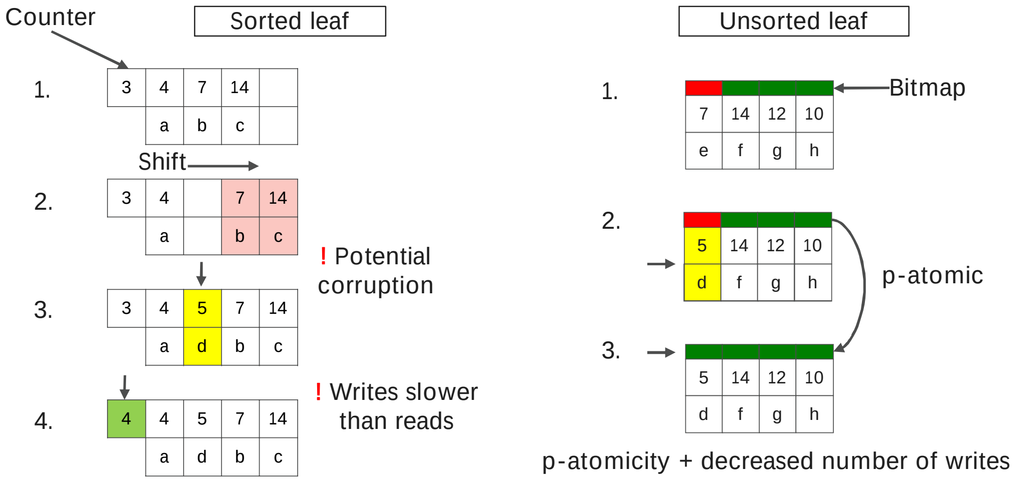

Figure 4.2: Comparison of insertions in a sorted node and an unsorted node.

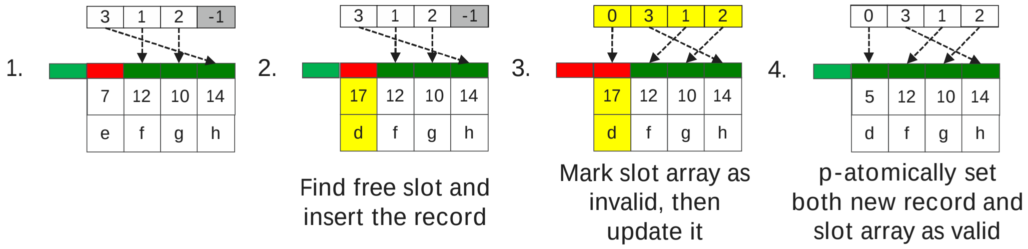
1.
3 1 2 -1
7 12 10 14
e f g h
2.
3 1 2 -1
17 12 10 14
d f g h
Find free slot and insert the record
3.
0 3 1 2
17 12 10 14
d f g h
Mark slot array as invalid, then update it
4.
0 3 1 2
5 12 10 14
d f g h
p-atomically set both new record and slot array as valid

Figure 4.3: Insertion in an unsorted node with a bitmap and an indirection slot array.

To remedy this issue, the authors extended their work by proposing the write-atomic B$^+$-Tree (wB-Tree) [21], a persistent tree that employs sorted indirection slot arrays in nodes to avoid linear search and enable binary search, thus reducing the number of SCM accesses. This array keeps index positions of the keys and is sorted based on the order of the keys. Moreover, one bit in the bitmap is reserved to indicate the validity of the indirection slot array. The wBTree relies on the atomic update of the bitmap to achieve consistency, and on undo-redo logs for more complex operations such as node splits.

Figure 4.3 illustrates an insert operation in an unsorted node with an indirection slot array. After inserting the record out-of-place in a free slot, the indirection slot array is flagged as invalid and updated. In case of a failure at this point, the indirection slot array will be detected as invalid and reconstructed upon recovery. Finally, the bitmap is p-atomically updated to set both the indirection slot array and the new record as valid. This last step imposes that the bitmap be no larger than 8 bytes. Note that when the indirection slot array is smaller than 8 bytes, the bitmap can be removed as the indirection slot array can be p-atomically updated and serve as the validity flag.

4.1.3 NV-Tree

Following another approach, Yang et al. [180] proposed the NV-Tree, a persistent and concurrent B$^+$-Tree based on the CSB$^+$-Tree [141]. They proposed Selective Consistency, illustrated in Figure 4.4, which consists in enforcing the consistency of leaf nodes while relaxing that of inner nodes, and rebuilding them in case of failure, resulting in a reduced number of persistence primitives and a simpler implementation. This approach assumes that the whole tree is placed in SCM, while our

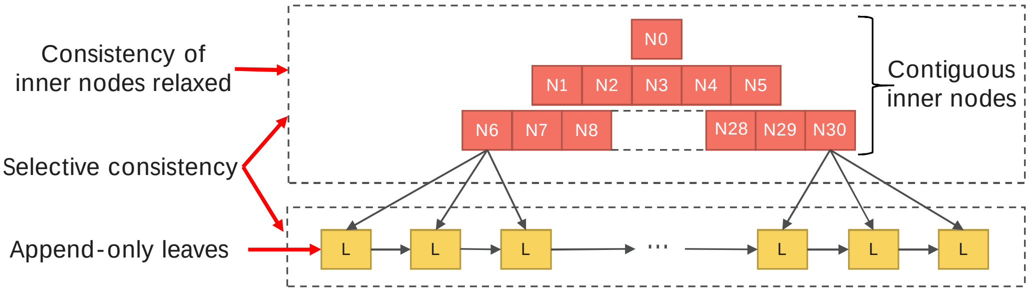

Figure 4.4: Overview of the architecture of the NV-Tree.

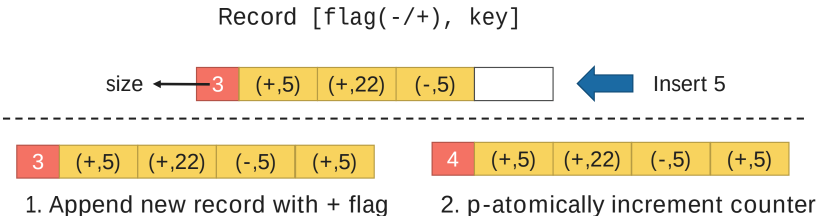
Record [flag(-/+), key]
size
3
(+,5)
(+,22)
(-,5)
Insert 5
4
1. Append new record with + flag
2. p-atomically increment counter

Figure 4.5: Insertion in an append-only leaf node of the NV-Tree.

proposed *Selective Persistence* assumes a hybrid SCM-DRAM configuration, stores only primary data in SCM, and keeps the rest in DRAM to enable better performance. The NV-Tree uses unsorted leaves with an append-only strategy to achieve fail-atomicity. Figure 4.5 shows an example of an insertion in an NV-Tree leaf node. The record is directly appended with a positive flag (or a negative flag in case of a deletion) regardless of whether the key exists or not. Then, the leaf counter is p-atomically incremented to reflect the insertion. To lookup a key, the leaf node is scanned backwards to find the latest version of a key: If its flag is positive, then the key exists, otherwise, the key has been deleted. Additionally, the NV-Tree keeps inner nodes contiguous in memory for better cache efficiency. However, this implies the need for costly rebuilds when a leaf parent node needs to be split. To avoid frequent rebuilds, inner nodes are rebuilt in a sparse way, which may lead to a high memory footprint.

4.1.4 Discussion

While the wBTree and the NV-Tree perform better than existing persistent trees, including the CDDS B^+-Tree, their performance is still significantly slower than fully transient counterparts. Additionally, they are oblivious to the problem of persistent memory leaks. Indeed, both the wBTree and the NV-Tree do not log the memory reference of a newly allocated or deallocated leaf, which makes these allocations prone to *persistent* memory leaks. Moreover, while the NV-Tree can retrieve its data thanks to using offsets, the wBTree does not elaborate on how data is recovered: It uses volatile pointers which become invalid after a restart, making data recovery practically infeasible.

To sum up, we can categorize existing techniques (including the ones we propose in this chapter) according to their objective as follows:

- **Achieving p-atomicity:** versioning, append-only updates, out-of-place updates (such as using bitmaps).
- **Reducing SCM writes:** unsorted nodes, selective consistency.
- **Reducing SCM accesses:** selective persistence, indirection slot arrays, fingerprints.

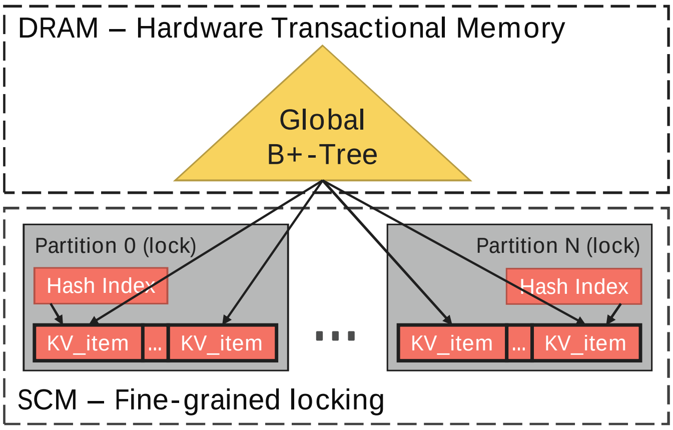

Figure 4.6: Illustration of the architecture of HiKV.

- **Concurrency schemes:** selective concurrency.

These techniques are mostly orthogonal and can be used as building blocks to design novel data structures that explore different design spaces. Two recent works illustrate the reuse of these building blocks: The Write-Optimal Radix Tree by Lee et al. [90] and the Hybrid Key-Value Store by Xia et al. [178]. Lee et al. [90] proposed three versions of a persistent radix tree, namely the Write-Optimal Radix Tree, the Write-Optimal Adaptive Radix Tree, and the Copy-on-Write Adaptive Radix Tree; the first one is an adaptation of a path-compressed radix tree [111], and the last two are an adaptation of the Adaptive Radix Tree (ART) [92]. The authors use a combination of bitmaps, indirection slot arrays, and 8-byte pointers, all of which can be updated p-atomically. Nevertheless, the authors rely on 8-byte normal volatile pointers, which makes their approach tied to using fixed-address memory mappings.

Xia et al. [178] presented HiKV, a hybrid key-value store that uses, as illustrated in Figure 4.6, a partitioned persistent hash index as its primary data, and a transient global B^+-Tree on top of the hash index as secondary data to provides range query capabilities. The B^+-Tree maintains in its leaves pointers to the keys, and is rebuilt from the hash index in case of failure. HiKV uses a combination of selective persistence, selective concurrency, and out-of-place updates. Additionally, the authors propose to update the global B^+-Tree asynchronously to speed up insertions. Nevertheless, they assume 16-byte p-atomic writes, which are not supported in current x86 CPUs. Furthermore, both works do not address the problem of memory leaks and do not elaborate on data discovery while using normal volatile pointers.

While all these works proposed valuable, reusable techniques, they do not rely on a sound programming model that addresses all the programming challenges we discussed in Chapter 3. We argue that adopting a sound programming model is necessary to be able to use persistent data structures as building blocks to design larger systems. Our FPTree successfully addresses all programming challenges.

While our focus is on tree-based data structures, for the sake of completeness, we mention that other works focused on other data structures. For instance, Schwalb et al. [149] proposed a persistent and concurrent hash map, while Zuo et al. [185] presented a hashing scheme that minimizes SCM writes and efficiently handles hash collisions (without providing data durability). Finally, Intel NVML [117] includes several implementation examples of persistent data structures, such as a linked list, a hash table, a binary search tree, and *pmemkv*, a key-value store based our own FPTree with the difference that copies of the keys and the fingerprints are kept in DRAM.

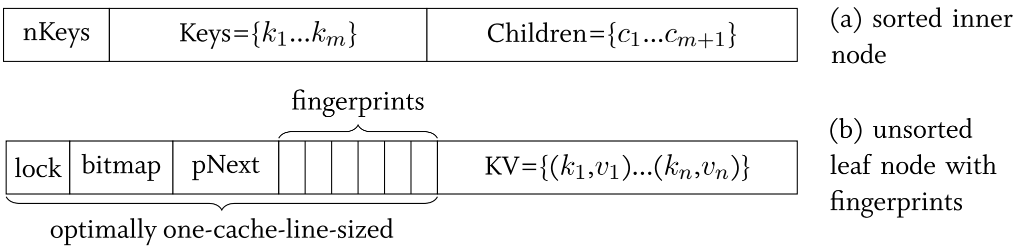
nKeys
Keys={k_1...k_m}
Children={c_1...c_{m+1}}
(a) sorted inner node
fingerprints
lock
bitmap
pNext
KV={(k_1,v_1)...(k_n,v_n)}
(b) unsorted leaf node with fingerprints
optimally one-cache-line-sized

Figure 4.7: FPTree inner node and leaf node layouts.

4.2 FPTREE DESIGN PRINCIPLES

We put forward the following design goals for the FPTree:

1. *Persistence.* The FPTree must be able to self-recover to a consistent state from any software crash or power failure scenario. We do not cover hardware failures in this work.
2. *Near-DRAM performance.* The FPTree must exhibit similar performance to transient counterparts.
3. *Robust performance.* The performance of the FPTree must be resilient to higher SCM latencies.
4. *Fast recovery.* The recovery time of the FPTree must be significantly faster than a complete rebuild of a transient B^+-Tree.
5. *High scalability.* The FPTree should implement a robust concurrency scheme that scales well in highly concurrent situations.
6. *Variable-size keys support.* The FPTree should support variable-size keys (e.g. strings) which is a requirement for many systems.

Figure 4.7 depicts the inner node and leaf node layouts of the FPTree. Since inner nodes are kept in DRAM, they have a classical main memory structure with sorted keys. Leaf nodes however keep keys unsorted and use a bitmap to track valid entries in order to reduce the number of expensive SCM writes, as first proposed by Chen et al [20]. Additionally, leaf nodes contain fingerprints which are explained in detail in Section 4.2.2. The next pointers in the leaves are used to form a linked list whose main goals are: (1) enable range queries, and (2) allow the traversal of all the leaves during recovery to rebuild inner nodes. The next pointers need to be *Persistent Pointers* in order to remain valid across failures. Finally, a one-byte field is used as a lock in each leaf. In the following we present our proposed design principles that enable us to achieve the above design goals.

4.2.1 Selective Persistence

Selective persistence can be described as keeping in SCM the minimal set of primary data on which all the implementation effort for consistency will be focused, and rebuilding all non-primary data that is placed in DRAM upon recovery. Applied to a B^+-Tree, as illustrated in Figure 4.8, the leaf nodes are placed in SCM using a persistent linked list, while inner nodes are placed in DRAM and can be rebuilt as long as the leaves are in a consistent state. As a result, only accessing the leaves is more expensive compared to a transient B^+-Tree. Additionally, inner nodes represent only a small fraction of the total size of the B^+-Tree. Hence, selective persistence should enable our persistent tree to have similar performance to that of a transient B^+-Tree, while using only a minimal portion of DRAM. Our

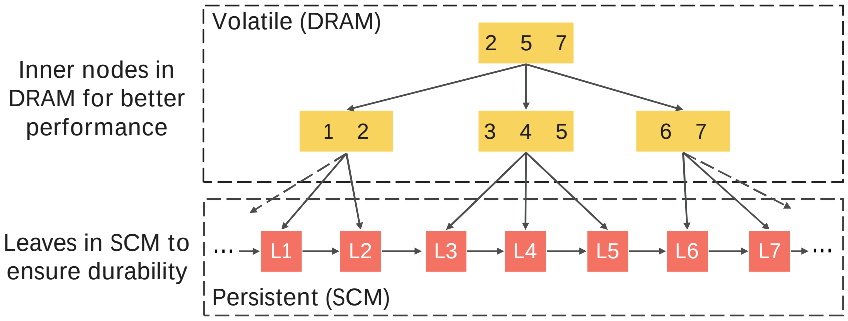
Volatile (DRAM)
2 5 7
1 2
3 4 5
6 7
Inner nodes in DRAM for better performance
Leaves in SCM to ensure durability
L1
L2
L3
L4
L5
L6
L7
Persistent (SCM)

Figure 4.8: Selective persistence applied to a B$^+$-Tree: inner nodes are kept in DRAM while leaf nodes are kept in SCM.

approach differs from that of the NV-Tree [180] in its underlying hardware assumptions: We assume a hybrid SCM-DRAM configuration while the NV-Tree assumes an SCM-only configuration.

In a nutshell, inner nodes will keep a classical structure and fully reside in DRAM without needing any special implementation effort, while leaf nodes will fully reside in SCM and require special care to ensure their consistency. This interplay between SCM and DRAM is crucial for our concurrency mechanism we present in Section 4.2.4.

4.2.2 Fingerprints

Unsorted leaves require an expensive linear scan in SCM. To enable better performance, we propose a technique called *Fingerprinting*. Fingerprints are one-byte hashes of leaf keys, stored contiguously at the beginning of the leaf as illustrated in Figure 4.7. By scanning them first during a search, fingerprints act as a filter to avoid probing keys that have a fingerprint that does not match that of the search key. In the following we show that, theoretically, Fingerprinting enables a much better performance than the wBTree and the NV-Tree. We consider only the case of unique keys, which is often an acceptable assumption in practice [52]. We demonstrate that, using Fingerprinting, the expected number of in-leaf key probes during a successful search is equal to *one*. In the following we compute this expected number. We assume a hash function that generates uniformly distributed fingerprints. Let m be the number of entries in the leaf and n the number of possible hash values ($n = 256$ for one-byte fingerprints).

First, we compute the expected number of occurrences of a fingerprint in a leaf, denoted $E[K]$, which is equivalent to the number of hash collisions in the fingerprint array plus one (since we assume that the search key exists):

$$E[K] = \sum_{i=1}^{m} i \cdot P[K = i]$$

where $P[K = i]$ is the probability that the search fingerprint has exactly i occurrences knowing that it occurs at least once. Let A and B be the following two events:

- A: the search fingerprint occurs exactly i times;
- B: the search fingerprint occurs at least once.

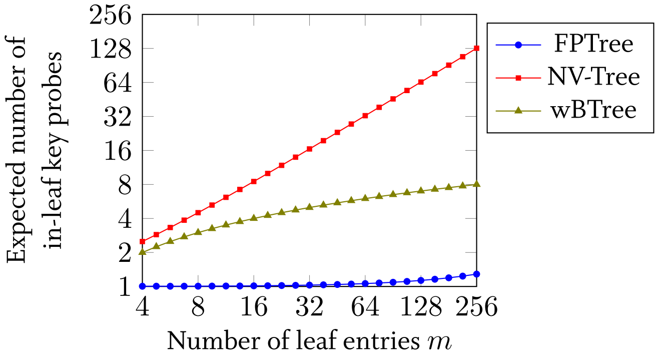

Figure 4.9: Expected number of in-leaf key probes during a successful search operation for the FPTree, NV-Tree, and wBTree.

Then, $P[K = i]$ can be expressed with the conditional probability:

$$P[K=i] = P[A|B] = \frac{P[A\cap B]}{P[B]} = \frac{\left(\frac{1}{n}\right)^i \left(1-\frac{1}{n}\right)^{m-i}\binom{m}{i}}{1-\left(1-\frac{1}{n}\right)^m}$$

The nominator reflects the binomial distribution, while the denominator reflects the condition, i.e., the probability that at least one matching fingerprint exists, expressed as the complementary probability of that of no matching fingerprint exists.

Knowing the expected number of fingerprint hits, we can determine the expected number of in-leaf key probes, denoted $E_{FPTree}[T]$, which is the expected number of key probes in a *linear search* of length $E[K]$ on the keys indicated by the fingerprint hits:

$$\begin{aligned}
E[T] = \frac{1}{2}\left(1+E[K]\right) &= \frac{1}{2}\left(1+\sum_{i=1}^{m} i \frac{\left(\frac{1}{n}\right)^i \left(1-\frac{1}{n}\right)^{m-i}\binom{m}{i}}{1-\left(1-\frac{1}{n}\right)^m}\right) \\
&= \frac{1}{2}\left(1+\frac{\left(\frac{n-1}{n}\right)^m}{1-\left(\frac{n-1}{n}\right)^m}\sum_{i=1}^{m}\frac{i\binom{m}{i}}{(n-1)^i}\right) \\
&= \frac{1}{2}\left(1+\frac{\left(\frac{n-1}{n}\right)^m}{1-\left(\frac{n-1}{n}\right)^m}\left(\frac{m}{n-1}\right)\sum_{i=0}^{m-1}\frac{\binom{m-1}{i}}{(n-1)^i}\right)
\end{aligned}$$

By applying the binomial theorem on the sum we get:

$$\begin{aligned}
E[T] &= \frac{1}{2}\left(1+\frac{\left(\frac{n-1}{n}\right)^m}{1-\left(\frac{n-1}{n}\right)^m}\left(\frac{m}{n-1}\right)\left(\frac{n}{n-1}\right)^{m-1}\right) \\
&= \frac{1}{2}\left(1+\frac{m}{n\left(1-\left(\frac{n-1}{n}\right)^m\right)}\right)
\end{aligned}$$

The wBTree is able to use binary search thanks to its sorted indirection slot arrays, hence, its expected number of in-leaf key probes is: $E_{\text{wBTree}}[T] = log_2(m)$. The NV-Tree scans a leaf by performing a reverse linear search, starting from the last entry of the leaf, so that if a matching key is found, it is guaranteed to be the most recent version. Then, the expected number of in-leaf key probes during a search operation for the NV-Tree is that of a linear search: $E_{\text{NV-Tree}}[T] = \frac{1}{2}(m+1)$. Figure 4.9 shows the expected number of in-leaf key probes for the FPTree, the wBTree, and the NV-Tree. We observe

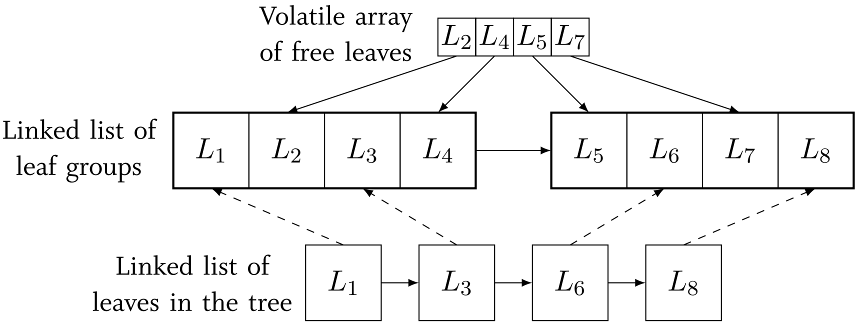

Figure 4.10: FPTree leaf group management.

that the FPTree theoretically enables a much better performance than the wBTree and NV-Tree. For instance, for $m = 32$, the FPTree needs a single in-leaf key probe, while the wBTree and NV-Tree need 5 and 16, respectively. Basically, fingerprinting requires less than two key probes in average up to $m \approx 400$. The wBTree outperforms the FPTree only starting from $m \approx 4096$. It is important to note that, in the case of variable-size keys, since only key references are kept in leaf nodes, every key probe results in a cache miss. Hence, every saved in-leaf key probe is a saved cache miss to SCM. This theoretical result is verified by our experimental evaluation as shown in Section 4.4.2.

4.2.3 Amortized Persistent Memory Allocations

Since persistent allocations are expensive, allocating new leaves during splits is costly to the overall performance of the persistent tree. To remedy this issue, we propose to amortize the overhead of those allocations by allocating blocks of multiple leaves at once. As illustrated in Figure 4.10, leaves are managed through two structures:

- A linked list of groups of leaves currently allocated;
- A transient array of leaves currently free and not used in the tree.

Two methods are used to get and free leaves:

- *GetLeaf*: if the vector of free leaves is not empty, we pop the last element and return it. If it is empty, we allocate a new leaf group, append it to the linked list of groups, and add its leaves to the vector of free leaves, except the one that we return.
- *FreeLeaf*: when a leaf is freed, it is pushed into the vector of free leaves. If its corresponding leaf group is completely free, it is deallocated.

Using leaf groups allows to decrease the number of expensive persistent memory allocations which leads to better insertion performance, as shown in Section 4.4.2.

4.2.4 Selective Concurrency

Transactional memory is a synchronization technique that simplifies concurrency by making a batch of writes atomically visible using transactions. Several hardware vendors provide hardware-supported transactional memory (HTM), such as IBM on Blue Gene/Q and POWER8 processors, and Intel with Transactional Synchronization Extensions (TSX). Although we use Intel TSX in this work, our algorithms are valid for any currently available HTM implementation.

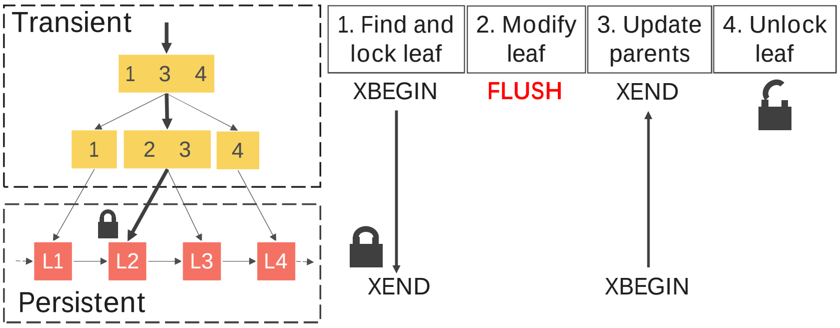

Figure 4.11: Selective concurrency applied to an insert operation in a hybrid data structure.

From a programmer's point of view, HTM is used as a coarse-grained lock around a critical section, but it behaves as a fine-grained lock from the hardware point of view: conflicts are detected between transactions at the granularity of a cache line. In the case of TSX, the critical code is put inside a transaction using the XBEGIN and XEND instructions. When a thread reaches the XBEGIN instruction, the corresponding lock is first read, and if it is available, a transaction is started without acquiring the lock. All changes made inside a transaction are made atomically visible to other threads by an atomic commit if the transaction is successful, that is, if it reaches the XEND instruction without detecting any conflicts. If the transaction aborts, all the buffered changes are discarded, and the operation is re-executed following a programmer-defined fall-back mechanism. In our implementation we use the *speculative spin mutex* of the Intel Threading Building Block library[2] that uses a global lock as a fall-back mechanism.

To detect conflicts, each transaction keeps read and write sets in the L1 cache. The read set comprises all the memory cache lines that the transaction reads, and the write set consists of all the memory cache lines that the transaction writes to. A conflict is detected by the hardware if a transaction reads from the write set of another transaction or writes to the read or write set of another transaction. When this happens, one of the two transactions is aborted. In this case, the aborted transaction falls back to a programmer-defined concurrency mechanism. To increase performance, a transaction is allowed to retry a few times before resorting to the fall-back mechanism. This is an optimistic concurrency scheme as it works under the assumption that only few conflicts will occur and the transactions will execute lock-free with high probability.

HTM is implemented in current architectures by monitoring changes using the L1 cache. Consequently, CPU instructions that affect the cache, such as CLFLUSH, are detected as conflicts which triggers the abortion of a transaction if they are executed within its read or write sets. A trivial implementation of HTM-based lock-elision for a standard B$^+$-Tree would be to execute its base operations within HTM transactions [77]. However, insert and delete operations would need to flush the modified records in the leaf, thus aborting the transaction and taking a global lock. This means that all insertion and deletion operations will in practice get serialized. Therefore, there is an apparent incompatibility between the use of HTM on the one hand and our need to flush the data to persistent memory to ensure consistency on the other hand. To solve this issue, we propose to use different concurrency schemes for the transient and the persistent parts of the data, in the same way we applied different consistency schemes for the data stored in DRAM and in SCM. We name our approach *Selective Concurrency*.

As illustrated in Figure 4.11, selective concurrency consists in performing the work that does not involve modifying persistent data inside an HTM transaction, and the work that requires persistence primitives outside HTM transactions. In the case of our FPTree, the traversal of the tree and changes

---

[2] `https://www.threadingbuildingblocks.org/`

to inner nodes only involve transient data. Therefore, these operations are executed within an HTM transaction and are thus protected against other operations done in concurrent HTM transactions. For other operations that cannot be executed inside the transaction, fine-grained locks are used. Basically, the leaf nodes to be modified are locked during the traversal of the tree inside the HTM transaction. After all modifications on the transient part are done, the transaction is committed. The remaining modifications on the persistent part are then processed outside of the transaction. Finally, the locks on the persistent part are released. The implementation of the base operations using TSX are detailed in Section 4.3.

4.3 FPTREE BASE OPERATIONS

We implement three different persistent trees:

1. *FPTree.* It is the single-threaded version that implements selective persistence, fingerprinting, amortized allocations, and unsorted leaves.
2. *Concurrent FPTree.* This version implements selective persistence, selective concurrency, fingerprinting, and unsorted leaves. As for amortized allocations, since they constitute a central synchronization point, we found that they hinder scalability. Hence, they are used only in the single-threaded version of the FPTree.
3. *PTree.* It reflects a light version of the FPTree that implements only selective persistence and unsorted leaves. Contrary to the FPTree and the wBTree, it keeps keys and values in separate arrays for better data locality when linearly scanning the keys.

In the following, Section 4.3.1 discusses the base operations of the FPTree with fixed-size keys. Thereafter, Section 4.3.2 presents a similar discussion for variable-size keys. Finally, Section 4.3.3 details the algorithms for managing the leaf groups in the single-threaded version of the FPTree.

In the course of this section, *speculative lock* denotes a TSX-enabled lock such as the Intel TBB speculative read write lock. Since leaf locks are only taken within TSX transactions, there is no need to modify them using atomics. As a result, if many threads try to write the same lock – thus writing to the same cache line – only one will succeed and the others will be aborted.

4.3.1 Fixed-Size Key Operations

This section discusses the find, range search, insert, delete, and update operations of the concurrent FPTree with fixed-size keys and explains how the FPTree can recover in a consistent state from any software crash or power failure scenario.

Find

Since search operations do not modify persistent data, they can be fully wrapped in a TSX transaction that protects them from conflicting with write operations of other threads. If another thread writes to a location read by the thread performing the lookup, the transaction will abort and retry, eventually taking a global lock if the retry threshold is exceeded. Search operations still need to check for any

Algorithm 4.1 FPTree Concurrent Find function.

```
function ConcurrentFind(Key K)
    while true do
        speculative_lock.acquire();
        Leaf = FindLeaf(K);
        if Leaf.lock == 1 then
            speculative_lock.abort();
            continue;
        for each slot in Leaf do
            if Leaf.Bitmap[slot] == 1 and Leaf.Fingerprints[slot] == hash(K) and Leaf.KV[slot].Key == K then
                Val = Leaf.KV[slot].Val;
                break;
        speculative_lock.release();
        return Val;
```

leaf locks that might have been taken by another thread to perform changes outside a TSX transaction. Algorithm 4.1 shows the pseudo-code for the *Find* operation.

The *concurrent Find* is executed until it succeeds, making it retry as long as it aborts, which occurs either because the target leaf is locked or because a conflict has been detected. The speculative lock can execute in two ways: either a regular TSX transaction is started with the XBEGIN instruction as long as the lock's retry threshold is not reached, or a global lock is taken.

A transaction can be aborted in multiple ways: if a regular TSX transaction was started, the XABORT instruction will undo all changes (not relevant here since no changes were made), and rewind to the XBEGIN instruction. If the global lock was taken, the XABORT instruction has no effect. In this case, the *while* loop and the *continue* directive play the role of aborting and retrying. Upon reaching the leaf, and if its lock is not already taken, a lookup for the key is performed without taking the leaf lock. If another thread takes the leaf lock during the search for the key, a conflict is detected and one of the two transactions is aborted.

Range Search

Similarly to the find operation, the range search operation is wrapped in a TSX transaction. The difference, however, is that fingerprints cannot be used to speed up a range search in the general case since hashing is not order-preserving. Though, in certain cases where data properties are known a priori, an order-preserving hashing scheme for the fingerprints can be devised. In the following we focus on the general case where fingerprints are not order-preserving.

A range search consists of two interleaved tree traversals, one following the min key, and the other one following the max key. The two traversals identify the start leaf and the end leaf of our range. Since leaves are unsorted, we need to fully scan the start leaf and the end leaf (which can be the same leaf) to extract only the keys that fall within the search range. As for the leaves that fall in between these two (if any), no key comparison is needed since key order is preserved across leaves. Thus, all keys fall within the search range. Overall, the range search operation does not benefit from the fingerprints and is slower than that of a B^+-Tree with sorted leaves. In scenarios where range search performance is critical, a remedy to this issue would be to use the indirection slot arrays of the wBTree in the FPTree to restore key order in the leaves.

Algorithm 4.2 FPTree Concurrent Insert function for fixed-size keys.

```
function ConcurrentInsert(Key K, Value V)
    Decision = Result::Abort;
    while Decision == Result::Abort do
        speculative_lock.acquire();
        (Leaf, Parent) = FindLeaf(K);
        if Leaf.lock == 1 then
            Decision = Result::Abort;
            speculative_lock.abort(); continue;
        Leaf.lock = 1;                              ▷ Writes to leaf locks are never explicitly persisted
        Decision = Leaf.isFull() ? Result::Split : Result::Insert;
        speculative_lock.release();
    if Decision == Result::Split then
        splitKey = SplitLeaf(Leaf);
    slot = Leaf.Bitmap.findFirstZero();
    Leaf.KV[slot] = (K, V); Leaf.Fingerprints[slot] = hash(K);
    Persist(Leaf.KV[slot]); Persist(Leaf.Fingerprints[slot]);
    Leaf.Bitmap[slot] = 1; Persist(Leaf.Bitmap);
    if Decision == Result::Split then
        speculative_lock.acquire();
        UpdateParents(splitKey, Parent, Leaf);
        speculative_lock.release();
    Leaf.lock = 0;
```

Insert

Algorithm 4.2 presents the pseudo-code of the *Concurrent Insert* operation. It follows three steps: (1) Inside a TSX transaction, the tree is traversed to reach a leaf and lock it, and the information of whether a split is needed is propagated; (2) Outside a TSX transaction, changes to the insertion leaf are applied: a leaf split if needed, and the insertion of the key-value pair. These operations use persistence primitives which would trigger an abort if used inside a TSX transaction; (3) If a leaf split occurred in step 2, the inner nodes are updated inside a second TSX transaction. This can be done in two ways: either by directly updating the leaf's parent node if it did not split while modifying the leaf, or by re-traversing the tree. The leaf lock is then released by setting it to 0. Note that Algorithm 4.2 does not use a *while* loop for the second transaction since inner nodes have no locks. Hence, there is no need to manually abort the transaction. When no leaf split is needed, the key-value pair and the fingerprint are written to their respective slots and persisted. The order of these writes does not matter since they are not visible as long as the bitmap is not updated. Therefore, in case a crash occurs while writing the key and the value, no action is needed and the operation is considered as not completed. The bitmap is then p-atomically updated and persisted. In brief, if a failure occurs before the bitmap is persisted, the key-value pair was not inserted, otherwise, the operation executed successfully. In both cases, no action is required.

Algorithm 4.3 represents the pseudo-code for a leaf split. To ensure the consistency of the tree in case of failure during a split, we need to use a micro-log that consists of two persistent pointers: one pointing to the leaf to split, denoted *PCurrentLeaf*, and another pointing to the newly allocated leaf, denoted *PNewLeaf*. The concurrent FPTree has two micro-log arrays that are indexed by transient lock-free queues: one for leaf splits and one for deletes. A micro-log is provided by the lock-free queue and is returned at the end of the operation. The split recovery function is shown in Algorithm 4.4. The split operation starts by writing the persistent address of the leaf to split to *PCurrentLeaf*. If a failure occurs at this point, we only need to reset the micro-log, since *PNewLeaf* is still null. Then, we allocate a new leaf and provide *PNewLeaf* as a reference to the allocator, which persists the address of the allocated memory in *PNewLeaf* before returning. If a crash occurs at this point, the split recovery

Algorithm 4.3 FPTree Split Leaf procedure.

```
 1: procedure SplitLeaf(LeafNode Leaf)
 2:     get $\mu$Log from SplitLogQueue;
 3:     set $\mu$Log.PCurrentLeaf to persistent address of Leaf;
 4:     Persist($\mu$Log.PCurrentLeaf);
 5:     allocate($\mu$Log.PNewLeaf, sizeof(LeafNode))
 6:     set NewLeaf to leaf pointed to by $\mu$Log.PNewLeaf;
 7:     Copy the content of Leaf into NewLeaf;
 8:     Persist(NewLeaf);
 9:     (splitKey, bmp) = FindSplitKey(Leaf);
10:     NewLeaf.Bitmap = bmp;
11:     Persist(NewLeaf.Bitmap);
12:     Leaf.Bitmap = inverse(NewLeaf.Bitmap);
13:     Persist(Leaf.Bitmap);
14:     set Leaf.Next to persistent address of NewLeaf;
15:     Persist(Leaf.Next);
16:     $\mu$Log.reset();
```

Algorithm 4.4 FPTree Recover Split Leaf procedure.

```
 1: procedure RecoverSplitLeaf(SplitLog $\mu$Log)
 2:     if $\mu$Log.PCurrentLeaf.isNull() then
 3:         return ;
 4:     if $\mu$Log.PNewLeaf.isNull() then
 5:         $\mu$Log.reset();                                  ▷ Crashed before SplitLeaf:5
 6:     else
 7:         set Leaf to leaf pointed to by $\mu$Log.PCurrentLeaf;
 8:         if Leaf.Bitmap.isFull() then
 9:             Continue leaf split from SplitLeaf:7;         ▷ Crashed before SplitLeaf:12
10:         else
11:             Continue leaf split from SplitLeaf:12;        ▷ Crashed after SplitLeaf:12
```

function checks whether *PNewLeaf* is null. If it is, it resets the micro-log and returns. Otherwise, it detects that the allocation did complete and thus continues the split operation. Thereafter, the content of the split leaf is persistently copied into the new leaf. The new key discriminator (split key) is then determined and the bitmap of the new leaf is updated accordingly. If a crash occurs during the latter two steps, the recovery function simply re-executes them when it detects that *PNewLeaf* is not null. Afterwards, the bitmap of the split leaf is updated and its next pointer is set to point to the new leaf. The latter write does not need to be p-atomic since in case of a failure, the recovery function will redo the split starting from the copy phase. Finally, the micro-log is reset.

Delete

The concurrency scheme of deletions, whose pseudo-code is shown in Algorithm 4.5, is very similar to that of insertions. The traversal of the tree is always done inside the TSX transaction which is aborted if the leaf is already locked by another thread. Upon reaching the leaf, three cases can arise: (1) The key to delete is not found in the leaf; (2) The leaf contains the key to delete and other keys; (3) The leaf contains only the key to delete.

In the first case, we simply return that the key was not found (not indicated in Algorithm 4.5). In the second case that is similar to an insertion with no split, the leaf is locked and the TSX transaction is committed. Outside of the transaction, the bitmap position corresponding to the value to delete is set to 0 and persisted. Then, the leaf is unlocked. As discussed earlier this operation is failure-atomic. In the third case, the leaf will be deleted. The inner nodes are modified inside the TSX transaction

Algorithm 4.5 FPTree Concurrent Delete function for fixed-size keys.

```
function ConcurrentDelete(Key K)
    Decision = Result::Abort;
    while Decision == Result::Abort do
        speculative_lock.acquire();
        (Leaf, PPrevLeaf) = FindLeafAndPrevLeaf(K);        ▷ PrevLeaf is locked only if Decision == LeafEmpty
        if Leaf.lock == 1 then
            Decision = Result::Abort;
            speculative_lock.abort(); continue;
        if Leaf.Bitmap.count() == 1 then
            if PPrevLeaf->lock == 1 then
                Decision = Result::Abort;
                speculative_lock.abort(); continue;
            Leaf.lock = 1; PPrevLeaf->lock = 1;
            Decision = Result::LeafEmpty;
        else
            Leaf.lock = 1; Decision = Result::Delete;
        speculative_lock.release();
    if Decision == Result::LeafEmpty then
        DeleteLeaf(Leaf, PPrevLeaf);
        PrevLeaf.lock = 0;
    else
        slot = Leaf.findInLeaf(K);
        Leaf.Bitmap[slot] = 0; Persist(Leaf.Bitmap[slot]);
        Leaf.lock = 0;
```

as no persistence primitives are needed. Basically, the key and the pointer corresponding to the leaf are removed from its parent, possibly triggering further inner node modifications. We note that the leaf to be deleted does not need to be locked because it will become unreachable by other threads after the update of the inner nodes completes. The only node that needs to be updated outside of the TSX transaction is the left neighbor of the deleted leaf; its next pointer is updated to point to the next leaf of the deleted leaf. Before committing the transaction, this left neighbor is retrieved and locked. Finally, outside of the transaction, the next pointer of the left neighbor is updated, its lock is released, and the deleted leaf is deallocated.

Algorithm 4.6 shows the pseudo-code for a leaf delete operation. Similarly to leaf splits, a leaf deletion requires a micro-log to ensure consistency. It consists of two persistent pointers, denoted *PCurrentLeaf* and *PPrevLeaf* that point to the leaf to be deleted and to its previous leaf, respectively. The leaf delete function first updates *PCurrentLeaf* and persists it. If *PCurrentLeaf* is equal to the head of the linked list of leaves, its head pointer must be updated. If a crash occurs at this point, the delete recovery procedure (shown in Algorithm 4.7) detects that *PCurrentLeaf* is set and either itself or its next pointer is equal to the head of the linked list of leaves, and continues the operation accordingly. If the leaf to be deleted is not the head of the linked list of leaves, *PPrevLeaf* is updated and persisted. Then, the next pointer of the previous leaf of the leaf to be deleted is updated to point to the next pointer of the latter. If a crash occurs at this point, the delete recovery procedure detects that the micro-log is fully set (i.e., both pointers are not null), and thus, it repeats the latter operation. Thereafter, in both cases, the deleted leaf is deallocated by passing *PCurrentLeaf* to the deallocate function of the allocator, which resets it to null. If a crash occurs at this point, the delete recovery function detects that *PCurrentLeaf* is null and resets the micro-log. Finally, the micro-log is reset.

Update

Algorithm 4.8 presents pseudo-code for the update operation. Although the update operation looks like an insert-after-delete operation, it is in fact much more optimized: It is executed out-of-place.

Algorithm 4.6 FPTree Delete Leaf procedure.

```
 1: procedure DeleteLeaf(LeafNode Leaf, LeafNode PPrevLeaf)
 2:     get the head of the linked list of leaves PHead
 3:     get $\mu$Log from DeleteLogQueue;
 4:     set $\mu$Log.PCurrentLeaf to persistent address of Leaf;
 5:     Persist($\mu$Log.PCurrentLeaf);
 6:     if $\mu$Log.PCurrentLeaf == PHead then          ▷ Leaf is the head of the linked list of leaves
 7:         PHead = Leaf.Next;
 8:         Persist(PHead);
 9:     else
10:         $\mu$Log.PPrevLeaf = PPrevLeaf;
11:         Persist($\mu$Log.PPrevLeaf);
12:         PrevLeaf.Next = Leaf.Next;
13:         Persist(PrevLeaf.Next);
14:     deallocate($\mu$Log.PCurrentLeaf);
15:     $\mu$Log.reset();
```

Algorithm 4.7 FPTree Recover Delete Leaf procedure.

```
 1: procedure RecoverDeleteLeaf(DeleteLog $\mu$Log)
 2:     get head of linked list of leaves PHead;
 3:     if $\mu$Log.PCurrentLeaf.isNotNull() and $\mu$Log.PPrevLeaf.isNotNull() then
 4:         Continue from DeleteLeaf:12;          ▷ Crashed between lines DeleteLeaf:12-14
 5:     else
 6:         if $\mu$Log.PCurrentLeaf.isNotNull() and $\mu$Log.PCurrentLeaf == PHead then
 7:             Continue from DeleteLeaf:7;          ▷ Crashed at line DeleteLeaf:7
 8:         else
 9:             if $\mu$Log.PCurrentLeaf.isNotNull() and $\mu$Log.PCurrentLeaf$\rightarrow$Next == PHead then
10:                 Continue from DeleteLeaf:14;          ▷ Crashed at line DeleteLeaf:14
11:             else
12:                 $\mu$Log.reset();
```

Concretely, the update operation relies on the fact that the bitmap can be updated p-atomically to reflect both the insertion and the deletion at the same time. This has the advantage of keeping the leaf size unchanged during an update, which makes leaf splits necessary only if the leaf that contains the record to update is already full. As for the recovery logic, it is exactly the same as for insertions, where a micro-log is used to ensure consistency only in case of a leaf split.

Recovery

Algorithm 4.9 shows the pseudo-code for the concurrent FPTree recovery function. It starts by checking whether the tree crashed during initialization by testing a state bit. Then, for each micro-log in the micro-logs arrays, it executes either the leaf split or the leaf delete recovery function. Afterwards, it rebuilds inner nodes by traversing the leaves, resetting their locks, and retrieving the greatest key in each leaf to use it as a discriminator key. This step is similar to how inner nodes are built in a bulk-load operation. Finally, the micro-log queues are rebuilt.

Note that micro-logs are cache-line-aligned. Thus, back-to-back writes to a micro-log that are not separated by other writes can be ordered with a memory barrier and then persisted together. In fact, when two writes target the same cache line, the first write is guaranteed to become persistent no later than the second one.

Algorithm 4.8 FPTree Concurrent Update function for fixed-size keys.

```
function ConcurrentUpdate(Key K, Value V)
    Decision = Result::Abort;
    while Decision == Result::Abort do
        speculative_lock.acquire();
        (Leaf, Parent) = FindLeaf(K);
        if Leaf.lock == 1 then
            Decision = Result::Abort;
            speculative_lock.abort(); continue;
        Leaf.lock = 1;
        prevPos = Leaf.findKey(K);
        Decision = Leaf.isFull() ? Result::Split : Result::Update;
        speculative_lock.release();
    if Decision == Result::Split then
        splitKey = SplitLeaf(Leaf);
    slot = Leaf.Bitmap.findFirstZero();
    Leaf.KV[slot] = (K, V); Leaf.Fingerprints[slot] = hash(K);
    Persist(Leaf.KV[slot]); Persist(Leaf.Fingerprints[slot]);
    copy Leaf.Bitmap in tmpBitmap;
    tmpBitmap[prevSlot] = 0; tmpBitmap[slot] = 1;
    Leaf.Bitmap = tmpBitmap; Persist(Leaf.Bitmap);                    ▷ p-atomic copy
    if Decision == Result::Split then
        speculative_lock.acquire();
        UpdateParents(splitKey, Parent, Leaf);
        speculative_lock.release();
    Leaf.lock = 0;
```

Algorithm 4.9 FPTree Recover procedure.

```
procedure Recover
    if Tree.Status == NotInitialized then
        Tree.init();
    else
        for each SplitLog in Tree.SplitLogArray do
            RecoverSplit(SplitLog);
        for each DeleteLog in Tree.DeleteLogArray do
            RecoverDelete(DeleteLog);
    RebuildInnerNodes();
    RebuildLogQueues();
```

4.3.2 Variable-Size Key Operations

To support variable-size keys (e.g., string keys), we replace the keys in inner nodes by regular (virtual) pointers to keys and those in leaf nodes by persistent pointers to keys. Ensuring consistency does not require any additional micro-logging compared to the case of fixed-size keys, although every insert or delete operation involves a persistent allocation or deallocation of a key, respectively. In the following we elaborate in detail on the concurrent FPTree insert, delete, and update operations for variable-size keys and their corresponding recovery procedures. Since search operations are similar to the concurrent FPTree with fixed-size keys, we do not discuss them in this section.

Insert

Algorithm 4.10 shows the pseudo code of the *Concurrent Insert* operation. It is similar to its fixed-size keys counterpart. In particular, the leaf split operation is identical to that of fixed-size keys. The only

Algorithm 4.10 FPTree Concurrent Insert function for variable-size keys.

```
function ConcurrentInsert_String(Key K, Value V)
    Decision = Result::Abort;
    while Decision == Result::Abort do
        speculative_lock.acquire();
        (Leaf, Parent) = FindLeaf(K);
        if Leaf.lock == 1 then
            Decision = Result::Abort;
            speculative_lock.abort(); continue;
        Leaf.lock = 1;
        Decision = Leaf.isFull() ? Result::Split : Result::Insert;
        speculative_lock.release();
    if Decision == Result::Split then
        splitKey = SplitLeaf(Leaf);
    slot = Leaf.Bitmap.findFirstZero();
    allocate(Leaf.KV[slot].PKey, strlen(K));
    set NewKey to key pointed to by Leaf.KV[slot].PKey;
    NewKey = K; Persist(NewKey);
    Leaf.KV[slot].Val = V; Leaf.Fingerprints[slot] = hash(K);
    Persist(Leaf.KV[slot].Val); Persist(Leaf.Fingerprints[slot]);
    Leaf.Bitmap[slot] = 1; Persist(Leaf.Bitmap);
    if Decision == Result::Split then
        speculative_lock.acquire();
        UpdateParents(splitKey, Parent, Leaf);
        speculative_lock.release();
    Leaf.lock = 0;
```

difference is that for variable-size keys, we need to allocate persistent memory to store the insertion key. To ensure consistency, we do not need any additional micro-logging compared to fixed-size keys. When the insertion position is found, the new key is allocated by passing the key persistent pointer of the insertion position to the allocator that writes the persistent address of the allocated memory to the provided persistent pointer. Then, the key to insert is persistently copied into the newly allocated key. Thereafter, the value and the fingerprint are persistently written in any order as they remain invisible until the bitmap is updated. Finally, the bitmap is persistently updated to make changes visible. If a crash occurs after the new key is allocated but before the bitmap is updated, the newly allocated key is a persistent memory leak. To detect this problem during recovery, it is sufficient to add the following additional check while traversing the leaves to rebuild inner nodes: for every unset bit in the bitmap of a leaf, check whether its corresponding key persistent pointer is null (as it should be). If it is not, then we might have crashed during an insert operation, after having allocated the new key but before having updated the bitmap to reflect the insertion. Deallocating the key, as shown in the recovery procedure (Algorithm 4.13), is sufficient to set the tree back to a state of leak-free consistency.

Delete

Algorithm 4.11 shows the pseudo code of the *Concurrent Delete* operation. It is similar to its fixed-size key counterpart. In particular, the leaf delete operation is identical to that of fixed-size keys. The only difference is that in this case, we need to deallocate the key that is deleted. Similarly to insert operations, there is no additional micro-log required to ensure failure-atomicity. Once the position of the key to be deleted is determined, the bitmap is updated and persisted to reflect the deletion. Finally, the deleted key is deallocated. A crash after updating the bitmap but before deallocating the key will lead to a persistent memory leak: The key will be invisible since the bitmap has been updated and thus the key will never get deallocated. During recovery however, it is sufficient to conduct the same

Algorithm 4.11 FPTree Concurrent Delete function for variable-size keys.

```
function ConcurrentDelete_String(Key K)
    Decision = Result::Abort;
    while Decision == Result::Abort do
        speculative_lock.acquire();
        (Leaf, PPrevLeaf) = FindLeafAndPrevLeaf(K);        ▷ PrevLeaf is locked only if Decision == LeafEmpty
        if Leaf.lock == 1 then
            Decision = Result::Abort;
            speculative_lock.abort(); continue;
        if Leaf.Bitmap.count() == 1 then
            if PPrevLeaf→lock == 1 then
                Decision = Result::Abort;
                speculative_lock.abort(); continue;
            Leaf.lock = 1; PPrevLeaf→lock = 1;
            Decision = Result::LeafEmpty;
        else
            Leaf.lock = 1; Decision = Result::Delete;
        speculative_lock.release();
    slot = Leaf.findInLeaf(K);
    Leaf.Bitmap[slot] = 0; Persist(Leaf.Bitmap);
    deallocate(Leaf.KV[slot].PKey);
    if Decision == Result::LeafEmpty then
        DeleteLeaf(Leaf, PPrevLeaf);
        PrevLeaf.lock = 0;
    else
        Leaf.lock = 0;
```

additional check as for insert operations: for every unset bit in the bitmap of a leaf, check whether its corresponding key persistent pointer is null (as it should be). If it is not, then we might have crashed during a delete operation, after having updated the bitmap but before having deallocation the deleted key. All there is to do to recover to a consistent and leak-free state is to deallocate the keys pointed to by these non-null persistent pointers, as shown in Algorithm 4.13.

Update

Algorithm 4.12 shows the pseudo code of the *Concurrent Update* operation. Similarly to the fixed-size key case, this operation is an optimized insert-after-delete operation where both the insertion and the deletion are made p-atomically visible by updating the bitmap. Compared to an insert operation, an update operation does not allocate memory, except when a split is needed. Instead of allocating a new key, the persistent pointer of the key is copied into a new location. After updating the bitmap, the persistent pointer of the old record location must be reset in order to ensure that a reference to a key exists only once. In the case of a crash after reflecting the update but before resetting the persistent pointer of the old record location, the recovery function might misinterpret this as a crash during an insert or a delete operation, and deallocate the key, as described previously. To avoid this issue, whenever a deleted record with a non-null key persistent pointer is found, the recovery function checks whether there is a valid record in the same leaf that points to the same key. If there is one, the key persistent pointer simply needs to be reset. Otherwise, this means that the crash occurred during an insert or a delete operation and the key needs to be deallocated.

Algorithm 4.12 FPTree Concurrent Update function for variable-size keys.

```
function ConcurrentUpdate_String(Key K, Value V)
    Decision = Result::Abort;
    while Decision == Result::Abort do
        speculative_lock.acquire();
        (Leaf, Parent) = FindLeaf(K);
        if Leaf.lock == 1 then
            Decision = Result::Abort;
            speculative_lock.abort(); continue;
        Leaf.lock = 1;
        prevPos = Leaf.findKey(K);
        Decision = Leaf.isFull() ? Result::Split : Result::Update;
        speculative_lock.release();
    if Decision == Result::Split then
        splitKey = SplitLeaf(Leaf);
    slot = Leaf.Bitmap.findFirstZero();
    Leaf.KV[slot].PKey = Leaf.KV[prevSlot].PKey;
    Leaf.KV[slot].Val = V; Leaf.Fingerprints[slot] = Leaf.Fingerprints[prevSlot];
    Persist(Leaf.KV[slot]); Persist(Leaf.Fingerprints[slot]);
    copy Leaf.Bitmap in tmpBitmap;
    tmpBitmap[prevSlot] = 0; tmpBitmap[slot] = 1;
    Leaf.Bitmap = tmpBitmap; Persist(Leaf.Bitmap);                ▷ p-atomic copy
    Leaf.KV[prevSlot].PKey.reset();
    if Decision == Result::Split then
        speculative_lock.acquire();
        UpdateParents(splitKey, Parent, Leaf);
        speculative_lock.release();
    Leaf.lock = 0;
```

Recovery

The recovery procedure of the FPTree with variable-size keys is similar to that with fixed-size keys, except for rebuilding inner nodes where the additional memory-leak checks described above are added. Algorithm 4.13 shows the pseudo-code of the inner node rebuilding function.

4.3.3 Leaf group management

In this section we discuss how insert and delete operations make use of leaf groups in the single-threaded version of the FPTree.

Insert

The insert operation using leaf groups differs from the concurrent version of the FPTree in the split operation. The non-concurrent version of the FPTree employs leaf groups and does not allocate memory on every split. The same recovery logic as for insert operations without leaf groups applies and only the leaf allocation step is replaced by a call to the *GetLeaf* function (described in Algorithm 4.14). This function requires a micro-log that contains a single persistent pointer, denoted *PNewGroup*. Instead of directly allocating a new leaf, *GetLeaf* first checks whether there is a leaf that is available in the queue of free leaves, and if not, it will allocate a leaf group, add it to the linked list of leaf groups, and

Algorithm 4.13 FPTree Inner Nodes Rebuild procedure for variable-size keys.

```
procedure RebuildInnerNodes_String
    let MaxVector be a vector of keys;
    for each $Leaf_i$ in linked-list of leaves do
        let MaxKey be a key set to the smallest value of its domain;
        for each slot in $Leaf_i$.Bitmap do                              ▷ Find max key
            if $Leaf_i$.Bitmap[slot] == 1 then
                set K to key pointed to by $Leaf_i$.KV[slot].PKey;
                MaxKey = max(K, MaxKey);
            else
                if $Leaf_i$.KV[slot].PKey.isNotNull() then            ▷ Test if there is a memory leak
                    if KeyExists($Leaf_i$, $Leaf_i$.KV[slot].PKey) then   ▷ If key exists in another slot
                        $Leaf_i$.KV[slot].PKey.reset();
                    else
                        deallocate($Leaf_i$.KV[slot].PKey);
            MaxVector[i] = MaxKey;
    rebuild inner nodes using MaxVector;
```

Algorithm 4.14 FPTree Get Leaf procedure.

```
procedure GetLeaf(PLeafNode PLeaf)
    $\mu$Log = Tree.GetLeafLog;
    if Tree.FreeLeavesQueue.isEmpty() then
        allocate($\mu$Log.PNewGroup, sizeof(LeafNode)*GROUP_SIZE);
        Tree.PGroupsListTail.Next = $\mu$Log.PNewGroup;
        Persist(Tree.PGroupsListTail.Next);
        Tree.PGroupsListTail = $\mu$Log.PNewGroup;
        Persist(Tree.PGroupsListTail);
        $\mu$Log.reset();
        insert Tree.PGroupsListTail in FreeLeavesQueue;
    return Tree.FreeLeavesVector.pop();
```

insert its members into the transient queue of free leaves, except the one that is returned. The corresponding recovery function is shown in Algorithm 4.15: if *PNewGroup* is not null, this means that the allocation took place and we can continue the operation as indicated in the pseudo-code. Otherwise, no action is required since the queue of free leaves is transient and rebuilt at recovery time.

Delete

The only difference between the Delete operation of the concurrent FPTree and the single-threaded FPTree is the leaf delete procedure; the FPTree uses leaf groups and does not require a deallocation on every leaf deletion. Algorithm 4.16 shows the pseudo-code of the *FreeLeaf* function that replaces the deallocation function. This operation requires a micro-log that contains two persistent pointers, denoted *PCurrentGroup* and *PPrevGroup*. First, the procedure checks whether the leaf group to which the deleted leaf belongs is completely free. If it is, it will deallocate the leaf group and update the head of the linked list of groups if needed. Otherwise, it will push the deleted leaf into the transient queue of free leaves. The corresponding recovery function is depicted in Algorithm 4.17 and follows the same logic as the leaf delete recovery function that is detailed in Section 4.3: if *PCurrentGroup* is not null, this means that the micro-log was set but the deallocation did not take place. We can continue the operation starting by either updating the head of the linked list of groups, or by deallocating the group, as indicated in Algorithm 4.17. If *PCurrentGroup* is null, no action is needed since the queue of free leaves is transient and rebuilt at restart time. Note that to speed up *GetPrevGroup*, it can be implemented using a transient index on top of the linked list of free leaves.

Algorithm 4.15 FPTree Recover Get Leaf procedure.

```
procedure RecoverGetLeaf(GetLeafLog μLog)
    if μLog.PNewGroup.isNotNull() then
        if Tree.PGroupsListTail == μLog.PNewGroup then
            μLog.reset();                    ▷ Everything was done except resetting the micro-log
        else
            Continue from line GetLeaf:5;
```

Algorithm 4.16 FPTree Free Leaf procedure.

```
procedure FreeLeaf(LeafNode Leaf)
    get head of the linked list of Groups PHead;
    μLog = Tree.FreeLeafLog;
    (Group,PPrevGroup) = GetLeafGroup(Leaf);
    if Group.isFree() then
        FreeLeavesQueue.delete(Group);
        set μLog.PCurrentGroup to persistent address of Group;
        Persist(μLog.PCurrentGroup);
        if μLog.PCurrentGroup == PHead then
            PHead = Group.Next;              ▷ Group is the head of the linked list of Groups
            Persist(PHead);
        else
            μLog.PPrevGroup = PPrevGroup;
            Persist(μLog.PPrevGroup);
            PrevGroup.Next = Group.Next;
            Persist(PrevGroup.Next);
        deallocate(μLog.PCurrentGroup);      ▷ the deallocate function resets PCurrentGroup
        μLog.reset();
    else
        FreeLeavesVector.push(Leaf);
```

Recovery

The recovery function of the non-concurrent FPTree is similar to that of its concurrent version, except that instead of iterating over the arrays of micro-logs, the non-concurrent version contains only one leaf split micro-log and one leaf delete micro-log. Additionally, they differ in how the inner nodes are rebuilt; the single-threaded FPTree traverses the linked list of leaf groups instead of traversing the linked list of leaves, which allows for more data locality. Furthermore, the keys that are retrieved from the leaves are unsorted and require to be sorted before proceeding to rebuilding inner nodes. Nevertheless, the benefits of increased data locality outperformed the cost of the additional sort, as shown in Section 4.4.2. We note that the transient vector of free leaves is rebuilt while traversing the list of leaf groups. f

4.4 EVALUATION

In this section we compare the performance of the FPTree with that of state-of-the-art persistent and transient trees. We first evaluate single-threaded, then multi-threaded base operation performance. Thereafter, to conduct an end-to-end evaluation, we integrate the evaluated trees in our prototype database SOFORT and in a popular key-value cache.

Algorithm 4.17 FPTree Recover Free Leaf procedure.

```
procedure RecoverFreeLeaf(FreeLeafLog $\mu$Log)
    get head of linked list of groups PHead;
    if $\mu$Log.PCurrentGroup.isNotNull() and $\mu$Log.PPrevGroup.isNotNull() then
        Continue from FreeLeaf:15;                                ▷ Crashed between lines FreeLeaf:15-17
    else
        if $\mu$Log.PCurrentGroup.isNotNull() and $\mu$Log.PCurrentGroup == PHead then
            Continue from FreeLeaf:10;                            ▷ Crashed at line FreeLeaf:10
        else
            if $\mu$Log.PCurrentGroup.isNotNull() and $\mu$Log.PCurrentGroup→Next == PHead then
                Continue from FreeLeaf:17;                        ▷ Crashed at line FreeLeaf:14
            else
                $\mu$Log.reset();
```

4.4.1 Experimental Setup

In addition to the PTree and the FPTree, we re-implemented the wBTree with indirection slot arrays and the NV-Tree as faithfully as possible with regard to their description in their respective original paper. To ensure the NV-Tree has the same level of optimization as the FPTree, we placed its inner nodes in DRAM. For the same purpose, we replaced the wBTree's undo-redo logs with the more lightweight FPTree micro-logs. As a reference transient implementation, we use the STXTree, an open-source optimized main memory B$^+$-Tree [154]. The test programs were compiled using *GCC-4.7.2*. We used *jemalloc-4.0* as DRAM allocator, and our own persistent allocator for SCM.

To emulate different SCM latencies, we use the Intel SCM Emulation Platform that we described in Chapter 2. This SCM evaluation platform is equipped with two Intel Xeon E5 processors. Each one has 8 cores, running at 2.6 GHz and featuring each 32 KB L1 data and 32 KB L1 instruction cache as well as 256 KB L2 cache. The 8 cores of one processor share a 20 MB last level cache. The system has 64 GB of DRAM and 192 GB of emulated SCM. The same type of emulation system was used in [5, 39, 128]. In the experiments, we vary the latency of SCM between $160\,\mathrm{ns}$ (the lowest latency that can be emulated) and $650\,\mathrm{ns}$. Additionally, we use *ext4* with Direct Access [35] (DAX) support to emulate a DRAM-like latency of SCM ($90\,\mathrm{ns}$).

Unfortunately, the emulation system does not support TSX which prevents us from testing concurrency on this system. Hence, we use for concurrency tests a system equipped with two Intel Xeon E5-2699 v4 processors that support TSX. Each one has 22 cores (44 with HyperThreading) running at 2.1 GHz. The system has 128 GB of DRAM. The local-socket and remote-socket DRAM latencies are respectively $85\,\mathrm{ns}$ and $145\,\mathrm{ns}$. We mount *ext4 DAX* on a reserved DRAM region to emulate SCM.

We conducted a preliminary experiment to determine the best node sizes for every tree considered in the evaluation. Table 4.1 summarizes the results. We note that the best node sizes for the single-threaded and the concurrent versions of the FPTree differ. This is because larger inner nodes increase the probability of conflicts inside TSX transactions.

4.4.2 Single-Threaded Microbenchmarks

In this sub-section, we focus on the single-threaded performance of the base operations of the trees. In all our microbenchmarks, we use uniformly distributed generated data. For fixed-size keys, keys and values are 8-byte integers, while for variable sized-keys, keys are 16-byte strings and values are 8-byte integers.

Tree	# inner node entries	# leaf node entries	Key size	Memory
PTree	4096	32	8 bytes	SCM + DRAM
FPTree	4096	32	8 bytes	SCM + DRAM
NV-Tree	128	32	8 bytes	SCM + DRAM
wBTree	32	64	8 bytes	SCM
STXTree	16	16	8 bytes	DRAM
FPTreeC	128	64	8 bytes	SCM + DRAM
NV-TreeC	128	32	8 bytes	SCM + DRAM
PTreeVar	256	32	16 bytes	SCM + DRAM
FPTreeVar	2048	32	16 bytes	SCM + DRAM
NV-TreeVar	128	32	16 bytes	SCM + DRAM
wBTreeVar	32	64	16 bytes	SCM
STXTreeVar	8	8	16 bytes	DRAM
FPTreeCVar	64	64	16 bytes	SCM + DRAM
NV-TreeCVar	128	32	16 bytes	SCM + DRAM

Table 4.1: Chosen node sizes (in number of entries) for the evaluated trees. Values are 8-byte integers for all trees. The suffixes *C* and *Var* indicate, respectively, the concurrent and variable-size key versions of the trees.

Base Operations

To study the performance of the *Find*, *Insert*, *Update*, and *Delete* operations, we first warm up the trees with 50 million key-values, then we execute back-to-back 50 million *Finds*, *Inserts*, *Updates*, and *Deletes*. Figures 4.12 and 4.13 show the performance results for different SCM latencies. For fixed-size keys, we observe that with an SCM latency of 90 ns (DRAM's latency), the FPTree outperforms the PTree, NV-Tree, and wBTree by a factor of 1.18/1.48/1.08/1.08, 1.47/1.83/2.63/1.79, and 1.97/2.05/1.81/2.05 for *Find*/*Insert*/*Update*/*Delete*, respectively. The speedup factors increase up to 1.19/1.63/1.08/1.02, 1.92/2.97/3.65/2.82, and 3.93/4.89/4.09/5.48, respectively, with an SCM latency of 650 ns. We notice that compared with the STXTree, the FPTree and the PTree have better *Delete* performance with the lower SCM latencies because deletions simply flip a bit in the bitmap, while the STXTree executes a sorted delete. Additionally, the FPTree exhibits a slowdown factor of only 1.51/1.67/1.93/1.21 and 2.56/2.17/2.76/1.70, for SCM latencies of 250 ns and 650 ns, respectively. The slowdown factors for the PTree, NV-Tree, and wBTree are 1.76/2.46/2.04/1.21, 2.47/3.51/5.78/2.60, and 4.32/5.16/5.25/4.26 for an SCM latency of 250 ns, and 3.05/3.55/2.99/1.73, 4.92/6.46/10.09/4.79, and 10.07/10.63/11.30/9.31 for an SCM latency of 650 ns. Moreover, we notice that the difference in performance between the FPTree and the PTree is greater for *Inserts* than for *Finds* and *Deletes*, showing the benefit of using leaf groups in addition to fingerprints.

At an SCM latency of 650 ns, the average time of an FPTree *Find* is 1.3 µs, which corresponds to the cost of two SCM cache misses: the first one to access the bitmap and fingerprints of the leaf node, and the second one to access the searched key-value. This is in line with our theoretical result of Section 4.2.2.

As for variable-size keys, the benefit of using fingerprints is more salient since any additional string key comparison involves a pointer dereferencing, and thus a cache miss. For *Find*/*Insert*/*Update*/*Delete*, the FPTree outperforms the PTree, NV-Tree, and wBTree by a factor of 1.82/1.65/1.71/1.24, 1.72/1.93/4.80/ 1.78, and 2.20/1.62/2.15/1.64 respectively for an SCM latency of 90 ns, and by an increased speedup factor of 2.15/2.16/2.36/1.35, 2.50/2.42/8.19/2.14, and 2.93/2.93/5.43/2.86 for an SCM latency of 650 ns. Another important observation is that the curves of the FPTree tend to be more flattened than those of the other trees, which denotes a decreased dependency with respect to the latency of SCM. Additionally, the FPTree outperforms the STXTree for *Find*/*Insert*/*Update*/*Delete* by a factor of 2.10/1.13/1.71/ 1.22 at a latency of 90 ns, and thanks to fingerprinting, it is still 1.23×/1.02× faster for *Find*/*Update* at a latency of 650 ns, while the STXTree is 2.04×/1.99× faster for *Insert*/*Delete*.

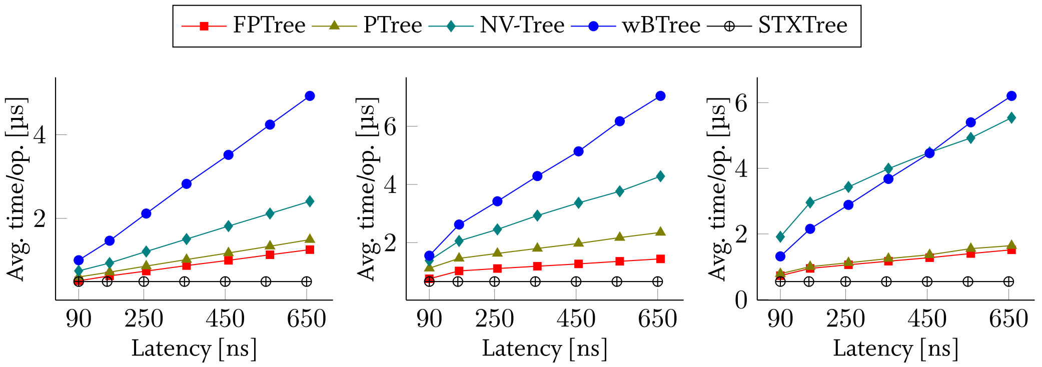

(a) Find (b) Insert (c) Update

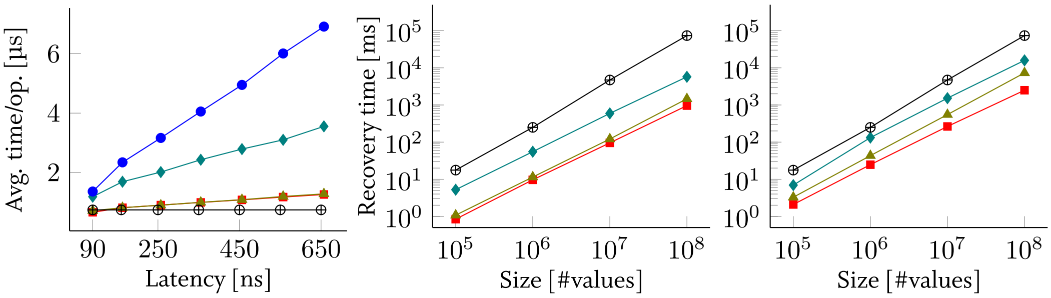

(d) Delete (e) Recovery 90ns (f) Recovery 650ns

Figure 4.12: Effect of the latency of SCM on the performance of the *Find*, *Insert*, *Update*, *Delete*, and *Recovery* tree operations with fixed-size keys.

Recovery

We evaluate the recovery performance of the trees, both for fixed-size and variable-size keys for different tree sizes and SCM latencies. Figures 4.12 and 4.13 depict the experimental results. Since the wBTree resides fully in SCM, it exhibits constant recovery time, in the order of one millisecond, and thus it is not depicted in the figure. We observe that for a tree size of 100M entries, the FPTree recovers 1.52×/2.93×, and 5.97×/6.38× faster than the PTree and the NV-Tree for an SCM latency of 90 ns/650 ns, respectively. This difference between the FPTree and the PTree is explained by the leaf groups that provide more data locality when traversing the leaves. The slower recovery time of the NV-Tree is due to the inner nodes being rebuilt in a sparse way, requiring a large amount of DRAM to be allocated. The recovery of the FPTree is 76.96× and 29.62× faster than a full rebuild of the STXTree in DRAM, for an SCM latency of 90 ns and 650 ns, respectively.

Regarding variable-size keys, most of recovery time of the PTree, the FPTree and the NV-Tree is spent dereferencing the persistent pointers to the keys in the leaves to retrieve the greatest key in each leaf. The rebuild of the inner nodes itself represents only a minor part in the total rebuild time. This explains why all three implementations tend to perform the same for recovery. Nevertheless, for a tree size of 100M entries, the recovery of the FPTree is 24.68× and 5.68× faster than a full rebuild of the STXTree in DRAM, for an SCM latency of 90 ns and 650 ns, respectively.

Memory Consumption

Figure 4.14 shows DRAM and SCM consumption of the trees with 100 million key-values and a node fill ratio of ~70%. Since the wBTree resides fully in SCM, it does not consume DRAM. We observe

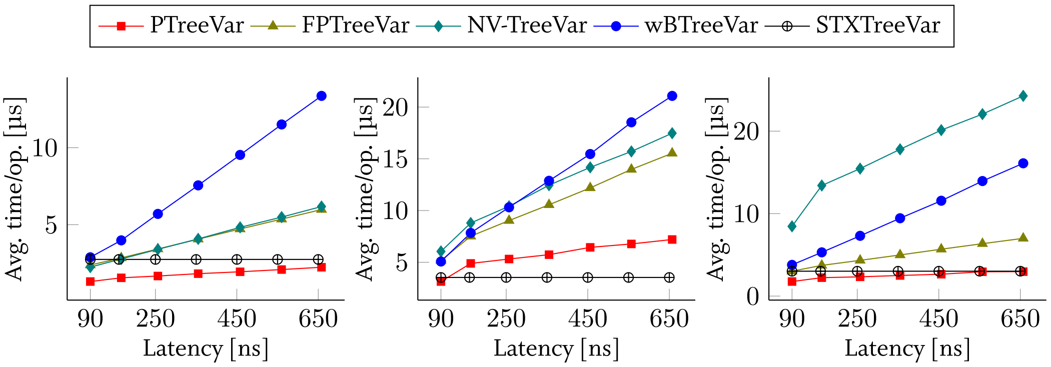

(a) Find (b) Insert (c) Update

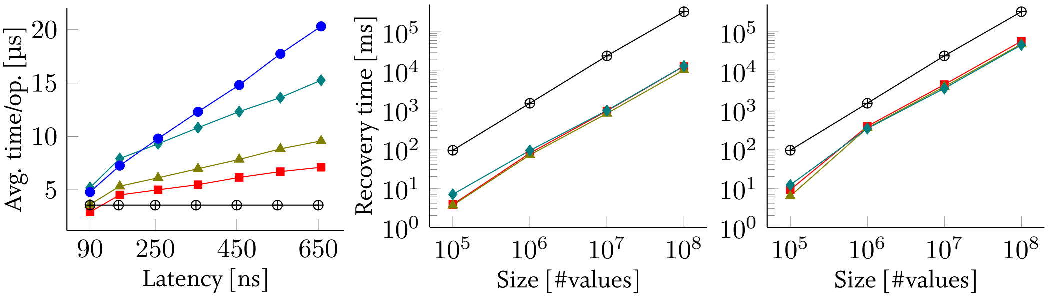

(d) Delete (e) Recovery 90ns (f) Recovery 650ns

Figure 4.13: Effect of the latency of SCM on the performance of the *Find*, *Insert*, *Update*, *Delete*, and *Recovery* tree operations with variable-size keys.

that for fixed-size keys, the FPTree needs 2.24 GB of SCM and only 64.12 MB of DRAM, i.e., only 2.71% of the total size of the tree. The PTree needs slightly more DRAM (5.19% of the size of the tree) because of its smaller leaves that lead to more inner nodes. The NV-Tree requires much more SCM and DRAM than the FPTree and the PTree: 3.62 GB of SCM and 1.09 GB of DRAM– which corresponds to 23.19% of the size of the tree. On the one side, the increase in SCM consumption is due to the additional flag that is added to every key-value and to the alignment of the leaf entries to be cache-line-aligned. On the other side, the increase in DRAM consumption is due to creating one leaf parent per leaf node when rebuilding the contiguous inner nodes. We observe similar results with variable-size keys, where consumed DRAM corresponds to 1.76% (108.73 MB), 3.78% (194.56 MB), and 12.67% (1.20 GB) of the total size of the tree for the FPTree, PTree, and NV-Tree, respectively. We note that the FPTree consumes slightly more SCM than the PTree due to the additional fingerprints in the leaves. The most salient observation is that the FPTree consumes one order of magnitude less DRAM than the NV-Tree.

4.4.3 Concurrent Microbenchmarks

For concurrency experiments, we use the system that supports Intel TSX. We compare the fixed-size and variable-size concurrent versions of the FPTree and the NV-Tree. The experiments consist of warming up the trees with 50 million key-values, then executing in order 50 million concurrent *Finds*, *Inserts*, *Updates*, and *Deletes* with a fixed number of threads. We also consider a mixed workload made of 50% *Inserts* and 50% *Finds*. To eliminate result variations, we use the *numactl* utility to bind every thread to exactly one core. The resource allocation strategy is to first allocate all physical cores before allocating the HyperThreads. When the two sockets are used, the cores are split equally between them.

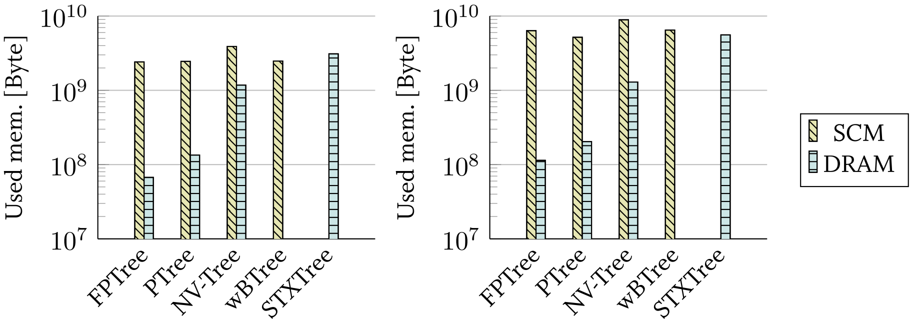

(a) Fixed-size keys (b) Variable-size keys

Figure 4.14: DRAM and SCM consumption of trees with 100M key-value: 8-byte and 16-byte keys for fixed-size and variable-size keys versions, respectively.

We evaluate concurrency in three scenarios: on a single socket (up to 44 logical cores), on two sockets (up to 88 logical cores), and on one socket with a higher SCM latency. For each scenario we depict throughput figures alongside speedup figures over single-threaded execution. Ideal speedup is depicted with the mark-less line.

Single-Socket Experiments

Figure 4.15 depicts the results for scalability experiments on one socket. We observe that the FPTree scales well for both fixed-size and variable-size keys throughout the range of threads considered. In the case of fixed-size keys, performance increases with 22 threads over single-threaded execution by a factor of 18.3/18.4/18.3/18.5/18.4 for the *Find*/*Insert*/*Update*/*Delete*/*Mixed* benchmarks, respectively. With 44 threads, and thus HyperThreading limiting the scaling, performance increases over the execution with 22 threads by a factor of 1.57/1.55/1.56/1.63/1.56 for the *Find*/*Insert*/*Update*/*Delete*/*Mixed* benchmarks, respectively. Compared with the FPTree, the NV-Tree has a lower base performance, and scales less. For fixed-size keys, its performance increases with 22 threads over single-threaded execution by a factor of 16.4/11.5/14.1/11.2/15.1 for the *Find*/*Insert*/*Update*/*Delete*/*Mixed* benchmarks, respectively. Performance increases with 44 threads over the execution with 22 threads by a factor of 1.49/1.73/1.07/1.74/1.61 for the *Find*/*Insert*/*Update*/*Delete*/*Mixed* benchmarks, respectively. We witness the same scalability patterns with variable-size keys. Between 45 and 88 threads, the performance of both the FPTree and the NV-Tree is stable and resists over-subscription.

Two-Socket Experiments

Results of the two-socket experiments are presented in Figure 4.16. We notice that the FPTree scales well for both fixed-size and variable-size keys. In the former case, the performance of the FPTree increases using 44 threads compared with single-threaded execution by a factor of 36.8/36.3/37.5/37.6/36.7 for the *Find*/*Insert*/*Update*/*Delete*/*Mixed* benchmarks, respectively. Using HyperThreading, performance increases with 88 threads over the execution with 44 threads by a factor of 1.50/1.30/1.34/1.53/1.37 for the *Find*/*Insert*/*Update*/*Delete*/*Mixed* benchmarks, respectively. As for the NV-Tree, it scales less than in the single socket scenario: performance increases with 44 threads compared with single-threaded execution by a factor of 31.2/10.5/10.9/9.1/15.6 for the *Find*/*Insert*/*Update*/*Delete*/*Mixed* benchmarks, respectively. With 88 threads, performance increases over the execution with 44 threads by

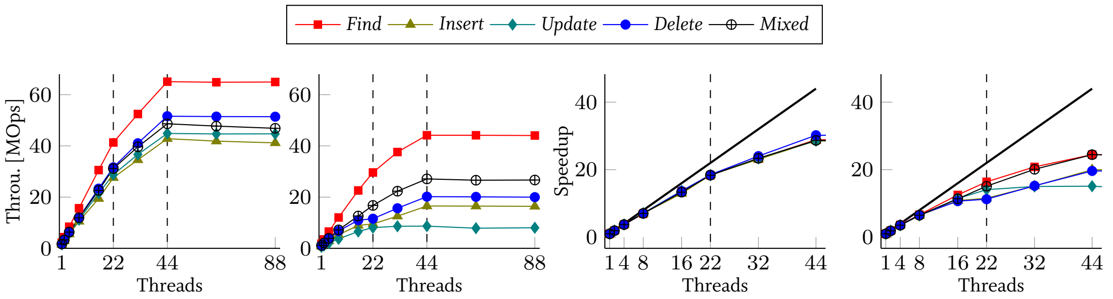

(a) FPTreeC (b) NV-TreeC (c) FPTreeC Speedup (d) NV-TreeC Speedup

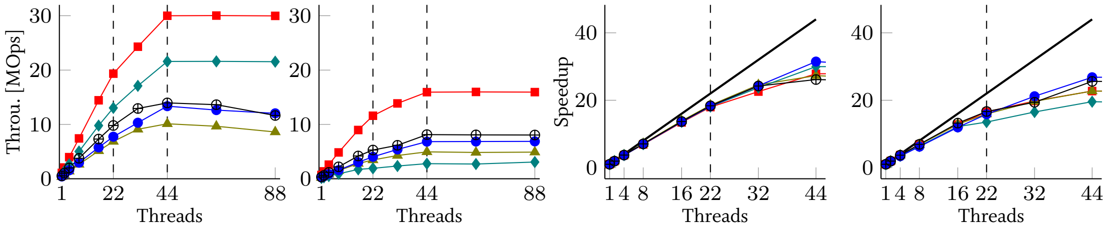

(e) FPTreeCVar (f) NV-TreeCVar (g) FPTreeCVar Speedup (h) NV-TreeCVar Speedup

Figure 4.15: Concurrency performance on one socket – 50 million key-values warmup followed by 50 million operations. Ideal speedup is depicted with the mark-less line.

a factor of 1.18/1.81/2.01/1.97/1.61 for the *Find*/*Insert*/*Update*/*Delete*/*Mixed* benchmarks, respectively. The latter factors are larger than expected, because when fully utilizing the logical cores, NUMA effects on performance fade out as consumed DRAM is homogeneously distributed over the sockets which enables the NV-Tree to catch its lost performance up. Yet, it exhibits significantly lower performance than the FPTree.

Regarding variable-size keys, the performance of the FPTree increases with 44 threads compared with single-threaded execution by a factor of 37.2/35.0/38.4/38.5/34.9 for the *Find*/*Insert*/*Update*/*Delete*/*Mixed* benchmarks, respectively. Using HyperThreading, performance increases with 88 threads over the execution with 44 threads by a factor of 1.54/1.63/1.63/1.62/1.67 for the *Find*/*Insert*/*Update*/*Delete*/*Mixed* benchmarks, respectively.

We observe that *Inserts* scale less than with fixed-size keys, and that the performance of *Deletes* flattens after 64 threads. The reason for that is threefold. First, these operations systematically involve an *expensive* allocation or a deallocation of a key in SCM. The persistent allocator implements concurrency by having one allocator object per physical core. While allocations are done by the core on which the requesting thread is running, ensuring good scalability, deallocations are executed by the object that allocated the memory in the first place. Hence, a high number of deallocations can create contention. Second, in HyperThreading mode, the two logical processors on the same core share its L1 cache that is used by TSX. This reduces the effective read and write set sizes of TSX transactions [66]. In fact, we observe a surge in transaction abortions that are due to full cache sets. We verify that by witnessing increased cache-set-related transaction abortions using the Intel Software Development Emulator [65]. Third, the hardware prefetcher speculatively prefetches data, which can exacerbate the previous problem. In conclusion, highly robust performance requires a scalable fall-back mechanism. However, we leave this to future work. As for the NV-Tree, it scales similarly to its fixed-size keys version since its base performance is slow enough so that persistent memory allocations and deallocations do not hinder scalability. Yet, it still exhibits a significantly lower performance than the FPTree.

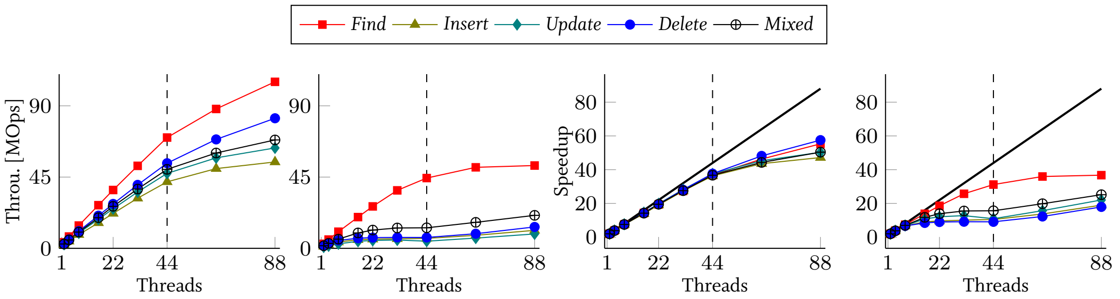

(a) FPTreeC (b) NV-TreeC (c) FPTreeC Speedup (d) NV-TreeC Speedup

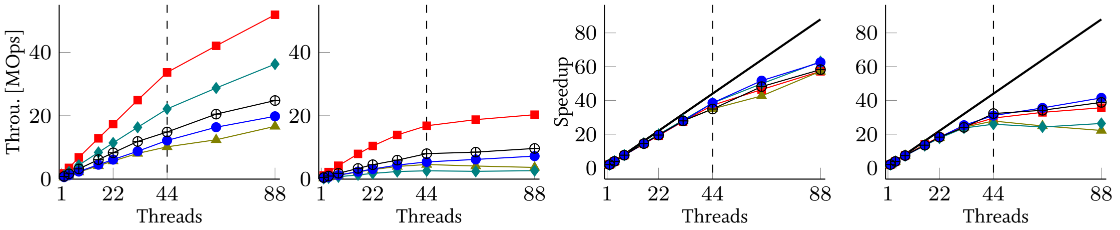

(e) FPTreeCVar (f) NV-TreeCVar (g) FPTreeCVar Speedup (h) NV-TreeCVar Speedup

Figure 4.16: Concurrency performance on two sockets – 50 million key-values followed by 50 million operations. Ideal speedup is depicted with the mark-less line.

Single-Socket Experiments with a Higher Latency

To emulate a higher SCM latency, we bind the CPU and DRAM resources to one socket and use the memory of the second socket as emulated SCM. Hence, latency increases from 85 ns (local socket latency) to 145 ns (remote socket latency). Figure 4.17 depicts the results for scalability experiments on one socket with an SCM latency of 145 ns. We observe that both the FPTree and the NV-Tree scale the same as with an SCM latency of 85 ns. The only difference is the decrease in throughput which is expected due to the higher emulated latency of SCM. Therefore, the scalability of our selective concurrency is not affected by the latency of SCM.

Overall, the FPTree has better scaling and throughput performance than the NV-Tree, both for fixed-size and variable-size keys, for the three scenarios, namely using one socket, two sockets, and one socket with a higher SCM latency.

Payload Size Impact on Tree Performance

In this experiment we study the effect of the payload (value) size on the performance of the evaluated trees. We follow the same experimental setup as in previous experiments while varying the payload size from 8 bytes to 112 bytes. Figures 4.18b to 4.18d depict single-threaded performance results with an SCM latency set to 360 ns, while Figures 4.18e to 4.18f depict multi-threaded performance on a single socket with 44 threads. We observe two patterns: (1) The NV-Tree stands out as the tree that is most affected by larger payloads, which is explained by the fact that linear scan of leaves needs to read larger amounts of data; (2) Insert operations tend to suffer more from larger payloads, which stems from the need for larger, more expensive SCM allocations. In general however, the performance of the FPTree and wBTree vary only slightly with larger payloads, thanks to them having respectively constant and logarithmic average leaf scan costs.

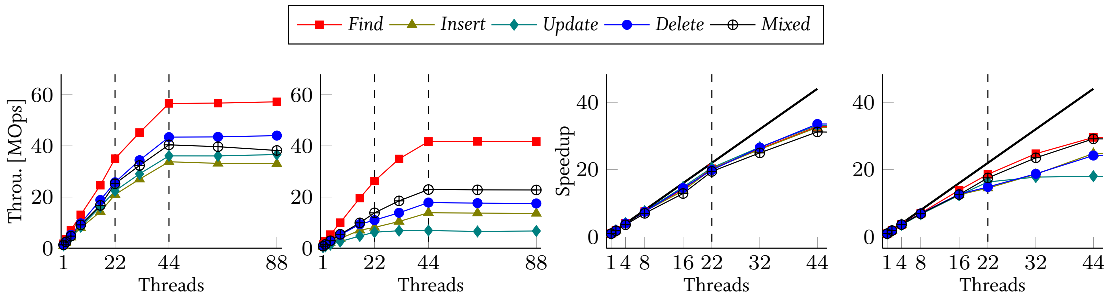

(a) FPTreeC (b) NV-TreeC (c) FPTreeC Speedup (d) NV-TreeC Speedup

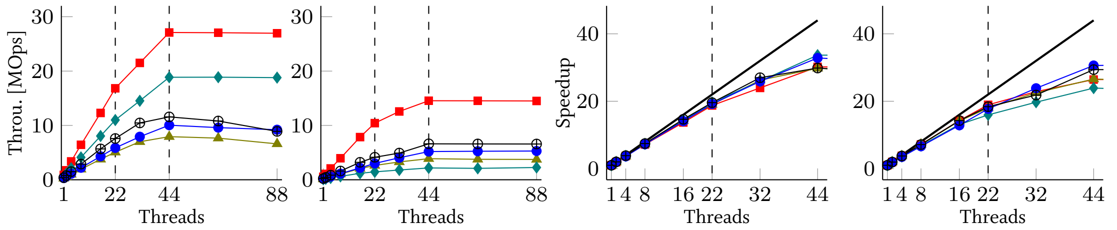

(e) FPTreeCVar (f) NV-TreeCVar (g) FPTreeCVar Speedup (h) NV-TreeCVar Speedup

Figure 4.17: Concurrency performance on one socket with an SCM latency of 145 ns – 50 million key-values warmup followed by 50 million operations. Ideal speedup is depicted with the mark-less line.

4.4.4 End-to-End Evaluation

We integrated the evaluated trees in two systems: our database prototype SOFORT, and *memcached*, a popular key-value cache.

Database Experiments

We replace the dictionary index of the dictionary-encoded, columnar storage engine of SOFORT by the evaluated trees. Only the fixed-size keys versions of the trees are needed for the dictionary index. To measure the impact of the persistent trees on transaction performance, we run the read-only queries of the Telecom Application Transaction Processing Benchmark [155] (TATP) with 50 million subscribers and 8 clients on the emulation system. The primary data size is 45 GB.

During the warm-up phase where the database is created, *Subsriber Ids* are sequentially generated, thus creating a highly skewed insertion workload, a situation that the NV-Tree was unable to handle. This is because highly skewed insertions happen most often in the same leaf node. A last-level inner node will then quickly become full and trigger a costly rebuild of the inner nodes. The workload-adaptivity scheme of the NV-Tree tries to space the rebuild phases by dynamically increasing the size of write-intensive nodes at split time, which defers but does not solve the issue of frequent rebuilds in presence of sorted insertions. Eventually, the NV-Tree will have one parent node per leaf node which provokes a memory overflow in our system. To avoid this issue, we set the size of leaf nodes to 1024 and that of inner nodes to 8. The large leaf nodes aim at decreasing the number of inner node rebuilds, while the small size of inner nodes aims at keeping the memory footprint of inner nodes small, even in the case of having one parent node per leaf node.

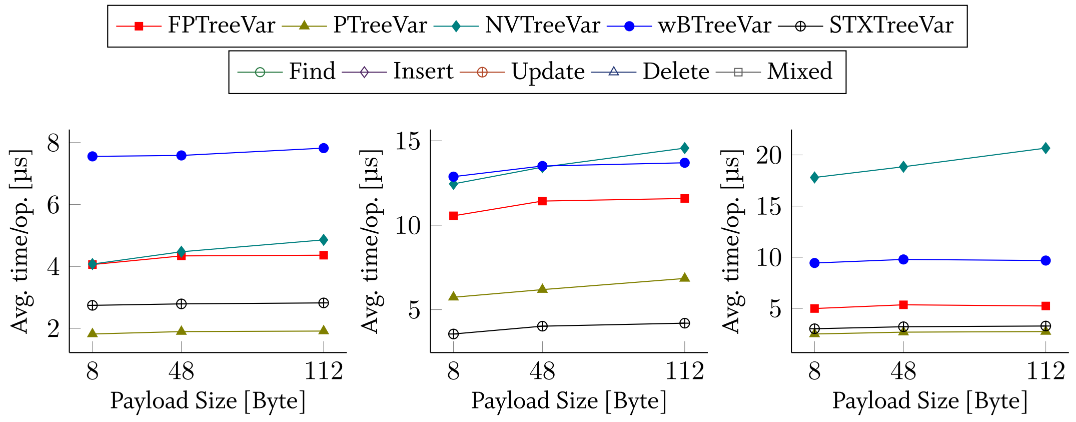

(a) Find (b) Insert (c) Update

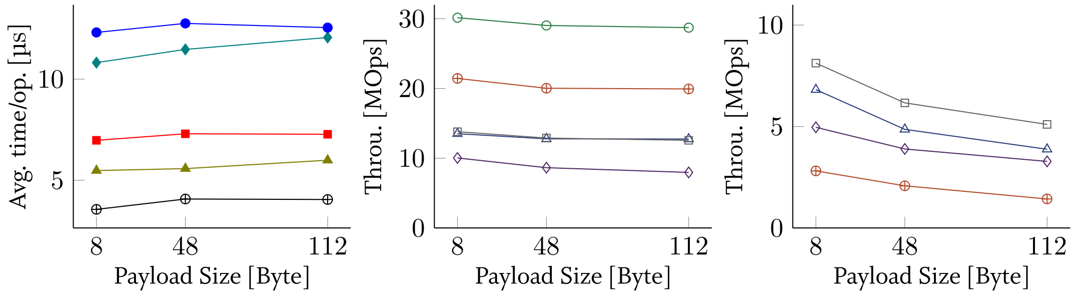

(d) Delete (e) FPTreeVar – 44 thr. (f) NVTreeVar – 44 thr.

Figure 4.18: Impact of payload size on the single-threaded and multi-threaded performance of the evaluated trees.

The results are depicted in Figure 4.19a. We observe that compared with using the fully transient STXTree, the FPTree incurs an overhead of only 8.74%/12.80% for an SCM latency of 160 ns/650 ns, while the overheads incurred by the PTree, NV-Tree, and wBTree are 16.98%/16.89%, 39.61%/51.77%, and 24.27%/48.23%, respectively. On the one side, the limited slowdown caused by the FPTree and the PTree shows the significant benefit of selective persistence from which stems a decreased dependency with respect to the latency of SCM. On the other side, the FPTree outperforming the PTree shows the benefits of the fingerprints. The decrease in throughput with higher SCM latencies is due to other database data structures being placed in SCM. Note that because of its larger leaves, the NV-Tree performs worse than the wBTree.

To measure the impact on database recovery, we simulate a crash and monitor the restart time. We use the same benchmark settings as in the previous experiment. Recovery consists of checking the sanity of SCM-based data and rebuilding DRAM-based data. The recovery process is parallelized and uses 8 cores. Figure 4.19b shows restart time results. Since the wBTree resides fully in SCM, recovery is near-instantaneous –in the order of tens of milliseconds. However, using the wBTree incurs a severe overhead on query performance, as shown in Figure 4.19a. We observe that the FPTree, PTree, and NV-Tree allow respectively 40.17x/21.56x, 26.05x/8.32x, and 21.42x%/9.58% faster restart times for an SCM latency of 160 ns/650 ns than using the STXTree. One can note that the NV-Tree performs on par with the PTree thanks to its larger leaves which allow for more data locality while scanning the leaf nodes during recovery. Still, the FPTree outperforms the NV-Tree thanks to rebuilding compact inner nodes, and outperforms the PTree thanks to using leaf groups that provide better data locality when traversing the leaves during recovery.

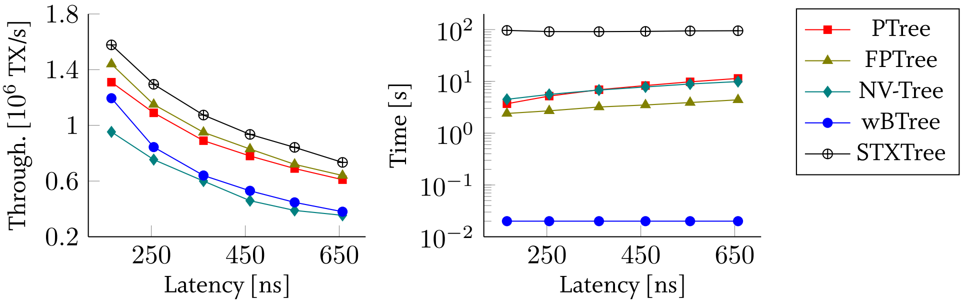

(a) DB throughput

(b) DB restart time

Figure 4.19: Trees impact on database throughput and restart performance – TATP with 50 million subscribers, primary data size ~45 GB.

Memcached Experiments

Memcached [104] is a key-value cache that uses a main-memory hash table internally. It employs a locking mechanism on two levels: global locks on the LRU lists of items, and locks on the buckets of the hash table. We replace the hash table by the variable-size keys versions of the evaluated trees. Furthermore, we remove the bucket locking mechanism and either replace it with global locks for non-concurrent trees, or rely on the concurrency scheme for the concurrent trees. Another necessary change is to insert the full string key in the trees instead of its hash value to avoid collisions.

To measure the impact on performance, we run the *memcached* server on the HTM system, and the *mc-benchmark* [103] with 50 clients on the emulation system. The measured network bandwidth between the two machines is 940 Mbits/s. We found that using 2 workers in *memcached* yielded the best results for the single-threaded trees while 4 workers was the optimal for the concurrent ones. The *mc-benchmark* executes 50 million SET requests followed by 50 million GET requests. Additionally, we use the same method as in the concurrency experiments to emulate a higher latency, that is, we bind *memcached* to one socket and use the memory of the other socket for SCM.

Figure 4.20 summarizes the experimental results. We observe that the NV-Tree and the concurrent version of the FPTree (denoted *FPTreeC* in the figure) perform nearly equally to vanilla *memcached* with the hash map table, for both latencies (85 ns and 145 ns) because their concurrent nature allows them to service requests in parallel and saturate the network. In fact, the incurred overhead is less than 2% for the concurrent FPTree, and less than 3% for the NV-Tree. The single-threaded trees however incur significant overheads: For SET/GET requests, the overheads incurred by the single-threaded FPTree, PTree, and wBTree are respectively 11.45%/0.29%, 40.37%/3.40%, and 45.57%/3.81% for an SCM latency of 85 ns. These overheads surge to respectively 37.28%/2.39%, 54.90%/24.06%, and 59.88%/32.40% with a higher SCM latency of 145 ns. As for the STXTree that resides fully in DRAM, it incurs an overhead of 28.29%/4.83% for SET/GET requests, respectively.

In conclusion, in both microbenchmarks and end-to-end scenarios, the FPTree performs nearly equally to its transient counterparts, significantly outperforms state-of-the-art persistent trees, and scales well in highly-concurrent situations.

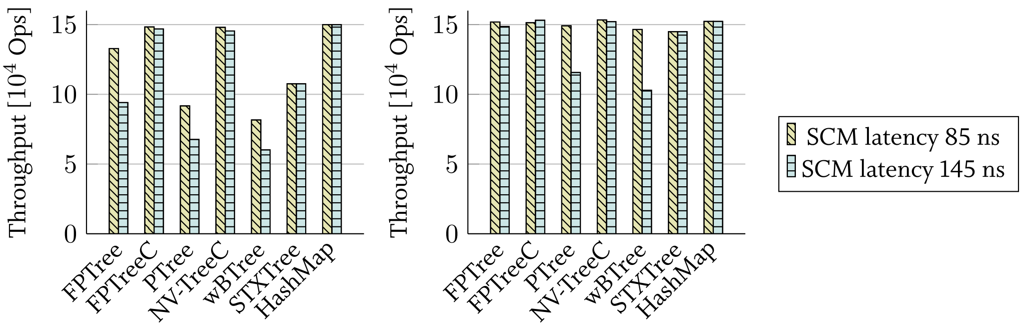

(a) SET requests (b) GET requests

Figure 4.20: Trees impact on *memcached* performance for different latencies – *mc-benchkark* with 50 million operations.

4.5 SUMMARY

In this chapter, we proposed the *FPTree*, a novel hybrid SCM-DRAM persistent, concurrent B^+-Tree that supports both fixed-size and variable-size keys. Pivotal to the design of the FPTree are the following key principles: fingerprinting, selective persistence, selective concurrency, and unsorted leaves with out-of-place updates.

These design principles make it possible to achieve the goals we put forward for our work: (1) The FPTree is persistent and guarantees any-point crash recovery to a consistent state without loss of information; (2) The FPTree exhibits fast recovery compared to a full rebuild; (3) The performance of the FPTree is similar to that of transient data structures, is resilient to high SCM latencies, and scales well under high concurrency.

We performed an extensive experimental evaluation which showed that our FPTree exhibits significantly better base operation performance compared with state-of-the-art persistent trees, while using DRAM for less than 3% of its total size. Moreover, the FPTree recovery performance is almost one order of magnitude faster than a full rebuild. We conducted an end-to-end evaluation using *memcached* and a prototype database. We show that compared with a fully transient tree, the overhead of using the FPTree is limited to less than 2% and 13% for *memcached* and our prototype SOFORT, respectively, while using state-of-the-art persistent trees incur an overhead of up to 60% and 52%, respectively.

Perhaps most importantly, the FPTree relies on a sound programming model that addresses all the programming challenges we identified in Chapter 3, which we argue is an important step towards devising sound building blocks that can be used to design and implement larger and more complex systems, such as SOFORT.

5

SOFORT: A HYBRID SCM-DRAM TRANSACTIONAL STORAGE ENGINE

In the previous chapters, we devised necessary building blocks, namely memory management and data structures for the design and implementation of SCM-based data-management systems. In this chapter we demonstrate such a system and present SOFORT, a hybrid SCM-DRAM dictionary-encoded columnar transactional engine tailored for hybrid transactional and analytical workloads and fast data recovery[1]. SOFORT is a single-level store, i.e., the working copy of the data is the same as the durable copy of the data. To achieve this, SOFORT leverages the byte-addressability of SCM to persist data in small increments at cache-line granularity. Since the database state is always up-to-date, SOFORT does not need a redo log. SOFORT implements serializable multi-version concurrency control (MVCC) coupled with cooperative garbage collection.

SOFORT is architected as a twin-store columnar main-memory database, with a larger static immutable read-optimized store and a smaller dynamic read/write store. The dynamic store is periodically merged into the static store to do compaction. This keeps the size of the dynamic store small, and therefore results in an optimal performance for reads and writes. The results of the microbenchmarks shown in Section 2.1.2 led us to envision that the static store can be entirely kept in SCM at a negligible cost for query execution, and instantly recovered after failure [3]. Therefore, we focus only on the dynamic part in this dissertation.

To track conflicts between transactions, MVCC keeps for every transaction, among other metadata, a write set that contains the row IDs of the tuples that the transaction inserted or deleted. This information is enough to undo a transaction in case it is aborted. We make the observation that the same information can be used to undo the effects of in-flight transactions during recovery. Therefore, to provide durability, SOFORT places the MVCC write set in SCM, which enables it to remove the traditional write-ahead log from the critical path of transactions. SOFORT stores its columns contiguously in memory, which complicates memory reclamation of deleted tuples. Indeed, the latter would require a writer-blocking process which would replace the current columns with new, garbage-free ones. To remedy this issue, we propose to keep track of deleted rows and re-use them when inserting new tuples whenever possible instead of appending them to the table.

Through an extensive experimental evaluation, we show that SOFORT exhibits competitive OLTP performance despite being a column-store. We also demonstrate the effectiveness and scalability of our garbage collection. We defer the performance evaluation of recovery to Chapter 6. The contributions of this chapter are as follows:

---

[1] The material in this chapter is partially based on [122, 128]

- the design of SOFORT, an OLAP-friendly columnar storage engine that achieves competitive OLTP performance;
- an adaptation of MVCC to SCM in a way that removes traditional write-ahead logging from the critical path of transactions;
- an extension of our SCM-optimized MVCC that enables SOFORT to continue unfinished transactions after failure;
- an efficient garbage collection scheme for a column-store.

This chapter is organized as follows: Section 5.1 surveys state-of-the-art multi-versioned database systems following four dimensions, namely concurrency control, version storage, indexing, and garbage collection. Thereafter, following the same structure, Section 5.2 presents the architecture of SOFORT, contrasting our design decisions with those of the state of the art. Afterwards, Section 5.3 presents the implementation details of SOFORT, with a focus on how it achieves failure atomicity. Moreover, Section 5.4 elaborates on how SOFORT can continue unfinished transactions after failure. We provide a performance evaluation in Section 5.5. Finally, Section 5.6 summarizes this chapter.

5.1 DESIGN SPACE EXPLORATION

Multi-Version Concurrency Control (MVCC) was first proposed by Reed in 1978 [144]. Since then, MVCC has co-existed with single-version concurrency control. However, the advent of main-memory database systems in the last decade made MVCC the de facto choice because it allows the database to better leverage the additional concurrency offered by hardware. Multi-versioning consists in keeping several versions of a single tuple, each of which representing the state of the tuple in mutually exclusive time intervals. Therefore, read queries can always read a consistent version of a tuple regardless of whether this tuple is being updated. By loosening the coupling between reads and writes, MVCC allows for more concurrency. Moreover, if old tuple versions are never deleted, any past state of the database can be queried. Wu et al. [176] presented an empirical survey of MVCC techniques. They distinguished four design dimentions: concurrency control, version storage, index management, and garbage collection. Based on their analysis, we propose in the following a summary of the design space of MVCC database systems.

5.1.1 Concurrency Control

MVCC usually keeps for each tuple the following metadata (all of which are initialized to zero):

- a creation timestamp (CTS) that indicates the time starting from which a tuple is visible;
- a deletion timestamp (DTS) indicating the time up to a tuple is visible;
- a transaction ID (TXID) that serves as a write lock for the tuple;
- a pointer to either the previous or the next version of this tuple (see Section 5.1.2 for more details).

MVCC has been extensively researched in the last decade. Since our goal is not to devise a new concurrency control protocol, but rather to adapt one to SCM, we only sample related work. Wu et al. [176] identified four main families of concurrency control protocols for multi-versioned database systems, which we present in the following.

Timestamp Ordering (MVTO)

MVTO is Reed's original proposed concurrency control protocol [144, 143]. The main idea behind MVTO is to use the start timestamp (STS) of transactions to determine their serial execution order. The STS serves as the TXID in this case. MVTO keeps additionally in the tuple's metadata the STS of the last transaction that read a tuple. We denote this field as read timestamp (RTS).

A transaction *T1* is allowed to read a tuple's latest version if: (1) the tuple is not locked by another transaction (i.e., its TXID is equal to zero or to *T1*'s TXID); and (2) *T1*'s TXID falls in between the tuple's CTS and DTS. If these conditions are satisfied, then *T1* sets the RTS of the tuple to its TXID if the existing RTS is lower than its TXID. If the conditions are not satisfied, then *T1* reads an older version of the tuple and does not need to update the tuple's RTS.

A transaction *T1* is allowed to update a tuple a_n if: (1) a_n is not locked by any active transaction; and (2) *T1*'s TXID is greater than a_n's RTS. The second condition ensures that the serial order of transactions, decided by their TXID, is respected. If these conditions are not satisfied, then *T1* is aborted. Otherwise, *T1* locks a_n, then updates it by creating a new (locked) version a_{n+1}. When *T1* commits, it sets the DTS of a_n to its TXID and the CTS and DTS of a_{n+1} to its TXID and infinity, respectively.

Finally, we discuss phantom prevention. Consider two transactions *T1* and *T2*, where *T1* logically precedes *T2* (i.e., the serial order is *T1* then *T2*). Since *T1* logically precedes *T2*, then *T2* must be able to see all tuples that *T1* inserted. Assume that *T2* reads a set of tuples that satisfy a specific predicate. Thereafter, *T1* inserts a tuple that satisfies the aforementioned predicate. *T2* is unable to see this tuple because it has already completed its read operation. Therefore, the newly inserted tuple is a *phantom*. MVTO as described above does not prevent such a scenario, therefore, it is not serializable. A way to remedy this issue is to use key range locks when reading [108, 54], which prevents other transactions from inserting new tuples that fall within the locked range.

Optimistic Concurrency Control (MVOCC)

Optimistic Concurrency Control (OCC) was first proposed by Kung et al. [81], and was adapted to multi-versioning by Larson et al. [84]. OCC relies on the assumption that conflicts between transactions are rare. Therefore, it allows transactions to read tuples without acquiring any locks. MVOCC splits a transaction in three phases: First, the transaction issues its read and write requests in the *read phase*. During this phase, the transaction keeps a read set that consists of references to all its read tuples. If the transaction is ready to commit, then it enters the *validation phase*, where all the transaction's read operations are redone, and the result intersected with the transaction's read set. If no new tuples are observed, then the transaction is allowed to enter the *write phase*, which starts by acquiring a commit timestamp, then updating the metadata of modified tuples, i.e., setting the CTS of created tuples and the DTS of deleted tuples to the commit timestamp. Otherwise, the transaction is aborted. Note that the checks of the *valiadtion phase* are able to detect phantoms.

When a transaction starts, it is assigned a unique TXID, and an STS equal to the current logical time. During the *read phase*, a transaction *T1* is allowed to read a tuple if: (1) The tuple is not locked and *T1*'s STS is in between the CTS and the DTS of the tuple; or (2) the tuple is locked for creation by another transaction that is in the *validation phase*; or (3) the tuple is locked for deletion by another transaction that is in the *read phase*. Basically, if a conflict with another transaction *T2* is detected, then MVOCC assumes that *T2* will successfully commit before *T1* if *T2* is in the *validation phase*, thereby proceeding optimistically. *T1* registers a dependency to *T2* and waits, during the *validation phase*, until *T2* commits. If *T2* aborts, then *T1* must abort as well. Keeping transaction dependencies might lead to cascaded aborts. *T1* is allowed to update a tuple if it is not locked. If *T1* successfully locks a tuple, then it updates it similarly to MVTO. Otherwise, *T1* is aborted.

The main advantage of MVOCC is that read operations do not require any locking. However, this comes at the cost of potentially expensive checks during the *validation phase*. Moreover, a transaction finds out that it must abort due to a conflict only in the *validation phase*.

There is a large body of work that focused on optimizing the implementation of MVOCC in the last years. For instance, Tu et al. [161] propose Silo, a main-memory storage engine that uses a decentralized, *epoch*-based design to achieve high scalability. Several systems, such as FOEDUS [172] and ERMIA [78] improved on top of Silo's ideas. Moreover, Neumann et al. [114] adapt *precision locking* [75] to MVOCC, which enables to significantly decrease the amount of metadata required for pre-commit validation. Finally, Wu et al. [177] propose to redo only conflicting reads or writes when retrying an aborted transaction, and reuse the results that did not conflict, thereby significantly decreasing the cost of retrying aborted transactions.

Two-Phase Locking (MV2PL)

Two-phase locking (2PL) [12] follows a pessimistic approach: a transaction must first acquire locks on both tuples it reads and modifies. To adapt 2PL to multi-versioning, we need to extend the metadata of tuples to encompass a read lock in the form of a counter (i.e., shared lock) that we denote RCTR. The tuple's TXID serves as an exclusive write lock. The RCTR of a tuple a_n is incremented whenever a transaction accesses a_n, and decremented whenever that transaction commits or aborts.

A transaction *T1* is allowed to read a tuple if: (1) the tuple is not locked for write (i.e., its TXID is equal to zero); and (2) *T1*'s TXID is in between the tuple's CTS and DTS. If these conditions are satisfied, then *T1* locks the tuple for read by atomically incrementing its RCTR. *T1* is allowed to modify a tuple if it is not locked neither for read nor for write (i.e., both the tuple's TXID and RCTR are equal to zero). If these conditions are satisfied, then *T1* locks the tuple for write. If *T1* fails to acquire either a read or a write lock, it can either wait until it acquires a lock, which might lead to deadlocks, or eagerly abort.

Similarly to MVTO, MV2PL as described above does not guarantee serializability because it does not prevent phantoms. To make MV2PL serializable, we need to employ key range locks.

Serialization Certifier

Another approach is to rely on a serialization certifier to arbitrate concurrent transactions. A certifier is usually employed on top of an existing, weaker isolation level to provide serializability. In essence, a certifier aims to offer the performance of the lower isolation level with the guarantees of serializability. The first certifier proposals relied on constructing offline a serialization graph for detecting transaction conflicts that would break serializability constraints [45]. Therefore, this approach does not support ad-hoc or data-dependant queries and requires a new analysis whenever the set of transaction templates of an application is changed.

To remedy this shortcoming, Cahill et al. [16] proposed Serializable Snapshot Isolation (SSI), a certifier-based concurrency algorithms that builds on top of snapshot isolation to provide serializability. Under snapshop isolation, when a transaction starts, it is assigned an STS, which will also serve as its commit timestamp. Instead of building an expensive serialization graph, SSI tracks only *anti-dependencies* between transactions. SSI maintains two booleans per transaction: *outConflict* and *inConflict*. An anti-dependency characterizes one of two scenarios: The first one is when a transaction *T1* reads a tuple that does not represent the latest version, because a transaction *T2* (that must have started after *T1*) updated it. When this scenario is encountered, there is an anti-dependency from *T1* to *T2*, therefore, SSI sets *T1.outConflict* and *T2.inConflict* to true. The second scenario is when a transaction *T1* reads the latest version of a tuple, then a subsequent transaction *T2* updates this tuple. When this scenario is encountered, there is an anti-dependency from *T1* to *T2*, therefore, SSI sets *T1.outConflict* and *T2.inConflict* to true. Detecting this scenario is more challenging than the previous one. To detect it, Cahill et al. [16] propose to introduce a new shared lock, denoted SIREAD, which is set when a transaction reads a version of a tuple. Anti-dependencies are then identified whenever both SIREAD and the write lock of a tuple are set. To set properly the transaction flags, the database must provide which transactions hold a particular SIREAD. SSI aborts a transaction whenever both its *outConflict* and *inConflict* flags are true, which is proven to be sufficient in preventing the anomalies of snapshot isolation [45]. Nevertheless, this condition is only sufficient, which means that there might be false positives.

More recently, Wang et al. [171] proposed the Serial Safety Net (SSN). SSN is more accurate and more powerful than SSI because it can serialize any isolation level that is at least as strict as read-committed, which is a weaker isolation level than snapshot isolation.

5.1.2 Version Storage

Multi-version storage engines usually chain together the versions of a tuple into a latch-free linked list using the pointer field of MVCC metadata. We find multiple ways of doing so in the literature. In the following we discuss the two major ones identified in the literature.

Append-Only Storage

An append-only MVCC storage scheme is characterized by the fact that any tuple update generates a new full tuple, even if only one attribute of the tuple is updated. In fact, a tuple update in an append-only table requires the following steps: (1) create and append a copy of the tuple (i.e., a new version) to the table; (2) update the attributes of the new version; and (3) link the new version to the previous versions of the tuple. Step (1) depends on how tuples are stored in a table. For instance, tuples can be stored contiguously in memory, or stored next to the keys of the primary index. Step (3) can be done by making the new tuple either the head or the tail of the version chain. Therefore, version chains are either ordered from oldest to newest (O2N), such as in the Hekaton [84] main-memory database, or from newest to oldest (N2O), such as in the MemSQL [105] main-memory database. O2N has the advantage that an update does not require updating indexes over non-updated attributes. However, the disadvantage of O2N is that read queries have to traverse the whole version chain to access the latest version of tuple, because the version chain is a simple linked-list. Therefore, the performance of O2N highly depends on the ability of the system to swiftly reclaim garbage versions. N2O remedies this issue by always indexing the latest version of a tuple. However, this comes at the cost of updating all the indexes of the table, regardless of whether the attributes they index are updated or not, when a tuple is updated.

A special case of append-only storage is *time travel storage*, in which an MVCC storage engine never deletes any versions to provide anytime snapshot isolation capability. In this scheme, each table encompasses two parts: the master table, and the time travel table. An advantage of time travel storage is that indexes always refer to the tuple in the master table, which lifts the need to update indexes over non-updated attributes. The master table contains the newest versions of the tuples, while the time travel table contains older versions (i.e., N2O version chain). A tuple update is performed by creating a copy of the newest version in the time travel table, then updating the tuple stored in the master table. Note that storing the oldest version in the main table and newer versions in the time travel table (i.e., O2N version chain) is possible and is implemented in some database systems such as SAP HANA [88].

Delta Storage

Delta storage keeps a master table that contains the master tuples (oldest if O2N, newest if N2O), and for each tuple, a list of delta versions such that each version contains only the attributes that are different from its preceding version. Delta versions are managed in a delta storage, called *undo buffer* in Hyper [114], which we use to illustrate how a tuple update in a delta storage scheme works. Hyper keeps transaction-local undo buffers, that are used to store the older tuple versions until they can be reclaimed by the garbage collector. Basically, tuples are updated in-place at the attribute level and the pre-image of their modified attributes is copied to the undo buffer. This improves the performance of concurrency control by reducing the amount of data that needs to be copied, and avoiding to update indexes that track non-updated attributes. It also speeds garbage collection because an undo buffer can be reclaimed entirely as a garbage unit.

By copying only modified attributes, delta storage significantly decreases the memory footprint of an MVCC system. However, to access a tuple version other than the master one, a transaction needs to traverse the version chain to reconstruct, potentially attribute by attribute, the desired tuple version.

5.1.3 Index Management

Indexing is an important and necessary part of any transactional system. MVCC introduces more complexity in index management since indexes have to account for different tuple versions. Tuple visibility metadata is decoupled from the indexes. Therefore, an index can contain entries for invisible versions. Primary and secondary indexes are managed differently in an MVCC system. An index maps a set of attributes, which constitutes the key, to a tuple reference, which constitutes the value. Depending on the version storage scheme, primary keys always reference either the newest or the oldest version of a tuple. In contrast, secondary indexes can reference any existing tuple version, because both their keys and values can change, while only the value can change in a primary index. Therefore, secondary indexes are more challenging to manage than primary indexes.

Transactions are allowed to update and insert in primary indexes, but only to insert in secondary indexes. Index delete operations are exclusively handled by the garbage collector to ensure snapshot visibility. In Section 5.1.2 we discussed when index updates are required for each version storage scheme. In particular, while the N2O append-only version storage scheme requires to update primary and secondary indexes when a tuple is updated, the O2N append-only and delta version storage schemes require only to update secondary indexes that index modified attributes. Moreover, in the case of an O2N version storage scheme, the garbage collector has the additional responsibility of updating primary indexes when reclaiming the oldest version of a tuple.

We distinguish two ways of implementing indexes depending on the nature of tuple references they employ. The first way is to use physical pointers to refer to a tuple, which is always possible for primary indexes since they reference the master tuple versions. However, secondary indexes can use physical pointers only in append-only version storage schemes, because each version is stored with all of its attributes. In the delta version storage scheme, non-master versions are stored as a sequence of modified attributes, which means that they cannot be referenced with a physical pointer. Examples of MVCC database systems that use physical pointers include Hekaton [84] and MemSQL [105].

The second way of implementing indexes is using logical pointers. In this approach, each tuple is associated with a unique ID. The system provides additionally a map that translates tuple IDs to the physical address of the master version of the corresponding tuple. This map needs to be updated whenever the master version of a tuple changes, e.g., when updating a tuple in an append-only version storage scheme. Delta version storage schemes adopt logical pointers by design. Nevertheless, logical pointers can be used with any version storage scheme. A straightforward implementation, exemplified by NuoDB [116], is to use the primary key as the unique ID, and the primary index as the mapping from tuple ID to physical pointer. In this case, secondary indexes need to store the whole primary key as its entry value. A lookup consists in retrieving the primary key, then probing the primary index to get the tuple physical pointer. This is not optimal, especially for large primary keys, because it incurs a significant memory overhead and a systematic, additional primary index lookup. An alternative is to generate unique integer tuple IDs, and map them to their corresponding tuple physical pointers in a hash table. Hyper [114] is an example of this approach.

The main advantage of logical pointers is that they alleviate the need to update indexes whose indexed attributes were not modified, thereby improving the system's update performance. However, this comes at the cost of read performance: Secondary index scans return tuple IDs, which then need to be translated into physical pointers to master tuple versions. However, the master version might not represent the indexed version. Therefore, the version chain needs to be traversed in order to find the appropriate version. In contrast, secondary indexes that use physical pointers give direct access to the right version. In summary, physical pointers favor reads while logical pointers favor writes.

5.1.4 Garbage Collection

The main purpose of garbage collection is to reclaim the space of deleted versions to limit the memory footprint of the system and prevent the system from running out of storage. Additionally, more garbage translates into longer version chains, which has a negative impact on performance. For instance, in an O2N scheme, a transaction needs to traverse the whole version chain to retrieve the latest version of a tuple, which is proportionally expensive to the number of versions, therefore, to the amount of garbage tuples. In an N2O scheme, indexes are updated for each tuple update, which means that indexes contain more garbage entries than in the O2N scheme. The performance of these indexes decreases proportionally to the number of garbage entries they contain. Hence, a second purpose of garbage collection is to delete garbage entries from indexes to maintain performance. In brief, garbage collection is essential for both limiting memory consumption and maintaining performance.

A tuple is considered as garbage if it was created by an aborted transaction, or if it was deleted and its DTS is lower or equal to the STS of the oldest active transaction. To reclaim a garbage tuple, the garbage collector removes it from its corresponding version chain, deletes its corresponding index entries, and claims its storage space. There are two approaches to garbage collection depending on the considered garbage unit. A garbage unit is either a single tuple version, or the set of deleted (created) tuples by a committed (aborted) transaction; these two approaches are referred to as *tuple-level* and *transaction-level* garbage collection, respectively.

Tuple-level garbage collection tests the visibility of each tuple to determine whether it can be reclaimed. It can be implemented in two ways. The first option, denoted *background vacuuming* and exemplified by Postgres [152], is to have background threads scan the database to identify garbage tuples. However, it does not scale to large database instances. There are several optimizations that can attenuate this, such as maintaining bitmaps or dirty blocks of tuples to avoid scanning blocks that were not modified since the last garbage collection pass. The second option, named *cooperative cleaning* and exemplified by Hekaton [84], makes transactions reclaim garbage versions they encounter when issuing scan requests. While cooperative cleaning scales better than background vacuuming, it is limited to the O2N append-only version storage scheme. Moreover, cooperative cleaning requires an additional periodic background garbage collector that reclaims old tuples that are never queried, hence, never detected by transactions.

Transaction-level garbage collection leverages the fact that garbage versions created by the same transaction share the same visibility. In the case of a committed transaction, the DTS of all its deleted tuples is equal to its commit timestamp, therefore, all these tuples qualify for reclamation if the commit timestamp is lower or equal to the smallest STS among active transactions. In the case of an aborted transaction, all its created rows qualify immediately for reclamation since they were never visible. The reclamation can either be done by background threads, or by the worker threads between running two transactions. Transaction-level garbage collection is simpler and more efficient than tuple-level garbage collection. However, it requires to keep a centralized data structure where transactions register their garbage, which might become a bottleneck if not implemented properly. Nevertheless, this can be mitigated by making transactions register their garbage in core-local structures [161]. The workers threads reclaim garbage only from their local garbage structure. Another optimization is to use *read-copy-update*-style epochs to reclaim garbage [161].

Garbage collection in hybrid OLTP and OLAP systems faces the challenge if long-running analytical transactions, which block the reclamation of old tuples. This leads to an accumulation of garbage, which both decreases performance and increases memory consumption. None of the solutions discussed above can efficiently address this problem. Lee et al. [89] propose a solution that identifies garbage versions based on timestamp visibility intervals, instead of the minimum STS among active transactions. The main idea is to block the reclamation of only the versions that should be visible to currently running transactions. Therefore, a long-running transaction can block the reclamation of only one version per tuple, instead of all versions in the minimum STS approach. The authors devise a hybrid solution, implemented in SAP HANA, that executes in three steps. The first one is to execute transaction-level garbage collection as described above. The second step is to execute *table-level garbage collection*, which consists in reclaiming the garbage of the tables that are not accessed by long-running transactions – known in the case of pre-compiled stored procedures. The third and final step is to execute tuple-level garbage collection based on timestamp visibility intervals.

5.2 SOFORT ARCHITECTURE

In this section we describe the architecture of SOFORT. We follow the same structure as the previous section to enable the reader to contrast our design decisions with those of the state of the art.

5.2.1 Concurrency Control

We choose to implement MVOCC in SOFORT because it favors read queries, which are frequent in hybrid OLTP and OLAP workloads. Indeed, MVOCC does not require any locking while reading. For simplicity of design, and to avoid the problem of cascading aborts, we choose to abort transactions whenever they encounter a locked tuple. This contrasts with the more optimistic approach of Larson et al. [84] where registering transaction dependencies allows to consider tuples locked by other transactions currently in their validation phase. In this case, a transaction must wait at commit time until all transactions it depends on are committed; if one of them aborts, then the transaction must also abort. This might lead to cascaded aborts.

An important design decision we made in our MVOCC is to have read-only transactions run at snapshot isolation level. This decision was motivated by the fact that long-running read-only transactions can suffer from starvation in MVOCC – a well-known limitation of OCC in general. Indeed, since reads do not require any locking, a long-running read-only transaction is likely to discover during pre-commit verification that it has to abort due to a conflict. We argue that running read-only transactions at snapshot isolation level does not break serializability: If we consider the start timestamp of the read-only transaction as its commit timestamp, then the read-only transaction satisfies serializability constraints.

In MVOCC, a transaction object maintains a read set and a write set that contain references to the read and modified tuples, respectively. An optimization of our MVOCC is to have one reusable transaction object per CPU core. We make the observation that a transaction object contains already all necessary metadata for recovering in-flight transactions. Therefore, we decided to split transaction objects into a transient part and a persistent part, such that the latter contains only necessary metadata for recovery, namely the commit timestamp and the write set. This is in contrast to Hyrise-NV which persists the whole transaction object [148]. Therefore, SOFORT achieves transaction atomicity across failures without relying on the traditional write-ahead log. Section 5.3 details our concurrency control implementation.

Nevertheless, the log is not only used to ensure transaction atomicity across failures. It contains a complete redo-history of the database, which enables point-in-time recovery. Furthermore, replication for high availability most often requires shipping the log to remote systems. Therefore, it is unlikely that any industrial system will do away with a traditional log. Nevertheless, SOFORT removes the log from the critical path of transactions; we envision that a traditional log could be shipped asynchronously while the transactions execute.

5.2.2 Version Storage

We adopt an append-only columnar strategy for two reasons: (1) An append-only columnar strategy yields better analytical performance, because attributes are stored contiguously in memory, which minimizes CPU cache misses; and (2) the design simplicity of an append-only strategy makes it ideal for SCM, because failure-atomicity is easy to reason about. Although we choose a columnar data organization to favor OLAP workloads, we show in Section 5.5 that we can achieve competitive OLTP performance as well. The tuple MVCC metadata consists of only a CTS and a DTS; we do not employ chain pointers. Instead, we rely on inverted indexes to track different versions of a tuple (more details in Section 5.2.3).

SOFORT is a dictionary-encoded column-store. Figure 5.1 gives an overview of data organization in SOFORT. Tables are stored as a collection of append-only columns. Each column c consists of

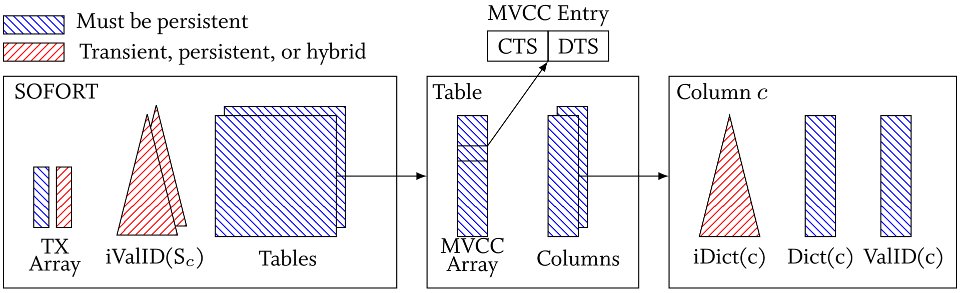

Figure 5.1: Overview of data layout in SOFORT.

an unsorted dictionary $Dict(c)[]$, stored as an array of the column's unique data values, and an array of value ids $ValID(c)[]$, where a value ID is simply a dictionary index (position). For a given column c, $Dict(c)[valueID]$ is the value, from the column domain, encoded as $valueID$, while $ValID(c)[rowID]$ is the $valueID$ of the column c at position $rowID$. These two arrays are sufficient to provide data durability: we refer to these as *primary* data. SOFORT uses SCM as memory and storage at the same time by keeping primary data, accessing it, and updating it directly in SCM. In other words, the working copy and the durable copy of the data are merged. Other data structures are required to achieve reasonable performance including, for each column c, a dictionary index $iDict(c)$ that maps values to value IDs, and for each table, a set of multi-column inverted indexes $iValID(S_c)$ that map sets of value IDs to the set of corresponding row IDs. We refer to these structures as *secondary* data since they can be reconstructed from the primary data. SOFORT can keep secondary data in DRAM or in SCM. Indeed, putting all indexes in DRAM gives the best performance but might put an unbearable stress on DRAM resources. In contrast, placing indexes in SCM exposes them to its higher latency and compromises performance. Therefore, SOFORT uses by default the FPTree, a hybrid SCM-DRAM B$^+$-Tree, as its default index. As shown in Chapter 4, the FPTree exhibits nearly the same performance as DRAM-based counterparts, while using only a small portion of DRAM.

Consider the following query:

```
SELECT a
FROM T
WHERE c=value
```

SOFORT evaluates this query as follows: First, the dictionary index $iDict(c)$ is consulted with $value$ as a search key. If $value$ is not found, then it does not exist in the dictionary and an empty result set is returned, else, the value ID, the encoding of $value$, is returned such that $valueID = iDict(c)[value]$. If $iDict(c)$ is not available, a linear scan of the dictionary array $Dict(c)$ is performed instead. Secondly, the inverted index $iValID(c)$ is looked up with $valueID$ as a search key, and a set of row IDs where $valueID$ occurs is returned: $R = iValID(c)[valueID]$. If $iValID(c)$ is not available, the set of row IDs is computed by doing a full column scan on $ValID(c)[]$ with an equality predicate, searching for all row IDs r, such that $R = \{r | ValID(c)[r] = valueID\}$. Lastly, based on R, the values for the column a are found by simple lookups in the primary data of column a, namely the value ID array $ValID(a)$ and the dictionary array $Dict(a)$:

$$result(Q) = \{v | v = Dict(a)[i], i \in \{i | i = ValID(a)[r], r \in R\}\}$$

The query result is materialized by decoding the rows from value IDs to values with simple lookups in the dictionary array – value IDs being simply indexes in the dictionary array. Overall, this query can potentially use two indexes: the dictionary index $iDict(c)$ and the inverted index $iValID(c)$ of column c. Hence, to optimally execute this query after failure, SOFORT needs to recover both indexes, otherwise, the query performance will be bound by the linear scan operations of $Dict(c)$ and $ValID(c)$.

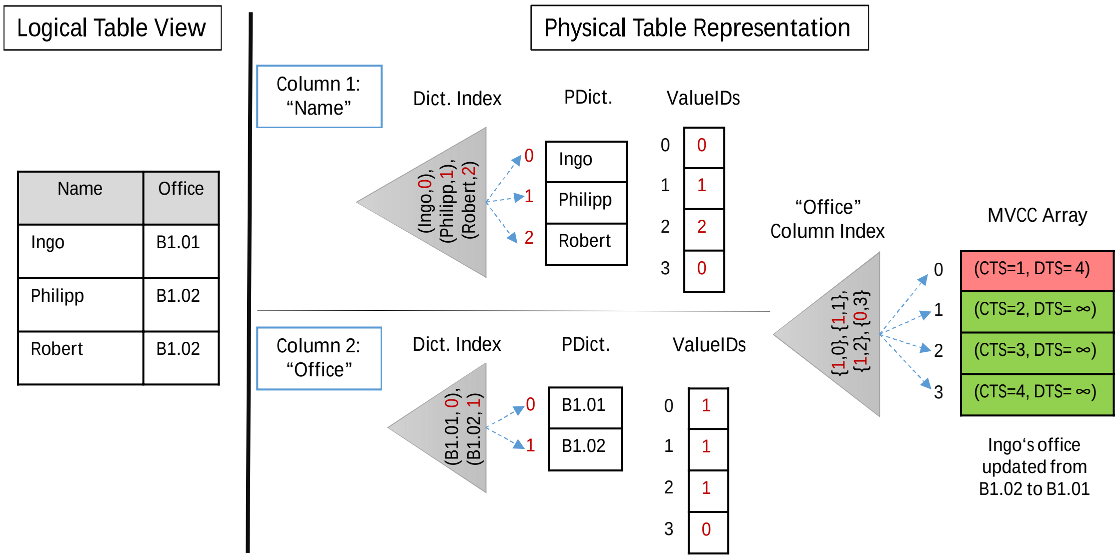

Figure 5.2: Example of a SOFORT table of employees and their offices.

5.2.3 Index Management

As mentioned in Section 5.2.1, we do not use chain pointers to link different versions of a tuple. Instead, we document them in the inverted indexes. Since column-stores scatter the attributes of a tuple, we cannot use physical pointers. Instead, our inverted indexes use the row ID, which is a *version ID* and not a *tuple ID*, as a reference to a tuple. This decouples indexes from the physical representation of tuples, while maintaining the benefits of physical pointers. To be able to identify each tuple distinctively, we implement our inverted indexes as sets, where the key is a pair consisting of an array of value IDs representing the indexed columns (attributes), and a row ID. Adding the row ID to the key makes it unique. Index entries are ordered first by their value ID arrays, then by their row ID. To retrieve all versions corresponding to a key, we issue a range query on the index for the range $[\{key, 0\}, \{key, MAX_ROWID\})$. This will return all index entries where key occurs.

SOFORT uses the FPTree as its default index. As we have discussed in Chapter 4, the unsorted leaves of the FPTree make it inefficient for range queries, and its fingerprints help only for point queries. Yet, inverted indexes are probed using range queries, which makes the FPTree perform poorly. To remedy this issue, we leverage our knowledge of the structure of the keys: Probed ranges are always in the form of $[\{key, 0\}, \{key, MAX_ROWID\})$, which means that the row ID part of index keys does not really matter. Therefore, we construct the fingerprints of the FPTree using only the value IDs array part of index keys. Therefore, we can leverage fingerprints during an index probe by testing for equality on the value IDs array rather than testing whether the full key falls within the queried range. Note that this optimization does not apply when we use another data structure than the FPTree for inverted indexes.

Figure 5.2 is an example of a SOFORT table of employees and their offices. It illustrates how multiple versions are managed. The table has an inverted index on column *Office*. When a row is updated (in the example, Ingo's office is updated from B1.2 to B1.1), the current version of the row is invalidated by updating the DTS of the corresponding MVCC entry, and a new version of the row is created, with its corresponding CTS and DTS equal to the DTS of the deleted row and infinity, respectively. The inverted index is updated by inserting a new pair consisting of the value ID of the office (0 in the example) and the row ID of the newly inserted tuple (row 3 in the example). At this point, the index retains the old version (value ID 1, row ID 0) until the garbage collector reclaims it.

An index lookup returns the row IDs of all rows where the key occurs, which might include garbage rows. In contrast, an MVCC system that indexes only the newest version of a tuple does need to check the visibility of older versions. In fact, the more garbage row IDs are returned by our index, the more visibility checks a transaction has to perform, hence, the lower the performance. Therefore, our indexing scheme makes SOFORT's transactional performance highly dependent on the ability of the garbage collection scheme to maintain a low rate of garbage. This motivated us to adopt an aggressive garbage collection scheme which we describe in the next section.

5.2.4 Garbage Collection

While row-stores and column-stores share the same garbage collection design patters, they differ in how the memory of deleted tuples are reclaimed. Row-stores usually allocate one block of memory per tuple, which makes memory reclamation during garbage collection as easy as freeing the memory dedicated to a deleted tuple. In column-stores, however, the attributes of a tuple are scattered across memory, which makes reclaiming the memory of deleted tuple versions less trivial. Indeed, this would require a writer-blocking process which would replace the current columns with new, garbage-free ones. To remedy this issue, we propose to keep track of deleted rows and re-use them when inserting new tuples whenever possible instead of appending them to the table. To do so, we maintain a transient queue of reusable row IDs per table.

SOFORT implements a form of transaction-level, cooperative garbage collection. When a transaction finishes, it registers the garbage it created (deleted rows for committing transactions, and created rows for aborting transactions) in the garbage list of its transaction object with an associated timestamp (the commit timestamp for committing transactions, and the minimum timestamp for aborting transactions). Transaction objects are core-local and get reused by subsequent transactions. Starting transactions check the garbage list of its transaction object, and collect any garbage that qualifies for reclamation. A garbage entry is reclaimable if its associated timestamp is lower or equal to the start timestamp of the oldest running transaction. This condition ensures that any running transaction is able to see versions that were visible when it started. Reclaiming a garbage entry consists in cleaning the inverted indexes and registering the reclaimed rows as reusable in their respective tables.

Our garbage collection scheme ensures that the system never lets garbage accumulate more than necessary. This is important for maintaining performance, since the performance of OLTP queries deteriorates with the accumulation of garbage. We verified this by evaluating a tuple-level vacuuming garbage collection scheme that relies on a single background thread that scans garbage. This scheme successfully maintained a very low garbage ratio with up to 10 worker threads. However, when the number of worker threads exceeds 10, the garbage collector thread is overwhelmed as the system produces garbage at a higher rate than what the garbage collector can handle. As a result, the system was slowed down until a balance was found between the rate of garbage production (i.e., transaction throughput) and garbage collection. Using more background threads solves the issue but wastes more CPU resources. Our transaction-level cooperative garbage collection prevents this scenario by making all transactions proactively collect garbage when they start. Finally, to address the problem of long-running transactions, we could use the timestamp visibility interval approach [89]. However, we leave this for future work since we focus on transactional behavior in this work.

5.3 SOFORT IMPLEMENTATION

In this section, we detail the core operations of SOFORT to demonstrate how serializable ACID transactions are performed. We also elaborate on how these operations achieve failure-atomicity: regardless of software crash conditions, we can recover the database to a consistent state, without relying on a traditional transactional log.

In this section, we use the following persistence functions: *Flush* calls the most advanced flushing instruction available, which might be asynchronous (e.g., CLFLUSHOPT and CLWB), while *Persist* is a *Flush* surrounded by two memory fences such as SFENCE (*MemBarrier*).

5.3.1 MVCC Structures

SOFORT implements a fixed-size array of transaction objects, whose size corresponds to the maximum number of allowed concurrent transactions (MaxParallelTX), e.g., the number of logical cores on a system. Each worker thread is assigned a transaction object and a unique ID corresponding to the position of its transaction object in the transaction object array. A worker thread reuses the same transaction object during its lifetime. A transaction object holds all necessary information to achieve serializability in our concurrency control protocol. As discussed in Section 5.2.1, we split this information in a transient part and a persistent part. The persistent part contains only necessary information for recovery (See Section 5.3.9 for recovery details), namely:

- a flag *IsCommitted* that indicates whether the transaction committed.
- the transaction commit timestamp;
- a create set that references all rows created by the transaction;
- a delete set that references all rows deleted by the transaction.

As for the transient part, it contains the following:

- a status variable that indicates whether a transaction is *Invalid*, *Active*, *Committed*, or *Aborted*;
- the transaction ID (TXID);
- the transaction start timestamp (STS);
- the transaction commit timestamp;
- a scan set containing all scan predicates issued by the transaction during its lifetime. The scan set is needed for the commit protocol (See Section 5.3.7 for full details);
- a read set that references all visible rows read by the transaction during its lifetime, excluding the rows referenced in the create and delete sets;
- a list of garbage entries registered by previous transactions that used the same transaction object;
- a flag *willAbort* that warns the transaction when it has to abort, e.g., when a conflict with another transaction is detected.

We keep the commit timestamp in both the persistent and the transient part of the transaction object.

MVCC entries are treated as a column of the table; there is one MVCC entry per row of a table. An MVCC entry consists of a commit timestamp (CTS) and a deletion timestamp (DTS) which are both initially equal to zero. Timestamps are 8-byte unsigned integers generated by a global timestamp counter (CurrentTime) which is atomically incremented for every commit. Additionally, SOFORT keeps another global timestamp used in garbage collection, denoted CurMinSTS, which keeps track of the lowest STS among active transactions. A transaction locks a row by setting the CTS (in case of

Algorithm 5.1 SOFORT Row Visibility function.

```
 1: function IsVisible(mvcc&, atTime, txid)
 2:     if mvcc.CTS == 0 or mvcc.DTS == 0 then                      ▷ CTS and/or DTS not initialized
 3:         return false;
 4:     do
 5:         cts = mvcc.CTS; dts = mvcc.DTS;                      ▷ Read current state of CTS and DTS
 6:         if dts >= kMinTS then                                            ▷ DTS is a timestamp
 7:             dtsVisible = atTime < dts;
 8:         else                                                        ▷ DTS is a transaction ID
 9:             rslt = GetTxInfo(dts).IsTsVisible(mvcc.DTS, atTime, txid);
10:             if rslt == -2 then
11:                 continue;                                      ▷ New transaction, redo check
12:             if rslt == -1 then
13:                 GetTxInfo(txid).willAbort = true;
14:                 return false;
15:             dtsVisible = !rslt;               ▷ txInfo.IsTsVisible returns 0 when DTS is visible
16:         if cts >= kMinTS then                                            ▷ CTS is a timestamp
17:             ctsVisible = atTime >= cts;
18:         else                                                        ▷ CTS is a transaction ID
19:             rslt = GetTxInfo(cts).IsTsVisible(mvcc.CTS, atTime, txid);
20:             if rslt == -2 then
21:                 continue;                                      ▷ New transaction, redo check
22:             if rslt == -1 then
23:                 GetTxInfo(txid).willAbort = true;
24:                 return false;
25:             ctsVisible = rslt;                ▷ txInfo.IsTsVisible returns 1 when CTS is visible
26:         return ctsVisible and dtsVisible;
27:     while true
```

a row creation) or the DTS (in case of a row deletion) to its TXID. To distinguish between timestamps and TXIDs, we split the value domain such that TXIDs are in the range $[1, 2^{63})$ and timestamps are in the range $[2^{63}, 2^{64})$. Therefore, a CTS or a DTS is interpreted as a TXID if it is lower than or equal to 2^{63}. We reserve zero as a special value that indicates that an MVCC entry is not initialized. We define two constants, kMinTS (2^{63}) and kInfinityTS ($2^{64} - 1$), corresponding respectively to the minimum and the maximum value of a timestamp. CurrentTime counter is initially set to kMinTS$+1$.

Algorithm 5.1 illustrates the function that decides whether a row is visible at a specific time such as an STS. If the DTS or the CTS of the row is not initialized (i.e., equal to zero), then the row is not visible (lines 2-3). Else, the function reads a copy of the CTS and the DTS of the checked row (line 5). This is important because their value might be changed by another transaction. For instance, if references are used instead of copies, DTS might be evaluated as a timestamp in line 6, but be changed to a TXID by another transaction before the comparison in line 7 is executed, thereby causing a visibility error.

If STS is greater than or equal to CTS and lower than DTS, then the row is visible. If either DTS or CTS is a TXID, then we need to check the state of the corresponding transaction (line 9 and 19, respectively), which is illustrated in Algorithm 5.2. A possible scenario is that the transaction is *Invalid* or that the TXID stored in CTS or DTS does not correspond to the TXID stored in the transaction object (line 3). This means that the transaction that was locking the checked row has finished, which implies that the timestamp (either CTS or DTS) that was interpreted as a TXID must have changed. Hence, the MVCC entry of the checked row must be read again and the visibility check redone from the beginning. If a row is locked by an *Active* or *Aborted* transaction, then it is considered invisible and the checking transaction is signaled to abort (lines 7-8). The only exception is if a transaction encounters its own created or deleted rows, in which case the former are considered visible while the latter are considered invisible (lines 5-6). If the transaction is *Committed*, then we compare CTS or DTS with its commit timestamp (line 9). This step is critical because the transaction status might change

Algorithm 5.2 SOFORT Cross-Transaction Row Visibility function.

```
 1: function TxInfo::IsTsVisible(ts, atTime, callerTxid)
 2:     locked_scope(mutex);
 3:     if ts != txid or status == kInvalid then                 ▷ If TX with ID 'ts' finished
 4:         return -2;                                           ▷ Must redo check from the beginning
 5:     if txid == callerTxid then                               ▷ Row is locked by the caller transaction
 6:         return 1;        ▷ Rows created (deleted) by a transaction are visible (invisible) to itself
 7:     if status != kCommitted then                             ▷ If TX is Active or Aborted
 8:         return -1;                                           ▷ Conflict. The transaction should be aborted
 9:     return atTime >= commitTS;                               ▷ Return 1 if expression is true, 0 otherwise
```

Algorithm 5.3 SOFORT Start Transaction function.

```
 1: function StartTransaction
 2:     GetPersTxInfo(txid).IsCommitted = FALSE;                 ▷ Persistly mark this TX as uncommitted
 3:     Persist(&GetPersTxInfo(txid).IsCommitted);
 4:     txInfo = GetTxInfo(txid);
 5:     txid = txInfo.txid + m_MaxParallelTX;                    ▷ Compute transaction ID
 6:     txInfo.STS = m_currentTime;                              ▷ Set TX start timestamp to current time
 7:     txInfo.SetActive(txid);                                  ▷ Set txid, commitTS, and status
 8:     if workerID() == 0 then
 9:         setCurMinSTS();                       ▷ Update CurMinSTS if worker thread ID is e.g. zero
10:     CollectGarbage(txInfo.garbage);
11:     return txid;
```

while reading the commit timestamp. Consider that transaction *T1* is checking the visibility of a row locked by transaction *T2*. After checking that transaction *T2* is *Committed*, the latter might finish and be replaced by another transaction which resets the commit timestamp before the timestamp comparison of line 9 is performed. To remedy this issue, we protect this function, as well as all functions that change the status of the transaction, namely *SetActive*, *SetCommitted*, *SetAborted*, and *SetInvalid*, with a shared lock to ensure that both the status and the commit timestamp are read consistently.

5.3.2 Start Transaction

The start transaction process, whose pseudo-code is depicted in Algorithm 5.3, is responsible for initializing the transaction object of a new transaction. When a transaction starts, it first persistently updates its *IsCommitted* flag to indicate its uncommitted state (lines 2-3). Then, it is assigned a unique TXID (line 5). TXIDs are assigned in a decentralized way: Transaction objects are initially assigned a TXID equal to their index position in the transaction object array. A new transaction is then assigned a TXID by adding MaxParallelTX to the current TXID. It is also assigned a start timestamp (STS) which is equal to the current logical time (line 6). Then, the transaction executes the function *SetActive* (line 7), which sets, in the transaction object, the TXID to the assigned value, the commit timestamp to kInfinityTS, and clears the read and scan sets, then changes its status to *Active*. As discussed in Section 5.3.1, *SetActive* shares the same lock as *IsTsVisible* in order to ensure that the status and the commit timestamp of a transaction are always read consistently. Finally, although it is ready to start, the transaction has to do its share of cooperative garbage collection. This is done in two parts: First, under a certain condition, e.g., if the worker ID is equal to zero, the transaction updates CurMinSTS by getting the lowest STS of all active transaction (lines 8-9). Second, it collects the garbage that is referenced in the garbage list of its transaction object (line 10). The garbage collection process is detailed in Section 5.3.10.

Algorithm 5.4 SOFORT Select function.

```
 1: function SELECT(tableName, predicates, colFilter, txid, rslt)
 2:     txInfo = GetTxInfo(txid);
 3:     (tabID, pTab) = GetTablePointer(tableName);
 4:     for (i = 0; i < colFilter.size(); ++i) do        ▷ Translate filter from column names to column Ids
 5:         colFilterIDs[i] = pTab->GetColID(colFilter[i]);
 6:     rowIDs = GetVisibleRows(pTab, predicates, txInfo.STS, txid);
 7:     if txInfo.willAbort then        ▷ GetVisibleRows sets willAbort if a row is locked by another TX
 8:         abort(txid);
 9:         return false;
10:     txInfo.scanSet.push_back({tabID, predicates});        ▷ Update scan set
11:     for each rowID in rowIDs do        ▷ Update read set
12:         txInfo.readSet.Append({tabID, rowID});
13:     pTab->GetRows(rowIDs, colFilterIDs, rslt);        ▷ Materialize selected attributes into rslt
14:     return true;
```

5.3.3 Select

The *Select* operation returns a list of materialized attributes based on a table name, a list of predicates, and a filter indicating which attributes are selected. Algorithm 5.4 shows the pseudo-code of this operation. First, the table name is translated, thanks to a mapping, to a table pointer and a table ID (line 3). Then, the attribute filter is transformed, thanks to a mapping, from a list of column names to a list of column IDs (line 4-5). Thereafter, the function *GetVisibleRows*, which we detail below, returns the row IDs of all visible rows that satisfy the list of predicates (line 6). If the latter function encounters a row that is locked by another transaction, then it signals its caller, by setting its *willAbort* flag to *true*, that the transaction should abort. If this is the case, the transaction is aborted (lines 7-9). If *willAbort* is not set, then the table ID and the list of predicates are appended to the scan set (line 10). Furthermore, the row IDs of the returned visible rows are inserted in the transaction's read set (lines 11-12). Finally, the selected attributes of the visible rows are materialized and returned to the user (line 13).

Algorithm 5.5 depicts pseudo-code of the *GetVisibleRows* function. This function is used by the *Select*, *Insert*, *Delete*, and *Update* operations to get the row IDs of visible rows that satisfy a list of predicates, such as equality and range predicates. The first step is to get the row IDs of row candidates using index or column scans (line 2). To do so, SOFORT sorts the predicates according to a combination of their selectivity and the cost of the associated scans. Basically, SOFORT selects, among the indexes that at least partially cover one of the attributes of a given predicate, the one that would return the lowest number of rows. If this number is too high, or if there are no partially matching indexes, then SOFORT falls back to full column scans. Selectivity is estimated based on the size of the dictionaries, which indicates the number of distinct values in a column, and the size of the ValueID array. Thereafter, the predicates are sorted starting with the cheapest and most selective one. After the latter predicate is evaluated, the remaining ones are evaluated either by following the computed predicate plan if the intermediate result is big (i.e., the number of returned rows is high), or by evaluating the predicate directly on the intermediate result if the number of rows is low.

Once the final result of row candidates is obtained, we check their visibility and construct the set of visible ones (lines 4-5). As shown in Algorithm 5.1, the visibility check function sets the transaction's *willAbort* flag to *true* if it encounters a row that is locked by another transaction. If this happens, then *GetVisibleRows* returns an empty result (lines 6-8) and the calling function will abort the transaction.

Algorithm 5.5 SOFORT Get Visible Rows function.

```
function GetVisibleRows(pTab, predicates, atTime, txid)
    rowIDs = pTab->GetRowIDs(predicates);                    ▷ Get row candidates using index/column scans
    for each rowID in rowIDs do                              ▷ Check visibility of candidates
        if IsVisible(pTab->MVCC[rowID], atTime, txid) then
            rslt.push_back(rowID);                           ▷ Add visible row to result
        if GetTxInfo(txid).willAbort then                    ▷ IsVisible sets willAbort if row is locked by another TX
            rstl.clear();                                    ▷ TX will abort; Return an empty result
            break;
    return rslt;
```

Algorithm 5.6 SOFORT Insert function.

```
1: function Insert(tableName, rowValues, txid)
2:     txInfo = GetTxInfo(txid);
3:     (tabID, pTab) = GetTablePointer(tableName);
4:     rowID = pTab->Insert(rowValues);                                  ▷ Insert row and update inverted indexes
5:     GetPersTxInfo(txid).createSet.PersistentAppend({tabID, rowID});   ▷ Update create set
6:     pTab->MVCC[rowID].CTS = txid;                                     ▷ Lock row by setting its CTS to txid
7:     pTab->MVCC[rowID].DTS = kInfinityTS;
8:     return true;
```

5.3.4 Insert

The *Insert* operation inserts a row in a specified table. Algorithm 5.6 illustrates the core steps of this operation. First, it gets the table pointer and the table ID corresponding to the table name (line 3). Then, it inserts the row into the table (line 4). Inserting the row involves translating its attribute values to value IDs, which might necessitate inserting new dictionary entries. A table then inserts the translated row by checking whether there is a reusable row in its reusable row queue. If there is one, then it is used to insert the new row, and its corresponding MVCC entry is left unchanged. Otherwise, the new row is appended to the table, in which case both its CTS and DTS will be equal to zero. In fact, the MVCC column is initialized to zero when it is first allocated. The value IDs of the new row are inserted into the ValueIDs Array using non-temporal stores, which necessitate a memory barrier to ensure that they are drained to SCM. However, we need this guarantee only at commit time. Non-temporal stores allow for better performance, because regular persistent writes require a round trip to SCM: First, they fetch data from SCM to the CPU cache, apply the writes, then flush the changes to SCM. Non-temporal stores bypass the CPU cache, which allows to avoid the read-before-write effect of regular writes.

Moreover, the table updates its inverted indexes to reflect the insertion. If these indexes are persistent or hybrid, then these updates are persistent; otherwise, they are transient. Next, the row ID of the newly inserted row is persistently appended to the transaction's create set (line 5). If a failure occurs after the insertion but before updating the create set (i.e., between lines 4 and 5), then the recovery garbage collection process will collect the inserted row since its DTS is either equal to an old timestamp or to zero (more details in Section 5.3.10). Then, the new row's CTS is set to the TXID to indicate that this row is locked (line 6), while its DTS is set to kInfinityTS (line 7); there is no need to persist these values at this stage, because the recovery process has enough information (i.e., the create set) to undo the row insertion in case of a failure. The last two steps must follow this order, because if the changes to the MVCC entry propagate to SCM before the update to the create set, then the recovery process will not be able to undo the row insertion.

Algorithm 5.7 SOFORT Delete function.

```
 1: function DELETE(tableName, predicates, txid)
 2:     txInfo = GetTxInfo(txid);
 3:     (tabID, pTab) = GetTablePointer(tableName);
 4:     rowIDs = GetVisibleRows(pTab, predicates, txInfo.STS, txid);
 5:     if txInfo.willAbort then
 6:         abort(txid);
 7:         return false;
 8:     txInfo.scanSet.Append({tabID, predicates});                    ▷ Update scan set
 9:     for each rowID in rowIDs do
10:         GetPersTxInfo(txid).deleteSet.PersistentAppend({tabID, rowID});    ▷ Update delete set
11:         if !TryToDelete(rowID, txid) then    ▷ Try to lock row by atomically setting its DTS to txid
12:             abort(txid);                                 ▷ Abort if failed to delete row
13:             return false;
14:     return true;
```

5.3.5 Delete

The *Delete* operation removes all the rows that satisfy a list of predicates from a specified table. Algorithm 5.7 describes the main steps of this operation. Similar to the *Select* and the *Insert* operations, the first step is to translate the table name to a table pointer and a table ID (line 3). Then, similar to the *Select* operation, *GetVisibleRows* is executed to get the list of row IDs of visible rows that satisfy the list of predicates (line 4). If the transaction's *willAbort* flag was set to *true* during the visibility check, then the transaction is aborted (lines 5-7). Otherwise, since we performed scan operations, the scan set must be updated (line 8). Note, however, that we do not need to update the scan set for point predicates that contain the primary key, because these are immune to the phantom problem. Thereafter, the visible rows are locked for deletion by setting their DTS to the TXID, under the condition that the DTS is equal to kInfinityTS, using a compare-and-swap atomic instruction (line 11); we do not need to enforce the durability of the DTS at this stage. Although the durability of the DTS is not enforced, the CPU might evict it from the cache and make it durable in SCM. If a failure occurs after the DTS was made durable but before the delete set was updated, then the recovery process will not be able to unlock this row. Hence, before trying to lock each row, we must first persistently append its table ID and row ID to the delete set of the transaction (line 10). If locking one of the rows fails, it means that another transaction was faster in locking this row, therefore, the transaction is aborted (line 12).

Finally, we discuss the case of a failure or an abort after a first transaction registered a row in its delete set, then failed to lock it because a second transaction was faster in locking it. In this case, the delete set of the first transaction references a row that was not locked by it. While recovering or aborting, the DTS of this row might be equal to the TXID of the second transaction, or even to its commit timestamp. A corruption might arise if when undoing the first transaction, the DTS of the row is reset to kInfinityTS. To remedy this issue, the abort process checks whether the DTS of a row is equal to the TXID of the aborting transaction before updating it. As for the recovery case, we discuss it in detail in Section 5.3.9.

5.3.6 Update

The *Update* operation updates all the rows that satisfy a list of predicates in a specified table. The update can concern only a subset of attributes specified in an attribute filter. Algorithm 5.8 illustrates the different steps of the *Update* operation. After translating the table name to a table pointer and a table ID (line 3), we get the list of row IDs of all visible rows that satisfy the list of predicates (line

Algorithm 5.8 SOFORT Update function.

```
 1: function UPDATE(tableName, predicates, colFilter, newValues, txid)
 2:     txInfo = GetTxInfo(txid);
 3:     (tabID, pTab) = GetTablePointer(tableName);
 4:     rowIDs = GetVisibleRows(pTab, predicates, txInfo.STS, txid);
 5:     if txInfo.willAbort then
 6:         abort(txid);
 7:         return false;
 8:     txInfo.scanSet.Append({tabID, predicates});                        ▷ Update scan set
 9:     for each rowID in rowIDs do
10:         GetPersTxInfo(txid).deleteSet.PersistentAppend({tabID, rowID});   ▷ Update delete set
11:         if !TryToDelete(rowID, txid) then     ▷ Try to lock row by atomically setting its DTS to txid
12:             abort(txid);                                     ▷ Abort if failed to delete row
13:             return false;
14:     rows = pTab->GetValIDs(rowIDs);                         ▷ get ValueIDs of the deleted rows
15:     UpdateRows(rows, colFilter, newValues);                              ▷ Apply update to rows
16:     for each row in rows do                                        ▷ Insert back updated rows
17:         rowID = pTab->Insert(row);
18:         GetPersTxInfo(txid).createSet.PersistentAppend({tabID, rowID});
19:         pTab->MVCC[rowID].CTS = txid;                      ▷ Lock row by setting its CTS to txid
20:         pTab->MVCC[rowID].DTS = kInfinityTS;
21:     return true;
```

4). If a conflict with another transaction was detected during the row visibility checks, then the transaction is aborted (lines 5-7). Otherwise, we append the table ID and the list of predicates to the transaction's scan set (line 8). Similarly to the *Delete* operation, we do not need to update the scan set for point predicates that contain the primary key. Thereafter, we proceed to update the rows. Each row update consists of a deletion followed by an insertion. First, we try to lock all visible rows for deletion. Similar to the *Delete* operation, we first persistently append to the transaction's delete set a reference to the row we try to delete (line 10). Then, with an atomic compare-and-swap instruction, we try to lock the row for deletion by setting its DTS to the TXID under the condition that the DTS is equal to kInfinityTS (line 11). If locking one of the rows fails, then the transaction must be aborted (lines 12-13). Similar to the *Delete* operation, a failing transaction (because of an abort or a failure) may contain in its delete set a reference to a row it failed to lock. The same remedies we discussed in Section 5.3.5 apply.

If the deletion phase is successful, then we move to the insertion phase. First, we gather the value IDs of all locked rows (line 14). Then, we apply the update to the gathered rows by translating the new values into value IDs, which might involve inserting new dictionary entries (line 15). The attribute filter indicates which attributes need to be updated. Thereafter, the updated rows are inserted back into the table following the same process as an *Insert* operation. Each row is first inserted into the table, either by reusing a deleted row if available, or by appending it to the table (line 17). Then, we update the transaction's create set by persistently appending a reference to the inserted row (line 18). Finally, we update the MVCC entry of the inserted row by setting its CTS to the TXID (line 19), which serves as a lock for the row, and its DTS to kInfinityTS (line 20). As discussed for the *Insert* and the *Delete* operations, we do not need to enforce the durability of MVCC entries at this stage.

5.3.7 Commit Transaction

The commit protocol, whose pseudo-code is depicted in Algorithm 5.9, starts by checking whether the transaction is read-only (line 4). This is the case when the create set and the delete set of the committing transaction are both empty. If it is the case, then we can skip the commit checks by considering that the commit timestamp of the transaction is its STS. In other words, read-only transaction can execute at snapshot isolation level without breaking serializability requirements. The transaction is then terminated by setting its status to *Invalid* (line 5). Note that if a transaction is known a priori to be read-only, then we can do away with the scan set and avoid aborting when detecting a conflict with another transaction.

If the transaction is not read-only, then it is assigned a commit timestamp by atomically incrementing CurrentTime (line 7). Note that the transaction is not yet considered as committed. The next step is to redo all the scans that the transaction performed during its lifetime, which are referenced in its scan set (lines 8-11). The goal is to ensure that the set of visible rows at STS time is the same as the one at commit time, which is a requirement for serializability. Then, the difference between the resulting set of visible rows and the transaction's read set is computed (line 12). The only rows that are allowed to be in the resulting difference set are those modified by the transaction itself (lines 13-17), which can happen because transactions do not insert modified rows in their read sets. If this condition is not met, the transaction is aborted because its scans at STS time are not the same as its scans at commit time, which breaks serializability requirements. If the condition is satisfied, then the transaction updates, in this order enforced with a memory barrier (line 19), its commit timestamp (line 18) and its *IsCommitted* flag (line 20), in the persistent part of its transaction object, and persists them in SCM with a single *Persist* since they are guaranteed to reside in the same cache line (line 21). Then, it changes its status to *Committed* (line 22); respecting this order is important because persisting the commit timestamp and the *IsCommitted* flag will indicate during recovery that this transaction has committed, upon which the recovery process will roll-forward the commit process. If the status change occurs first, then another transaction might see the newly committed rows before failure, but not see them after failure because the first transaction was rolled back since it did not persist its commit timestamp and set its *IsCommitted* flag.

After this step, the transaction updates the MVCC entries of its modified rows: First, it sets the DTS of the rows in its delete set to its commit timestamp (lines 23-24). Second, it sets the CTS of the rows in its create set to its commit timestamp (lines 25-26). Third, it persists the MVCC entries of both its created and deleted rows (lines 27-30). Since the order of persistence is not important, we employ asynchronous flushes (when available) because, contrary to synchronous flushes, they can execute in parallel (line 29). Since asynchronous flushes are not ordered with writes, we need to wrap the asynchronous flushes with two memory barriers; the first one ensures that the updates to the MVCC entries finish executing before the flushes are issued (line 27), and the second one ensures that the flushes finish executing, i.e., that all changes to the MVCC entries have been made durable (line 30). MVCC entries are not allowed to span two cache lines, which means that a single flushing instruction drains both the CTS and the DTS to SCM. Afterwards, the transaction adds a garbage entry consisting of its commit timestamp and the rows contained in its delete set (line 31). The create set and delete set are cleared (lines 32-33) before the transaction terminates by setting its status to *Invalid* (line 34).

5.3.8 Abort Transaction

A transaction can abort either because of a conflict with another transaction, or because the user decided to abort it. Algorithm 5.10 depicts the pseudo-code of SOFORT's *Abort* process. When a transaction aborts, it first changes its status to *Aborted* (line 4). Then, it reactivates the rows that it deleted (referenced in its delete set) by setting their DTS to kInfinityTS (lines 5-7). However, since the delete set might include a row that was not locked by the aborting transaction (See discussion in Section 5.3.5), we update the DTS of a row only if it is equal to the TXID of the aborting transaction (line 6). Thereafter, the abort process invalidates its created rows, referenced in its create set, by setting their CTS to zero and their DTS to CurMinSTS (lines 8-10). Next, it persists the MVCC entries

Algorithm 5.9 SOFORT Commit Transaction function

```
 1: function COMMIT(txid)
 2:     txInfo = GetTxInfo(txid);
 3:     pTxInfo = GetPersTxInfo(txid);
 4:     if pTxInfo.createSet.Empty() and pTxInfo.deleteSet.Empty() then          ▷ Read-only TX
 5:         txInfo.SetInvalid();                    ▷ Terminate TX (startTS is used as commitTS)
 6:         return true;
 7:     txInfo.commitTS = AtomicIncrement(m_currentTime);                      ▷ Acquire commitTS
 8:     for each scan in txInfo.scanSet do                           ▷ Redo all scans at time commitTS
 9:         rowIDs = GetVisibleRows(m_tables[scan.tabID], scan.predicates, txInfo.commitTS, txid);
10:         for each rowID in rowIDs do
11:             newReadSet.Append({scan.tabID, rowID});
12:     readSetDiff = Difference(txInfo.readSet, newReadSet)
13:     for each row in readSetDiff do          ▷ Only rows modified by TX are allowed to be in readSetDiff
14:         mvcc = m_tables[row.tabID]->MVCC[row.rowID];
15:         if mvcc.CTS != txid and mvcc.DTS != txid then
16:             abort(txid);
17:             return false;
18:     pTxInfo.commitTS = info.commitTS;                           ▷ Persist commit timestamp in pTxInfo
19:     MemBarrier();                                  ▷ Ensure ordering of writes to commitTS and IsCommitted
20:     pTxInfo.IsCommitted = TRUE;                              ▷ Persist information that this TX committed
21:     Persist(&(pTxInfo.IsCommitted));                   ▷ commitTs and IsCommitted share the same cache line
22:     txInfo.SetCommitted();                                           ▷ Set TX status to committed
23:     for each row in pTxInfo.deleteSet do                               ▷ Update DTS of deleted rows
24:         m_tables[row.tabID]->MVCC[row.rowID].DTS = txInfo.commitTS;
25:     for each row in pTxInfo.createSet do                               ▷ Update CTS of created rows
26:         m_tables[row.tabID]->MVCC[row.rowID].CTS = txInfo.commitTS;
27:     MemBarrier();                                   ▷ Ensure that all updates to mvcc entries finish executing
28:     for each row in pTxInfo.createSet ∪ pTxInfo.deleteSet do       ▷ Flush mvcc of created and deleted rows
29:         Flush(&m_tables[row.tabID]->MVCC[row.rowID]);                              ▷ Asynchronous flush
30:     MemBarrier();                                            ▷ Ensure that all flushes finish executing
31:     txInfo.addGarbage(info.commitTS, pTxInfo.deleteSet);                 ▷ Register deleted rows as garbage
32:     pTxInfo.createSet.Clear();                                                       ▷ Clear create set
33:     pTxInfo.deleteSet.Clear();                                                       ▷ Clear delete set
34:     txInfo.SetInvalid();                                                                ▷ Terminate TX
35:     return true;
```

of its changed rows using asynchronous flushes (when available) and memory barriers (lines 11-14). Afterwards, the transaction collects its garbage (line 15), which consists of its created rows. Collecting garbage at this point is possible because the created rows were never visible to any other transaction, therefore, they can be collected immediately. Then, the create set and delete set are cleared (lines 16-17). Finally, the transaction is terminated by setting its status to *Invalid* (line 18).

Processing the delete set before the create set is important. Consider the case of a row that was created then deleted by the same transaction. This row will be present in both the create and the delete sets. If the create set is processed first, then the DTS of the row will be set to CurMinSTS, which is important to distinguish pre-failure garbage from post-recovery garbage (see Section 5.3.10 for more details). However, the DTS of the row will be overwritten to kInfinityTS when processing the delete set, thereby incapacitating the recovery garbage collection process from distinguishing whether this row is pre-failure or post-recovery garbage. In contrast, the commit process can process the create and delete sets in either order.

Algorithm 5.10 SOFORT Abort Transaction function.

```
function ABORT(txid)
    txInfo = GetTxInfo(txid);
    pTxInfo = GetPersTxInfo(txid);
    txInfo.SetAborted();                                              ▷ Set status to Aborted
    for each row in pTxInfo.deleteSet do                              ▷ Reactivate deleted rows
        if m_tables[row.tabID]->MVCC[row.rowID].DTS == txid then     ▷ If DTS is locked by this TX
            m_tables[row.tabID]->MVCC[row.rowID].DTS = kInfinityTS;
    for each row in pTxInfo.createSet do                              ▷ Set created rows as invalid
        m_tables[row.tabID]->MVCC[row.rowID].CTS = 0;                 ▷ Mark row as invalid
        m_tables[row.tabID]->MVCC[row.rowID].DTS = CurMinSTS;         ▷ Set DTS to CurMinSTS
    MemBarrier();                         ▷ Ensure that all updates to mvcc entries finish executing
    for each row in pTxInfo.createSet ∪ pTxInfo.deleteSet do          ▷ Flush mvcc of changed rows
        Flush(&m_tables[row.tabID]->MVCC[row.rowID]);                 ▷ Asynchronous flush
    MemBarrier();                                          ▷ Ensure that all flushes finish executing
    CollectGarbage({kMinTS, pTxInfo.createSet});                ▷ Collect garbage (created rows)
    pTxInfo.deleteSet.Clear();                                        ▷ Clear delete set
    pTxInfo.createSet.Clear();                                        ▷ Clear create set
    txInfo.SetInvalid();                                              ▷ Terminate TX
```

5.3.9 Recovery

Upon restart, memory management (PAllocator) is the first component that is recovered. Then, SOFORT is recovered following the process depicted in Algorithm 5.11. The first step is to recover the work pointers of SOFORT (line 2). A work pointer is a regular volatile pointer resulting from the conversion of a persistent pointer. Since a restart renders volatile pointers invalid, we have to reset them to the conversion of their corresponding persistent pointers. Then, SOFORT recovers the persistent structures of its tables (lines 3-4), which includes recovering its columns and building a new reusable row queue, but does not include the recovery of transient or hybrid secondary data structures. Every persistent or hybrid data structure has a *Recover* function that checks the sanity of its state, restores work pointers from persistent pointers, and recovers from problematic situations, such as crashing in the middle of a table resize.

Afterwards, SOFORT recovers the persistent transaction objects in order to either undo in-flight uncommitted transactions, or finish committed ones. In Section 5.3.5 we discussed the challenge that a first transaction might reference in its delete set a row that it failed to lock. If that row was locked by a second transaction which successfully committed, then updating the DTS of this row during recovery based on the delete set of the first transaction will lead to a corruption. Moreover, both transactions might still be unfinished, with the second one in a committed state. To handle this case, the recovery process must first finish all committed transactions (lines 5-7) before undoing uncommitted ones (lines 8-10). This ensures that the DTS of any deleted row will be equal to a valid timestamp. When undoing uncommitted transactions, it is then sufficient to update the DTS of a row in a delete set only if it is a TXID.

Algorithm 5.12 depicts pseudo-code of the transaction recovery process. After recovering the delete and create sets (lines 2-3), we set the DTS of all rows in the delete set with the condition that it is a TXID, to a timestamp provided as a parameter (lines 4-6). Then, we set the CTS of all rows in the create set to the provided timestamp, and their DTS to either kInfinityTS if the transaction is committed or CurMinSTS if it is uncommitted (lines 7-12). The provided timestamp is either a valid commit timestamp if the transaction had committed but did not finish updating the MVCC entries of its modified rows, or equal to kInfinityTS otherwise. Afterwards, we persist the MVCC entries of all modified rows using asynchronous flushes (when available) and memory barriers (line 13-16). Finally, the create and delete sets are cleared (lines 17-18). We do not need to collect garbage rows of in-flight

Algorithm 5.11 SOFORT Recovery function.

```
 1: function RecoverDB
 2:     RecoverWorkingPointers();    ▷ Set working pointers by converting their relative PPtrs
 3:     for each pTab in m_tables do    ▷ Recover table contents
 4:         pTab->Recover();
 5:     for each pTxInfo in m_persTxInfoArray do    ▷ Finish committed TXs
 6:         if pTxInfo.IsCommitted == TRUE then
 7:             RecoverTransaction(pTxInfo, pTxInfo.commitTS);
 8:     for each pTxInfo in m_persTxInfoArray do    ▷ Undo uncommitted TXs
 9:         if pTxInfo.IsCommitted == FALSE then
10:             RecoverTransaction(pTxInfo, kInfinityTS);
11:     m_txInfoArray = new TxTransientInfo[m_MaxParallelTX];    ▷ Build new txInfoArray
12:     for (txid = 0; txid < m_MaxParallelTX; ++txid) do    ▷ Initialize txid of each txInfo
13:         m_txInfoArray[i].txid = txid;
14:     m_currentTime = MaxCommitTS();    ▷ Set current time to max commiTS in persTxInfoArray
15:     m_curMinSTS = m_currentTime;    ▷ Set CurMinSTS to current time
16:     thread recoverGarbage(m_curMinSTS, tableSizes);    ▷ Recover garbage in the background
17:     RecoverSecondaryDataStructures();    ▷ Recover transient or hybrid indexes
```

Algorithm 5.12 SOFORT Transaction Recovery function.

```
 1: function RecoverTransaction(pTxInfo, ts)
 2:     pTxInfo.createSet.Recover();    ▷ Recover create set
 3:     pTxInfo.deleteSet.Recover();    ▷ Recover delete set
 4:     for each row in pTxInfo.deleteSet do
 5:         if m_tables[row.tabID]->MVCC[row.rowID].DTS < kMinTS then    ▷ If DTS is at txid
 6:             m_tables[row.tabID]->MVCC[row.rowID].DTS = ts;    ▷ Finish commit or undo row creation
 7:     for each row in pTxInfo.createSet do
 8:         m_tables[row.tabID]->MVCC[row.rowID].CTS = ts;    ▷ Finish commit or undo row creation
 9:         if pTxInfo.IsCommitted == TRUE then
10:             m_tables[row.tabID]->MVCC[row.rowID].DTS = kInfinityTS;    ▷ Set DTS if TX committed
11:         else
12:             m_tables[row.tabID]->MVCC[row.rowID].DTS = CurMinSTS;    ▷ Set DTS to CurMinSTS
13:     MemBarrier();    ▷ Ensure that all updates to mvcc entries finish executing
14:     for each row in pTxInfo.createSet ∪ pTxInfo.deleteSet do    ▷ Flush mvcc of changed rows
15:         Flush(&m_tables[row.tabID]->MVCC[row.rowID]);
16:     MemBarrier();    ▷ Ensure that all flushes finish executing
17:     pTxInfo.createSet.Clear();
18:     pTxInfo.deleteSet.Clear();
```

transactions since the background garbage recovery will take care of it. Similarly to the abort process, it is important to process the delete set before the create set to enable the recovery garbage collector to distinguish between pre-failure and post-recovery garbage (more details in Section 5.3.10).

Back to Algorithm 5.11, SOFORT builds new transient transaction objects (line 11), and initializes their TXIDs as explained in Section 5.3.2 (lines 12-13). We decided against persisting CurrentTime, because every flush would evict it from the cache, which would jeopardize performance considering that it is frequently incremented. During recovery, we set it to the largest commit timestamp stored in the persistent transaction objects (line 14). This guarantees that no committed transaction, and therefore no MVCC entry, has a timestamp larger than CurrentTime. Afterwards, SOFORT sets CurMinSTS to the current time (line 15) and launches a background garbage collection process (line 16, see Section 5.3.10 for further details). All the above recovery steps execute near-instantaneously as they consume very little time. Finally, SOFORT recovers its transient and hybrid secondary data structures (line 17), such as dictionary indexes and inverted indexes. This is the only time-consuming operation in the recovery process, making it the recovery bottleneck. It can be executed synchronously or in the background, single-threaded or multi-threaded. We tackle this bottleneck in depth in Chapter 6.

Algorithm 5.13 SOFORT Garbage Collection function.

```
1: function CollectGarbage(garbage&)
2:     for each garbageEntry in garbage do
3:         if garbageEntry.TS > m_curMinSTS then
4:             break;                                          ▷ Cannot yet collect this garbage
5:         for each row in garbageEntry.Rows do
6:             m_tables[row.tabID]->collectRow(row.rowID);     ▷ Collect garbage row
7:         garbage.erase(garbageEntry);        ▷ Remove collected garbage from garbage list
```

Algorithm 5.14 SOFORT Row Collection function.

```
1: function PTable::CollectRow(rowID)
2:     for each index in m_Indexes do        ▷ Delete index entries corresponding to this row
3:         key = GetKey(index.GetIndexedCols());        ▷ Get valIDs of indexed columns
4:         index->Erase({key, rowID});
5:     m_reusableRows.Push(rowID);                      ▷ Mark row as reusable
```

5.3.10 Garbage Collection

As shown in the previous sections, each transaction object keeps a list of garbage entries, each of which comprises a list of rows and a timestamp that indicates when these rows can be collected. To qualify for collection, the timestamp of a garbage entry must be lower or equal to CurMinSTS. This way, we ensure that any running transaction is able to see all versions that should be visible at its STS. CurMinSTS is updated by one or more worker threads in the start transaction function. In Algorithm 5.3 we illustrated this by having only one worker thread update CurMinSTS. This is good enough even if this worker thread is executing a long-running transaction, in which case CurMinSTS could be off by MaxParallelTX in the worst case – the real CurMinSTS becomes eventually the STS of the long-running transaction. Nevertheless, it is possible to have more than one worker thread update CurMinSTS.

Garbage is collected in a cooperative way by transactions when they start (see Algorithm 5.3). Algorithm 5.13 presents pseudo-code of the garbage collection process. To collect garbage, a transaction goes through the list of garbage in its transaction object. If the timestamp of a garbage entry is greater than CurMinSTS, then the garbage entry cannot be collected yet (lines 3-4). In this case the garbage collection process is stopped, because garbage entries are chronologically ordered in the garbage list, which means that if the head of the list does not qualify for collection, then the remaining entries do not either. If a garbage entry qualifies for collection, then its rows are collected at the table level (lines 5-6). Finally, collected entries are deleted from the garbage list (line 7).

Algorithm 5.14 shows pseudo-code for the row collection function provided by PTable. First, the function cleans the indexes of the table (lines 2-4). To do so, it constructs the corresponding index keys by fetching the value IDs of the indexed columns (line 2), then it uses this key and the row ID to delete the corresponding index entry (line 4). Finally, the row ID of the collected row is pushed into the reusable row queue.

To decrease the number of accesses to SCM, we decided to place the garbage lists of the transaction objects and the reusable row queues in DRAM. Therefore, these lists are lost upon failure. To collect the lost garbage during recovery, a background garbage collector scans the MVCC column of all tables. Algorithm 5.15 shows pseudo-code of this process. The recovery garbage collector scans tables only up to their pre-failure size, because any garbage past this limit will be already referenced in the garbage lists of the transaction objects. A row is considered as garbage if its DTS is equal to zero, or if it is a valid timestamp and lower or equal to failure time.

Algorithm 5.15 SOFORT Background Garbage Collection Recovery function.

```
function RecoverGarbage(minTS, tableSizes)
    for (i = 0; i < m_numTables; ++i) do                              ▷ Recover garbage for each table
        pTab = m_tables[i];
        for (rowID = 0; rowID < tableSizes[i]; ++rowID) do            ▷ Scan table up to pre-failure size
            mvcc = pTab->MVCC[rowID];
            if mvcc.DTS == 0 or (kMinTS <= mvcc.DTS <= minTS) then
                pTab->collectRow(rowID);
```

Since collected rows can be reused by running transactions, the recovery garbage collector can conflict with the regular garbage collection process. Consider the scenario where, while the recovery garbage collector is running, transaction *T1* deletes a row, which is then reused by transaction *T2*. If transaction *T2* aborts, it will register this row as garbage. If the recovery garbage collector did not scan this row yet, it might race with the regular garbage collection process, which might lead to the row being pushed twice in the reusable row queue, eventually causing a data corruption. To avoid such a scenario, the recovery garbage collector must be able to distinguish between pre-failure and post-recovery garbage. To achieve this, when a transaction is aborted or rolled back during recovery, we set the DTS of its created rows to CurMinSTS. This ensures that any pre-failure garbage row has its DTS equal to a timestamp that is lower or equal to failure time. Hence, garbage rows with a DTS lower than or equal to failure time are pre-failure garbage, while ones with a DTS greater than failure time are post-recovery garbage.

Finally, we discuss the case of garbage rows whose MVCC entries were updated while handling in-flight transactions during recovery. If an uncommitted transaction was rolled back, then the rows in its create set need to be collected. However, the create set might not include all created rows following a failure. For instance, a failure can occur after inserting a row in a table but before appending its row ID to the create set (e.g., between lines 4 and 5 in Algorithm 5.6). In this case, the DTS of this row will be equal to either zero if it was a newly appended row, or to an old timestamp (the commit timestamp of the transaction that deleted it) if it was a reused row. In both cases, the recovery garbage collector will be able to identify it as pre-failure garbage. If a committed transaction was rolled forward, then the rows in its delete set need to be collected. Their DTS is set to failure time, therefore, the recovery garbage collector is able to identify them as pre-failure garbage.

5.4 CONTINUING UNFINISHED TRANSACTIONS

In this section we discuss a special configuration of SOFORT that allows the user to continue executing open transactions after a system failure. SOFORT achieves this by segregating between the statements of a transaction. In contrast to traditional systems, SOFORT makes the changes of each statement durable in SCM, before executing the next one. The changes, which are durable, are not visible to other transactions and will only become atomically visible when the transaction commits by updating the MVCC commit time-stamps. To empower SOFORT to continue in-flight transactions, the following changes to its MVCC structures are necessary:

- we persist the whole transaction object, including the STS, the read set, the scan set, and the status variables;
- we add a new statement ID persistent counter in the transaction object;
- in addition to the table ID and row ID, we also add the statement ID to the read, create, and delete sets.

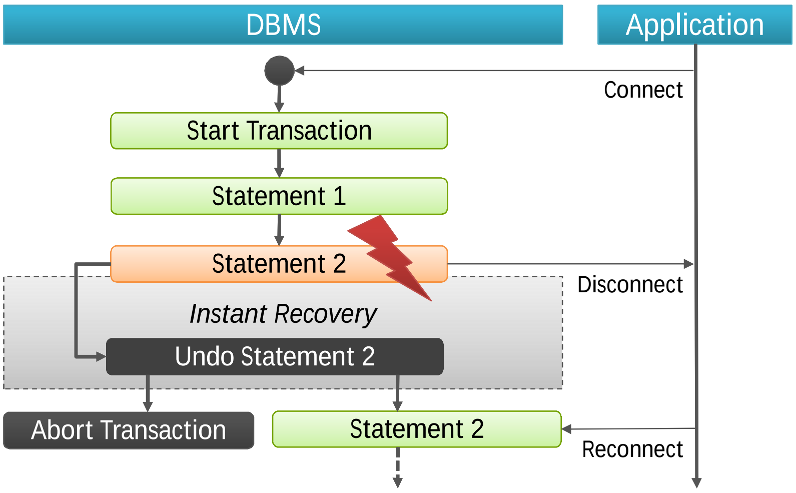

Figure 5.3: Transaction flow during a system failure.

When a transaction starts, it resets its statement ID counter to zero. When a statement is issued, it is assigned an ID equal to the current value of the statement ID counter. The latter is persistently incremented only at the end of each statement, as an indicator that this statement finished executing. In the case of a system failure, SOFORT first checks the status of the transaction: If it is aborted or committed, then the transaction is rolled back or finished, respectively. Otherwise, SOFORT checks the value of the statement ID counter, which is equal to the ID of the last active statement (if any). Then, SOFORT rolls back this unfinished statement by removing the statement's entries from the read and scan sets, and undoing its changes documented in the create and delete sets. This is made possible by the fact that SOFORT keeps the statement ID for each entry in the latter sets. Thereafter, the transaction can be resumed with the same STS it had before failure. Nevertheless, only read-only transactions need to be resumed with the same STS since they execute in snapshot isolation mode; read-write transactions could be resumed with an STS equal to the recovery time. Finally, persisting the read and scan sets allows to ensure the serializability of resumed transactions.

Figure 5.3 shows what happens in case of a system failure during the processing of a statement of a transaction. Every executed statement is guaranteed to have its incurred changes persisted. If the system crashes before a statement is finished, the latter is first undone, then re-executed right after recovery. With no transaction rollbacks after failure and instant recovery, the application or user will not notice that the system has crashed and will continue executing his transaction as if nothing happened. If the application does not reconnect to the DBMS after a crash, its transactions are aborted after a timeout. This approach is highly beneficial especially for long-running interactive transactions, such as ones in e-commerce applications, which justifies the overhead of persisting additional transaction metadata.

5.5 EVALUATION

This section presents an experimental evaluation of SOFORT's OLTP performance. Since our goal is to show that a column-store can exhibit competitive OLTP performance, we do not evaluate OLAP performance which we assume is competitive given our design decisions. First, we compare the performance of SOFORT to that of two existing systems. Then, we explore the impact of different secondary data placement strategies and higher SCM latencies on SOFORT's performance. Thereafter, we study the cost of durability in SOFORT. Finally, we briefly evaluate SOFORT's recovery time and compare it to a setting where SOFORT is placed on traditional storage media. A more detailed experimental evaluation of recovery is provided in Chapter 6.

5.5.1 Experimental Setup

Based on the data structure used to implement the column and dictionary indexes, we consider three SOFORT configurations:

- SOFORT-FPTree: all indexes are kept in a hybrid SCM-DRAM format and implemented using the FPTree [126]. This is the default configuration.
- SOFORT-STXTree: all indexes are placed in DRAM and implemented using a transient B^+-Tree, namely the STXTree [154];
- SOFORT-wBTree: all indexes are persisted in SCM and implemented using the wBTree [21], a persistent B^+-Tree fully residing in SCM.

These three configurations are used to investigate the effect of different secondary data placement strategies. SOFORT-STXTree and SOFORT-wBTree represent the extreme cases where all secondary data is placed in DRAM and in SCM, respectively, while SOFORT-FPTree represents our advocated hybrid SCM-DRAM strategy.

We use two OLTP benchmarks in our experiments: TATP and TPC-C. TATP [155] is a simple but realistic OLTP benchmark that simulates a telecommunication application. The schema of the benchmark comprises four tables and the benchmark consists of seven transaction templates. TATP is read-mostly as its standard mix comprises 80% read-only transactions and 20% read-write transactions. TPC-C [159] is the industry standard OLTP benchmark. Its schema encompasses nine tables and it consists of five transaction templates. TPC-C is write-heavy since its standard mix consists of 92% read-write transactions and only 8% read-only transactions. In the following experiments, we run the standard TATP and TPC-C mixes.

To emulate different SCM latencies, we use the Intel SCM Emulation Platform that we described in Chapter 2. It is equipped with two Intel Xeon E5 processors. Each one has 8 cores, running at 2.6 GHz and featuring each 32 KB L1 data and 32 KB L1 instruction cache as well as 256 KB L2 cache. The 8 cores of one processor share a 20 MB last level cache. The system has 64 GB of DRAM and 192 GB of emulated SCM. In the experiments, we vary the latency of SCM between 160 ns (the lowest latency that can be emulated) and 650 ns.

Since the emulation platform does not support TSX– upon which the concurrency scheme of the FPTree depends – we use for concurrency experiments a platform equipped with two Intel Xeon E5-2699 v4 processors that support TSX. Each one has 22 cores (44 with HyperThreading) running at 2.1 GHz. The system has 128 GB of DRAM. The local-socket and remote-socket DRAM latencies are respectively 85 ns and 145 ns. We mount *ext4 DAX* on a reserved DRAM region belonging to the second socket to emulate SCM, and bind our programs to run on the first socket, thereby emulating an SCM latency of 145 ns.

5.5.2 OLTP Performance

In this section we evaluate the OLTP performance of SOFORT; we consider only the (default) configuration SOFORT-FPTree, as it is the most optimized for high concurrency. To provide a comparison baseline, we also experiment with two OLTP systems, namely Shore-MT [73] and SILO [161]. Shore-MT is a disk-based transactional storage engine designed for multi-core systems. We place the database and the log of Shore-MT on SCM to get an upper bound of Shore-MT's performance. We tuned the configuration of Shore-MT baseline to get the highest possible throughput, e.g., by ensuring that all data fits in the buffer pool. SILO is a state-of-the-art highly scalable main-memory

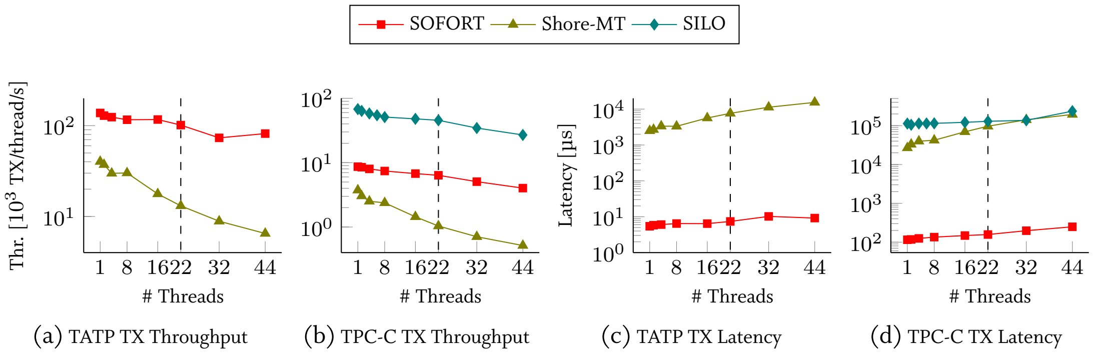

(a) TATP TX Throughput (b) TPC-C TX Throughput (c) TATP TX Latency (d) TPC-C TX Latency

Figure 5.4: Transaction throughput and latency of SOFORT, SILO, and Shore-MT for the TATP (10 million Subscribers) and TPC-C (48 Warehouses) benchmarks.

transactional storage engine that relies on epoch-based concurrency control. It stores data row-wise in indexes based on the Masstree [101]. We place SILO's log in SCM to ensure a fair comparison. We emphasize that both Shore-MT and SILO are designed purely for OLTP workloads, while SOFORT is designed for hybrid OLTP and OLAP workloads.

We use the TSX-enabled platform in this experiment. While we run the TPC-C benchmark on the three evaluated storage engines, we run the TATP benchmark only on SOFORT and Shore-MT, because SILO does not provide a TATP implementation. Figure 5.4 shows transaction throughput and latency per thread for an increasing number of threads. The first observation is that both SOFORT and SILO are able to retain nearly-constant transaction throughput and latency per thread until 22 threads, which is the number of available physical cores. When using hyperthreading (22-44 threads), SOFORT's metrics per thread deteriorate slightly, emphasizing that it is still able to leverage the additional logical cores for more performance. In contrast, Shore-MT scales only up to 8 threads due to resource contention. However, with Dora [130], Shore-MT resists to a certain extent to resource contention.

Regarding throughput, despite being a column-store, SOFORT outperforms Shore-MT in TATP by 4.6×-16.7×, and in TPC-C by 2.3×-7.8×, stressing the superiority in performance of main-memory over disk-based database architectures, even when the latter fits in memory. However, SILO outperforms SOFORT by 6.8×-7.8× in TPC-C. Given that SILO is a purely OLTP-optimized main-memory engine, this difference – less than one order of magnitude – is in fact smaller than expected. Therefore, we argue that SOFORT exhibits competitive OLTP performance for a hybrid analytical and transactional system. Regarding transaction latency, SOFORT delivers up to three orders of magnitude lower transaction latency than Shore-MT and SILO, because both systems use variants of group commit, which SOFORT does away with thanks to its fine-grained and decentralized transaction management.

5.5.3 Data Placement Impact on OLTP Performance

In this experiment we study the effect of different secondary data placement strategies and increasing SCM latencies on the performance of SOFORT. To eliminate any concurrency artifacts from the experimental results, we run SOFORT single-threaded. We use the SCM emulation platform and vary the latency of SCM between 160 ns and 650 ns. Figure 5.5 depicts the TATP and TPC-C transaction throughput for each configuration of SOFORT relative to a baseline latency of 160 ns. First, we observe that the impact of higher SCM latencies depends on the workload: TATP throughput deteriorates faster than that of TPC-C. Second, we notice that the impact of higher SCM latencies highly depends on the secondary data placement strategy: the more secondary data is placed in DRAM, the

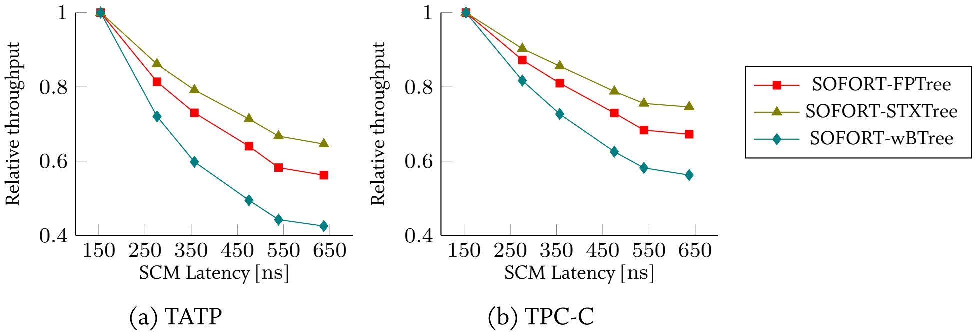

(a) TATP (b) TPC-C

Figure 5.5: Impact of higher SCM latencies on SOFORT's OLTP performance for the TATP (10 million Subscribers) and TPC-C (48 Warehouses) benchmarks. Depicted throughput is relative to a baseline SCM latency of 160 ns.

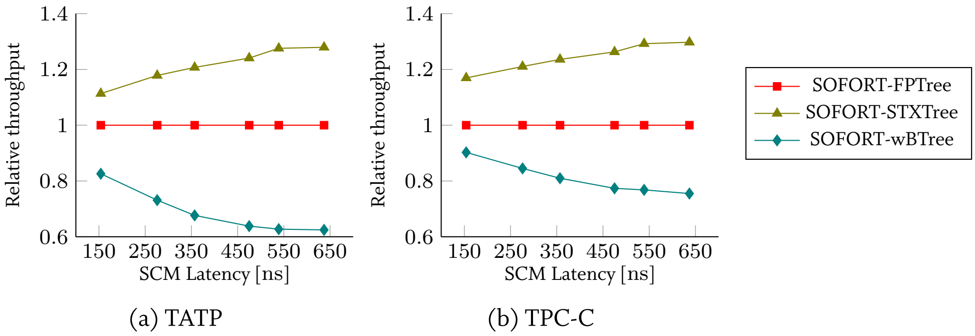

(a) TATP (b) TPC-C

Figure 5.6: SOFORT's OLTP performance with different secondary data placement strategies for the TATP (10 million Subscribers) and TPC-C (48 Warehouses) benchmarks. Depicted throughput is relative to SOFORT-FPTree.

less the impact on performance. For instance, increasing the latency of SCM to 650 ns (4× higher than the baseline latency) incurs a 43.8%, 35.4%, and 57.5% TATP throughput decrease and 32.7%, 25.4%, and 43.7% TPC-C throughput decrease for the FPTree, STXTree, and wBTree SOFORT configurations, respectively. While the performance impact is significant, it is far less than the 4× increase in latency.

To analyze the performance impact of different secondary data placement strategies, we depict in Figure 5.6 TATP and TPC-C throughput of SOFORT-STXTree and SOFORT-wBTree relative to that of SOFORT-FPTree for different SCM latencies. We observe that the more secondary data is placed in DRAM, the higher the throughput. Moreover, the gap between the different configurations widens as the latency of SCM increases, due to their different sensitivity to higher SCM latencies. Concretely, SOFORT-STXTree delivers respectively 1.11×-1.28× and 1.17×-1.29× higher TATP and TPC-C throughput than SOFORT-FPTree. Compared to SOFORT-wBTree, SOFORT-STXTree delivers respectively 1.35×-2.05× and 1.30×-1.72× higher TATP and TPC-C. We conclude that while placing all secondary data in DRAM yields the best performance, a hybrid SCM-DRAM architecture incurs only a limited performance impact compared to an all-in-SCM approach. Moreover, a hybrid architecture requires only a small portion of DRAM relative to SCM, as discussed in the next paragraph.

Figure 5.7 shows DRAM and SCM consumption of each SOFORT configuration. At one extreme, SOFORT-STXTree requires almost a 1:1 ratio of DRAM and SCM, which might not be optimal if DRAM is a scarce resource. At the other extreme, SOFORT-wBTree requires a 1:600 ratio of DRAM

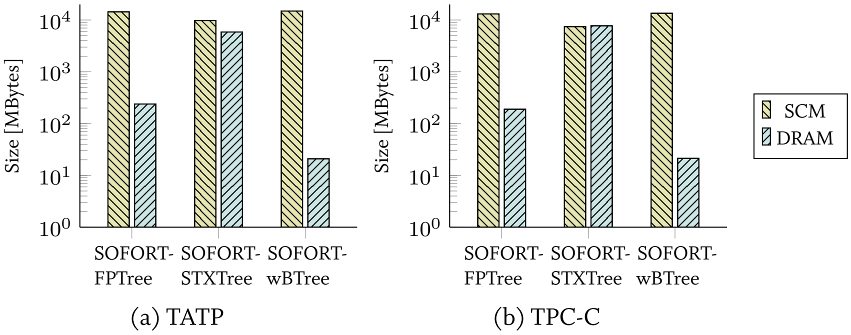

(a) TATP (b) TPC-C

Figure 5.7: SOFORT DRAM and SCM consumption with different data placement strategies for the TATP (10 million Subscribers) and TPC-C (48 Warehouses) benchmarks.

and SCM, which is optimal when DRAM is very scarce, but incurs a significant performance impact. In the middle, SOFORT-FPTree offers an appealing ratio of 1:60 ratio of DRAM and SCM – especially considering the fact that SCM is projected to be cheaper than DRAM – while decreasing the sensitivity towards SCM latency and limiting the impact on query performance.

5.5.4 Durability Cost

In this section we measure the cost of using the cache-line flushing instructions (CLFLUSH in our case) in SOFORT, which corresponds to the cost of providing data durability guarantees. Similarly to the previous experiment, we run SOFORT single-threaded. Figure 5.8 shows the decrease in percentage of SOFORT's throughput for the TATP and TPC-C benchmarks for different SCM latencies. We observe that for TATP, which is read-mostly, the overhead of flushing instructions is less than 12% and similar for the three SOFORT configurations, with the STXTree configuration suffering the lowest overhead. In contrast, we notice that for TPC-C, which is write-heavy, flushing instructions incur different overheads on the three configurations of SOFORT: 15.7%-18.2%, 8.6%-14.3%, and 18.8%-24% on the FPTree, STXTree, and wBTree configurations. As expected, the STXTree configuration suffers the lowest overhead, followed by the FPTree one, then the wBTree one.

To sum up, in comparison to an all-in-SCM approach, a hybrid SCM-DRAM approach not only decreases the impact of higher SCM latencies, it also decreases that of flushing instructions. An interesting observation is that while increasing the latency of SCM impacts the overall performance of the system, the relative cost of flushing instructions remains stable, that is, it does not necessarily increase when increasing the latency of SCM. We explain this by two factors: (1) the system emulates symmetric (instead of asymmetric) read and write latencies; and therefore (2) higher SCM latencies impact reads as much as writes.

We expect the overhead of flushing instructions to be significantly reduced with the new CLWB instruction, which writes back a cache line to main memory without evicting it. Additionally, in contrast to the serializing CLFLUSH, CLWB executes asynchronously, which enables issuing multiple CLWB instructions per cycle. In conclusion, the cost of cache-line flushing instructions can be as much as 24% depending on the workload and the data placement strategy. In hybrid transactional and analytical workloads, we expect this overhead to be less than 10%. Still, we argue that providing non-volatile caches – which is at the discretion of hardware vendors – would be the better solution. If that were to happen, then SOFORT can do away with flushing instructions but must retain memory fences, because writes need to ordered the same way with volatile or non-volatile caches.

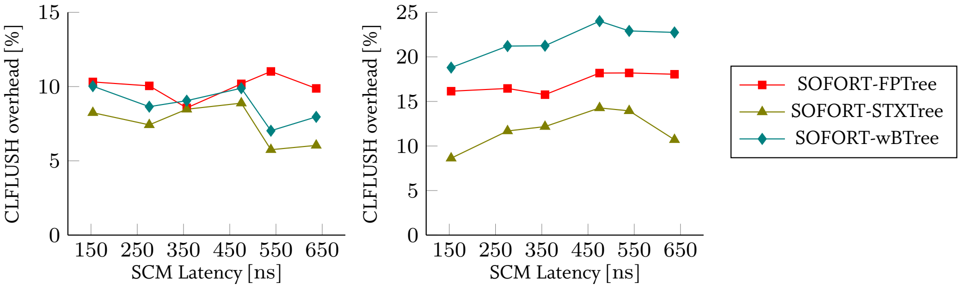

(a) TATP (b) TPC-C

Figure 5.8: Cost of flushing instructions in SOFORT with different secondary data placement strategies for the TATP (10 million Subscribers) and TPC-C (48 Warehouses) benchmarks.

5.5.5 Recovery Time

In this experiment, we measure SOFORT's recovery time for the three investigated data placement strategies above. Additionally, to provide a baseline for comparison, we substitute SCM with the following storage media:

- A SATA-attached Western Digital Disk (WD1002FAEX-00Z3A0) with a measured read bandwidth of 126 MB/s;
- An PCIe-attached Intel SSD (SSDPEDMD400G4) with a measured read bandwidth of 2.7 GB/s.

Since the above storage media are available on the TSX-enabled platform, we use it for this experiment. In contrast to SCM, disk or SSD-resident files are buffered in DRAM when accessed via memory mapping. To force primary data to be loaded from storage to main memory, we use the flag *MAP_POPULATE* of *mmap*, which populates the page table, thereby causing a read-ahead on the file. Note that SOFORT on disk and SSD does not provide any durability guarantees, because SOFORT relies on cache-line flushing instructions, which evict data from the CPU cache to main memory – in this case, DRAM. Therefore, writes are not propagated to the disk or the SSD.

SOFORT first recovers its persistent primary and secondary data, rolls back unfinished transactions, then rebuilds its transient secondary data. We allow using up to 8 threads in SOFORT's recovery process. Figure 5.9 depicts recovery time for the TATP and TPC-C schema with 20 million Subscribers and 128 Warehouse, respectively. For the sake of concision, and since we observe the same patterns for the TATP and the TPC-C schema, we limit the discussion below to the TATP schema. We observe that when using the disk or the SSD, the recovery time of the three SOFORT configurations is similar. When using the disk, SOFORT takes 234.9 s, 166.4 s, and 237.8 s when using the FPTree, STXTree, and the wBTree, respectively. SOFORT-STXTree takes less time to recover because less data is persisted in SCM. When using the SSD, the recovery time is decreased to 21.7 s, 21.7 s, and 19.7 s for the FPTree, STXTree, and the wBTree configurations, respectively, which is still significant. In contrast, when using SCM, the recovery time of the three SOFORT configurations drift apart: It takes only 1.9 s, 8.7 s, and 0.3 s to recover SOFORT when using the FPTree, STXTree, and the wBTree, respectively. The reason behind this difference is that when using a disk or an SSD, the recovery bottleneck consists in loading the durable data from storage to main memory – a well-known bottleneck in the recovery of main-memory database system. Persisting data in SCM alleviates this bottleneck because data does not need to be loaded, rather, it is discovered in SCM and directly accessed from it. As for the difference in recovery time between the three SOFORT configurations, it is explained by the cost of rebuilding transient secondary data, which is very small when using the SCM-based wBTree, moderate when using the hybrid SCM-DRAM FPTree, and high when using the DRAM-based STXTree.

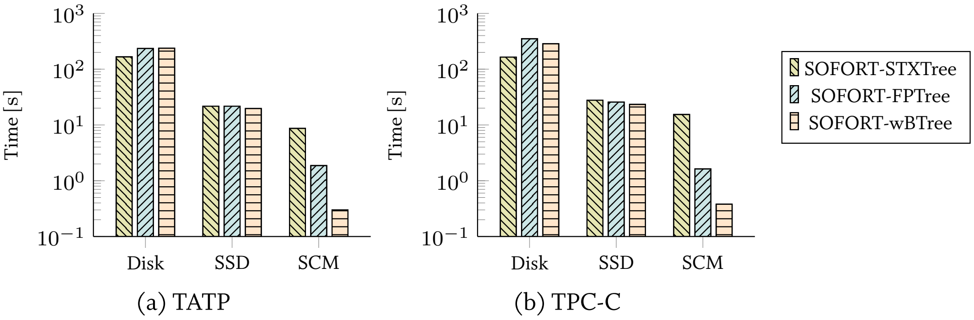

(a) TATP

(b) TPC-C

Figure 5.9: SOFORT Recovery time with different storage technologies and data placement strategies for the TATP (20 million Subscribers) and TPC-C (128 Warehouses) benchmarks.

While near-instant recovery at full speed is possible (such as in SOFORT-wBTree) and beneficial in applications where availability is critical, placing latency-sensitive secondary data in SCM incurs a significant cost on query performance, as shown previously. Our hybrid SCM-DRAM approach offers a good trade-off between recovery time, query performance, and DRAM usage. We conclude that the new recovery bottleneck in SCM-based database systems is rebuilding transient secondary data. We tackle this bottleneck in the next chapter.

5.6 SUMMARY

In this chapter we demonstrated how we assembled the building blocks we devised in previous chapters, namely persistent memory management and hybrid SCM-DRAM persistent data structures, into SOFORT, a novel columnar single-level transactional engine. Our architecture enables near-instant recovery: The redo phase and loading data from storage to main memory are not needed anymore. We presented a new MVCC design, including efficient indexing and garbage collection, tailored to SOFORT's architecture. By persisting part of transactions' MVCC metadata, we demonstrated how to remove traditional write-ahead logging from the critical path of transactions. Nevertheless, removing the logging component does not decrease the overall complexity, because its logic is spread over the persistent data structures. Additionally, we presented a special configuration where SOFORT is able to continue unfinished transactions after a failure.

Through an experimental evaluation, we showed that, despite being a column-store, SOFORT exhibits competitive OLTP performance, and achieves low transaction latency since its design alleviates the need for group commit. Furthermore, we showed that secondary data placement in DRAM or in SCM has a direct impact on query performance and recovery time. At one extreme, all secondary data is placed in SCM, which enables near-instant recovery but incurs a significant overhead on query performance. At the other extreme, all secondary data is placed in DRAM, which is optimal for query performance but makes recovery time dependent on the size of secondary data to be rebuilt. Our advocated hybrid SCM-DRAM approach showed promising results by limiting the impact on query performance, decreasing the sensitivity towards SCM latency, and exhibiting fast recovery. Finally, the new recovery bottleneck in single-level storage architectures is rebuilding transient secondary data, which we address in the next chapter.

6

SOFORT RECOVERY TECHNIQUES

Availability guarantees form an important part of many service level agreements (SLAs) for production database systems [25]. Database recovery time has a significant and direct impact on database availability as many database crash conditions are transient (e.g., software bugs, hardware faults, and user errors) and for these, restarting is a reasonable approach to recovery. To ensure transaction durability, traditional in-memory DBMSs periodically persist a copy (checkpoint) of the database state and log subsequent updates. Recovery consists of reloading the most recent persisted state, applying subsequent updates, and undoing the effects of unfinished transactions. For in-memory DBMSs reloading the persisted state is typically the bottleneck in this process.

SCM has empowered a new class of database architectures where memory and storage are merged [5, 122, 79, 148]. SCM-enabled database systems such as SOFORT keep a single copy of the data that is stored, accessed, and modified directly in SCM. This eliminates the need to reload a consistent state from durable media to memory upon recovery, as primary data is accessed directly in SCM. Hence, the new recovery bottleneck is rebuilding DRAM-based data structures. SOFORT allows trading off query performance for recovery performance by judiciously placing certain secondary data structures in SCM. However, while this is beneficial for systems with critical availability needs, database systems are generally optimized for query performance. In this chapter we aim to improve recovery performance without compromising query performance. Therefore, we assume that all latency-sensitive secondary data structures are kept in DRAM.

After recovering its SCM-based data structures, SOFORT rebuilds DRAM-based secondary data structures, then starts accepting requests. If DRAM-based secondary data structures are large, restart times can still be unacceptably long. To address this, we propose an *Instant Recovery* strategy. It allows queries to be processed concurrently with the rebuilding of DRAM-based data structures. However, while the secondary data structures are being rebuilt, request throughput is reduced. Part of the performance drop is due to the overhead of rebuilding but a more significant factor is the unavailability of the DRAM-based secondary data structures, resulting in sub-optimal access plans.

In this chapter[1], we propose a novel recovery strategy, *Adaptive Recovery*. It is inspired by the observation that not all secondary data structures are equally important to a given workload. It improves on instant recovery in two ways. First, it prioritizes the rebuilding of DRAM-based secondary data structures based on their benefit to a workload (instant recovery simply uses an arbitrary order). Second, it releases most of the CPU resources dedicated to recovery once all of the important secondary data

---

[1] This chapter is partially based on the material in [128, 129].

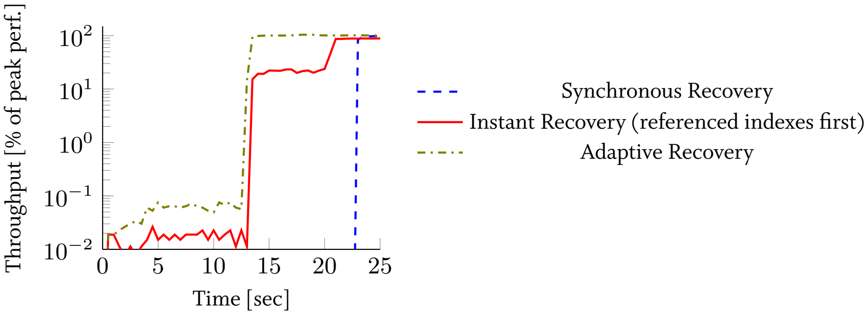

Figure 6.1: Results overview: TPC-C transaction throughput during recovery.

structures have been rebuilt (instant recovery statically splits CPU resources between recovery and query processing for the entire recovery period).

Adaptive recovery aims at approaching peak performance of the database as fast as possible by tuning the rebuild order of secondary data structures to optimize the workload run concurrently with the recovery process. To determine the optimal rebuild order, we conduct a characterization of secondary data structures. Although we focus on indexes in this work, the characterization and the recovery algorithms are generic and apply to most runtime data structures. We identify a set of properties that are intrinsic to secondary data structures and infer from them the criteria based on which they should be ranked, namely: (1) the usefulness to the workload before failure and during recovery, (2) the cost of rebuilding each secondary data structure, and (3) workload-related dependencies between secondary data structures.

We propose two ranking functions that take into account these properties. The first one satisfies items (1) and (2) while the second one satisfies all three of them. Additionally, the ranking of secondary data structures is adjusted dynamically to accommodate workload changes during the recovery period. Furthermore, we introduce a resource allocation algorithm that releases recovery resources to query processing when it detects that all important secondary data structures have been rebuilt.

We conduct a detailed experimental evaluation that shows the benefits of our approach. Figure 6.1 shows an overview of recovery performance results using the TPC-C benchmark. Our adaptive recovery approach significantly outperforms synchronous recovery, since in adaptive recovery, the database approaches its peak performance well before the end of the recovery process: approaching peak performance is no more a function of the size of all secondary data structures but only of a small subset of them, namely the relevant ones to the current workload.

The rest of this chapter is structured as follows: Section 6.1 explores the design space of the recovery of secondary data structures. Thereafter, Section 6.2 formalizes the problem we tackle in this chapter and elaborates in details on our adaptive recovery approach. Afterwards, we implement adaptive recovery in SOFORT and conduct a thorough experimental evaluation in Section 6.3. Finally, Section 6.4 briefly surveys related work while Section 6.5 summarizes this chapter.

6.1 RECOVERY OF SECONDARY DATA STRUCTURES

In this section we discuss the two main design dimensions for the recovery of secondary data structures: The first dimension is whether to recover secondary data structures synchronously or asynchronously, which determines when the system starts being responsive again. The second dimension pertains to secondary data placement in DRAM or in SCM, which determines a trade-off between query performance and recovery performance.

6.1.1 System Responsiveness

SOFORT recovers by first recovering primary data that is persisted in SCM at a negligible cost, then undoing the effects of unfinished transactions [122]. The last phase of the recovery procedure, that is, rebuilding secondary data, can be handled in two different ways: In the first approach, denoted *Synchronous Recovery*, SOFORT does not accept requests until the end of the recovery process, i.e., until all secondary data structures have been rebuilt. The main advantage of this approach is that it rebuilds secondary data structures as fast as possible since all system resources are allocated to recovery. However, this approach suffers from the fact that the database is not responsive during the whole recovery period, which might be long as its duration depends directly on the size of secondary data structures to be rebuilt.

In the second approach, denoted *Instant Recovery*, SOFORT starts accepting new transactions right after recovering the persistent data structures. This is possible because all of the primary data are persistent in SCM, allowing us to process transactions without the vanished transient data structures. However, since the latter are responsible for speeding up query processing, the transaction throughput could be low at this point in time. Moreover, the rebuilding of the transient data structures can be done in a specific order, e.g., based on the transactions which need to be continued during recovery. To achieve instant recovery, SOFORT adopts a *crawl before run* approach: it uses primary data, which is recovered at a negligible cost, to answer queries, while secondary data structures are rebuilt in the background. For example, lookups to a dictionary index and an inverted index are replaced by scans of the corresponding dictionary array and the value ID arrays, respectively. Partially rebuilt DRAM-based indexes can be progressively leveraged as they are being rebuilt. For instance, a regular dictionary index lookup is replaced by the following sequence: look up the partially rebuilt dictionary index; if the value is not found, then scan only the portion of the dictionary array that has not been indexed yet. As for hybrid SCM-DRAM indexes, we can only scan their persistent part before they are fully recovered. Hence, transaction throughput during recovery continuously increases until it reaches, once all data structures have been completely rebuilt, its value observed before failure. The main advantage of this approach is that it enables instant recovery, i.e., instant responsiveness of the database after failure. However, it takes the database a considerable amount of time, potentially longer than for synchronous recovery, to approach peak performance observed before failure. This is because system resources are split between recovery and query processing, while in synchronous recovery, all system resources are allocated to recovery.

6.1.2 Balancing Query Performance with Recovery Performance

As we have shown in Section 2.1.2, latency-sensitive data structures, such as indexes, perform up to several times better when they are located in DRAM, because of its low latency. However, storing secondary index structures in DRAM causes a significant drop in transaction throughput immediately after recovery, since they have to be rebuilt before the database system can leverage such indexes for optimized query processing. Operational database systems often require certain guarantees in terms of minimum transaction throughput per second. To enable SOFORT to meet such constraints, we allow placing a certain amount of transient data structures (or all in the extreme scenario) in SCM to store them in a persistent way. By varying the amount of transient and persistent data structures, we are able to balance between a high transaction throughput during usual query processing and a guaranteed minimum throughput during recovery. While SOFORT can achieve near instant recovery if most secondary data structures are stored in SCM, there is a query performance cost, as many of these data structures are latency-sensitive and SCM is expected to have higher latencies than DRAM (cf. Section 5.5).

6.1.3 Discussion

From the above description of different recovery trade-offs, we observe that the bottleneck of recovery is shifted in SCM-enabled databases from reloading primary data from durable media to main memory, to rebuilding secondary data structures. Optimizing the latter did not get much attention in the past because it was shadowed by the former, more prominent bottleneck. In this chapter we propose a solution to overcome this new bottleneck. For operational databases with critical availability requirements, placing all secondary data in SCM provides near-instant recovery. However, operational databases most often optimize for query performance; we focus on the latter scenario in this chapter. Therefore, we assume in the remainder of this chapter that all latency-sensitive secondary data structures are kept in DRAM as our goal is to improve recovery performance without compromising query performance. Although synchronous recovery and instant recovery exhibit interesting advantages, they both suffer from (different) noticeable shortcomings. We try to cure the shortcomings of both approaches by achieving instant responsiveness and reaching peak performance quickly, well before the end of the recovery process. The following section formalizes the problem and explains in details how we achieve this.

6.2 ADAPTIVE RECOVERY

Adaptive recovery is based on the observation that not all secondary data structures are equally important to a specific workload. Therefore, rebuilding the most relevant ones first should significantly improve the performance of the workload run concurrently with the recovery process, eventually improving the overall recovery performance. The following questions arise: What are the characteristics of secondary data structures? How are secondary data structures rebuilt? How can the *benefit* of a secondary data structure be measured and estimated for a specific workload?

In this section, we answer these questions in order. We discuss the recovery procedure of secondary data structures based on a characterization of their recovery properties. Then, we introduce benefit functions centered on the usefulness and rebuild cost of these structures given a recovery workload. As the recovery process is usually a very short period of time compared with the time the system is in normal operation, the benefit functions must quickly adapt to the current workload to maximize performance of the system during recovery. A recovery manager will take into account the workload right before the crash and the workload during recovery to decide the recovery procedure of the secondary data structures by answering these questions: What resources are allocated to the recovery process? Does the recovery happen in a background process or synchronously with the statements needing them? And what is the recovery order?

6.2.1 Characterization of Secondary Data Structures

Secondary data structures can reside in SCM or in DRAM. The decision for this characteristic can be decided as part of the database physical design process, based on cost estimated that takes into account the schema, the base data properties, the workload, and how fast the recovery process must be. In a robust system, when recovery must be guaranteed to be almost instantaneous, it may be desired to have all primary data and secondary data structures in SCM for fast recovery. However, this approach will significantly impact query performance as discussed in Section 2.1.2.

Secondary data structures, such as indexes, materialized views, intermediate cached results are structures that can be completely rebuilt from primary data. In this work, we identify and assume the following general properties of using and maintaining secondary data structures:

1. query processing can be correctly done (i.e. correct result sets) without using any secondary data structures;
2. secondary data structures are used for improving global performance;
3. the decisions to build and use them is cost-based taking into account the cost of maintaining them, and the performance benefit their usage will bring;
4. for a particular statement, the decision to use an available secondary data structure is cost-based;
5. secondary data structures may be useful when they are only partially built, and the query optimizer will build correct plans capable of compensating for missing data. For example, this can be implemented using partially materialized views or cracked indexes.

In an SCM-DRAM hybrid system such as SOFORT, secondary data structures can be built and stored as follows:

- *Transient data structures* fully residing in DRAM. These structures must be fully rebuilt from primary data at restart to reach a consistent state similar to the state before the crash.
- *Persistent data structures* fully residing in SCM and persisted in real-time. These structures are available to be used by query processing, almost instantaneously, after a *recover* process which includes sanity checks and repairs if needed.
- *Hybrid transient-persistent data structures* partially residing in DRAM, and partially in SCM (e.g., the FPTree [126]). The persistent part must go through a *recovery* process which includes sanity checks and repairs if needed. The transient part is rebuilt based on one or both of the persistent part and the primary data.

Regardless of the type of a secondary data structure, the rebuild or reload can be executed to completion for the whole structure, or it can be partially done on a need-to-do basis based on the workload, e.g., data cracking techniques [63]. Each secondary data structure can be rebuilt right after restart or on demand, e.g., when this structure is first needed by a transaction (for writes or reads). These decisions should be cost-based, balancing the performance benefit for the workload during recovery with the overhead of recovery, i.e., reloading and rebuilding.

6.2.2 Benefit Functions for Secondary Data

Regardless of where a secondary data structure resides or what the recovery process for a specific secondary data structure is, we can compare and rank them based on the usefulness to past and current workloads, and how expensive it is to rebuild them at recovery time. Our goal is to maximize performance of the workload run in parallel with the recovery process. In real database systems, the workload right after restart can be similar to the workload at crash time (e.g., unfinished transactions are resubmitted after restart), it can be very different (e.g., the system must execute a specific restart workload), or a mixed workload including both special restart transactions and resubmitted transactions. As the recovery time can be very short, the benefit functions for secondary data structures must quickly adapt to the current workload and available resources for recovery process.

At first glance, using benefit functions to rank the usefulness of secondary data structures is similar to techniques used for indexes and materialized views selection. Index selection has been studied in the research literature, and most commercial database systems have a physical design adviser tool (see, for example, [146] for a survey). The main characteristics of index selection are:

1. Index selection works with a large, known workload that is representative of normal usage of the database system;
2. Algorithms for index selection are run off-line, and can take hours;

3. Index selection deals with multi-objective functions, for maximizing workload performance and minimizing the total space requirements for selected indexes;
4. The interaction among recommended indexes is implicitly captured in the algorithms employed by index advisers which heuristically enumerate subsets of indexes and compare them based on their estimated benefit. In [146], authors address the issue of measuring interactions among indexes for a given set of recommended indexes, with experiments showing that this particular method can take minutes to run for a medium size set of indexes;

In contrast, computing the benefit of secondary data structures during recovery is characterized by the following:

1. It is applied to a dynamic restart workload that can be very different from the observed normal workload; this workload is run for a very short period of time;
2. It is applied to a well defined schema of secondary data structures, all of which must be rebuilt before the end of the recovery process. However, many of them are not useful to this restart workload.

Our proposed method is based on computing, when the recovery starts (at time 0), an original ranking based on the immediate past workload, and dynamically adjusting this ranking during recovery based on the current workload. This dynamic ranking function can use a benefit function that captures the estimated usefulness of an index compared to other indexes. Below, we discuss the general algorithm for ranking based on a given benefit function. We then introduce two possible benefit functions that can be used for ranking. We compare their properties and discuss how these can be computed on-line during the recovery process.

We denote by $\mathcal{S}_{SCM}$ the set of secondary data structures residing in SCM that do not need to be rebuilt as they are available almost instantly at restart time, and $\mathcal{S}$ the set of all secondary data structures defined in the database schema. During recovery, all secondary data structures in $\mathcal{S} \setminus \mathcal{S}_{SCM}$ must be rebuilt.

We assume that a *query benefit* function is available, $Benefit(s, Q, \mathcal{S})$ which estimates the benefit of a secondary data structure $s \in \mathcal{S}$ with respect to the set $\mathcal{S}$ and the statement Q, such as the ones we will introduce below, namely $Benefit_{indep}$ and $Benefit_{dep}$. Given a workload W, a multi-set of statements (i.e., repeated statements are considered) and $Benefit(s, Q, \mathcal{S})$, we define the *benefit* of a secondary data structure s with respect to $\mathcal{S}$ for W as:

$$Benefit(s, W, \mathcal{S}) = \Sigma_{Q \in W} Benefit(s, Q, \mathcal{S}) \tag{6.1}$$

The rank of a secondary data structure s at restart time $rank(s, 0)$ can be computed based on the observed workload in the immediate past of the crash $WoPast$ and taking into account the estimated rebuild cost (denoted here by $rebuild(s)$):

$$\begin{aligned} rank(s, 0) = {} & Benefit(s, WoPast, \mathcal{S}) \\ & - rebuild(s) \end{aligned} \tag{6.2}$$

During recovery, the benefit of an index changes as the current workload, run in parallel with the recovery procedure, progresses. The content of the workload since the restart and up to current time t, $WoRestart(t)$, can be used to adjust the ranking $rank(s, t)$ of the yet-to-be-built structure $s \in \mathcal{S}$. The ranking function must be effective for all scenarios: the workload after restart is the same as before, very different, or a combination. We propose a weighted average with adjusted weights based on the number of statements observed since the restart. As the recovery manager considers what to recover next, rankings are adjusted and next best ranked index is rebuilt. Because rebuild cost is considered in the $rank()$ formula, the ranks can be negative for data structures for which the rebuild cost exceeds the benefit to the workload. With $n = sizeof(WoRestart(t))$, the following formula computes the ranking at time t:

$$\begin{aligned} rank(s,t) = &\alpha(n) * Benefit(s, WoPast, \mathcal{S}) \\ &+ (1-\alpha(n)) * Benefit(s, WoRestart(t), \mathcal{S}) \\ &- rebuild(s) \end{aligned} \tag{6.3}$$

$\alpha(n)$ can be defined such that it decays exponentially with n (e.g., $\alpha(n) = \alpha^n$ with $0 \leq \alpha \leq 1$) to increase the weight of the current workload as more statements are seen during the recovery period.

6.2.3 Benefit Functions Benefit$_{dep}$ and Benefit$_{indep}$

The above formulas require that a query benefit function, denoted $Benefit(s, Q, \mathcal{S})$, is available. We use in this work two benefit functions, one, $Benefit_{indep}$, based solely on the independent effect of an index s on a statement Q, while the other, $Benefit_{dep}$ captures the effect of the index s with respect to the whole set of defined secondary data structures $\mathcal{S}$.

We assume that the query optimizer can generate an optimal plan, denoted by $plan(Q, I)$ and its estimated cost, denoted by $Cost(Q, I)$, for a statement Q when only a subset of indexes $I \subseteq \mathcal{S}$ are available for the query execution. If a secondary data structure $s \in I$ is used in $plan(Q, I)$, we use the notation $s \in \mathcal{S}(plan(Q, I))$. We assume that there exists a well-behaved optimizer which consistently builds the same optimal plan in the presence of the same indexes: i.e., if $I_1 \subseteq I_2$, and $\mathcal{S}(plan(Q, I_2)) \subseteq I_1 \subseteq I_2$, then $plan(Q, I_2) = plan(Q, I_1)$.

We denote by t_Q, the time during $WoRestart(t)$ when the query Q was run, hence $t_Q \leq t$; and by $S(t)$ the set of indexes available for query execution at time t. Note that $S(0) = S_{SCM}$, as the only secondary data structures available at the start of recovery are the indexes which are instantly recovered (i.e., stored in SCM).

$$\begin{aligned} &\text{for } Q \in WoRestart(t), WoPast: \\ &Benefit_{indep}(s, Q, \mathcal{S}) = Cost(Q, \mathcal{S}_{SCM}) \\ &\qquad\qquad - Cost(Q, \mathcal{S}_{SCM} \cup \{s\}) \end{aligned} \tag{6.4}$$

$Benefit_{indep}$, in Equation 6.4, is defined completely in isolation from and independent of the other indexes in $S \setminus S_{SCM}$. Using this function, $rank(s,t)$ (cf. Equation 6.3), captures what is the benefit of having available just $\mathcal{S}_{SCM} \cup \{s\}$ when the workloads $WoPast$ or $WoRestart(t)$ are run.

$$\begin{aligned} &\text{for } Q \in WoRestart(t): \\ &Benefit_{dep}(s, Q, \mathcal{S}) = Cost(Q, \mathcal{S}(t_Q)) \\ &\qquad\qquad - Cost(Q, \mathcal{S}(t_Q) \cup \{s\}) \end{aligned} \tag{6.5}$$

$$\begin{aligned} &\text{for } Q \in WoPast: \\ &Benefit_{dep}(s, Q, \mathcal{S}) = \\ &\begin{cases} Cost(Q, \mathcal{S}_{SCM}) - Cost(Q, \mathcal{S}), & s \in \mathcal{S}(plan(s, Q)) \\ 0, & \text{otherwise} \end{cases} \end{aligned} \tag{6.6}$$

In contrast, $Benefit_{dep}$ (Equations 6.5 and 6.6) captures the dependency of indexes that are used together in the best plans: for any index s participating in the optimal plan of Q at the time t_Q, i.e.,

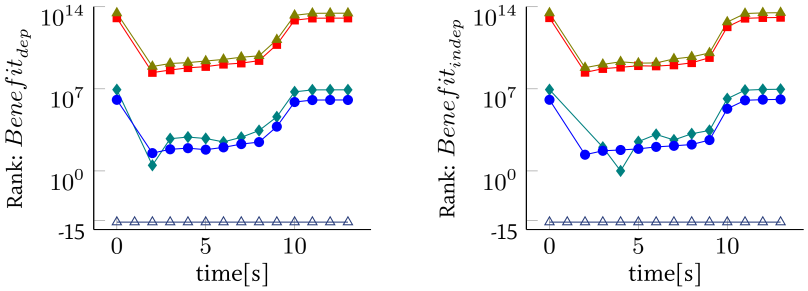

(a) TATP $rank(s, t)$ w/ $Benefit_{dep}$

(b) TATP $rank(s, t)$ w/ $Benefit_{indep}$

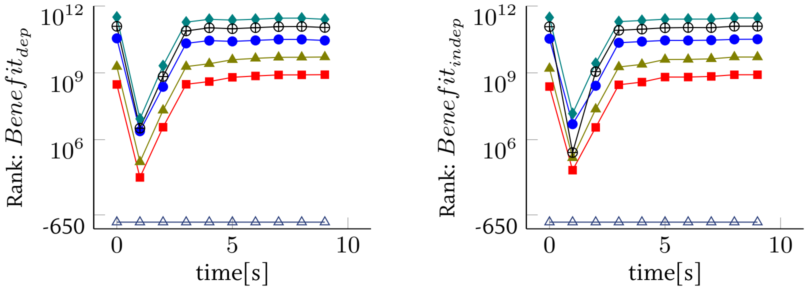

(c) TPC-C $rank(s, t)$ w/ $Benefit_{dep}$

(d) TPC-C $rank(s, t)$ w/ $Benefit_{indep}$

Figure 6.2: $rank(s, t)$ for TATP (20 Mio subscribers) and TPC-C (50 Warehouses) during recovery : $Benefit_{dep}$ vs. $Benefit_{indep}$.

$s \in \mathcal{S}(plan(Q, \mathcal{S}(t_Q) \cup \{s\}))$, the cost difference between the current plan and the plan using s, i.e., $Cost(Q, \mathcal{S}(t_Q)) - Cost(Q, \mathcal{S}(t_Q) \cup \{s\})$, is added to $rank(s, t)$ as per in Equation 6.3.

To show how ranking is progressing during recovery, we picked a set of interesting indexes from the TATP and TPC-C benchmarks used in the evaluation section and plotted the evolution of their $rank(s, t)$ functions during recovery in Figure 6.2, for both $Benefit_{dep}$ and $Benefit_{indep}$. We choose $\alpha(n) = 0.99^n$, which decays exponentially as the number of observed statements n increases. $\mathcal{S}$ has 51 dictionary indexes (one per column) and 5 inverted indexes in TATP, and 94 dictionary indexes and 10 inverted indexes in TPC-C, all of which are stored in DRAM. In these figures, each $rank(s, t)$ function has the same line style for the same index s. Note that indexes that have the same rank using $Benefit_{indep}$ (Figures 6.2b & 6.2d) may not have the same rank using $Benefit_{dep}$ (Figures 6.2a & 6.2c). However, for these particular benchmarks, both query benefit functions result in the same ranking among indexes, which gives the same rebuild order.

If s is not used in any optimal plans, its benefit for the workload is 0 (for both $Benefit_{indep}$ and $Benefit_{dep}$), hence $rank(s, 0)$ is negative because of the $rebuild(s)$ cost, and $rank(s, t)$ (which is equal to $rank(s, 0)$) is also negative until s is rebuilt during recovery. Figure 6.2 shows a set of unused indexes during $WoPast$ and $WoRestart(t)$ and their negative ranking.

As we assume that the decision to use a secondary data structure during query processing is cost-based, the estimated costs $Cost(Q, \mathcal{S}_{SCM})$, $Cost(Q, \mathcal{S}_{SCM} \cup \{s\})$, and $Cost(Q, \mathcal{S})$ needed in $Benefit_{dep}$ and $Benefit_{indep}$ functions are computed by the query optimizer during the query optimization of the statement Q. For example, in Equation 6.5, $Cost(Q, S(t_Q))$ is exactly the estimated cost of the best plan executed when Q was run at time t_Q during recovery, with the available indexes in $S(t_Q)$. The workload statistics capturing $WoPast$ can be collected as statement identifiers, with frequencies, for a fixed window of time. Such statistics are usually recorded anyway by real systems, for example, for security purposes, and performance tuning.

Algorithm 6.1 SOFORT Adaptive Recovery procedure.

```
1: procedure AdaptiveRecoveryProcedure
2:     $R$ = maximum available resources
3:     while $\exists$ secondary data structure yet-to-be built and $\exists$ free resources out of $R$ do
4:         $I = NextToRebuild(R)$
5:         Adjust resources based on $I$
6:         $R'$ = available resources to recover $I$
7:         rebuild a subset of $I$ using $R'$
```

Algorithm 6.2 Get Next Indexes to Rebuild function.

```
function NextToRebuild($R$)                                        ▷ Input: available resources $R$
    $t =$ currrent time
    $n = sizeof(WoRestart(t))$
    for $\forall s$, a secondary data structure not yet rebuilt do
        $rank(s,t) = \alpha(n) * Benefit(s, WoPast, \mathcal{S})$
        $+(1-\alpha(n)) * Benefit(s, WoRestart(t), \mathcal{S}) - rebuild(s)$
    $I =$ top ranked secondary data structures to be built using $R$ resources
    return $I$;                          ▷ Output: a set $I$ of secondary data structure to recover next
```

6.2.4 Recovery Manager

In SOFORT, recovery starts with a *recovery* process of all persistent data structures residing in SCM. This is an almost instantaneous process. As all primary data is persisted in SCM, SOFORT will not be available for new transactions until this initial recover process is finished. According to definitions in SLAs, a system is considered as *available* if users are able to connect. Hence, in SOFORT, availability is almost instantaneous after software failures. For *Instant Recovery* and *Adaptive Recovery*, SOFORT allows new connections right after recovering primary data. These new connections yield, at each time t, the restart workload denoted by $WoRestart(t)$. In parallel, SOFORT performs the recovery of secondary data structures which need to be rebuilt, i.e., the ones residing in DRAM. As resource allocation between the usual restart workload and the recovery process adapts to the current state, resources can be fully allocated to the recovery process. All secondary data structures need to be eventually rebuilt even if they are not useful to the current workload. Under these constraints, the main goal is to maximize throughput during recovery time.

The recovery process, as implemented in SOFORT, for secondary data structures can be achieved in different ways: (1) recover all secondary data structure before allowing any connections (referred here as *Synchronous Recovery*); (2) recover a secondary data structure right before executing a statement that needs it. This decision is cost-based on the rebuild time and the benefit to the statement; (3) in a background recovery process that is invoked by the recovery manager with either fixed or adjustable resources, using or not using a ranking algorithm (referred here as *Adaptive Recovery*). In the most optimized operation mode, the recovery manager consults a ranking component that provides an updated ranking of the yet-to-be built secondary data structures, and adapts the resource allocation between query processing and recovery based on the new ranking.

Figure 6.3 shows the general recovery framework which handles the recovery of secondary data structures. Right after restart, the recovery manager starts recovery procedures for the highly ranked secondary data structure. The recovery process is run in parallel with other statements unless all resources are allocated to the recovery process. The ranking at restart time $rank(s, 0)$ is based on the workload before the crash. the recovery manager can use adaptive or static resource allocation as described in Algorithm 6.1 (line 5). As recovery jobs finish and resources become available to the recovery process again (line 7 in Algorithm 6.1), a current ranking is computed and next secondary data structures candidates are chosen using Algorithm 6.2. Secondary data structures with negative

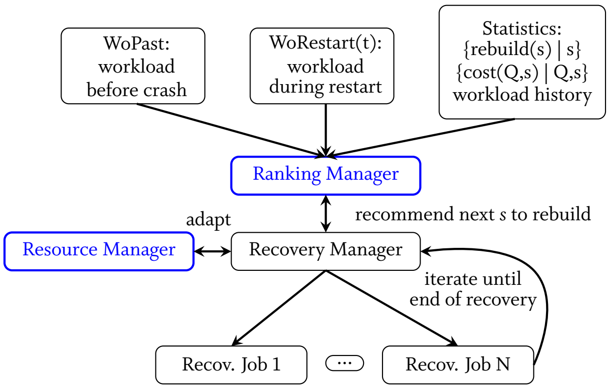

Figure 6.3: Recovery framework of secondary database objects.

benefits will be built last. Note that one way to adapt resource allocation is based on the observed benefit of the most highly ranked secondary data structure: the lower this benefit, the more resources we release to query processing.

6.3 EVALUATION

This section provides an experimental evaluation for recovery performance. First, we evaluate the impact of secondary data placement on recovery performance. Then, we evaluate different aspects of our adaptive recovery approach.

6.3.1 Experimental Details

In our experiments, we use the SCM emulator that is described in Section 2.2.3. We fix the latency of SCM to 200 ns which is more than 2 x higher than the latency of DRAM (90 ns) in the emulation system. Except if mentioned otherwise, we bind all tests to a single socket (with 8 cores) to isolate NUMA effects from the effects of SCM's higher latency. Hyperthreading is disabled.

We use the TATP benchmark [155] and the TPC-C [159] benchmark we previously used in Section 5.5. The TPC-C schema encompasses nine tables and it consists of five transaction templates. The TATP schema comprises four tables and the benchmark consists of seven transaction templates. Unless specified otherwise, we run the following query mixes in the experiments below: (1) the ORDER STATUS (50%) and STOCK LEVEL (50%) queries of TPC-C, and (2) the GET SUBSCRIBER DATA (50%) and GET ACCESS DATA (20%) of TATP. The experiments were run using TPC-C scale factor 128 (i.e, 128 Warehouses) and TATP scale factor 2000 (i.e., 20 Mio Subscribers), which corresponds to an initial primary data size of 18 GB and 19 GB, respectively. Additionally, we designed a synthetic benchmark that encompasses 10 tables with 10 integer columns each; we create an inverted index for each column. All tables have 100 million rows of distinct values, which corresponds to an initial primary data size of 17 GB. We run a mix that consists of 20 queries, each of which executes a simple select with a predicate on a single, distinct column. Only two columns are queried from each table. We run all benchmarks with eight users (clients) in all experiments. Table 6.1 shows the labels used for each experimental configuration, and helps understand the legends of the figures in this section.

We evaluate recovery performance with respect to two metrics: (1) The number of transactions that the database is able to execute during recovery; and (2) The time it takes to achieve the pre-failure throughput which we denote *recovery delta*.

Experiment	Query Processing Resources	Recovery Resources	Ranking
$rk.Qx.Rz$	static x cores	static z cores	yes
$\neg rk.Qx.Rz$	static x cores	static z cores	no
$rk.Q^{ad}.Rz^{ad}$	adaptive	adaptive, start with z cores	yes

Table 6.1: Experimental Configurations of SOFORT Recovery Experiments.

6.3.2 Secondary Data Placement Impact on Recovery Performance

In this experiment, we run the aforementioned benchmarks, then, we crash the database and monitor the throughput variation during the recovery process by sampling it every $500\,\text{ms}$. We use recovery configuration $\neg rk.Q0.R8$, i.e., synchronous recovery, where all CPU resources are allocated to the recovery process until its end, and new transactions are not allowed before the end of recovery. Therefore, the total recovery time is the recovery delta. We consider three data placement scenarios:

- SOFORT-FPTree: all indexes are kept in a hybrid SCM-DRAM format and implemented using the FPTree [126];
- SOFORT-STXTree: all indexes are placed in DRAM and implemented using a transient B^+-Tree, namely the STXTree [154];
- SOFORT-wBTree: all indexes are persisted in SCM and implemented using the wBTree [21], a persistent B^+-Tree fully residing in SCM.

Figure 6.4 depicts the experimental results. We observe that it takes SOFORT-STXTree $10.5\,\text{s}$, $22.6\,\text{s}$, and $32.1\,\text{s}$ to perform recovery for TATP, TPC-C, and the synthetic benchmark, respectively. As shown in Table 6.2, SOFORT-STXTree's recovery time is dominated by the rebuilding of its DRAM-based indexes. In comparison to SOFORT-STXTree, SOFORT-FPTree is able to reduce recovery time by $3.6\times$, $5.9\times$, and $5.0\times$ for TATP, TPC-C, and the synthetic benchmark, respectively. However, this comes at the cost of query performance: In comparison to SOFORT-STXTree, SOFORT-FPTree exhibits a decreased throughput by 16.6%, 32.7%, and 25.6% for TATP, TPC-C, and the synthetic benchmark, respectively, which is explained by two factors. First, due to its higher latency, accessing data in SCM is more expensive than accessing it in DRAM. Second, persisting data in SCM requires expensive flushing instructions. The recovery delta of both SOFORT-STXTree and SOFORT-FPTree is a function of the size of the transient data structures to be rebuilt. In the third scenario, namely SOFORT-wBTree, recovery time takes only a few milliseconds for all benchmarks, thereby demonstrating not only near-instant responsiveness, but also near-instant regain of pre-failure throughput independently of primary and secondary data size. This scenario is optimal when the system must provide guaranteed throughput right after failure. However, SOFORT-wBTree shows a decreased maximum throughput by 35.2%, 47.1%, and 51.1% for TATP, TPC-C, and the synthetic benchmark, respectively, in comparison to SOFORT-STXTree.

Table 6.2 shows the duration of the different recovery steps, namely recovering memory management (PAllocator), primary data, secondary data, and pre-failure garbage. We observe that for all data placement strategies and benchmarks, the recovery of PAllocator and primary data takes only a few milliseconds, while the recovery of secondary data is highly dependent on whether they are persisted in SCM or not. This confirms that the recovery of DRAM-based data is the new recovery bottleneck. Additionally, we observe that pre-failure garbage recovery time does not depend on secondary data placement strategies, but rather on the benchmark which determines the amount of MVCC columns that the garbage recovery process needs to scan. Depending on the benchmark, pre-failure garbage recovery takes between $0.95\,\text{s}$ and $3.4\,\text{s}$, which is much faster than the recovery of secondary data

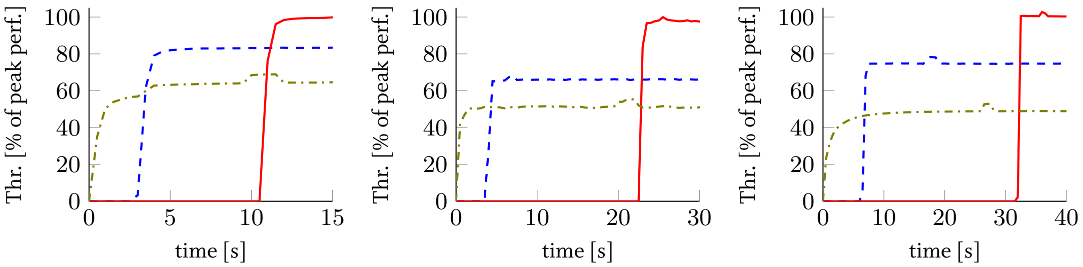

(a) TATP (b) TPC-C (c) Synthetic

Legend Entry	TATP		TPC-C		Synthetic	
	Rec. End	Max Throu.	Rec. End	Max Throu.	Rec. End	Max Throu.
—— SOFORT-STXTree	10.5 s	100%	22.6 s	100%	32.1 s	100%
- - - SOFORT-FPTree	2.9 s	83.4%	3.8 s	67.3%	6.4 s	74.4%
-·-·- SOFORT-wBTree	6.4 ms	64.8%	13.3 ms	52.9%	7.3 ms	48.9%

Figure 6.4: Impact of secondary data placement on recovery performance. Maximum throughput is relative to the performance of SOFORT-STXTree.

SOFORT Configuration		Recovery Duration			
		PAllocator	Primary Data	Secondary Data	Garbage
SOFORT-FPTree	TATP	1.2 ms	3.3 ms	2.9 s	3.4 s
	TPC-C	6.8 ms	5.1 ms	3.8 s	1.1 s
	Synthetic	2.7 ms	4.0 ms	6.4 s	1.8 s
SOFORT-STXTree	TATP	0.6 ms	4.1 ms	10.5 s	3.4 s
	TPC-C	0.7 ms	4.0 ms	22.6 s	1.2 s
	Synthetic	1.2 ms	4.5 ms	32.1 s	1.8 s
SOFORT-wBTree	TATP	1.2 ms	4.4 ms	0.8 ms	3.3 s
	TPC-C	7.0 ms	4.6 ms	1.7 ms	0.95 s
	Synthetic	2.5 ms	4.6 ms	0.4 ms	1.2 s

Table 6.2: Breakdown of recovery time. Recovery duration of memory management (PAllocator), primary data, secondary data, and garbage recovery times.

in SOFORT-STXTree. Note that garbage recovery is performed asynchronously, independent of secondary data recovery.

The distribution of the data structures over SCM and DRAM used in these scenarios are just one of many possible distributions. The more secondary data structures we put on DRAM, the higher the performance during usual query processing and the lower the performance of recovery. In contrast, the more secondary data structures in SCM, the lower the performance during usual query processing and the better the recovery performance. In conclusion, depending on the scenario and the database requirements, we can trade-off between query performance and recovery performance.

6.3.3 Recovery Strategies

In this experiment, we observe the recovery behavior of different recovery strategies, where the restart workload *WoRestart* is the same as the workload observed before the crash. The results are depicted in Figure 6.5.

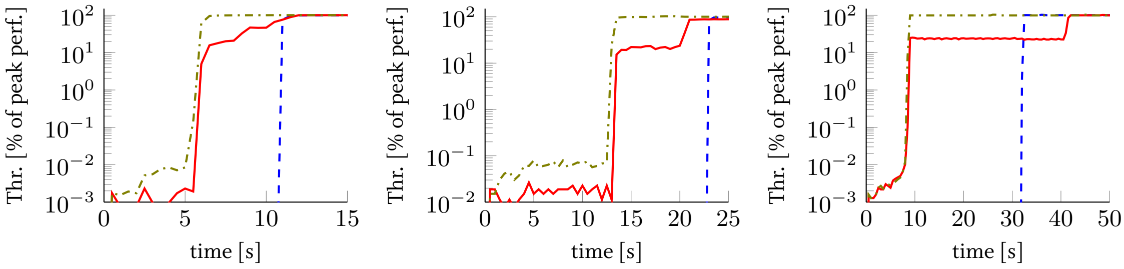

(a) TATP (b) TPC-C (c) Synthetic

Legend Entry	TATP		TPC-C		Synthetic	
	Rec. End	#TXs t=15 s	Rec. End	#TXs t=25 s	Rec. End	#TXs t=50 s
- - - $\neg rk.Q0.R8$	10.5 s	4.51 M	22.6 s	125.5 K	32.1 s	47.9 M
—— $\neg rk.Q2.R6$	11.4 s	6.1 M	26.7 s	300 K	41.2 s	30.7 M
-·-·- $rk.Q^{ad}.R6^{ad}$	50.9 s	27.9 M	115.4 s	419 K	201.7 s	84.5 M

Figure 6.5: Different recovery strategies with logarithmic scale.

- $\neg rk.Q0.R8$: the recovery process is run synchronously. We use this strategy as a baseline.
- $\neg rk.Q2.R6$: the recovery process is run in parallel with the recovery workload *WoRestart*, and the secondary data structures are not ranked, i.e., they are recovered by prioritizing referenced indexes. We observe a noticeable increase in performance before the end of recovery. This approach outperforms $\neg rk.Q0.R8$ for TATP and TPC-C, both in terms of recovery delta and the number of transactions executed during recovery. Nevertheless, $\neg rk.Q2.R6$ performs worse than $\neg rk.Q0.R8$ for the synthetic benchmark. Indeed, the recovery delta of $\neg rk.Q2.R6$ is 41.2 s, while that of $\neg rk.Q0.R8$ is 32.1 s. Furthermore, 50 s after the start of recovery, $\neg rk.Q0.R8$ executed 17.2 million more transactions than $\neg rk.Q2.R6$. This result emphasizes the importance of ordering the rebuild of secondary data structures according to their importance for the workload. A careless ranking strategy can backfire and prove to be harmful to recovery performance.
- $rk.Q^{ad}.R6^{ad}$: the recovery process is run in parallel with the recovery workload *WoRestart*, and the secondary data structures are rebuilt based on our ranking function. Adaptive resource allocation is enabled. This strategy outperforms both previous strategies as throughput gradually increases to reach peak performance. The performance of query processing surges earlier than in $\neg rk.Q2.R6$ in all three benchmarks. Although the end of recovery occurs much later than in the previous two configurations, the recovery delta is decreased by 1.9×, 1.7×, and 3.8× for TATP, TPC-C, and the synthetic benchmark, respectively, compared to $\neg rk.Q0.R8$. Moreover, $rk.Q^{ad}.R6^{ad}$ executed up to 23.4 million, 293.5 thousand, and 53.8 million more transactions during recovery than $\neg rk.Q0.R8$ and $\neg rk.Q2.R6$ for TATP, TPC-C, and the synthetic benchmark, respectively.

Although query throughput is less than 1% of peak performance at the beginning of recovery in $\neg rk.Q2.R6$ and $rk.Q^{ad}.R6^{ad}$, this still represents thousands of transactions per second, which allows to run high priority queries.

Another important dimension is resource sharing between recovery and query processing. We experiment with several static resource allocation configurations and report the results in Figure 6.6. We notice that the more resources we allocate to the recovery process the better the performance (cf. legend table): The best configuration, $rk.Q0.R8$, has a lower recovery delta and executes more transactions during recovery than the other configurations. This result emphasizes the importance of resource allocation. We also observe that the curves are shaped like stairs, where a peak corresponds

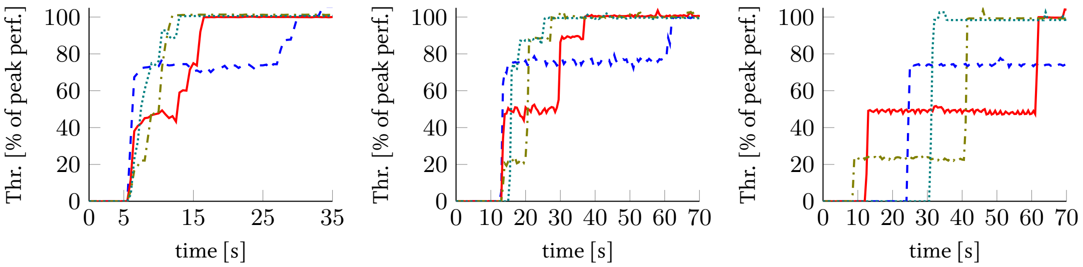

(a) TATP (b) TPC-C (c) Synthetic

Legend Entry	TATP		TPC-C		Synthetic	
	Rec. End	#TXs t=35 s	Rec. End	#TXs t=70 s	Rec. End	#TXs t=70 s
- - - $rk.Q6.R2$	29.3 s	24.2 M	62.2 s	2.4 M	121.1 s	89.9 M
—— $rk.Q4.R4$	15.9 s	25.4 M	36.6 s	2.5 M	61.3 s	86.5 M
-·-·- $rk.Q2.R6$	11.4 s	27.4 M	27.1 s	2.6 M	41.0 s	96.7 M
········ $rk.Q0.R8$	10.6 s	28.3 M	25.0 s	2.8 M	31.2 s	102.2 M

Figure 6.6: Static resource allocation impact on recovery.

to the end of the recovery of an important secondary data structures group. The reason why the increase in throughput is in stair-steps and not linear is the design of the benchmark: all users run the same mix of queries, which means that even if only one single query did not regain its optimal performance, it will drain the query throughput down across all users. Hence, substantial improvements in throughput occur only once the performance of all queries improves. This setup is not in favor of our approach, as earlier benefits of our approach could be observed in a different setup where users run different queries from each other, or run the same queries on different copies of the data.

We also notice that the more resources allocated to recovery, the sooner the first stair-step appears and the lower it is. This is due to the fact that more resources for recovery means faster rebuild of secondary data structures (hence faster appearance of stair-steps) and slower query processing due to the lack of resources (hence, the lower the stair-steps). The last peak that brings each configuration back to peak performance takes place at the end of the recovery process, which again happens sooner with more recovery resources, but configurations with less recovery resources compensate with higher stair-steps. An intuition that stems from this result is that a combination of all configurations, such that recovery starts with more resources and releases them gradually whenever query performance surges might lead to a better recovery performance.

6.3.4 Adaptive Resource Allocation Algorithm

In this experiment, we investigate the efficiency of our adaptive resource allocation algorithm. The recovery manager is given specific resources and is free to use them fully and/or return them partially/fully to query processing. Basically, the recovery manager decides to give back recovery resources to query processing once it detects, based on the benefit value of the most highly ranked index, that enough secondary data structures have been rebuilt to allow the system to run at nearly full speed. The remaining secondary data structures are recovered in the background whenever the CPU idles.

Figure 6.7 summarizes the results of this experiment. Theoretically, allocating more resources to recovery should enable the database to reach peak performance sooner. Notably, we observe that for TATP and TPC-C, all investigated recovery configurations perform nearly equally. This is explained

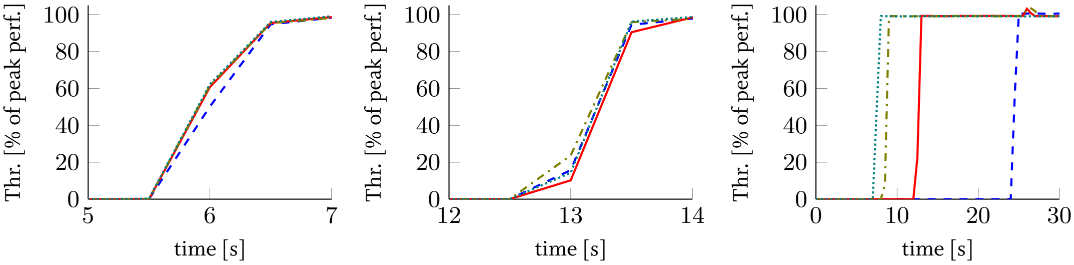

(a) TATP (b) TPC-C (c) Synthetic

Legend Entry	TATP		TPC-C		Synthetic	
	Rec. End	#TXs t=7 s	Rec. End	#TXs t=14 s	Rec. End	#TXs t=30 s
- - - $rk.Q^{ad}.R2^{ad}$	50.9 s	1.25 M	115.4 s	55.5 K	200.4 s	7.7 M
—— $rk.Q^{ad}.R4^{ad}$	50.9 s	1.30 M	115.5 s	53 K	201.7 s	28.2 M
-·-·- $rk.Q^{ad}.R6^{ad}$	50.9 s	1.30 M	115.4 s	58 K	205.6 s	56.4 M
········ $rk.Q^{ad}.R8^{ad}$	50.9 s	1.35 M	115.5 s	57.5 K	217.5 s	59.7 M

Figure 6.7: Adaptive resource allocation impact on recovery.

by two factors. First, the set of important indexes is small in our benchmarks, which means that only a few recovery resources are needed. Second, in both TATP and TPC-C, there is one large index in the set of useful indexes that dominates the recovery delta. This is because each secondary data structure is recovered single-threaded. We can remedy this issue by implementing a mix of inter and intra parallel index rebuilding. We do not observe this phenomenon in the synthetic benchmark, because all indexes are of the same size. In this case, we notice that the more resources we allocate to recovery, the faster we reach peak performance.

Accepting queries during recovery allows to gain more knowledge of the current workload, hence swiftly narrowing down the set of important indexes to recover. The recovery manager can then invest all available resources in rebuilding as quickly as possible these indexes, and then give back all the resources to query processing and continue rebuilding the remaining secondary data structures in the background. As a consequence, the system reaches peak performance before the end of the recovery process. An interesting observation is that the stair-steps in the figure are not as explicit as in static resource allocation. Actually, the gradual increase in throughput results from the fact that some resources finish their job and are released earlier than others.

Figure 6.8 shows a comparison between the best configuration for static resource allocation and the best configuration for adaptive resource allocation. We observe that, despite a much larger total recovery time compared to $rk.Q0.R8$, $rk.Q^{ad}.R8^{ad}$ decreases recovery delta by $1.9\times$, $1.9\times$, and $4.3\times$ for TATP, TPC-C, and the synthetic benchmark, respectively. Moreover, $rk.Q^{ad}.R8^{ad}$ executes 2.3 million, 222 thousand, and 62.3 million more transactions during recovery than $rk.Q0.R8$. Additionally, for static resource allocation, peak performance is regained only at the end of the recovery process while for adaptive resource allocation, peak performance is regained before the end of the recovery process. Therefore, recovery delta is decoupled from the total recovery time. From this point on, unless specified otherwise, we experiment with adaptive resource allocation enabled. The adaptive approach brings a noticeable enhancement in recovery performance over the static one, but has the drawback of prohibiting query processing at the beginning of recovery in configuration $rk.Q^{ad}.R8^{ad}$. For scenarios where allowing query processing right from the beginning of recovery is crucial, configurations $rk.Q^{ad}.R6^{ad}$ and $rk.Q^{ad}.R4^{ad}$ might be more interesting. Moreover, allowing query processing as early as possible has the advantage of enriching knowledge about $WoRestart$, hence allowing to adapt to workload changes.

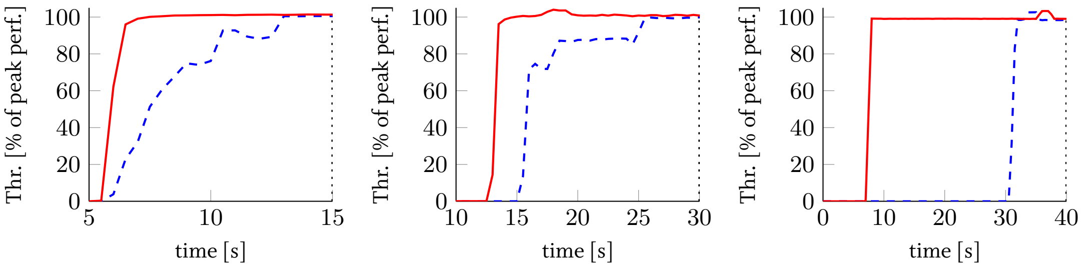

(a) TATP (b) TPC-C (c) Synthetic

Legend Entry	TATP		TPC-C		Synthetic	
	Rec. End	#TXs t=15 s	Rec. End	#TXs t=30 s	Rec. End	#TXs t=40 s
- - - $rk.Q0.R8$	10.6 s	7.4 M	25.0 s	691 K	31.2 s	23.9 M
—— $rk.Q^{ad}.R8^{ad}$	50.9 s	9.7 M	115.5 s	913 K	217.5 s	86.2 M

Figure 6.8: Best of static vs. best of adaptive resource allocation.

6.3.5 Resilience to Workload Change

This experiment is dedicated to studying the effect of changing workloads during recovery. To do so, we execute different workloads before and after the crash: before failure, the full original TATP and TPC-C mixes are run; as for the synthetic benchmark, we expand the mix described in Section 6.3.1 to comprise four queryable columns per table (instead of two). After failure however, only the TATP, TPC-C, and synthetic queries described in Section 6.3.1 are run. This approach has the benefit that the workload before failure uses a superset of the indexes used by the workload after failure. Basically, a subset of the indexes is used more often while others are not used anymore after failure, which makes it a good example to study the importance of considering *WoPast* and *WoRestart*. We run configuration $rk.Q^{ad}.R6^{ad}$ to allow adaptive recovery to gain knowledge of *WoRestart*.

Figure 6.9 illustrates the results of this experiment. We observe that the adapting approach achieves a $1.02\times$, $1.03\times$, and $2.1\times$ lower recovery delta than the non-adapting one for TATP, TPC-C, and the synthetic benchmark, respectively. While the improvement might seem marginal for TATP and TPC-C, there is a large difference in the number of executed transactions during recovery: The adapting approach executes 3.1 million, 117.2 thousand, and 47.9 million more transactions than the non-adapting one for TATP, TPC-C, and the synthetic benchmark, respectively. These results clearly show the benefit of adapting to changing workloads during recovery. Also, not taking into account *WoRestart* in the ranking function could lead to a scenario similar to the one discussed in Section 6.3.3, where $\neg rk.Q2.R6$ is outperformed by synchronous recovery. Other scenarios, such as using completely different secondary data structures before and after failure, would highlight much more the importance of considering *WoRestart* in the benefit function.

6.3.6 Impact of SCM Latency

In this experiment we run the TATP, TPC-C, and synthetic mixes described in Section 6.3.1 with configuration $rk.Q0.R8$, and vary the latency of SCM between 200 ns and 700 ns. We report the results in Figure 6.10. We notice that while the peak performance of the system suffers from higher SCM latencies, recovery does not. This is because primary data is accessed sequentially in SCM to rebuild secondary data in DRAM. The system reaches its peak performance approximately at the same time

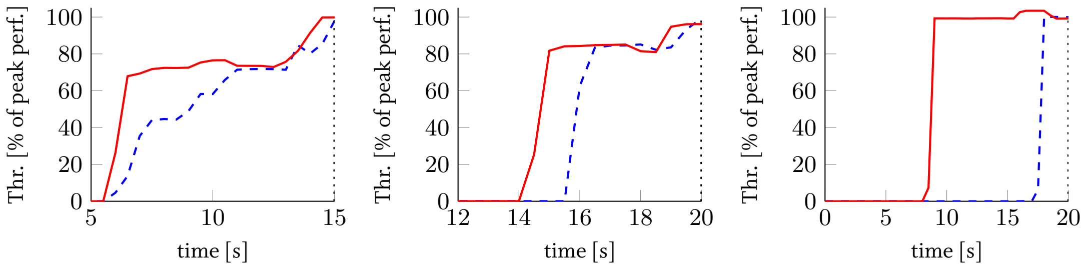

(a) TATP (b) TPC-C (c) Synthetic

Legend Entry	TATP		TPC-C		Synthetic	
	Rec. End	#TXs t=15 s	Rec. End	#TXs t=20 s	Rec. End	#TXs t=20 s
- - - no adapt to *WoRes.*	23.1 s	11.7 M	97.8 s	402.6 K	162.8 s	13.4 M
—— adapt to *WoRes.*	32.9 s	14.8 M	95.4 s	519.8 K	202.4 s	61.3 M

Figure 6.9: Impact of workload change during recovery.

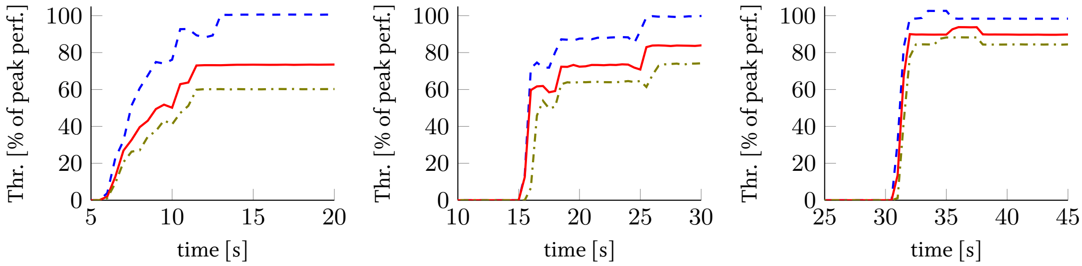

(a) TATP (b) TPC-C (c) Synthetic

Legend Entry	TATP Rec. End	TPC-C Rec. End	Synthetic Rec. End
- - - 200 ns	10.6 s	25.0 s	31.3 s
—— 450 ns	10.8 s	24.9 s	31.4 s
-·-·- 700 ns	10.9 s	25.7 s	31.7 s

Figure 6.10: SCM latency impact on recovery performance. Throughput is depicted relative to a baseline SCM latency of 200 ns.

for all latency configurations. In brief, the benefits of our approach are almost independent from the latency of the SCM. Note that the performance degradation is partially attributed to the materialization phase, where at least one random SCM access per column is executed, thereby exposing the higher latency of SCM.

6.3.7 Limits of Adaptive Recovery

To conduct a worst case analysis, we use our synthetic benchmark with a mix consisting of 100 queries, each of which executes a simple select with a predicate on a single, distinct column. Overall, all columns are uniformly queried. We run recovery configurations $rk.Q^{ad}.R8^{ad}$ and $\neg rk.Q0.R8$. We report the experimental results in Figure 6.11. Theoretically $rk.Q^{ad}.R8^{ad}$ and $\neg rk.Q0.R8$ should perform nearly equally. This is because all indexes have similar benefits and are equally important to the workload. Hence, all orders of recovery should yield similar recovery performance. As expected, the difference in performance is marginal: The recovery time and the number of executed

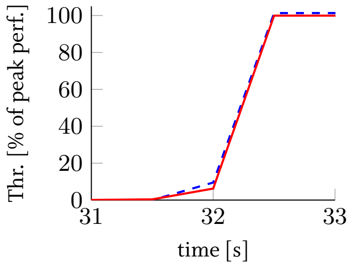

Legend Entry	Rec. End	#TXs t=33 s
- - - $\neg rk.Q0.R8$	32.0 s	7.64 M
—— $rk.Q^{ad}.R8^{ad}$	32.1 s	7.48 M

Figure 6.11: Worst case analysis: Adaptive recovery Vs. Synchronous recovery.

transactions by the end of recovery is nearly the same for both configurations. However, in a setting such as TATP or TPC-C, where certain large data structures can dominate recovery time, adaptive resource allocation will release resources as soon as the recovery job queue is empty, while in synchronous recovery no resources are released until all recovery jobs are finished. Therefore, in such a scenario, adaptive recovery would slightly outperform synchronous recovery. We conclude that the performance of synchronous recovery is a lower bound to that of adaptive recovery.

6.4 RELATED WORK

We divide related work into two categories: efforts to leverage SCM to improve databases recovery performance, and traditional main-memory database recovery related works. We refer the reader to Chapter 2 for a detailed discussed of the impact of SCM on database systems, including the recovery aspect. Since our design avoids traditional logging, most existing recovery techniques do not apply to our work. Nevertheless, for the sake of completeness, we briefly review state of the art database recovery techniques.

Garcia-Molina et al. [47] provide a detailed discussion of traditional recovery techniques, such as techniques presented by Jagadish et al. [69, 70], Eich et al. [40], and Levy et al. [96] for main-memory databases. All of them rely on logging and snapshotting, which are not needed in our recovery algorithm. In this family of traditional recovery techniques, ARIES [109] is without doubt the most well-known recovery technique.

The Shore-MT team focused on improving logging efficiency by eliminating log-related contention [74, 130, 131]. Additionally, Cao et al. [17] propose a main-memory checkpoint recovery algorithm for frequently consistent applications. Furthermore, Lomet et al. [99] and Malviya et al. [100] investigate logical logging-based recovery techniques. Moreover, Goetz et al. [53] present a technique called *Instant Recovery with Write-Ahead Logging*, that is based on on-demand single-page recovery. However, this technique does not apply to our architecture, as we do not use paging.

More recently, Yao et al. [182] studied the recovery cost of distributed main-memory database systems, investigating in particular the differential in recovery cost between transaction-level and tuple-level logging. Additionally, Wu et al. [176] proposed Pacman, a fast and parallel recovery mechanism for main-memory databases. Pacman assumes database transactions to be executed exclusively through stored procedures, which it analyzes at compile time to identify independent parts that can be executed in parallel during recovery.

6.5 SUMMARY

The advent of SCM has enabled single-level database architectures to emerge. These store, access, and modify data directly in SCM, alleviating the traditional recovery bottleneck of main-memory databases, i.e., reloading data from storage to memory. Thus, the new recovery bottleneck for such systems is rebuilding DRAM-based data. In this chapter we addressed this bottleneck following two orthogonal dimensions: The first one pertains to secondary data placement in SCM, in DRAM, or in a hybrid SCM-DRAM format. We showed that near-instant recovery is achievable if all secondary data is persisted in SCM. However, this comes at the cost of a decreased query performance by up to 51.1%. Nevertheless, near-instant recovery offers guarantees that are appealing to business applications where availability is critical. Hybrid SCM-DRAM data structures offer a good compromise by reducing recovery time by up to $5.9\times$ while limiting the impact on query performance between 16.6% and 32.7%. The second dimension is optimizing the recovery of DRAM-based data independent of data placement. To address this problem, we presented a novel recovery technique, named adaptive recovery, that relies on: (1) a characterization of secondary data structures, (2) a ranking function for secondary data structures that takes into account the workload before and after crash, and (3) an adaptive resource allocation algorithm. We presented two benefit functions for secondary data structures: the first one considers indexes independently while the second one takes into account indexes interdependence. Our recovery algorithm aims at maximizing performance of the workload run in parallel with recovery. We have implemented adaptive recovery in SOFORT, our SCM-enabled database prototype. Through our experimental evaluation, we showed that SOFORT regains its maximum performance up to $4.3\times$ faster with adaptive recovery than with synchronous recovery, while allowing the system to be responsive near-instantly. Additionally, the adaptive resource allocation algorithm brings a significant performance improvement over static resource allocation. We have demonstrated that our ranking functions adapt well to workload changes during recovery and regains pre-failure throughput up to $2.1\times$ faster than rankings that do not take into consideration the recovery workload.

7

TESTING OF SCM-BASED SOFTWARE

The advent of SCM is disrupting the database landscape and driving novel database architectures that store data, access it, and modify it directly from SCM at a cache-line granularity. However, the *no free lunch* folklore conjecture holds more than ever as SCM brings unprecedented challenges that we detailed in Chapter 3. Consistency failure scenarios and recovery strategies of software that persists data depend on the underlying storage technology. In the traditional case of block-based devices, illustrated in the left side of Figure 7.1, software has full control over when data is made persistent. Basically, software schedules I/O to persist modified data at a page granularity. The application has no direct access to the primary copy of the data and can only access copies of the data that are buffered in main memory. Hence, software errors can corrupt data only in main memory which can be reverted as long as the corruption was not explicitly propagated to storage. In fact, crash-safety for block-based software highly depends on the correctness of the underlying file system. In contrast, SCM is byte-addressable and is accessed via a long volatility chain that includes store buffers and CPU caches, over all of which software has little control. As a side effect, changes can be speculatively propagated from the CPU cache to SCM at any time, and compilers and out-of-order CPU execution can jeopardize consistency by reordering memory operations. Moreover, changes are made persistent at a cache line granularity which necessitates the use of CPU persistence primitives. This adds another level of complexity as enforcing the order in which changes are made persistent cannot be delayed like with block-based devices, and must be synchronous. Hence, storing the primary copy of the data in SCM and directly updating it in-place significantly aggravates the risk of data corruption. In addition to data consistency, memory leaks in SCM have a deeper impact than in DRAM. This is because SCM allocations are persistent, hence, a memory leak would also be persistent.

Several proposals tackled these challenges following two main approaches. The first one focuses on providing global software-based solutions, mainly transactional-memory-like libraries, to make it easier for developers to write SCM-based software. The second and more mainstream approach is to rely solely on existing hardware persistence primitives, such as cache line flushing instructions and memory barriers to achieve consistency. Nevertheless, all approaches have in common that SCM-related errors may result in data corruption. In contrast to volatile RAM where data corruption can be cured with a restart of the program, data corruption in SCM might be irreversible as it is persistent. Therefore, we argue for the need of testing the correctness of SCM-based software against software crashes and power failures–which result in the loss of the content of the CPU cache. We remark that testing is orthogonal to devising recovery strategies that solve the challenges introduced by SCM.

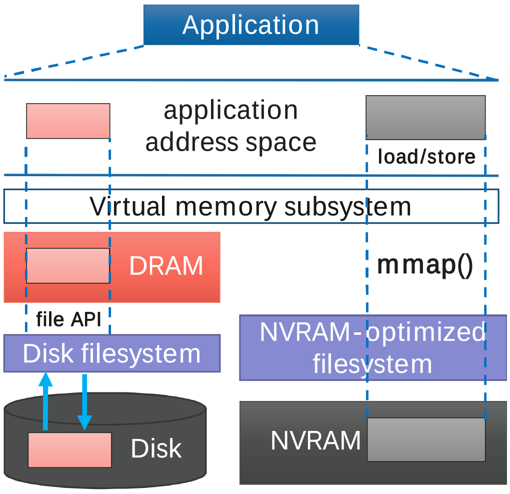

Figure 7.1: Contrast between the traditional disk-based storage architecture (on the left side) and the single-level SCM-based direct access architecture (on the right side).

In this chapter we propose a lightweight automated on-line testing framework that helps detect and debug a wide range of SCM-related bugs that can arise upon software or power failures[1]. We particularly focus on detecting missing cache line flushing instructions. Our testing framework is based on a *suspend-test-resume* approach and employs shadow memory to simulate different crash scenarios including the loss of the content of the CPU cache. An important feature of our testing framework is its ability to avoid excessive duplicate testing by tracking the call stack information of already tested code paths, which leads to achieving fast code coverage. Additionally, our testing framework is able to partially detect errors that might arise due to the compiler or the CPU speculatively reordering memory operations. An additional capability of our testing framework is simulating crashes in the recovery procedure of the tested program, which we argue is important since hidden SCM-related errors in the recovery procedure may compromise the integrity of the data upon every restart.

We show with an experimental evaluation on the FPTree and PAllocator that our testing framework achieves fast testing convergence, even in the case of nested crash simulations, and is fast enough to be used on fairly large software systems. In particular, we demonstrate that taking into account the call stack can improve the testing time by several orders of magnitude.

The rest of this chapter is organized as follows: Section 7.1 discusses related work and elaborates on our memory model assumptions. Then, Section 7.2 presents our testing framework and its different optimizations. Thereafter, we evaluate our testing framework in Section 7.3. Finally, Section 7.4 summarizes this chapter and outlines future directions.

7.1 BACKGROUND

In this section we first present relevant related work. Then, we elaborate on our memory model assumptions for this work.

---

[1] Parts of the material in this chapter are based on [123]

7.1.1 Related Work

Crash-safety for disk-based software has been extensively researched and several tools that combine experimental testing and model checking have been proposed [135, 181]. Although they share the same goals, crash-safety testing for disk-based and SCM-based software are different in that they have to address radically different failure modes.

Consistency and recovery testing of SCM-based software did not get much attention so far. Lantz et al. proposed Yat [83], a hypervisor-based off-line testing framework for SCM-based software. Yat is based on a record-and-replay approach. First, it records all SCM write operations by logging hypervisor exits that are caused by writes to SCM. Persistence primitive instructions need to be replaced in tested software by illegal instructions to make them traceable by causing a VMM exit. Yat then divides the memory trace into *segments*, each of which is delimited by two persistence barriers. It considers that SCM write operations can be arbitrarily reordered within a segment, with the exception of writes to the same cache line which are considered to be of fixed order. Yat replays the trace until a non-tested segment and runs the recovery procedure of the tested software for every possible reordering combination inside that segment. Since the number of combinations can grow exponentially, the authors propose to limit the number of combinations per segment to a certain threshold.

Given a program that covers the whole code base of the tested software, and given a sanity check program that detects any present data corruption – both of which are challenging to produce – Yat can achieve comprehensive testing for single-threaded SCM-based software. In practice however, that may still require prohibitive testing time. In the case of a multi-threaded program, Yat records the sequence of operations executed by the various threads, which can differ between two runs due to the non-determinism of multi-threading. Hence, comprehensive testing of a recorded sequence does not imply comprehensive testing of the software.

In contrast to Yat, our testing framework performs on-line testing and is non-invasive as it does not require software changes in most cases. While it covers only partially memory-reordering-related errors, our testing framework achieves fast code coverage by limiting duplicate testing, and is able to automate crash testing inside the recovery procedure of a program, both of which Yat does not provide. We explain in Section 7.2.7 how our testing framework can be combined with Yat to make up for the limitations of both tools.

Moreover, we mention an experimental persistent memory extension to Valgrind [163]. It provides several functionalities, such as indicating when:

- Writes are not guaranteed to be durable (e.g., missing flushing instruction);
- Multiple writes are made to the same location without flushing the first one, which hints to possible consistency issues;
- Flushes made to non-dirty cache lines, which hints to possible optimizations.

However, the program must be modified to notify Valgrind about persistent memory operations such as flushing instructions, memory fences, and persistent memory mappings, so that Valgrind can track and shadow persistent memory.

We conjecture that providing comprehensive consistency and recovery testing for large SCM-based software is – as of now – impractical. Instead, our focus is on improving the *quality* of such software by covering a wide range of SCM-related errors in a reasonable amount of time. We argue that similarly to concurrent software, providing theoretical correctness guarantees should be a prerequisite for any SCM-based software, and that experimental testing should not (and cannot) make up for the lack of such theoretical guarantees.

It is also woth mentioning that techniques to prevent data corruption in SCM-based software start to emerge, such as the work of Moraru et al. [110] who proposed to use virtual memory protection keys to prevent dangling pointers from corrupting data in SCM. This is, however, orthogonal to the challenges we tackle in this chapter.

7.1.2 Memory Model

In this work we assume, without loss of generality, an Intel x86 architecture that provides the following persistence primitives [64]:

- CLFLUSH evicts a cache line from the CPU cache and writes it back to memory. CLFLUSH executes synchronously.
- SFENCE guarantees that all preceding stores have been executed.
- CLFLUSHOPT evicts a cache line and writes asynchronously its content to memory. It is ordered with SFENCE but not with writes.
- CLWB asynchronously writes back a cache line without invalidating it. It is ordered with SFENCE but not with writes.

CLFLUSHOPT and CLWB need to be wrapped by two SFENCE to be fully ordered and serialized; the first SFENCE ensures that the latest version of the data is flushed, while the second one ensures that the flushing instruction finishes executing. In the following we refer to a serialized flushing operation by the *persist* function.

The Intel x86 architecture implements a total store order, with two exceptions: 1) non-temporal stores are not ordered between themselves or with other writes [66]. Hence, they can be arbitrarily reordered; and 2) the read-before-right effect. Consequently, normal store instructions cannot be reordered and reach the store buffer of the CPU in the same order in which they were executed. As we will show, the flexibility of our testing framework makes it easy to take into account other, more relaxed memory ordering models, such as the ones implemented by ARM and IBM POWER [102].

7.2 TESTING OF SCM-BASED SOFTWARE

We propose a lightweight on-line testing framework that is able to simulate software crashes and power failures that cover a wide range of consistency and recovery bugs. As an implementation example, we integrate the framework with PAllocator, our own persistent SCM allocator. The persistent allocator creates large files, referred to as *segments*, and then logically divides them into smaller blocks for allocation.

7.2.1 Crash Simulation

In this section we explain how our testing framework is able to simulate software and power failures. The main challenge in simulating a power failure is to simulate the loss of the content of the CPU caches. To achieve this, we devise the following strategy that is based on a *suspend-test-resume* approach:

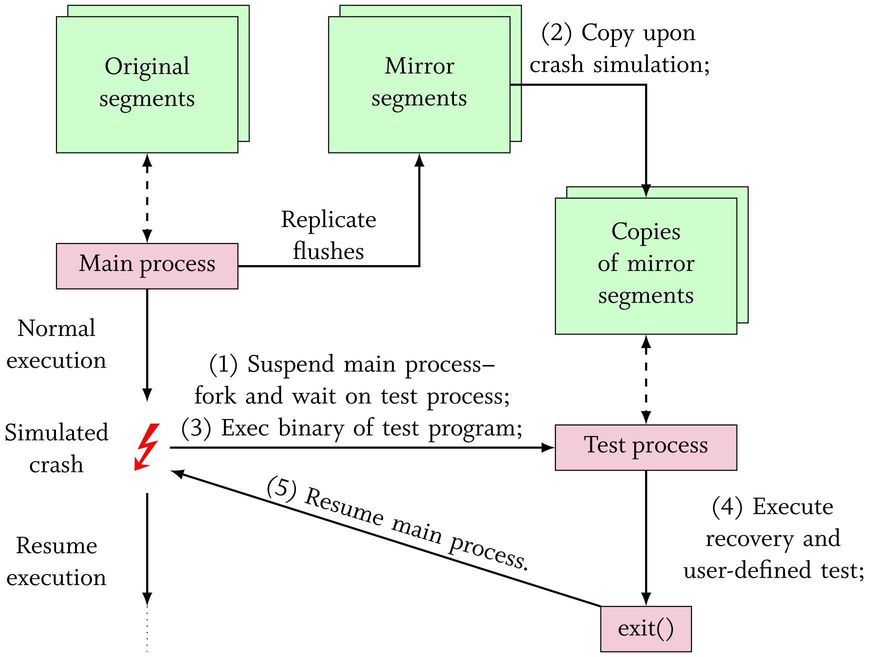
Original segments
Mirror segments
(2) Copy upon crash simulation;
Copies of mirror segments
Main process
Replicate flushes
Normal execution
(1) Suspend main process–fork and wait on test process;
(3) Exec binary of test program;
Simulated crash
Test process
(5) Resume main process.
(4) Execute recovery and user-defined test;
Resume execution
exit()

Figure 7.2: Illustration of crash simulation in the testing framework.

- For every segment created by the persistent allocator, a corresponding *mirror segment* is created, similar to shadow memory techniques [113].
- When a cache line is explicitly flushed, its content is copied from the original segment to the same offset in its corresponding mirror segment. Therefore, only explicitly flushed data is present in the mirror segments.
- *Malfunctions* that simulate a crash are randomly triggered when calling persistent primitive functions. These simulated crashes proceed as follows, as illustrated in Figure 7.2: (1) Suspend (pause) the main process by forking a test process and waiting on it; (2) the test process creates a copy of each mirror segment; and (3) the test process executes the binary of the test program which recovers using the created copies of the mirror segments. The test process starts then the recovery procedure the same way as would have done the main process if it crashed where it was suspended. After recovery, the test process executes a user-defined consistency check procedure (step (4) in Figure 7.2).
- Once the test process exits, the copies of the mirror segments are deleted and the main program resumes execution (step (5) in Figure 7.2) until the next crash simulation.

This strategy is fully *automated* and the state of the main process is never changed during the crash simulation phase. More specifically, the state of the original segments and the mirror segments is never changed during the crash simulation phase. Capturing explicit flushes and replicating them in the mirror segments allows to simulate the loss of the CPU cache. In fact, this corresponds to the case where no cache lines are evicted from the CPU cache without being explicitly flushed. In a real scenario, some of the content of the CPU cache might have been speculatively written back. Nevertheless, we argue that by capturing only explicitly flushed data, we can more reliably detect missing flushes in the tested code.

Crash simulations are triggered inside the *Flush* function, as shows in Algorithm 7.1, because it is the only function that modifies the state of the mirror segments. In the case of a detected error or a crash in the recovery procedure or in the user-defined checking procedure, the test process is suspended and a debugger can be attached to both the main process and the test process. This greatly helps in finding the reason of the crash, since both the simulated crash scenario in the main process and

Algorithm 7.1 Crash simulation inside the Flush procedure.

```
procedure FLUSH(PPtr PAddr, Char Content[CacheLineSize])
    crashProb ← rand(0, 1)                              ▷ Get a random crash probability
    if crashProb < 0.5 then                             ▷ Crash with a probability of 0.5
        SimulateCrash()
    copyToMirror(PAddr, Content)
    crashProb ← rand(0, 1)
    if crashProb < 0.5 then
        SimulateCrash()
```

the recovery crash in the test process can be fully traced and the content of their corresponding data structures examined. To help reproduce errors, it is also possible to allow crash simulations only in a specific code region.

To illustrate different classes of errors that our testing framework can detect, we consider in the following the case of a simplified array append operation. The correct code is:

```
array[size] = val;
persist(&array[size]);
size++;
persist(&size);
```

The newly appended value must be persisted *before* $size$ is incremented and persisted. Consider the following code:

```
array[size] = val;
size++;
persist(&size);
```

The following figure illustrates the contents of an array in the CPU cache and in SCM after inserting the values A, B, C, and D using the above code:

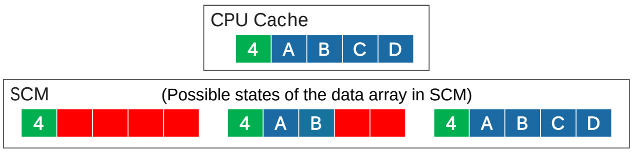

In this case there is no guarantee that $size$ will refer to only valid entries in the array after a failure, because appended values are never explicitly persisted. Hence, the array can be in an arbitrary state, as illustrated in the figure above. Using our testing framework, the content of the array in the CPU cache, the original segment, and the mirror segment using the same erroneous insertion code are illustrated as follows:

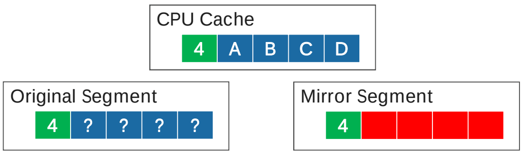

Our testing framework successfully detects such errors since $array$ will never be updated in the mirror segments and a simple check of the content of $array$ during a simulated crash will detect this issue.

Algorithm 7.2 Crash Simulation procedure with call-stack awareness.

```
procedure GetCrashProbability(CallStack S)
    (prob, found) ← CallStackMap.find(S)
    if found then
        return prob
    else                                        ▷ First time visiting this call stack
        CallStackMap.insert(S, 1)
        return 1                                ▷ Simulate crash
procedure RussianRoulette(CallStack S)
    prob ← GetCrashProbability(S)
    crashProb ← rand(0,1)
    if crashProb < prob then
        SimulateCrash()
        CallStackMap.update(S, prob/2)
```

7.2.2 Faster Testing with Copy-on-Write

In practice, the cost of making copies of the mirror segments for every simulated crash is proportional to the size and number of segments. Therefore, this step can be prohibitively expensive for programs with a large memory footprint. To remedy this issue, we use *copy-on-write memory mapping*[2]. Copy-on-write enables to read data directly from the mirror segments while copying only the memory pages that are modified by the test process. When the test program terminates, the memory pages that hold the changes that were made to the mirror segments are discarded. Hence, both the original segments and the mirror segments remain unchanged during the crash simulation phase, but at a much lower cost than that of making copies of the mirror segments.

7.2.3 Faster Code Coverage with Call Stack Tracing

Triggering crash simulations purely randomly gives no code coverage guarantees as some critical paths might not be tested while others might be tested multiple times. An alternative to the purely random approach is systematic crash simulation, similar to the one followed by Yat. This approach has the disadvantage of testing the same critical path as many times as it is executed. For instance, if a program appends one thousand values to a persistent array, systematic crash simulation will test the append function of the persistent array one thousand times, leading to prohibitive testing times.

To solve this issue, we propose to capture the program call stack when a crash is simulated as a means to limit duplicate testing. Basically, we cache the call stacks of the scenarios that were already tested and avoid triggering a crash simulation when the same call stack is visited again. However, the same call stack does not mean the exact same scenario. We argue that testing the same call stack several times is beneficial in the sense that corner cases are more likely to be covered. Consider the following code for the previous example:

```
array[size] = val;
persist(array);
size++;
persist(&size);
```

---

[2] See the MAP_PRIVATE flag of *mmap*: `http://man7.org/linux/man-pages/man2/mmap.2.html`

The error is that it is always the first cache-line-sized piece of *array* that is flushed instead of the cache line that holds the newly appended value. Similarly to the previous examples, we illustrate the contents of the array in the CPU cache, the original segment, and the mirror segment:

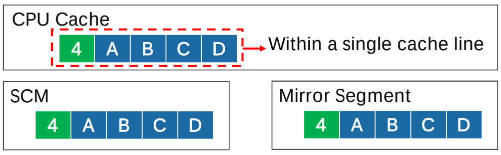

If a crash is simulated only once in the append operation, this error might remain unnoticed since the first appended value will be located in the first cache-line-sized piece of *array*. Therefore, we propose to exponentially decrease the probability of simulating a crash with the same call stack. Algorithm 7.2 illustrates the different steps of this process. Basically, we map tested call stacks to a corresponding probability. If the call stack has never been visited before, we insert the new call stack in the map together with a corresponding probability of 1. This probability is divided by two whenever a crash is simulated at the same call stack. We use our own call stack unwinder that unwinds up to 10 frames to avoid any ambiguity.

7.2.4 Memory Reordering

Although it is advised to always protect a flushing instruction with two memory barriers, it can sometimes be useful to group several flushing instructions together for optimization purposes – e.g., when the order of writes is not important. However, such optimizations may stem from wrong ordering assumptions, hence leading to errors. Consider again the previous example:

```
1 array[size] = val;
2 sfence();
3 clwb(&array[size]);
4 /* Missing memory barrier */
5 size++;
6 persist(&size);
```

The code above tries to optimize by skipping one memory barrier that should be at line 4. As a result, lines 3 and 5 might be reordered by the CPU and the new value of *size* might be made persistent before the newly appended value.

Errors caused by memory reordering are one of the most challenging situations for SCM-based software. We propose an extension to our testing framework that enables us to partially take them into account during testing. Instead of directly copying flushed cache lines into the mirror segments, we propose to stash them first in a map where the key is the persistent address of the cache-line-sized piece of data, and the value is the content of that piece of data. Whenever a call stack is tested, we simulate a crash for each possible subset of the stash. As a consequence, the number of crash simulations increases exponentially with the size of the stash. However, testing SOFORT and its different components unveiled very small stash sizes (typically up to three). The stash is emptied whenever a memory barrier is issued. Basically, we take into account the reordering of consecutive flushes that were not ordered by memory barriers. As a side effect, the stash enables us also to detect the case when several cache-line flushing instructions are issued to the same cache line without being ordered, which hints to a potential programming error. Algorithm 7.3 shows the pseudo-code of the overloaded *Flush* and *Barrier* functions, as well as the procedure *RussianRoulette* whose purpose is to trigger crash

Algorithm 7.3 Crash Simulation procedure with call-stack awareness and stashed writes.

```
procedure RussianRoulette(CallStack S, Map Stash)
    prob ← GetCrashProbability(S)
    crashProb ← rand(0,1)
    if crashProb < prob then
        for each $subset$ of Stash do
            Copy $subset$ to mirror segments
            SimulateCrash()
            Undo $subset$
        CallStackMap.update(S, prob/2)
procedure Flush(PPtr PAddr, Char Content[CacheLineSize])
    found ← Stash.find(PAddr)
    if found then
        Stash.update(PAddr, Content)
    else
        Stash.insert(PAddr, Content)
procedure Barrier
    if Stash is not empty then
        S ← getCallStack()
        RussianRoulette(S, Stash)
    for (PAddr, Content) in Stash do
        copyToMirror(PAddr, Content)
```

simulations. The latter function is systematically called inside the *Barrier* function, because it replaces the *Flush* function as the only one that changes the state of the mirror segments. These functions abstract memory barriers and cache-line flushing instructions – for the sake of generality. For instance, *Barrier* could be implemented with an *sfence* and *Flush* with a *clwb*. Section 7.2.7 elaborates on the memory reordering cases that are not covered by our framework.

7.2.5 Crash Simulation During Recovery

Contrary to Yat, our testing framework is able to *automatically* simulate crashes during the recovery procedure. To achieve this, we allow crash simulation in both the main process and the test process. To be able to simulate crashes in the test process, we need new segment copies in which we replicate the data that is explicitly flushed by the test process. Therefore, we need to first make copies of the mirror segments before the test process starts executing. When a crash simulation is triggered in the test process, a third process which we denote as recovery test process, is forked and will perform recovery using the copies of the mirror segments with copy-on-write. We keep these copies until the test process finishes executing, upon which we delete them. Hence, only one copy of the mirror segments is needed during the lifetime of the test process regardless of the number of crash simulations that are triggered in it.

To limit the higher cost of nested testing, we propose to (1) test the software without allowing crashes in the test process; (2) devise a minimalistic test program whose crash scenarios cover the whole recovery procedure; (3) test the latter program while allowing crash simulation in the test process. The goal of the minimalistic test program is to mitigate the higher cost of nested crash simulation which requires the additional step of making copies of the mirror segments. If a crash occurs during testing, a debugger can be attached to the three processes, namely the main process, the test process, and the recovery test process. Figure 7.3 gives a global overview of the complete testing framework, with all the optimizations and features discussed so far.

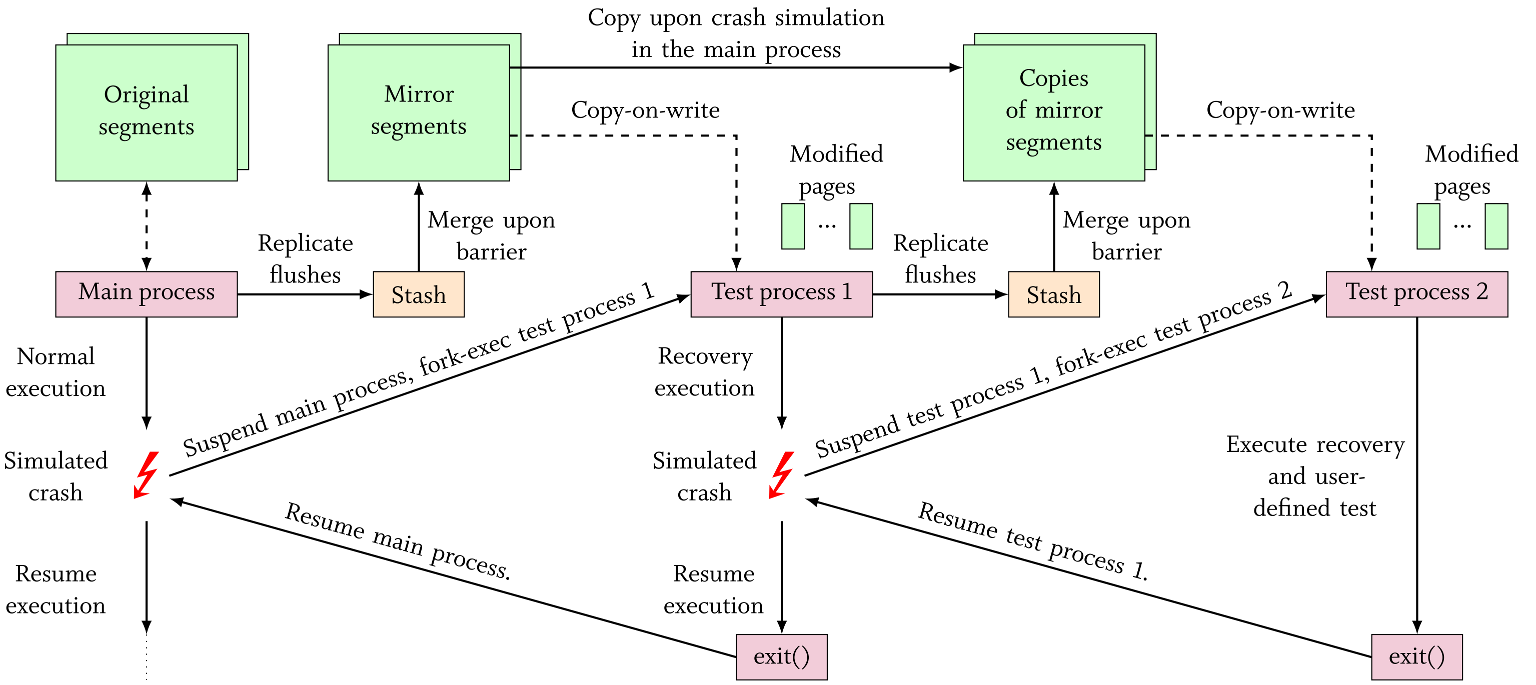

Figure 7.3: Global overview of the testing framework including copy-on-write optimizations, memory reordering, and nested crash simulation.

7.2.6 Crash Simulation in Multi-Threaded Programs

Single-threaded consistency and recovery correctness in addition to concurrency correctness (e.g., no race conditions) is a good indicator of multi-threaded consistency and recovery correctness. However, there are programming errors that cannot be detected in single-threaded execution. These errors typically concern code paths that execute only in multi-threaded mode. Consider the following example where two threads try to increment one of two persistent counters, $ctr1$ and $ctr2$:

```
 1 mutex m1, m2;
 2 if(m1.try_lock()){
 3     ctr1++;
 4     persist(&ctr1);
 5     m1.unlock();
 6 }else if(m2.try_lock()){
 7     ctr2++;
 8     persist(&ctr1) /* Should be ctr2 */
 9     m2.unlock();
10 }
```

The error in the code above is at line 8 where $ctr1$ is persisted instead of $ctr2$. In the case of single-threaded execution, lock $m1$ will always be successfully acquired, hence, lines 7 to 9 will never be executed and the error will not be detected.

Our testing framework is capable of testing multi-threaded programs. Indeed, it is possible to suspend all the threads of a process as long as the process keeps references to all its threads. Only when this is not the case (e.g. if some threads are detached) the program needs to be changed to provide a procedure that halts all its threads. Additionally, the call stack map and the stash of pending writes need to be made thread-safe using global locks so that only one thread is allowed to try and trigger a crash simulation at a time. Avoiding duplicate testing by caching the call stack of the thread that triggered the crash simulation becomes less effective in a multi-threaded environment. This is because the crash scenario depends on the state of all threads and not only the thread that triggered the crash simulation. Nevertheless, exhaustive testing for multi-threaded programs is infeasible because thread scheduling is non-deterministic, hence, two runs of the same multi-threaded program may produce different scenarios.

7.2.7 Limitations and Complementarity with Yat

While our testing framework is able to detect a wide range of consistency-related errors, it is unable to find errors that stem from the reordering of consecutive SCM writes whose persistence is delayed but still enforced in the right order. Consider the following code snippet of an array append operation:

```
array[size] = val;
size++;
persist(&array[size]);
persist(&size);
```

The issue in the code above is that the new value of $size$ can be speculatively evicted from the CPU cache and become persistent before the newly appended value. A power failure at this same instant would leave the array in an inconsistent state. Similarly to the previous examples, we illustrate below the content of CPU cache, the original segment, and the mirror segment:

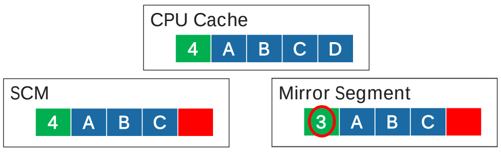

Our testing framework cannot detect this issue because it captures only *persistence primitives* and not *individual SCM writes*. If lines 3 and 4 are swapped, our testing framework would detect it as a wrong persistence order. In contrast, Yat is able to detect such errors since it captures all SCM writes.

We advocate coupling our testing framework with Yat. Our testing framework can quickly test several classes of SCM-related errors, leaving out only the class of errors described above, for which Yat can be used. Yat can eliminate the scenarios that were tested using our testing framework and focus instead only on SCM write reordering between two cache line flushing instructions. This significantly decreases the amount of combinations that Yat needs to test.

Unfortunately, there is another class of errors that neither our testing framework nor Yat can detect. Consider the example of Section 7.2.3:

```
1 array[size] = val;
2 persist(&array);
3 size++;
4 persist(&size);
```

The error in this case is in line 2 where we persist the first cache-line-sized piece of $array$ instead of the appended value. If the test program appends only a few values which fit in a single cache line, line 2 will still persist the newly appended value. Hence, the error will remain unnoticed both in our testing framework and in Yat. If in the release version of the software the array spans more than one cache line, data consistency will not be guaranteed.

7.3 EVALUATION

We evaluated our testing framework on a persistent B^+-Tree, namely the our FPTree, and on a persistent SCM allocator, namely our PAllocator. The allocator code base is around 7000 lines of code (excluding blank lines and comments). We consider the following test scenarios:

- *PTree-N:* The main program consists of inserting N key-value pairs in the persistent B^+-Tree, then erasing them. The test program that is executed upon crash simulation consists in executing recovery and checking that the tree is in a consistent state.
- *PAlloc-N*: The main program consists of interleaving N allocation and N deallocation of blocks of sizes between 128 Bytes and 1 KB. The test program consists in executing recovery, deallocating all currently allocated blocks, then inspecting the allocator against memory leaks.

In the case of PTree-N, the persistent tree uses the persistent SCM allocator. Hence, some of the simulated crashes will be triggered inside the allocator code. This is useful because it will stress the scenarios where a memory leak might happen because the persistent tree did not properly track its own allocations or deallocations.

Test	Main program stats		#Crash simulation		Time	
	#Flush	#Barrier	w/o CS	w/ CS	w/o CS	w/ CS
PTree-100	747	1238	966	234	20.5 s	5 s
PTree-1000	4488	8440	8524	390	179 s	8 s
PTree-10000	42494	81436	84392	834	1795 s	20 s
PAlloc-100	2254	4346	4034	322	84 s	7 s
PAlloc-1000	17643	38730	34902	452	730 s	10 s
PAlloc-10000	173479	384046	346580	702	7199 s	23 s

Table 7.1: Performance of the testing framework with nested crash simulation disabled. Call stack is abbreviated as CS.

Test	Time	
	without call stack	with call stack
PTree-100	218 s	98 s
PTree-1000	710 s	126 s
PTree-10000	6120 s	273 s
PAlloc-100	DNF (≈ 1.3 d)	227 s
PAlloc-1000	DNF (≈ 11.5 d)	414 s
PAlloc-10000	DNF (≈ 114.8 d)	1349 s

Table 7.2: Performance of the testing framework with nested crash simulation enabled.

First, we execute the test scenarios without allowing crash simulation in the test process (i.e. no nested crash simulation). Table 7.1 illustrates the number of persistence primitives, the number of crash scenarios, and the total testing time with and without taking into account the call stack. We observe that when not taking into account the call stack, the number of crash scenarios grows linearly with the number of operations. When taking into account the call stack however, the number of crash scenarios grows very slowly, which allows speedups of 41.7x and 30.5x for PTree-10000 and PAlloc-10000, respectively, compared with not taking into account the call stack.

We depict in Figure 7.4 the frequency of simulated crashes in visited call stacks for PTree-10000 and PAlloc-10000. We observe that when taking into account the call stack, the highest number of simulated crashes with the same call stack is limited to 16. When not taking into the account the call stack, this number increases up to 10000 (as expected). Hence, our approach efficiently limits duplicate testing. We argue again that removing all duplicate testing is not necessarily a good option: while testing the persistent allocator and the persistent B^+-Tree, duplicate testing allowed us to detect errors stemming from corner cases in already visited call stacks.

As a second step, we allow nested crash simulation in order to test the crash-safety of recovery procedures. We set a limit of one day per run. We report the results in Table 7.2. As expected, the testing time is higher than without nested crash simulation. Still, taking into account the call stack keeps the testing cost reasonable and yields significant speedups: 22.4x and 7352.6x for PTree-10000 and PAlloc-10000, respectively, compared with not taking into account the call stack. The three call-stack-oblivious PAlloc test scenarios exceeded the one-day threshold and we report an estimation of their running time. This is explained by the fact that the recovery procedure of PAlloc is larger and more complex than that of PTree. Hence, the number of nested crash simulations is much higher for PAlloc than for PTree.

The testing framework detected many errors, such as missing flushes, in the persistent allocator and the persistent B^+-Tree. Some errors however were non-trivial such as errors in the logic of recovery

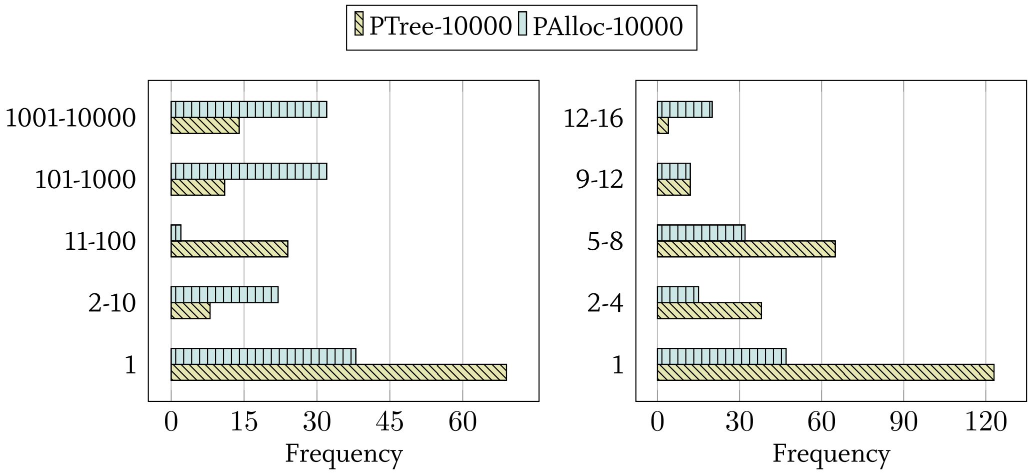

(a) without call stack

(b) with call stack

Figure 7.4: Frequency distribution of the the number of simulated crashes per call stack. The y axis represents the considered range groups of the number of crash simulations per call stack, while the x axis represents the cardinality of these groups.

procedures. These errors would not have been detected without nested crash simulation. Importantly, the call-stack-oblivious version of the framework did not detect any errors that were not detected by the call-stack-aware version. We conclude that thanks to its call stack awareness, our testing framework enables fast crash-safety testing, even with nested crash simulation, without compromising the quality of testing.

7.4 SUMMARY AND FUTURE WORK

In this chapter we presented a lightweight automated testing framework for software that uses SCM as a universal memory. Our testing framework can simulate software crashes and power failures following a suspend-test-resume approach. It makes efficient usage of copy-on-write memory mapping to speedup the testing process. Additionally, it achieves fast code coverage by caching the call stacks of the already tested crash scenarios. Our testing framework is also able to simulate nested crashes in a fully automated way, that is, crashes that occur during the recovery procedure of a test program executing in an ongoing crash simulation. Our experimental evaluation shows that our testing framework successfully finds a wide range of consistency and recovery errors, and is fast enough to be used continuously during development of fairly large software systems.

The focus of our testing framework is to improve the quality of SCM-based software rather than to achieve comprehensive crash-safety testing, which we argue is impractical. For future work, our testing framework could be extended to take into account data that is speculatively evicted from the CPU cache in order to better simulate power failures. Furthermore, it would be interesting to adapt our testing framework to other, more relaxed memory ordering models. Moreover, we identify a need to investigate new development life cycles that are fit for SCM-based software and that involve model-based verification. Indeed, we argue that theoretical consistency and recovery guarantees must precede experimental verification. Finally, we believe that testing of SCM-based software will receive increasing attention in the near future as real SCM-based systems start to emerge.

8

CONCLUSION

SCM is emerging as a disruptive memory technology that might have the same level of impact as high core counts and large main-memory capacities, requiring us to rethink current database system architectures. In this dissertation, we endeavored to explore this potential by building a hybrid transactional and analytical database system from the ground up that leverages SCM as persistent main memory. This led us to devise several database building blocks. This chapter concludes this dissertation by first summarizing our contributions, then sketching promising directions for future work.

8.1 SUMMARY OF CONTRIBUTIONS

SCM Programming Model. We identified several SCM programming challenges, namely data consistency, data recovery, persistent memory leaks, and partial writes. To address these challenges, we devised a sound programming model that relies on lightweight persistence primitives to achieve data consistency. To provide data recovery, we propose to use persistent pointers in the form of a file ID and an offset within that file. Persistent pointers remain valid across restarts, thereby enabling data recovery. Additionally, we provide a swizzling mechanism from persistent pointers to volatile pointers and vice versa. To avoid persistent memory leaks, we employ reference passing, which consists in extending the allocation interface to take a reference to a persistent pointer belonging to the caller data structure. Furthermore, to avoid partial writes, we use p-atomic flags to indicate when a large write operation is completed. We argue that our sound programming model is the guarantee of the technical feasibility and correctness of the work presented in this dissertation.

Persistent Memory Management. The ability to allocate and deallocate SCM is a fundamental building block for building SCM-based data structures. Therefore, we propose PAllocator, a persistent and highly scalable SCM allocator. In contrast to transient memory allocators, our persistent allocator retains the topology of its allocated blocks across restarts. PAllocator's design is tailored to the versatile needs of large-scale hybrid transactional and analytical SCM-based database system. As a result, PAllocator adopts radically different design decisions compared to state-of-the-art transient and persistent allocators. PAllocator implements its memory pool using multiple files, which allows to easily grow and shrink the memory pool, in contrast to state-of-the-art persistent allocators that use a single-file pool. For concurrency, PAllocator creates core-local memory pools, which, in contrast to thread-local memory pools, has the advantage of decoupling local pool management from thread management.

To provide robust performance for a wide range of allocation sizes and to minimize fragmentation, PAllocator relies on three allocation strategies: a segregated-fit strategy for small blocks, a best-fit strategy for large blocks, and creating one file per allocation for huge blocks. Furthermore, PAllocator addresses the important issue of persistent memory fragmentation by providing a defragmentation algorithm that relies on the hole punching feature of sparse files. Our experiments show that PAllocator outperforms both transient and persistent state-of-the-art allocators under high contention.

Hybrid SCM-DRAM Persistent Data Structures. Motivated by the observation that placing tree-based data structures in SCM significantly slows them down, we propose the FPTree, a novel hybrid SCM-DRAM B^+-Tree. The FPTree builds on a number of design principles, namely selective persistence, unsorted leaves, fingerprinting, and selective concurrency. Selective persistence consists in placing primary data in SCM and secondary data, which can be rebuilt from primary data, in DRAM. Applied to the FPTree, this corresponds to placing inner nodes in DRAM and leaf nodes in SCM. Hence, when traversing the FPTree, only accessing the leaf nodes is more expensive compared to a transient B^+-Tree. Moreover, to decrease the number of writes and simplify failure atomicity of updates, we keep the FPTree's leaf nodes unsorted and track valid entries using a bitmap. Nevertheless, looking up unsorted leaves requires a linear scan, which is more expensive (in case of large leaf nodes) than the traditional binary search. To remedy this issue, we introduce fingerprinting, which consists of keeping in leaf nodes one-byte hashes of the keys used as filters. Through an asymptotic analysis as well as an experimental evaluation, we show that fingerprints limit the number of key probes in leaf nodes to exactly one. Furthermore, we devise selective concurrency, a highly scalable hybrid concurrency scheme that uses HTM for the concurrency of inner nodes and fine-grained locks for that of leaf nodes, thereby solving the apparent incompatibility of HTM and SCM.

SOFORT. We use the above building blocks to build SOFORT, a novel single-level hybrid SCM-DRAM columnar transactional engine. SOFORT places its primary data in SCM and its secondary data either in DRAM, in SCM, or in a hybrid SCM-DRAM format. We propose an adaptation of MVCC to SCM that removes traditional write-ahead logging from the critical path of transactions. We achieve this by persisting part of MVCC transaction metadata, namely the write set and the commit timestamp, in SCM. Furthermore, we show that by persisting additional MVCC transaction metadata, SOFORT avoids aborting in-flight transaction during recovery; instead, SOFORT rolls back only the last unfinished statement, and offers the user the ability to continue in-flight transactions. Additionally, we propose an efficient recoverable garbage collection scheme in conjunction with our MVCC scheme. The decentralized design of SOFORT removes the need for group commit, which translates into low transaction latencies. Upon recovery, SOFORT simply discovers primary data in SCM, which removes the traditional bottleneck of main-memory database recovery, namely loading data from storage to main memory. Since committed transactions are guaranteed to have persisted their changes, SOFORT does not require a redo phase. Thereafter, SOFORT rebuilds its transient secondary data from its primary data. By investigating several secondary data placement strategies, we show that on one extreme, persisting all secondary data in SCM enables near-instant recovery at full speed, but at a significant query performance cost due to the higher latency of SCM. On the other extreme, placing all secondary data in DRAM yields the best query performance, but incurs slow restart times due to the large amount of secondary data that needs to be rebuilt. Using our hybrid FPTree proved to be a promising compromise as it limits the impact on query performance while speeding up recovery by more than one order of magnitude compared to using DRAM-based secondary data, all of which while requiring only a 1:60 DRAM to SCM ratio.

Recovery Techniques. The new recovery bottleneck in SCM-based database systems is rebuilding transient secondary data structures. To address this bottleneck, we propose two recovery techniques: instant recovery and adaptive recovery. Motivated by the observation that primary data is sufficient to answer queries, instant recovery allows accepting queries right after recovering primary data, thereby enabling near-instant responsiveness of the database. This is achieved by statically splitting CPU resources between query processing and the recovery of secondary data structures. However, our experimental evaluation showed that it takes SOFORT a significant amount of time to regain its pre-failure throughput due to the slow recovery of secondary data. To remedy this issue, we proposed adaptive recovery, a new secondary data recovery technique that builds on the observation that not all secondary data are equally important. Adaptive recovery uses a ranking function that takes into account the pre-failure workload as well as the recovery workload to prioritize the rebuild of the most important secondary data structures. Moreover, adaptive recovery gradually releases its resources to query processing as it finishes rebuilding the most important secondary data structures, and continues rebuilding the remaining ones in the background. As a result, adaptive recovery enables SOFORT to regain its pre-failure throughput well before the end of the recovery process while still providing near-instant responsiveness.

Testing Framework for SCM-Based Software. Programming SCM as persistent main memory introduces new failure scenarios, such as missing persistence primitives, wrong writes ordering, and failure-induced persistent memory leaks. To tackle this issue, we propose an online testing framework that relies on a suspend-test-resume strategy. Our testing framework creates for each SCM file a mirror file that contains only explicitly flushed data. Our testing framework automatically triggers crash simulations at the boundaries of persistence primitives by halting the main process, then forking a test process that executes recovery on the mirror files using copy-on-write semantics. Since they contain only explicitly flushed data, the mirror files simulate the loss of the CPU caches, which allows catching missing or misplaced flushing instructions. By using copy-on-write semantics, any changes to the mirror files are discarded when the test process exits, enabling the main process to resume execution and reuse the mirror files for future crash simulations. To limit duplicate testing, we proposed to associate the call-stack of each crash scenario with a crash probability that is exponentially decreased each time a crash is simulated for that scenario. This significantly reduces testing time, thereby making it feasible to test fairly large SCM-based software systems. Moreover, our testing framework supports nested crash simulation, i.e., simulating crashes in the test process; this enables to thoroughly test recovery procedures, which are otherwise not tested in the main process.

To summarize, our pathfinding work led us to identify the challenges and opportunities brought by SCM for database systems. As a result, we devised a set of building blocks, including a programming model, an SCM allocator, a hybrid SCM-DRAM data structure, an adaptation of MVCC for SCM, new database recovery techniques, and a testing tool for SCM-based software. These building blocks can be used to build more complex systems, thereby paving the way for future database systems on SCM.

8.2 FUTURE WORK

Research on SCM-based databases is still in its early stages. Some database research areas, such as query optimization and query processing, need to be extended, but not rewritten, to account for SCM and its asymmetric read write latency and bandwidth. In contrast, other areas, such as storage and replication, need to be revisited from the ground up, while new areas, such as testing of SCM-based data structures, require fundamental groundwork. In this context, we present promising research directions for SCM in the following. Our focus is twofold: (1) hardware, software, and theoretical groundwork advancements that can catalyze the adoption of SCM; and (2) ideas that can build on top of the contributions of this dissertation.

Persistent Memory Management

Similar to programming multi-threaded software, programming SCM as a persistent main memory will require a set of mature tools and programming models to be adopted by a larger audience. While several programming models have been proposed, none can claim to have reached standard status. One major concern hindering the widespread adoption of SCM programming is the need to explicitly order and persist writes at a cache line granularity. Libraries providing an interface like transactional memory can hide this complexity, but at the cost of doubling the number of writes (and flushes) to SCM due to systematic undo or redo logging. We envision that new hardware features could dramatically decrease this overhead, thereby making these libraries competitive with hand-tuned code. Such hardware features could include:

- *Hardware-Managed Undo-Redo Logs*. SCM transactional libraries usually rely on either redo or undo logging to ensure failure atomicity. We conceive that hardware-driven undo-redo logging would decrease the overhead of these libraries. For instance, Ogleari et al. [118] propose a hardware-based undo-redo logging scheme that uses a combination of cache-resident and SCM-resident buffers. Writes are kept in cache-resident buffers and flushed to SCM only if their dependent writes are evicted from the cache. This has the advantage of decreasing the cost of flushing instructions and relaxing write ordering constraints.
- *SCM Support in HTM*. As explained in Chapter 4, HTM transactions must buffer changes in the L1 CPU cache to ensure their atomic visibility at the end of the transaction. Therefore, flushing instructions will automatically abort HTM transactions. Extending HTM to support SCM would further ease the adoption of SCM and provide a baseline for concurrency support in SCM transactional libraries. Research works on the subject started to emerge, exemplified by PhyTM [8], which requires only the ability to commit one bit atomically to SCM to support SCM transactions.
- *Providing Non-Volatile Caches*. This would remove the need for flushing instructions, which would significantly reduce the overhead of SCM transactional libraries. Moreover, this would facilitate SCM support in HTM because data changes can be buffered in the L1 CPU cache without jeopardizing data durability.

In 1983, Atkinson et al. [7] formulated the concept of decoupling the data representation from data manipulation. In other words, each data object can be persistent or transient, independent of its internal representation. It would be interesting to revisit this concept in light of SCM, especially since transient (DRAM-based) and persistent (SCM-based) data structures share most of their layout optimization techniques. Additionally, this concept could be implemented in SCM transactional libraries.

Furthermore, fragmentation will be a major issue in SCM memory management. We addressed this issue in this dissertation for the versatile needs of hybrid analytical and transactional systems. However, other systems with more predictable memory management needs, such as FOEDUS [79] – a purely transactional system – can opt to go back to the fundamentals of buffer pool management, that is, dividing memory into fixed-size chunks, thereby avoiding any fragmentation. We expect different systems with different needs to devise tailor-made SCM management techniques. These techniques will exploit knowledge of the memory allocation patterns of the underlying system to minimize fragmentation or avoid it completely when possible.

Finally, it is worth considering rewriting part or all of the operating system such that it intrinsically supports SCM. One can argue that the support for SCM that is currently being built in Linux and Windows treats SCM as a second-class citizen. For instance, the Direct Access (DAX) filesystem feature [35] builds on top of block-based filesystem architectures. Several SCM-optimized filesystem proposals, such as NOVA [179], have showcased the benefits of rearchitecting file management for SCM. Following a more radical approach, Bryson et al. [15] are working on Twizzler, a novel operating system designed from scratch around SCM. We believe that such endeavors are essential to unveil the full potential of SCM.

Persistent Data Structures

Looking ahead, we envision that the next evolution of hybrid SCM-DRAM data structures will be morphing data structures that can dynamically adjust their data placement between SCM and DRAM, following performance and memory constraints. Figure 8.1 illustrates a generalization of our selective persistence model towards the morphing persistence model. Furthermore, log-structured data structures, such as the Log-Structured Merge Tree (LSM) [119], are natural candidates for SCM given their append-only nature and their wide use in key-value databases; works investigating LSMs on SCM start to emerge [93, 94] and we expect to see more research in that direction.

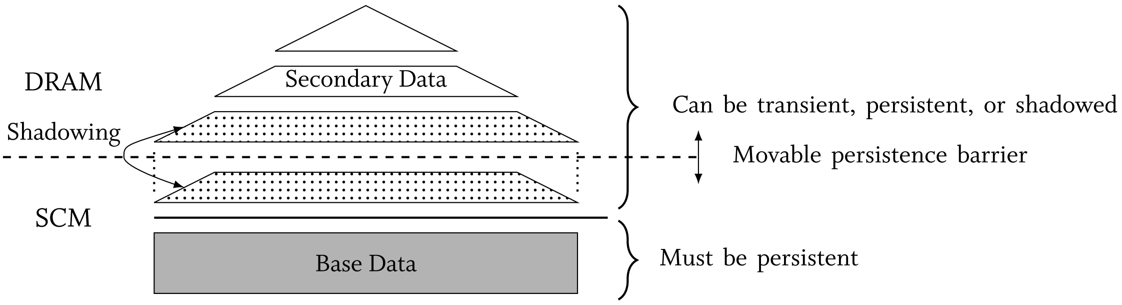
DRAM
Secondary Data
Shadowing
SCM
Base Data
Can be transient, persistent, or shadowed
Movable persistence barrier
Must be persistent

Figure 8.1: Illustration of a morphing SCM-DRAM data structure.

Regarding concurrency, we see the need to extend our selective concurrency scheme to efficiently handle skew. In fact, highly skewed writes abort HTM transactions as conflicts are detected. After a programmer-defined number of retries, a hardware transaction falls back to a programmer-defined lock-based concurrency scheme. In the absence of skew, this can be simply a global lock, as demonstrated with our FPTree [126]. However, under highly skewed workloads, a global lock would constitute a contention point. Therefore, to ensure robust concurrency scalability, the fall-back concurrency mechanism *must* be scalable and skew resilient. This way, HTM would provide linear scaling when skew is low and the fall-back concurrency scheme would provide resilience to skewed workloads.

High Availability

In this dissertation, we have dealt only with software and power failures. Nevertheless, high-availability cannot be achieved without accounting for hardware failures. Hardware failures are usually handled in one of the following two ways:

- *Data replication.* It consists of replicating primary data either by mirroring, such as using RAID storage systems, or by replicating enough information to redo the changes, i.e., log shipping. The advantage of these approaches is their low cost as they require only additional storage media. However, recovery can be very costly as it depends directly on the amount of data to restore or the amount of changes to replay.
- *System replication.* It consists of replicating the state of the whole system on several interconnected machines. For instance, H-Store [151] provides high-availability by replicating the state of main memory on several nodes of a cluster without providing single-node persistence. The advantage of this approach is that a node failure has minimal effect on the availability of the system. However, a major disadvantage is the total cost of ownership (TCO), which is many times higher than for data replication.

We conceive an approach that combines the benefits of both data and system replication while avoiding their disadvantages. While RDMA has been used mostly for transient data in DRAM, we propose to achieve fine-grained, low-level replication using RDMA with SCM and high-speed interconnects. Novel high-speed interconnects are expected to provide low RDMA latencies comparable to remote-socket memory latencies on large multi-socket machines. This approach does not require an active computing unit on top of SCM, therefore reducing TCO compared to system replication. Additionally, it does not require data to be reloaded, replayed, or reconstructed as it is stored in SCM, thereby eliminating the shortcoming of data replication.

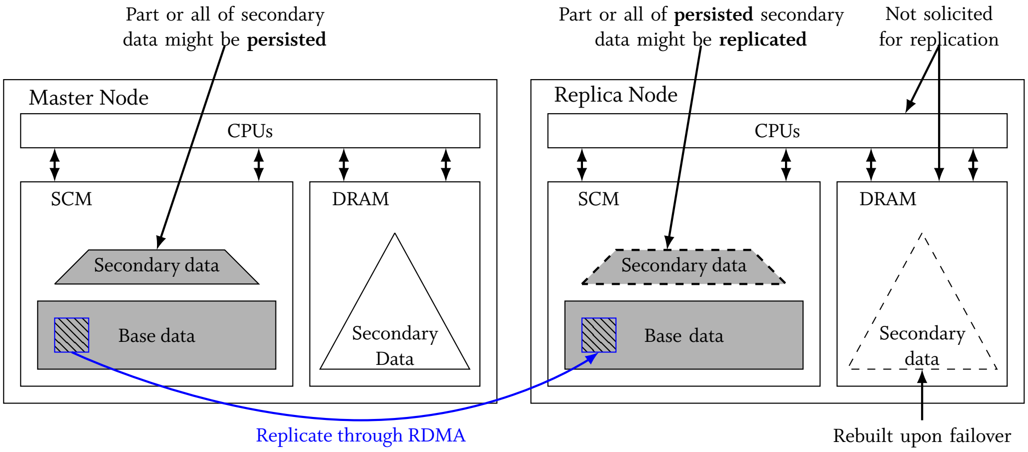

Figure 8.2: Fine-grained replication using SCM and RDMA.

Figure 8.2 illustrates our envisioned replication approach. Data persistence and replication can vary following two dimensions. The first one is *which data to replicate*. Primary data as well as potentially part or all of secondary data is persisted in SCM. While primary data *must* be replicated, persisted secondary data might or might not be replicated. Additionally, the more secondary data is replicated, the faster the fail-over to the replica node and potentially the lower the performance on the master node. Therefore, we plan to investigate several data replication thresholds and evaluate each scenario based on the set of criteria defined earlier, in addition to fail-over time. The second dimension is *what to persist on the master node*. Although we investigated this question in Chapter 5, replication through RDMA introduces additional overhead and potentially stall time, which can then be used to persist additional secondary data parts, e.g., using shadowing techniques. Therefore, we need to revisit the SCM-DRAM data placement dimension in conjunction with replication.

Testing of SCM-Based Software

We argue that testing the correctness and fail-atomicity of SCM-based data structures is one of the most important and challenging aspects of SCM programming. Still, research in this field has yet to gain traction. While experimental testing is beneficial, providing theoretical correctness guarantees is necessary. Therefore, we foresee that model checking techniques will be applied to SCM-based data structures to prove their correctness. Perhaps the first building block towards this is to formally define the correctness of an SCM-based data structure. The groundwork of Izraelevitz et al. [68] goes into that direction. The authors formally define correctness criteria of SCM-based data structures assuming current hardware, with transient registers and CPU caches. They further formalize the notion of *durable serializability* to govern the safety of concurrent objects. Formalizing constraints lays the ground for both feature-exhaustive formal and experimental testing tools. Furthermore, it facilitates the identification of optimization opportunities, such as writes whose ordering can be relaxed. We expect theoretical work on SCM-based data structures to play a major role in enabling the widespread adoption of SCM as persistent main memory.

BIBLIOGRAPHY

[1] *3D XPoint Technology*. `https://www.micron.com/about/our-innovation/3d-xpoint-technology` *(Last accessed: September 24, 2017)*.

[2] Rakesh Agrawal and H Jagadish. "Recovery algorithms for database machines with non-volatile main memory". In: *Database Machines* (1989), pp. 269–285.

[3] Mihnea Andrei, Christian Lemke, Guenter Radestock, Robert Schulze, Carsten Thiel, Rolando Blanco, Akanksha Meghlan, Muhammad Sharique, Sebastian Seifert, Surendra Vishnoi, Thomas Peh, Ivan Schreter, Werner Thesing, and Mehul Wagle. "SAP HANA Adoption of Non-Volatile Memory". In: *Proceedings of the VLDB Endowment* (2017).

[4] Joy Arulraj and Andrew Pavlo. "How to Build a Non-Volatile Memory Database Management System". In: *Proceedings of the 2017 ACM International Conference on Management of Data*. ACM. 2017, pp. 1753–1758.

[5] Joy Arulraj, Andrew Pavlo, and Subramanya R Dulloor. "Let's talk about storage & recovery methods for non-volatile memory database systems". In: *Proceedings of the 2015 ACM SIGMOD International Conference on Management of Data*. ACM. 2015, pp. 707–722.

[6] Joy Arulraj, Matthew Perron, and Andrew Pavlo. "Write-behind logging". In: *PVLDB* 10.4 (2016), pp. 337–348.

[7] Malcolm P. Atkinson, Peter J. Bailey, Ken J Chisholm, Paul W Cockshott, and Ronald Morrison. "An approach to persistent programming". In: *The computer journal* 26.4 (1983), pp. 360–365.

[8] Hillel Avni and Trevor Brown. "PHyTM: Persistent hybrid transactional memory for databases". In: *Proceedings of the VLDB Endowment* 10.4 (2016), pp. 409–420.

[9] Daniel Bausch, Ilia Petrov, and Alejandro Buchmann. "Making cost-based query optimization asymmetry-aware". In: *Proceedings of the Eighth International Workshop on Data Management on New Hardware*. ACM. 2012, pp. 24–32.

[10] Naama Ben-David, Guy E Blelloch, Jeremy T Fineman, Phillip B Gibbons, Yan Gu, Charles McGuffey, and Julian Shun. "Parallel algorithms for asymmetric read-write costs". In: *Proceedings of the 28th ACM Symposium on Parallelism in Algorithms and Architectures*. ACM. 2016, pp. 145–156.

[11] Emery D Berger, Kathryn S McKinley, Robert D Blumofe, and Paul R Wilson. "Hoard: A scalable memory allocator for multithreaded applications". In: *ACM Sigplan Notices* 35.11 (2000), pp. 117–128.

[12] Philip A Bernstein, Vassos Hadzilacos, and Nathan Goodman. *Concurrency Control and Recovery in Database Systems*. Addison- Wesley, 1987.

[13] Kumud Bhandari, Dhruva R. Chakrabarti, and Hans-J. Boehm. "Makalu: Fast Recoverable Allocation of Non-volatile Memory". In: *OOPSLA 2016*. ACM, 2016, pp. 677–694.

[14] Guy E Blelloch, Jeremy T Fineman, Phillip B Gibbons, Yan Gu, and Julian Shun. "Sorting with asymmetric read and write costs". In: *Proceedings of the 27th ACM symposium on Parallelism in Algorithms and Architectures*. ACM. 2015, pp. 1–12.

[15] Matt Bryson, Daniel Bittman, Darrell Long, and Ethan Miller. "Twizzer: The Design and Implementation of a NVM Aware OS". In: *8th Annual Non-Volatile Memories Workshop (NVMW'17)*. 2017.

[16] Michael J Cahill, Uwe Röhm, and Alan D Fekete. "Serializable isolation for snapshot databases". In: *ACM Transactions on Database Systems (TODS)* 34.4 (2009), p. 20.

[17] Tuan Cao, Marcos Vaz Salles, Benjamin Sowell, Yao Yue, Alan Demers, Johannes Gehrke, and Walker White. "Fast checkpoint recovery algorithms for frequently consistent applications". In: *Proceedings of the 2011 ACM SIGMOD International Conference on Management of data*. ACM. 2011, pp. 265–276.

[18] Dhruva R Chakrabarti, Hans-J Boehm, and Kumud Bhandari. "Atlas: Leveraging locks for non-volatile memory consistency". In: *ACM SIGPLAN Notices* 49.10 (2014), pp. 433–452.

[19] Andreas Chatzistergiou, Marcelo Cintra, and Stratis D Viglas. "REWIND: Recovery write-ahead system for in-memory non-volatile data-structures". In: *Proceedings of the VLDB Endowment* 8.5 (2015), pp. 497–508.

[20] Shimin Chen, Phillip B Gibbons, and Suman Nath. "Rethinking Database Algorithms for Phase Change Memory." In: *CIDR*. 2011, pp. 21–31.

[21] Shimin Chen and Qin Jin. "Persistent b+-trees in non-volatile main memory". In: *Proceedings of the VLDB Endowment* 8.7 (2015), pp. 786–797.

[22] Howard Chu. *MDB: A memory-mapped database and backend for openldap*. Tech. rep. 2011.

[23] Leon Chua. "Memristor-the missing circuit element". In: *IEEE Transactions on circuit theory* 18.5 (1971), pp. 507–519.

[24] Joel Coburn, Adrian M Caulfield, Ameen Akel, Laura M Grupp, Rajesh K Gupta, Ranjit Jhala, and Steven Swanson. "NV-Heaps: making persistent objects fast and safe with next-generation, non-volatile memories". In: *ACM Sigplan Notices* 46.3 (2011), pp. 105–118.

[25] Rod Colledge. *SQL Server 2008 Administration in Action*. English. Manning Publications, Aug. 2009. ISBN: 9781933988726.

[26] Jeremy Condit, Edmund B Nightingale, Christopher Frost, Engin Ipek, Benjamin Lee, Doug Burger, and Derrick Coetzee. "Better I/O through byte-addressable, persistent memory". In: *Proceedings of the ACM SIGOPS 22nd symposium on Operating systems principles*. ACM. 2009, pp. 133–146.

[27] George Copeland, Tom W Keller, Ravi Krishnamurthy, and Marc G Smith. "The case for safe RAM". In: *VLDB*. 1989, pp. 327–335.

[28] Jonathan Corbet. *Linux 5-Level Page Table. https://lwn.net/Articles/717293/ (Last accessed: September 24, 2017)*.

[29] Jonathan Corbet. *Supporting file systems in persistent memory. https://lwn.net/Articles/610174/ (Last accessed: September 24, 2017)*.

[30] M. Dayarathna, Y. Wen, and R. Fan. "Data Center Energy Consumption Modeling: A Survey". In: *IEEE Communications Surveys Tutorials* 18.1 (2016), pp. 732–794. ISSN: 1553-877X. DOI: 10.1109/COMST.2015.2481183.

[31] Justin DeBrabant, Joy Arulraj, Andrew Pavlo, Michael Stonebraker, Stan Zdonik, and Subramanya Dulloor. "A prolegomenon on OLTP database systems for non-volatile memory". In: *ADMS@ VLDB* (2014).

[32] Justin DeBrabant, Andrew Pavlo, Stephen Tu, Michael Stonebraker, and Stan Zdonik. "Anti-Caching: A new approach to database management system architecture". In: *Proceedings of the VLDB Endowment* 6.14 (2013), pp. 1942–1953.

[33] *Deprecating the PCOMMIT Instruction.* https://software.intel.com/en-us/blogs/2016/09/12/deprecate-pcommit-instruction *(Last accessed: September 24, 2017).*

[34] David J DeWitt, Randy H Katz, Frank Olken, Leonard D Shapiro, Michael R Stonebraker, and David A. Wood. "Implementation Techniques for Main Memory Database Systems". In: *SIGMOD Rec.* 14.2 (June 1984), pp. 1–8. ISSN: 0163-5808. DOI: 10.1145/971697.602261.

[35] *Direct Access for files.* https://www.kernel.org/doc/Documentation/filesystems/dax.txt *(Last accessed: September 24, 2017).*

[36] *Disclosure of H/W prefetcher control on some Intel®processors.* https://software.intel.com/en-us/articles/disclosure-of-hw-prefetcher-control-on-some-\intel-processors (Last accessed: September 24, 2017).

[37] Xiangyu Dong, Xiaoxia Wu, Guangyu Sun, Yuan Xie, Helen Li, and Yiran Chen. "Circuit and microarchitecture evaluation of 3D stacking magnetic RAM (MRAM) as a universal memory replacement". In: *Design Automation Conference, 2008. DAC 2008. 45th ACM/IEEE*. IEEE. 2008, pp. 554–559.

[38] Subramanya R. Dulloor. "Systems and Applications for Persistent Memory." PhD thesis. Georgia Institute of Technology, 2016.

[39] Subramanya R Dulloor, Sanjay Kumar, Anil Keshavamurthy, Philip Lantz, Dheeraj Reddy, Rajesh Sankaran, and Jeff Jackson. "System software for persistent memory". In: *Proceedings of the Ninth European Conference on Computer Systems*. ACM. 2014, p. 15.

[40] Margaret H Eich. "Main memory database recovery". In: *Proceedings of 1986 ACM Fall Joint Computer Conference*. IEEE Computer Society Press. 1986, pp. 1226–1232.

[41] Ahmed Eldawy, Justin Levandoski, and Per-Åke Larson. "Trekking through Siberia: Managing cold data in a memory-optimized database". In: *Proceedings of the VLDB Endowment* 7.11 (2014), pp. 931–942.

[42] *Ext4 file system.* https://www.kernel.org/doc/Documentation/filesystems/ext4.txt *(Last accessed: September 24, 2017).*

[43] Ru Fang, Hui-I Hsiao, Bin He, C Mohan, and Yun Wang. "High performance database logging using storage class memory". In: *Data Engineering (ICDE), 2011 IEEE 27th International Conference on*. IEEE. 2011, pp. 1221–1231.

[44] Franz Färber, Sang Kyun Cha, Jürgen Primsch, Christof Bornhövd, Stefan Sigg, and Wolfgang Lehner. "SAP HANA database: data management for modern business applications". In: *ACM Sigmod Record* 40.4 (2012), pp. 45–51.

[45] Alan Fekete, Dimitrios Liarokapis, Elizabeth O'Neil, Patrick O'Neil, and Dennis Shasha. "Making snapshot isolation serializable". In: *ACM Transactions on Database Systems (TODS)* 30.2 (2005), pp. 492–528.

[46] Shen Gao, Jianliang Xu, Bingsheng He, Byron Choi, and Haibo Hu. "PCMLogging: reducing transaction logging overhead with PCM". In: *Proceedings of the 20th ACM international conference on Information and knowledge management*. ACM. 2011, pp. 2401–2404.

[47] Hector Garcia-Molina and Kenneth Salem. "Main memory database systems: An overview". In: *IEEE Transactions on knowledge and data engineering* 4.6 (1992), pp. 509–516.

[48] Sanjay Ghemawat and Jeff Dean. *LevelDB.* https://www.voltdb.com/ *(Last accessed: September 24, 2017).*

[49] Sanjay Ghemawat and Paul Menage. *TCMalloc: Thread-Caching Malloc.* http://goog-perftools.sourceforge.net/doc/tcmalloc.html *(Last accessed: September 24, 2017).*

[50] B Govoreanu, GS Kar, YY Chen, V Paraschiv, S Kubicek, A Fantini, IP Radu, L Goux, S Clima, R Degraeve, et al. “10× 10nm 2 Hf/HfO x crossbar resistive RAM with excellent performance, reliability and low-energy operation”. In: *Electron Devices Meeting (IEDM), 2011 IEEE International*. IEEE. 2011, pp. 31–6.

[51] Goetz Graefe. “A survey of B-tree locking techniques”. In: *ACM Transactions on Database Systems (TODS)* 35.3 (2010), p. 16.

[52] Goetz Graefe. “Modern B-tree techniques”. In: *Foundations and Trends in Databases* 3.4 (2011), pp. 203–402.

[53] Goetz Graefe, Wey Guy, and Caetano Sauer. *Instant Recovery with Write-Ahead Logging: Page Repair, System Restart, Media Restore, and System Failover, Second Edition*. Synthesis Lectures on Data Management. Morgan & Claypool Publishers, 2016.

[54] Goetz Graefe and Hideaki Kimura. “Orthogonal key-value locking.” In: *BTW*. 2015, pp. 237–256.

[55] Goetz Graefe, Hideaki Kimura, and Harumi Kuno. “Foster B-trees”. In: *ACM Transactions on Database Systems (TODS)* 37.3 (2012), p. 17.

[56] Jim Gray. “Notes on Data Base Operating Systems”. In: *Operating Systems, An Advanced Course*. 1978, pp. 393–481.

[57] Martin Grund, Jens Krüger, Hasso Plattner, Alexander Zeier, Philippe Cudre-Mauroux, and Samuel Madden. “HYRISE: a main memory hybrid storage engine”. In: *Proceedings of the VLDB Endowment* 4.2 (2010), pp. 105–116.

[58] Heather Hanson and Karthick Rajamani. “What computer architects need to know about memory throttling”. In: *Computer Architecture*. Springer. 2012, pp. 233–242.

[59] M Hosomi, H Yamagishi, T Yamamoto, K Bessho, Y Higo, K Yamane, H Yamada, M Shoji, H Hachino, C Fukumoto, et al. “A novel nonvolatile memory with spin torque transfer magnetization switching: Spin-RAM”. In: *Electron Devices Meeting (IEDM)*. IEEE. 2005, pp. 459–462.

[60] *How to emulate persistent memory.* *http://pmem.io/2016/02/22/pm-emulation.html* *(Last accessed: September 24, 2017).*

[61] *HPE Integrity MC990 X Server.* *https://www.hpe.com/us/en/product-catalog/servers/integrity-servers/pip.hpe-integrity-mc990-x-server.1008798952.html* *(Last accessed: September 24, 2017).*

[62] Jian Huang, Karsten Schwan, and Moinuddin K Qureshi. “NVRAM-aware logging in transaction systems”. In: *Proceedings of the VLDB Endowment* 8.4 (2014), pp. 389–400.

[63] Stratos Idreos, Martin L Kersten, Stefan Manegold, et al. “Database Cracking.” In: *CIDR*. Vol. 7. 2007, pp. 68–78.

[64] *Intel 64 and IA-32 Architectures Software Developer Manuals.* *http://software.intel.com/en-us/intel-isa-extensions* *(Last accessed: September 24, 2017).*

[65] *Intel Software Development Emulator.* *https://software.intel.com/en-us/articles/intel-software-development-emulator* *(Last accessed: September 24, 2017).*

[66] *Intel®64 and IA-32 Architectures Optimization Reference Manual*. Tech. rep. http://www.intel.com/content/dam/www/public/us/en/documents/manuals/64-ia-32-architectures-optimization-manual.pdf (Last accessed: September 24, 2017).

[67] *International Technology Roadmap for Semiconductors 2.0, Beyond CMOS, 2015.* *http://www.semiconductors.org/clientuploads/Research_Technology/ITRS/2015/6_2015%20ITRS%202.0%20Beyond%20CMOS.pdf* *(Last accessed: September 24, 2017).*

[68] Joseph Izraelevitz, Hammurabi Mendes, and Michael L Scott. "Linearizability of persistent memory objects under a full-system-crash failure model". In: *International Symposium on Distributed Computing*. Springer. 2016, pp. 313–327.

[69] Hosagrahar V Jagadish, Daniel Lieuwen, Rajeev Rastogi, Abraham Silberschatz, and S Sudarshan. "Dali: A high performance main memory storage manager". In: *VLDB*. Vol. 94. 1994, pp. 12–15.

[70] HV Jagadish, Abraham Silberschatz, and S Sudarshan. "Recovering from Main-Memory Lapses." In: *VLDB*. Vol. 93. 1993, pp. 391–404.

[71] *JEDEC Announces Support for NVDIMM Hybrid Memory Modules.* `https://www.jedec.org/news/pressreleases/jedec-announces-support-nvdimm-hybrid-memory-modules` *(Last accessed: September 24, 2017).*

[72] *jemalloc Memory Allocator.* `http://jemalloc.net/` *(Last accessed: September 24, 2017).*

[73] Ryan Johnson, Ippokratis Pandis, Nikos Hardavellas, Anastasia Ailamaki, and Babak Falsafi. "Shore-MT: a scalable storage manager for the multicore era". In: *Proceedings of the 12th International Conference on Extending Database Technology: Advances in Database Technology*. ACM. 2009, pp. 24–35.

[74] Ryan Johnson, Ippokratis Pandis, Radu Stoica, Manos Athanassoulis, and Anastasia Ailamaki. "Aether: a scalable approach to logging". In: *Proceedings of the VLDB Endowment* 3.1-2 (2010), pp. 681–692.

[75] JR Jordan, J Banerjee, and RB Batman. "Precision locks". In: *Proceedings of the 1981 ACM SIGMOD international conference on Management of data*. ACM. 1981, pp. 143–147.

[76] Robert Kallman, Hideaki Kimura, Jonathan Natkins, Andrew Pavlo, Alexander Rasin, Stanley Zdonik, Evan PC Jones, Samuel Madden, Michael Stonebraker, Yang Zhang, et al. "H-Store: a high-performance, distributed main memory transaction processing system". In: *Proceedings of the VLDB Endowment* 1.2 (2008), pp. 1496–1499.

[77] Tomas Karnagel, Roman Dementiev, Ravi Rajwar, Konrad Lai, Thomas Legler, Benjamin Schlegel, and Wolfgang Lehner. "Improving in-memory database index performance with Intel® Transactional Synchronization Extensions". In: *High Performance Computer Architecture (HPCA), 2014 IEEE 20th International Symposium on*. IEEE. 2014, pp. 476–487.

[78] Kangnyeon Kim, Tianzheng Wang, Ryan Johnson, and Ippokratis Pandis. "Ermia: Fast memory-optimized database system for heterogeneous workloads". In: *Proceedings of the 2016 International Conference on Management of Data*. ACM. 2016, pp. 1675–1687.

[79] Hideaki Kimura. "FOEDUS: OLTP engine for a thousand cores and NVRAM". In: *Proceedings of the 2015 ACM SIGMOD International Conference on Management of Data*. ACM. 2015, pp. 691–706.

[80] Masaru Kitsuregawa, Hidehiko Tanaka, and Tohru Moto-Oka. "Application of hash to data base machine and its architecture". In: *New Generation Computing* 1.1 (1983), pp. 63–74.

[81] Hsiang-Tsung Kung and John T Robinson. "On optimistic methods for concurrency control". In: *ACM Transactions on Database Systems (TODS)* 6.2 (1981), pp. 213–226.

[82] Leslie Lamport. "Time, clocks, and the ordering of events in a distributed system". In: *Communications of the ACM* 21.7 (1978), pp. 558–565.

[83] Philip Lantz, Dulloor Subramanya Rao, Sanjay Kumar, Rajesh Sankaran, and Jeff Jackson. "Yat: A Validation Framework for Persistent Memory Software." In: *USENIX Annual Technical Conference*. 2014, pp. 433–438.

[84] Per-Åke Larson, Spyros Blanas, Cristian Diaconu, Craig Freedman, Jignesh M Patel, and Mike Zwilling. “High-performance concurrency control mechanisms for main-memory databases”. In: *Proceedings of the VLDB Endowment* 5.4 (2011), pp. 298–309.

[85] Doug Lea. *dlmalloc: A Memory Allocator.* `http://g.oswego.edu/dl/html/malloc.html` *(Last accessed: September 24, 2017)*.

[86] Benjamin C Lee, Engin Ipek, Onur Mutlu, and Doug Burger. “Architecting phase change memory as a scalable dram alternative”. In: *ACM SIGARCH Computer Architecture News*. Vol. 37. 3. ACM. 2009, pp. 2–13.

[87] Benjamin C Lee, Ping Zhou, Jun Yang, Youtao Zhang, Bo Zhao, Engin Ipek, Onur Mutlu, and Doug Burger. “Phase-change technology and the future of main memory”. In: *IEEE micro* 30.1 (2010).

[88] Eunji Lee, Jee E Jang, Taeseok Kim, and Hyokyung Bahn. “On-demand snapshot: An efficient versioning file system for phase-change memory”. In: *IEEE Transactions on Knowledge and Data Engineering* 25.12 (2013), pp. 2841–2853.

[89] Juchang Lee, Hyungyu Shin, Chang Gyoo Park, Seongyun Ko, Jaeyun Noh, Yongjae Chuh, Wolfgang Stephan, and Wook-Shin Han. “Hybrid Garbage Collection for Multi-Version Concurrency Control in SAP HANA”. In: *Proceedings of the 2016 International Conference on Management of Data*. ACM. 2016, pp. 1307–1318.

[90] Se Kwon Lee, K. Hyun Lim, Hyunsub Song, Beomseok Nam, and Sam H. Noh. “WORT: Write Optimal Radix Tree for Persistent Memory Storage Systems”. In: *15th USENIX Conference on File and Storage Technologies (FAST 17)*. Santa Clara, CA: USENIX Association, 2017, pp. 257–270. ISBN: 978-1-931971-36-2.

[91] Tobin Jon Lehman. “Design and performance evaluation of a main memory relational database system”. PhD thesis. University of Wisconsin–Madison, 1986.

[92] Viktor Leis, Alfons Kemper, and Thomas Neumann. “The adaptive radix tree: ARTful indexing for main-memory databases”. In: *Data Engineering (ICDE), 2013 IEEE 29th International Conference on*. IEEE. 2013, pp. 38–49.

[93] Lucas Lersch, Ismail Oukid, Wolfgang Lehner, and Ivan Schreter. “An analysis of LSM caching in NVRAM”. In: *Proceedings of the 13th International Workshop on Data Management on New Hardware*. ACM. 2017, p. 9.

[94] Lucas Lersch, Ismail Oukid, Ivan Schreter, and Wolfgang Lehner. “Rethinking DRAM Caching for LSMs in an NVRAM Environment”. In: *Advances in Databases and Information Systems: 21th East European Conference (ADBIS’17)*. Springer. 2017.

[95] Justin J Levandoski, David B Lomet, and Sudipta Sengupta. “The Bw-Tree: A B-tree for new hardware platforms”. In: *Data Engineering (ICDE), 2013 IEEE 29th International Conference on*. IEEE. 2013, pp. 302–313.

[96] Eliezer Levy and Abraham Silberschatz. “Incremental recovery in main memory database systems”. In: *IEEE Transactions on Knowledge and Data Engineering* 4.6 (1992), pp. 529–540.

[97] *Linux LIBNVDIMM.* `https://www.kernel.org/doc/Documentation/nvdimm/nvdimm.txt` *(Last accessed: September 24, 2017)*.

[98] Qingyue Liu and Peter Varman. “Ouroboros Wear-Leveling: A Two-Level Hierarchical Wear-Leveling Model for NVRAM”. In: (2017).

[99] David Lomet, Kostas Tzoumas, and Michael Zwilling. “Implementing performance competitive logical recovery”. In: *Proceedings of the VLDB Endowment* 4.7 (2011), pp. 430–439.

[100] Nirmesh Malviya, Ariel Weisberg, Samuel Madden, and Michael Stonebraker. “Rethinking main memory OLTP recovery”. In: *Data Engineering (ICDE), 2014 IEEE 30th International Conference on*. IEEE. 2014, pp. 604–615.

[101] Yandong Mao, Eddie Kohler, and Robert Tappan Morris. “Cache craftiness for fast multicore key-value storage”. In: *Proceedings of the 7th ACM European Conference on Computer Systems*. ACM. 2012, pp. 183–196.

[102] Luc Maranget, Susmit Sarkar, and Peter Sewell. *A tutorial introduction to the ARM and POWER relaxed memory models*. Tech. rep. 2012.

[103] *MC-Benchmark – Redis benchmark for Memcached.* `https://github.com/antirez/mc-benchmark` *(Last accessed: September 24, 2017)*.

[104] *Memcached – Memory Object Caching Store..* `http://memcached.org/` *(Last accessed: September 24, 2017)*.

[105] *MemSQL.* `http://www.memsql.com/` *(Last accessed: September 24, 2017)*.

[106] Ross Mistry and Stacia Misner. *Introducing Microsoft SQL Server 2014*. Microsoft Press, 2014.

[107] Sparsh Mittal and Jeffrey S Vetter. “A survey of software techniques for using non-volatile memories for storage and main memory systems”. In: *IEEE Transactions on Parallel and Distributed Systems* 27.5 (2016), pp. 1537–1550.

[108] C Mohan. *ARIES/KVL: A Key-Value Locking Method for Concurrency Control of Multiaction Transactions Operating on B-Tree Indexes.* IBM Thomas J. Watson Research Division, 1989.

[109] C Mohan, Don Haderle, Bruce Lindsay, Hamid Pirahesh, and Peter Schwarz. “ARIES: a transaction recovery method supporting fine-granularity locking and partial rollbacks using write-ahead logging”. In: *ACM Transactions on Database Systems (TODS)* 17.1 (1992), pp. 94–162.

[110] Iulian Moraru, David G Andersen, Michael Kaminsky, Niraj Tolia, Parthasarathy Ranganathan, and Nathan Binkert. “Consistent, durable, and safe memory management for byte-addressable non volatile main memory”. In: *Proceedings of the First ACM SIGOPS Conference on Timely Results in Operating Systems*. ACM. 2013, p. 1.

[111] Donald R Morrison. “PATRICIA—practical algorithm to retrieve information coded in alphanumeric”. In: *Journal of the ACM (JACM)* 15.4 (1968), pp. 514–534.

[112] Onur Mutlu. “Memory scaling: A systems architecture perspective”. In: *Memory Workshop (IMW), 2013 5th IEEE International*. IEEE. 2013, pp. 21–25.

[113] Nicholas Nethercote and Julian Seward. “Valgrind: a framework for heavyweight dynamic binary instrumentation”. In: *ACM Sigplan notices* 42.6 (2007), pp. 89–100.

[114] Thomas Neumann, Tobias Mühlbauer, and Alfons Kemper. “Fast serializable multi-version concurrency control for main-memory database systems”. In: *Proceedings of the 2015 ACM SIGMOD International Conference on Management of Data*. ACM. 2015, pp. 677–689.

[115] *numactl: Control NUMA policy for processes or shared memory.* `https://linux.die.net/man/8/numactl` *(Last accessed: September 24, 2017)*.

[116] *NuoDB.* `https://www.nuodb.com/` *(Last accessed: September 24, 2017)*.

[117] *NVML Library.* `http://pmem.io/nvml/` *(Last accessed: September 24, 2017)*.

[118] Matheus A Ogleari, Ethan L Miller, and Jishen Zhao. “Relaxing Persistent Memory Constraints with Hardware-Driven Undo+ Redo Logging”. In: *8th Annual Non-Volatile Memories Workshop (NVMW'17)*. 2017.

[119] Patrick O'Neil, Edward Cheng, Dieter Gawlick, and Elizabeth O'Neil. “The log-structured merge-tree (LSM-tree)”. In: *Acta Informatica* 33.4 (1996), pp. 351–385.

[120] *Oracle Database Administrator's Guide: Managing Memory.* `https://docs.oracle.com/database/121/ADMIN/memory.htm` (Last accessed: September 24, 2017).

[121] Jiaxin Ou, Jiwu Shu, and Youyou Lu. "A high performance file system for non-volatile main memory". In: *EuroSys*. ACM. 2016, p. 12.

[122] Ismail Oukid, Daniel Booss, Wolfgang Lehner, Peter Bumbulis, and Thomas Willhalm. "SOFORT: A hybrid SCM-DRAM storage engine for fast data recovery". In: *Proceedings of the Tenth International Workshop on Data Management on New Hardware*. ACM. 2014, p. 8.

[123] Ismail Oukid, Daniel Booss, Adrien Lespinasse, and Wolfgang Lehner. "On testing persistent-memory-based software". In: *Proceedings of the 12th International Workshop on Data Management on New Hardware*. ACM. 2016, p. 5.

[124] Ismail Oukid, Daniel Booss, Adrien Lespinasse, Wolfgang Lehner, Thomas Willhalm, and Grégoire Gomes. "Memory management techniques for large-scale persistent-main-memory systems". In: *Proceedings of the VLDB Endowment* 10.11 (2017), pp. 1166–1177.

[125] Ismail Oukid, Robert Kettler, and Thomas Willhalm. "Storage class memory and databases: Opportunities and challenges". In: *it-Information Technology* (2017).

[126] Ismail Oukid, Johan Lasperas, Anisoara Nica, Thomas Willhalm, and Wolfgang Lehner. "FP-Tree: A Hybrid SCM-DRAM Persistent and Concurrent B-Tree for Storage Class Memory". In: *SIGMOD*. ACM. 2016, pp. 371–386.

[127] Ismail Oukid and Wolfgang Lehner. "Data Structure Engineering For Byte-Addressable Non-Volatile Memory". In: *Proceedings of the 2017 ACM International Conference on Management of Data*. ACM. 2017, pp. 1759–1764.

[128] Ismail Oukid, Wolfgang Lehner, Thomas Kissinger, Thomas Willhalm, and Peter Bumbulis. "Instant Recovery for Main-Memory Databases". In: *CIDR*. 2015.

[129] Ismail Oukid, Anisoara Nica, Daniel Dos Santos Bossle, Wolfgang Lehner, Peter Bumbulis, and Thomas Willhalm. "Adaptive Recovery for SCM-Enabled Databases". In: *ADMS@ VLDB*. 2017.

[130] Ippokratis Pandis, Ryan Johnson, Nikos Hardavellas, and Anastasia Ailamaki. "Data-oriented transaction execution". In: *Proceedings of the VLDB Endowment* 3.1-2 (2010), pp. 928–939.

[131] Ippokratis Pandis, Pinar Tözün, Ryan Johnson, and Anastasia Ailamaki. "PLP: page latch-free shared-everything OLTP". In: *Proceedings of the VLDB Endowment* 4.10 (2011), pp. 610–621.

[132] Steven Pelley, Kristen LeFevre, and Thomas F Wenisch. "Do Query Optimizers Need to be SSD-aware?" In: *ADMS@ VLDB*. 2011, pp. 44–51.

[133] Steven Pelley, Thomas F Wenisch, Brian T Gold, and Bill Bridge. "Storage management in the NVRAM era". In: *Proceedings of the VLDB Endowment* 7.2 (2013), pp. 121–132.

[134] *Peloton Database Management System.* `http://pelotondb.org` (Last accessed: September 24, 2017).

[135] Thanumalayan Sankaranarayana Pillai, Vijay Chidambaram, Ramnatthan Alagappan, Samer Al-Kiswany, Andrea C Arpaci-Dusseau, and Remzi H Arpaci-Dusseau. "All File Systems Are Not Created Equal: On the Complexity of Crafting Crash-Consistent Applications." In: *OSDI*. 2014, pp. 433–448.

[136] *Quartz: A DRAM-based performance emulator for NVM.* `https://github.com/HewlettPackard/quartz` (Last accessed: September 24, 2017).

[137] Moinuddin K Qureshi, Sudhanva Gurumurthi, and Bipin Rajendran. "Phase change memory: From devices to systems". In: *Synthesis Lectures on Computer Architecture* 6.4 (2011), pp. 1–134.

[138] Moinuddin K Qureshi, John Karidis, Michele Franceschini, Vijayalakshmi Srinivasan, Luis Lastras, and Bulent Abali. “Enhancing lifetime and security of PCM-based main memory with start-gap wear leveling”. In: *Proceedings of the 42nd Annual IEEE/ACM International Symposium on Microarchitecture*. ACM. 2009, pp. 14–23.

[139] Moinuddin K Qureshi, Vijayalakshmi Srinivasan, and Jude A Rivers. “Scalable high performance main memory system using phase-change memory technology”. In: *ACM SIGARCH Computer Architecture News* 37.3 (2009), pp. 24–33.

[140] Vijayshankar Raman, Gopi Attaluri, Ronald Barber, Naresh Chainani, David Kalmuk, Vincent KulandaiSamy, Jens Leenstra, Sam Lightstone, Shaorong Liu, Guy M Lohman, et al. “DB2 with BLU acceleration: So much more than just a column store”. In: *Proceedings of the VLDB Endowment* 6.11 (2013), pp. 1080–1091.

[141] Jun Rao and Kenneth A Ross. “Making B+-trees cache conscious in main memory”. In: *ACM SIGMOD Record*. Vol. 29. 2. ACM. 2000, pp. 475–486.

[142] *Real-Time Decision Making Using Hybrid Streaming, In-Memory Computing Analytics and Transaction Processing. Gartner, 2017.* `https://www.gartner.com/imagesrv/media-products/pdf/Kx/KX-1-3CZ44RH.pdf` *(Last accessed: September 24, 2017).*

[143] David P Reed. “Implementing atomic actions on decentralized data”. In: *ACM Transactions on Computer Systems (TOCS)* 1.1 (1983), pp. 3–23.

[144] David Patrick Reed. “Naming and synchronization in a decentralized computer system”. PhD thesis. Massachusetts Institute of Technology, 1978.

[145] *SAP HANA Memory Usage Explained.* `https://www.sap.com/documents/2016/08/205c8299-867c-0010-82c7-eda71af511fa.html` *(Last accessed: September 24, 2017).*

[146] Karl Schnaitter, Neoklis Polyzotis, and Lise Getoor. “Index interactions in physical design tuning: modeling, analysis, and applications”. In: *Proceedings of the VLDB Endowment* 2.1 (2009), pp. 1234–1245.

[147] David Schwalb, Tim Berning, Martin Faust, Markus Dreseler, and Hasso Plattner. “nvm malloc: Memory Allocation for NVRAM.” In: *ADMS@ VLDB*. 2015, pp. 61–72.

[148] David Schwalb, Girish Kumar BK, Markus Dreseler, S Anusha, Martin Faust, Adolf Hohl, Tim Berning, Gaurav Makkar, Hasso Plattner, and Parag Deshmukh. “Hyrise-NV: Instant Recovery for In-Memory Databases Using Non-Volatile Memory”. In: *International Conference on Database Systems for Advanced Applications*. Springer. 2016, pp. 267–282.

[149] David Schwalb, Markus Dreseler, Matthias Uflacker, and Hasso Plattner. “NVC-hashmap: A persistent and concurrent hashmap for non-volatile memories”. In: *Proceedings of the 3rd VLDB Workshop on In-Memory Data Mangement and Analytics*. ACM. 2015, p. 4.

[150] *SNIA NVM Programming Model V1.1.* Tech. rep. `http://www.snia.org/sites/default/files/NVMProgrammingModel_v1.1.pdf` (Last accessed: September 24, 2017).

[151] Michael Stonebraker, Samuel Madden, Daniel J Abadi, Stavros Harizopoulos, Nabil Hachem, and Pat Helland. “The end of an architectural era: (it’s time for a complete rewrite)”. In: *Proceedings of the 33rd international conference on Very large data bases*. VLDB Endowment. 2007, pp. 1150–1160.

[152] Michael Stonebraker and Lawrence A. Rowe. “The Design of POSTGRES”. In: *Proceedings of the 1986 ACM SIGMOD International Conference on Management of Data*. SIGMOD ’86. Washington, D.C., USA: ACM, 1986, pp. 340–355.

[153] Dmitri B Strukov, Gregory S Snider, Duncan R Stewart, and R Stanley Williams. “The missing memristor found”. In: *nature* 453.7191 (2008), pp. 80–83.

[154] *STX B^+-Tree C++ Template Classes.* `https://panthema.net/2007/stx-btree/` *(Last accessed: September 24, 2017)*.

[155] *Telecom Application Transaction Processing Benchmark.* `http://tatpbenchmark.sourceforge.net/` *(Last accessed: September 24, 2017)*.

[156] *The DB2 UDB memory model.* `https://www.ibm.com/developerworks/data/library/techarticle/dm-0406qi/` *(Last accessed: September 24, 2017)*.

[157] *Tile Based Architecture in Peloton.* `https://github.com/cmu-db/peloton/wiki/Tile-Based-Architecture` *(Last accessed: September 24, 2017)*.

[158] *Tmpfs file system.* `https://www.kernel.org/doc/Documentation/filesystems/tmpfs.txt` *(Last accessed: September 24, 2017)*.

[159] *TPC-C Benchmark.* `http://www.tpc.org/tpcc/` *(Last accessed: September 24, 2017)*.

[160] Irving L Traiger. "Virtual memory management for database systems". In: *ACM SIGOPS Operating Systems Review* 16.4 (1982), pp. 26–48.

[161] Stephen Tu, Wenting Zheng, Eddie Kohler, Barbara Liskov, and Samuel Madden. "Speedy transactions in multicore in-memory databases". In: *Proceedings of the Twenty-Fourth ACM Symposium on Operating Systems Principles*. ACM. 2013, pp. 18–32.

[162] *Using Non-volatile Memory (NVDIMM-N) as Byte-Addressable Storage in Windows Server 2016.* `https://channel9.msdn.com/events/build/2016/p470` *(Last accessed: September 24, 2017)*.

[163] *Valgrind extension for persistent memory.* `https://github.com/pmem/valgrind` *(Last accessed: September 24, 2017)*.

[164] Shivaram Venkataraman, Niraj Tolia, Parthasarathy Ranganathan, Roy H Campbell, et al. "Consistent and Durable Data Structures for Non-Volatile Byte-Addressable Memory." In: *9th USENIX Conference on File and Storage Technologies (FAST 11)*. Vol. 11. USENIX Association, 2011, pp. 61–75.

[165] Stratis D Viglas. "Adapting the B+-tree for asymmetric I/O". In: *East European Conference on Advances in Databases and Information Systems*. Springer. 2012, pp. 399–412.

[166] Stratis D Viglas. "Write-limited sorts and joins for persistent memory". In: *Proceedings of the VLDB Endowment* 7.5 (2014), pp. 413–424.

[167] Haris Volos, Guilherme Magalhaes, Ludmila Cherkasova, and Jun Li. "Quartz: A Lightweight Performance Emulator for Persistent Memory Software". In: *Proceedings of the 16th Annual Middleware Conference*. ACM. 2015, pp. 37–49.

[168] Haris Volos, Andres Jaan Tack, and Michael M Swift. "Mnemosyne: Lightweight persistent memory". In: *ACM SIGARCH Computer Architecture News* 39.1 (2011), pp. 91–104.

[169] *VoltDB.* `https://www.voltdb.com/` *(Last accessed: September 24, 2017)*.

[170] Tianzheng Wang and Ryan Johnson. "Scalable logging through emerging non-volatile memory". In: *Proceedings of the VLDB Endowment* 7.10 (2014), pp. 865–876.

[171] Tianzheng Wang, Ryan Johnson, Alan Fekete, and Ippokratis Pandis. "Efficiently making (almost) any concurrency control mechanism serializable". In: *The VLDB Journal* 26.4 (2017), pp. 537–562.

[172] Tianzheng Wang and Hideaki Kimura. "Mostly-optimistic concurrency control for highly contended dynamic workloads on a thousand cores". In: *Proceedings of the VLDB Endowment* 10.2 (2016), pp. 49–60.

[173] Thomas Willhalm, Nicolae Popovici, Yazan Boshmaf, Hasso Plattner, Alexander Zeier, and Jan Schaffner. "SIMD-scan: ultra fast in-memory table scan using on-chip vector processing units". In: *Proceedings of the VLDB Endowment* 2.1 (2009), pp. 385–394.

[174] Paul R. Wilson. "Pointer Swizzling at Page Fault Time: Efficiently Supporting Huge Address Spaces on Standard Hardware". In: *SIGARCH Comput. Archit. News* 19.4 (July 1991), pp. 6–13. ISSN: 0163-5964. DOI: `10.1145/122576.122577`.

[175] Xiaojian Wu and AL Reddy. "SCMFS: a file system for storage class memory". In: *Proceedings of 2011 International Conference for High Performance Computing, Networking, Storage and Analysis*. ACM. 2011, p. 39.

[176] Yingjun Wu, Joy Arulraj, Jiexi Lin, Ran Xian, and Andrew Pavlo. "An empirical evaluation of in-memory multi-version concurrency control". In: *Proceedings of the VLDB Endowment* 10.7 (2017), pp. 781–792.

[177] Yingjun Wu, Chee-Yong Chan, and Kian-Lee Tan. "Transaction healing: Scaling optimistic concurrency control on multicores". In: *Proceedings of the 2016 International Conference on Management of Data*. ACM. 2016, pp. 1689–1704.

[178] Fei Xia, Dejun Jiang, Jin Xiong, and Ninghui Sun. "HiKV: A Hybrid Index Key-Value Store for DRAM-NVM Memory Systems". In: *2017 USENIX Annual Technical Conference (USENIX ATC 17)*. Santa Clara, CA: USENIX Association, 2017.

[179] Jian Xu and Steven Swanson. "NOVA: a log-structured file system for hybrid volatile/non-volatile main memories". In: *14th USENIX Conference on File and Storage Technologies (FAST 16)*. USENIX Association, 2016, pp. 323–338.

[180] J. Yang, Q. Wei, C. Wang, C. Chen, K. Yong, and B. He. "NV-Tree: A Consistent and Workload-adaptive Tree Structure for Non-volatile Memory". In: *IEEE Transactions on Computers* PP.99 (2015). ISSN: 0018-9340. DOI: `10.1109/TC.2015.2479621`.

[181] Junfeng Yang, Can Sar, and Dawson Engler. "Explode: a lightweight, general system for finding serious storage system errors". In: *Proceedings of the 7th symposium on Operating systems design and implementation*. USENIX Association. 2006, pp. 131–146.

[182] Chang Yao, Divyakant Agrawal, Gang Chen, Beng Chin Ooi, and Sai Wu. "Adaptive logging: Optimizing logging and recovery costs in distributed in-memory databases". In: *Proceedings of the 2016 International Conference on Management of Data*. ACM. 2016, pp. 1119–1134.

[183] Matt T Yourst. "PTLsim: A cycle accurate full system x86-64 microarchitectural simulator". In: *Performance Analysis of Systems & Software, 2007. ISPASS 2007. IEEE International Symposium on*. IEEE. 2007, pp. 23–34.

[184] Songping Yu, Nong Xiao, Mingzhu Deng, Yuxuan Xing, Fang Liu, Zhiping Cai, and Wei Chen. "WAlloc: An efficient wear-aware allocator for non-volatile main memory". In: *IPCCC*. IEEE. 2015, pp. 1–8.

[185] Pengfei Zuo and Yu Hua. "A Write-friendly Hashing Scheme for Non-Volatile Memory Systems". In: (2017).

LIST OF FIGURES

1.1 Comparison of access latency of different memory technologies. Adapted from [137]. 6
1.2 SCM is mapped directly into the address space of the application, allowing direct access with load/store semantics. 6
1.3 Towards a hybrid SCM-DRAM single-level database storage architecture. 7
1.4 Organization of our contributions across the dissertation. 9

2.1 SCM as transient main memory extension. 13
2.2 SCM as disk replacement or as persistent main memory. 13
2.3 Measuring process termination duration. Experiment: memory map memory, touch it, then kill the process and measure termination duration. The experimental system has 32 E7-8890 v3 processors (1152 cores total) and 16 terabytes of DRAM. 14
2.4 Slowdown incurred by using SCM over DRAM in different microbenchmarks. 15
2.5 SIMD Scan performance on SCM relative to DRAM with and without hardware and software prefetching. 15
2.6 NUMA-based SCM emulation on a two-socket system. 16
2.7 Architecture overview of Intel's SCM emulation platform. 18
2.8 Traditional database architecture. 19
2.9 Database architecture with SCM as a primary data store. 22
2.10 Hybrid SCM-DRAM architecture of SOFORT. 28
2.11 Data layout overview in SOFORT. 29

3.1 Illustration of the volatility chain in a 2-core x86-like processors. 35
3.2 Illustration of process address space loss upon restart. 36
3.3 Example of data recovery using persistent pointers consisting of a file ID and an offset within that file. 39
3.4 Illustration of the segregated-fit allocation strategy for small block allocations. 43
3.5 Illustration of the best-fit allocation strategy for large block allocations. 43
3.6 16 KB allocation performance on an Intel Xeon CPU X5550 2.67GHz (16 cores). The core-local allocator scales better under high concurrency than thread-local counterparts. 44
3.7 Architecture overview of PAllocator. 46
3.8 Architecture overview of SmallPAllocator. 50
3.9 Data organization in SmallPAllocator. 51
3.10 Allocation process of SmallPAllocator. 52
3.11 Architecture overview of BigPAllocator. 53
3.12 Data organization in BigPAllocator. 53
3.13 Allocation process of BigPAllocator. 54
3.14 Defragmentation process of BigPAllocator. 55
3.15 Allocations concurrency scalability for different object sizes. 56
3.16 Allocations performance for different object sizes and SCM latencies. 57
3.17 Deallocation concurrency scalability for different object sizes. 58
3.18 Deallocation performance for different object sizes and SCM latencies. 59
3.19 Random allocation/deallocation benchmark with different distributions. 61
3.20 Larson benchmark with different random allocation ranges. 62
3.21 Recovery time for varying total allocation sizes and SCM latencies. 63

3.22 Allocator impact on FPTree performance. Solid lines represent PAllocator and dash-dotted lines NVML. 65

4.1 Node split after an insertion in the CDDS B^+-Tree. 69
4.2 Comparison of insertions in a sorted node and an unsorted node. 70
4.3 Insertion in an unsorted node with a bitmap and an indirection slot array. 70
4.4 Overview of the architecture of the NV-Tree. 71
4.5 Insertion in an append-only leaf node of the NV-Tree. 71
4.6 Illustration of the architecture of HiKV. 72
4.7 FPTree inner node and leaf node layouts. 73
4.8 Selective persistence applied to a B^+-Tree: inner nodes are kept in DRAM while leaf nodes are kept in SCM. 74
4.9 Expected number of in-leaf key probes during a successful search operation for the FPTree, NV-Tree, and wBTree. 75
4.10 FPTree leaf group management. 76
4.11 Selective concurrency applied to an insert operation in a hybrid data structure. . . . 77
4.12 Effect of the latency of SCM on the performance of the *Find*, *Insert*, *Update*, *Delete*, and *Recovery* tree operations with fixed-size keys. 92
4.13 Effect of the latency of SCM on the performance of the *Find*, *Insert*, *Update*, *Delete*, and *Recovery* tree operations with variable-size keys. 93
4.14 DRAM and SCM consumption of trees with 100M key-value: 8-byte and 16-byte keys for fixed-size and variable-size keys versions, respectively. 94
4.15 Concurrency performance on one socket – 50 million key-values warmup followed by 50 million operations. Ideal speedup is depicted with the mark-less line. 95
4.16 Concurrency performance on two sockets – 50 million key-values followed by 50 million operations. Ideal speedup is depicted with the mark-less line. 96
4.17 Concurrency performance on one socket with an SCM latency of 145 ns – 50 million key-values warmup followed by 50 million operations. Ideal speedup is depicted with the mark-less line. 97
4.18 Impact of payload size on the single-threaded and multi-threaded performance of the evaluated trees. 98
4.19 Trees impact on database throughput and restart performance – TATP with 50 million subscribers, primary data size ~45 GB. 99
4.20 Trees impact on *memcached* performance for different latencies – *mc-benchkark* with 50 million operations. 100

5.1 Overview of data layout in SOFORT. 110
5.2 Example of a SOFORT table of employees and their offices. 111
5.3 Transaction flow during a system failure. 126
5.4 Transaction throughput and latency of SOFORT, SILO, and Shore-MT for the TATP (10 million Subscribers) and TPC-C (48 Warehouses) benchmarks. 128
5.5 Impact of higher SCM latencies on SOFORT's OLTP performance for the TATP (10 million Subscribers) and TPC-C (48 Warehouses) benchmarks. Depicted throughput is relative to a baseline SCM latency of 160 ns. 129
5.6 SOFORT's OLTP performance with different secondary data placement strategies for the TATP (10 million Subscribers) and TPC-C (48 Warehouses) benchmarks. Depicted throughput is relative to SOFORT-FPTree. 129
5.7 SOFORT DRAM and SCM consumption with different data placement strategies for the TATP (10 million Subscribers) and TPC-C (48 Warehouses) benchmarks. 130
5.8 Cost of flushing instructions in SOFORT with different secondary data placement strategies for the TATP (10 million Subscribers) and TPC-C (48 Warehouses) benchmarks. 131

5.9 SOFORT Recovery time with different storage technologies and data placement strategies for the TATP (20 million Subscribers) and TPC-C (128 Warehouses) benchmarks. 132

6.1 Results overview: TPC-C transaction throughput during recovery. 134
6.2 $rank(s, t)$ for TATP (20 Mio subscribers) and TPC-C (50 Warehouses) during recovery : $Benefit_{dep}$ vs. $Benefit_{indep}$. 140
6.3 Recovery framework of secondary database objects. 142
6.4 Impact of secondary data placement on recovery performance. Maximum throughput is relative to the performance of SOFORT-STXTree. 144
6.5 Different recovery strategies with logarithmic scale. 145
6.6 Static resource allocation impact on recovery. 146
6.7 Adaptive resource allocation impact on recovery. 147
6.8 Best of static vs. best of adaptive resource allocation. 148
6.9 Impact of workload change during recovery. 149
6.10 SCM latency impact on recovery performance. Throughput is depicted relative to a baseline SCM latency of 200 ns. 149
6.11 Worst case analysis: Adaptive recovery Vs. Synchronous recovery. 150

7.1 Contrast between the traditional disk-based storage architecture (on the left side) and the single-level SCM-based direct access architecture (on the right side). 154
7.2 Illustration of crash simulation in the testing framework. 157
7.3 Global overview of the testing framework including copy-on-write optimizations, memory reordering, and nested crash simulation. 162
7.4 Frequency distribution of the the number of simulated crashes per call stack. The y axis represents the considered range groups of the number of crash simulations per call stack, while the x axis represents the cardinality of these groups. 166

8.1 Illustration of a morphing SCM-DRAM data structure. 171
8.2 Fine-grained replication using SCM and RDMA. 172

LIST OF TABLES

2.1 Comparison of current memory technologies with SCM candidates [107]. 12
2.2 Summary of state-of-the-art research on re-architecting database storage and recovery in presence of SCM. 25

3.1 Summary of existing libraries that address some or all of the programming challenges of SCM. PPtr stands for persistent pointer. 41
3.2 Summary of the design characteristics of existing persistent memory allocators. There are salient differences in the design decisions of PAllocator and state-of-the-art persistent allocators. 47
3.3 Fragmentation stress test results. 64

4.1 Chosen node sizes (in number of entries) for the evaluated trees. Values are 8-byte integers for all trees. The suffixes *C* and *Var* indicate, respectively, the concurrent and variable-size key versions of the trees. 91

6.1 Experimental Configurations of SOFORT Recovery Experiments. 143

6.2 Breakdown of recovery time. Recovery duration of memory management (PAllocator), primary data, secondary data, and garbage recovery times. 144

7.1 Performance of the testing framework with nested crash simulation disabled. Call stack is abbreviated as CS. 165
7.2 Performance of the testing framework with nested crash simulation enabled. 165

LIST OF ALGORITHMS

4.1 FPTree Concurrent Find function. 79
4.2 FPTree Concurrent Insert function for fixed-size keys. 80
4.3 FPTree Split Leaf procedure. 81
4.4 FPTree Recover Split Leaf procedure. 81
4.5 FPTree Concurrent Delete function for fixed-size keys. 82
4.6 FPTree Delete Leaf procedure. 83
4.7 FPTree Recover Delete Leaf procedure. 83
4.8 FPTree Concurrent Update function for fixed-size keys. 84
4.9 FPTree Recover procedure. 84
4.10 FPTree Concurrent Insert function for variable-size keys. 85
4.11 FPTree Concurrent Delete function for variable-size keys. 86
4.12 FPTree Concurrent Update function for variable-size keys. 87
4.13 FPTree Inner Nodes Rebuild procedure for variable-size keys. 88
4.14 FPTree Get Leaf procedure. 88
4.15 FPTree Recover Get Leaf procedure. 89
4.16 FPTree Free Leaf procedure. 89
4.17 FPTree Recover Free Leaf procedure. 90

5.1 SOFORT Row Visibility function. 114
5.2 SOFORT Cross-Transaction Row Visibility function. 115
5.3 SOFORT Start Transaction function. 115
5.4 SOFORT Select function. 116
5.5 SOFORT Get Visible Rows function. 117
5.6 SOFORT Insert function. 117
5.7 SOFORT Delete function. 118
5.8 SOFORT Update function. 119
5.9 SOFORT Commit Transaction function 121
5.10 SOFORT Abort Transaction function. 122
5.11 SOFORT Recovery function. 123
5.12 SOFORT Transaction Recovery function. 123
5.13 SOFORT Garbage Collection function. 124
5.14 SOFORT Row Collection function. 124
5.15 SOFORT Background Garbage Collection Recovery function. 125
6.1 SOFORT Adaptive Recovery procedure. 141
6.2 Get Next Indexes to Rebuild function. 141

7.1 Crash simulation inside the Flush procedure. 158
7.2 Crash Simulation procedure with call-stack awareness. 159
7.3 Crash Simulation procedure with call-stack awareness and stashed writes. 161

CONFIRMATION

I confirm that I independently prepared the dissertation and that I used only the references and auxiliary means indicated in the dissertation.

Walldorf, December 15, 2017